

CARDIFF UNIVERSITY

The molecular, cellular and clinical impacts of Suppressor of Cytokine Signalling in human wound healing

by

Yi Feng


**Cardiff China Medical Research Collaborative
School of Medicine, Cardiff University
Cardiff**

18/02/2017

Thesis submitted to Cardiff University for the degree of Doctor
of Philosophy


DECLARATION

This work has not been submitted in substance for any other degree or award at this or any other university or place of learning, nor is being submitted concurrently in candidature for any degree or other award.

Signed  (candidate) Date ...18/02/2017.....


STATEMENT 1

This thesis is being submitted in partial fulfillment of the requirements for the degree of PhD.

Signed  (candidate) Date ...18/02/2017.....


STATEMENT 2

This thesis is the result of my own independent work/investigation, except where otherwise stated. Other sources are acknowledged by explicit references. The views expressed are my own.

Signed  (candidate) Date ...18/02/2017.....


STATEMENT 3

I hereby give consent for my thesis, if accepted, to be available for photocopying and for inter-library loan, and for the title and summary to be made available to outside organisations.

Signed  (candidate) Date ...18/02/2017.....

STATEMENT 4: PREVIOUSLY APPROVED BAR ON ACCESS

I hereby give consent for my thesis, if accepted, to be available for photocopying and for inter-library loans **after expiry of a bar on access previously approved by the Academic Standards & Quality Committee.**

Signed  (candidate) Date ...18/02/2017.....

Acknowledgements

Firstly, I would like to thank my supervisors Professor Wen G. Jiang and Professor Keith G. Harding, and my sponsor, GlaxoSmithKline, for providing me with this great opportunity to pursue my PhD at Cardiff University. I also would like to express my gratitude to my co-supervisor, Dr Andrew Sanders, Miss Fiona Ruge and Dr Liam Morgan who have always been patient and supportive throughout the whole period of my PhD study. I also appreciate Dr Jun Cai, Dr Lin Ye and all the Chinese visiting scholars in CCMRC who helped me settle down very quickly when I first came to this new and daunting environment. Meanwhile, I would like to thank all the PhD, MD, post-doctoral, senior staff members and administrative staff members in CCMRC who have been really friendly and helpful all the time. In addition, I would like to express my thanks to the members in my Research Student Progress Monitoring Panel, Professor David Kipling and Dr Alex Tonks, who provided me with many valuable suggestions and guidance. Last, but not least, I am really grateful to Mr Bruno Bastos, Miss Robyn Bradbury, Miss Jeyna Resaul and Miss Bethan Frugtniet for the wonderful friendship during the last three years, and I wish we could be friends for ever.

Finally, I would like to dedicate this work to my parents and my wife whose support and encouragement gave me the motivation and determination to overcome all the difficulties and frustrations in order to complete my study.

At last I would like to address that this study is kindly supported and funded by GlaxoSmithKline.

Publications

Full papers (published):

FENG, Y., SANDERS, A. J., MORGAN, L. D., HARDING, K. G. & JIANG, W. G. 2016.

Potential roles of suppressor of cytokine signaling in wound healing. *Regen Med*, 11, 193-209.

FENG, Y., SANDERS, A. J., RUGE, F., MORRIS, C. A., HARDING, K. G. & JIANG, W. G.

2016. Expression of the SOCS family in human chronic wound tissues: Potential implications for SOCS in chronic wound healing. *Int J Mol Med*.

Full papers submitted and in preparation:

FENG, Y., SANDERS, A.J., MORGAN, L. D., RUGE, F., HARDING, K. G. & JIANG, W. G.

Functional significance of SOCS-3 and SOCS-4 in wound healing *in vitro* models.

Abstracts and conference presentations

Poster presentation:

Expression of the suppressor of cytokine signaling (SOCS) family members in chronic wound tissue. September, 2014. **Yi Feng**, Andrew J. Sanders, Fiona Ruge, Professor Wen G. Jiang, Professor Keith G. Harding. European Tissue Repair Society Annual Congress 2014, Edinburg, Scotland, United Kingdom.

Oral presentation:

Differences in expression of the suppressor of cytokine signaling (SOCS) family members in chronic wound tissue. September, 2014. **Yi Feng**, Andrew J. Sanders, Fiona Ruge, Professor Wen G. Jiang, Professor Keith G. Harding. International Conference on Repair, Regeneration and Reconstruction, London, England, United Kingdom.

Summary

Wound healing and the management of chronic, non-healing wounds represent a significant burden to the NHS and results in substantial patient morbidity. New methods to further understanding of wound chronicity and potential therapies are needed. This PhD study aims to explore the importance of the SOCS family in the wound healing process, exploring their potential to act as prognostic factors in clinical cohorts and exploring the potential of SOCS-3 and -4 to influence key cellular traits linked to the healing process.

Detection of SOCS family members within a clinical healing/non-healing cohort highlighted significant elevations of gene expression of SOCS-3 and -4 in non-healing chronic wounds compared to healing chronic wounds, though this trend was not as obvious in a smaller cohort of IHC stained samples. However, the IHC stained samples potentially indicated that SOCS-3 protein relocalisation, from wound edge to distal wound area, was evident in the non-healing chronic wound.

Subsequently, SOCS-3 expression and SOCS-4 knockdown lines were generated in human (HaCaT) keratinocytes and (HECV) endothelial cells to explore the functional significance of these molecules at a cellular level. In summary, SOCS-4 knockdown decreased the migration of both HaCaT and HECV cells on plastic cultureware, whereas downregulation of SOCS-4 only reduced the adhesion and tubule formation of HECV cells on matrigel matrix. SOCS-3 expression attenuated the proliferation of HaCaT cells but had no effect on HECV cells. In addition, SOCS-3 upregulation solely improved the adhesion and tubule formation of HECV cells on matrigel matrix. Moreover, the regulatory role of SOCS-3 and SOCS-4 in the migration and adhesion of HaCaT and HECV are likely to be substratum matrix dependent.

Finally, to explore potential mechanisms of action for SOCS-4 role in HaCaT cell line, a protein microarray was utilised to highlight a number of potential key pathways. Based on the results from protein microarray and wound healing assay as well as evidences from literature review, four potential mechanisms (FAK/Src/p130cas, HBEGF/EGFR, VEGF/VEGFR-2, IGF-1/IGF-1R/PI3K) of SOCS-4 regulating keratinocyte migration was highlighted for further validation, and the expression profile of FAK Y397 was verified by western blotting.

Hence, SOCS-3 and SOCS-4 may regulate keratinocyte and endothelial cell behaviour, and potentially have effect on the wound healing process..

Contents

Declaration	i
Acknowledgements	ii
Publications and presentations	iii
Abstrats and conference presentations.....	iv
Summary	v
List of figures	xi
List of tables	xiv
Abbreviations	xvi
Chapter I General Introduction	
1.1 History and background of wound healing.....	2
1.1.1 The emergance and development of wound healing treatments	2
1.1.2 The neccessity and importance of study on wound healing.....	3
1.2 Cellular and molecular biology of wound repair.....	11
1.2.1 Haemostasis	15
1.2.2 Inflammation phase	15
1.2.3 Proliferation and re-epithelialisation phase	17
1.2.4 Tissue remodelling phase.....	21
1.3 Role of cytokines / growth factors in wound healing	22
1.3.1 Cytokines, growth factors and wound healing	22
1.4 SOCS	30
1.4.1 Discovery of SOCS	31
1.4.2 Structure and structural related function.....	31
1.4.3 Biological functions of SOCS family members	41
1.5 Aims of the thesis.....	91
Chapter II Methods and materials	
2.1 Cells	94
2.2 Primers	96
2.3 Antibodies	99
2.4 General reagents and solutions	100
2.4.1 Reagents and chemicals.....	100
2.4.1.1 Solutions and reagent for cell culture.....	100

2.4.1.2	Solutions and reagent for molecular biology.....	100
2.4.1.3	Solutions and reagent for cloning.....	101
2.4.1.4	Solutions and reagent for western blotting.....	102
2.4.1.5	Solutions and reagent for microarray protein lysis	103
2.4.1.6	Solutions and reagents for immunohistochemical staining.....	104
2.5	Cell culture, maintenance, storage and revival	104
2.5.1	Preparation of growth medium and cell maintenance.....	104
2.5.2	Trypsinisation (detachment) of adherent cells and cell counting	105
2.5.3	Storage and revival of cells	106
2.6	Tissue collection and processing.....	106
2.7	Total RNA isolation.....	108
2.8	Reverse transcription polymerase chain reaction (RT-PCR)	110
2.9	Polymerase chain reaction (PCR)	111
2.10	Agarose gel electrophoresis.....	112
2.11	Generation of mutant HaCaT and HECV cell lines	113
2.11.1	Discovery and the catalytic mechanism of ribozymes.....	113
2.11.2	TOPO TA gene cloning and generation of stable transfectants	115
2.11.3	Plasmid amplification and extraction	118
2.11.4	Plasmid transfection via electroporation into HaCaT and HECV cell lines	119
2.11.5	siRNA transfection via DharmaFECT transfect reagent 1 into HaCaT and HECV cell lines.....	120
2.12	Real time quantitative polymerase chain reaction (q-PCR).....	121
2.13	Immunohistochemistry (IHC)	125
2.14	Cellular lysis and protein extraction	127
2.15	Protein sample quantification, denaturation and normalisation.....	128
2.16	Protein extraction and fluorometric protein quantification for Kinexus TM antibody microarrays.....	129
2.17	Tris-glycine sodium dodecyl sulphate polyacrylamide gel electrophoresis (SDS-PAGE) and western blotting	130
2.17.1	Gel preparation and gel running.....	130
2.17.2	Preparation and operation of gel transfer.....	133
2.17.3	Protein staining and immunoprobng	134
2.17.3.1	Membrane staining	134
2.17.3.2	Immunoprobng	134

2.17.3.3	Semi-quantitative analysis on western blot results by densitometry	136
2.18	Cell functional assays	136
2.18.1	Electric cell-substrate impedance sensing (ECIS) based initial attachment and spreading, and migration assay.....	136
2.18.2	<i>In vitro</i> thiazolyl blue tetrazolium bromide (MTT) cell proliferation assay	144
2.18.3	<i>In vitro</i> MTT cell adhesion assay	145
2.18.4	<i>In vitro</i> cell migration assay (wound healing assay).....	146
2.18.5	Tubule formation assay.....	147
2.19	Statistical analysis	148
Chapter III Expression of the suppressor of cytokine signalling (SOCS) family in human chronic wound tissues: potential implications for SOCS in chronic wound healing		
3.1.	Introduction	150
3.2.	Materials and methods.....	153
3.2.1	Primers	153
3.2.2	RNA extraction and reverse transcription	154
3.2.3	q-PCR.....	154
3.2.4	IHC.....	154
3.2.5	Statistical analysis	155
3.3.	Results.....	156
3.3.1	Gene expression levels of SOCS family members in healing/healed and non-healing chronic wounds.....	156
3.3.2	Protein expression levels of seven SOCS family members in chronic tissues	162
3.3.2.1	Negative staining in chronic tissues.....	162
3.3.2.2	SOCS-1 staining in chronic tissues.....	165
3.3.2.3	SOCS-2 staining in chronic wound tissues	170
3.3.2.4	SOCS-3 staining in chronic wound tissues	175
3.3.2.5	SOCS-4 staining in chronic wound tissues	180
3.3.2.6	SOCS-5 staining in chronic tissues.....	185
3.3.2.7	SOCS-6 staining in chronic tissues.....	190
3.3.2.8	SOCS-7 staining in chronic tissues.....	195
3.4.	Discussion.....	196

Chapter IV Establishment of SOCS-3 expression and SOCS-4 knockdown models

4.1	Introduction	202
4.2	Methods and materials	205
4.2.1	Synthesis of SOCS-4 targeting ribozyme by touchdown PCR.....	205
4.2.2	TOPO TA cloning of SOCS-4 targeting ribozyme into the pEF6/V5-His-TOPO plasmid vector and incorporated transgene orientation check	205
4.2.3	Amplification of complete coding sequence of SOCS-3 using PCR ...	206
4.2.3.1	SOCS-3 coding sequence primer pair specificity check and annealing temperature confirmation	206
4.2.3.2	Secondary screening of SOCS-3 on normal cell lines/tissues and SOCS-3 coding sequence amplification with high fidelity enzyme mix kit ...	206
4.2.4	Extraction of PCR product from agarose gel.....	207
4.2.5	TOPO TA cloning of SOCS-3 coding sequence into the pEF6/V5-His-TOPO plasmid vector and incorporated transgene orientation check	208
4.2.6	Statistical analysis	210
4.3	Results	211
4.3.1	Expression profile of seven SOCS family members (SOCS-1 to SOCS-7) in epithelial and endothelial cell line candidates.....	211
4.3.2	Generation of SOCS-4 knockdown models and SOCS-3 expression models	213
4.3.2.1	Generation of SOCS-4 knockdown models using ribozyme transgene	213
4.3.2.2	Verification of SOCS-4 knockdown by ribozyme transgene in epithelial and endothelial cell models through RT-PCR, q-PCR and western blotting	216
4.3.2.3	Generation of SOCS-4 knockdown cell models by siRNA.....	220
4.3.2.4	Generation of SOCS-3 overexpression HaCaT and HECV models .	235
4.4	Discussion.....	249

Chapter V Functional significance of SOCS-4 knockdown in HaCaT and HECV models and potential downstream mechanisms

5.1	Introduction	255
5.2	Methods and materials	256
5.2.1	<i>In vitro</i> MTT cell adhesion assay	256
5.2.2	<i>In vitro</i> MTT cell proliferation assay.....	256
5.2.3	Kinexus protein array and data analysis	256

5.2.4	Statistical analysis	258
5.3	Results.....	260
5.3.1	ECIS based initial attachment & spreading and migration assay.....	260
5.3.2	<i>In vitro</i> MTT cell adhesion assay	264
5.3.3	<i>In vitro</i> MTT cell proliferation assay.....	266
5.3.4	<i>In vitro</i> cell migration assay (wound healing assay).....	268
5.3.5	Tubule formation assay.....	272
5.3.6	Potential downstream signalling investigation.....	274
5.4	Discussion.....	278
Chapter VI Functional significance of SOCS-3exp on HaCaT and HECV models		
6.1	Introduction	285
6.2	Methods and materials.....	287
6.2.1	<i>In vitro</i> crystal violet matrigel adhesion assay	287
6.2.2	Statistical analysis	288
6.3	Results.....	289
6.3.1	ECIS based initial attachment & spreading assay and migration assay	289
6.3.2	<i>In vitro</i> crystal violet matrigel adhesion assay	293
6.3.3	<i>In vitro</i> MTT cell proliferation assay.....	295
6.3.4	<i>In vitro</i> cell migration assay (wound healing assay).....	297
6.3.5	Tubule formation assay.....	300
6.4	Discussion.....	302
Chapter VII General discussion		
7.1	The clinical significance of SOCS family members in chronic wounds.....	308
7.2	The cellular traits of SOCS-4 in essential cell types involved in the wound healing and its potential mechanism.....	311
7.3	The cellular traits of SOCS-3 in essential cell types involved in the wound healing	317
7.4	Main findings and significance.....	319
7.5	Future work.....	322

List of figures

Chapter I General Introduction

Figure 1-1: Overview of the four overlapping stages during the wound healing process	12
Figure 1-2 The phases of wound healing	13
Figure 1-3: Structure of the eight suppressor of cytokine signalling (SOCS) family members	34
Figure 1-4: Mechanisms of SOCS regulation on cytokine and growth factor signalling	37

Chapter II Methods and materials

Figure 2-1: Agarose gel electrophoresis apparatus	113
Figure 2-2: Diagram of the predicted secondary structure of human SOCS-4 mRNA	114
Figure 2-3: Diagram of hammerhead ribozyme secondary structure	115
Figure 2-4: Diagram of the pEF6/V5-His TOPO® vector feature (from pEF6-His TOPO® TA Expression Kit manual)	116
Figure 2-5: Diagram indicating the principle of the Amplifluor Uniprimer Universal system.	124
Figure 2-6: Diagram of standard curve generation.....	125
Figure 2-7: Acrylamide gel electrophoresis apparatus	131
Figure 2-8: Western blotting protein transfer equipment.....	134
Figure 2-9: Diagram of current flow following cell attachment to the gold electrode	137
Figure 2-10: Electric cell-substrate impedance sensing (ECIS) system and cultureware	140
Figure 2- 11: Diagram of ECIS based cell attachment and spreading assay-resistance trace following inoculation	141
Figure 2-12: Diagram of ECIS based cell migration assay-resistance trace following lethal electroporation (electrical wounding)	142
Figure 2- 13: Diagram of the relationship between cell migration and resistance trace following electrical wounding.....	143
Figure 2-14: EVOS® FL Auto Imaging System installed with EVOS® Onstage Incubator.....	147

Chapter III Expression of the suppressor of cytokine signalling (SOCS) family in human chronic wound tissues: potential implications for SOCS in chronic wound healing

Figure 3-1: The gene expression profile of SOCS-1, -2, -5 and -6 in clinical chronic wound biopsies.....	159
Figure 3-2: The gene expression profile of SOCS-3, -4 and -7 transcript in clinical chronic wound biopsies.....	160
Figure 3-3: Negative control staining in SOCS-1, -2 and -3 primary antibody group	163

Figure 3-4: Negative control staining in SOCS-4, -5 and -6 primary antibody group	164
Figure 3-5: The expression pattern of SOCS-1 at the wound edge of clinical chronic wound biopsies	167
Figure 3-6: The expression pattern of SOCS-1 distal to the wound edge in clinical chronic wound biopsies	169
Figure 3-7: The expression pattern of SOCS-2 at the wound edge in clinical chronic wound biopsies	172
Figure 3-8: The expression pattern of SOCS-2 distal to the wound edge in clinical chronic wound biopsies	174
Figure 3-9: The expression pattern of SOCS-3 at the wound edge in clinical chronic wound biopsies	177
Figure 3-10: The expression pattern of SOCS-3 distal to the wound edge in clinical chronic wound biopsies	179
Figure 3-11: The expression pattern of SOCS-4 at the wound edge in clinical chronic wound biopsies	182
Figure 3-12: The expression pattern of SOCS-4 distal to the wound edge in clinical chronic wound biopsies	184
Figure 3-13: The expression pattern of SOCS-5 at the wound edge in clinical chronic wound biopsies	187
Figure 3-14: The expression pattern of SOCS-5 distal to the wound edge in clinical chronic wound biopsies	189
Figure 3-15: The expression pattern of SOCS-6 at the wound edge in clinical chronic wound biopsies	192
Figure 3-16: The expression pattern of SOCS-6 distal to the wound edge in clinical chronic wound biopsies	194
Figure 3-17: The expression pattern of SOCS-7 in clinical chronic wound biopsies	195

Chapter IV Establishment of SOCS-3 expression and SOCS-4 knockdown models

Figure 4-1: Screening of SOCS-1 to SOCS-7 in HaCaT and HECV cell lines	212
Figure 4-2: Ribozyme transgene synthesis, incorporation and plasmid extraction	215
Figure 4-3: Verification of SOCS-4 knockdown in HaCaT and HECV by RT-PCR, q-PCR and western blotting	219
Figure 4-4: Initial investigation on SOCS-4 knockdown in HaCaT and HECV by siRNA	222
Figure 4-5: Transfect reagent concentration optimisation for HaCaT	225
Figure 4-6: Transfect reagent concentration optimisation for HECV	227
Figure 4-7: Time point evaluation of siRNA generated SOCS-4 knockdown in HaCaT	230
Figure 4-8: Time point evaluation of siRNA generated SOCS-4 knockdown in HECV	231
Figure 4-9: siRNA knockdown verification by western blotting	234

Figure 4-10: Initial screening for SOCS-3 expression on 10 potential cell lines.....	237
Figure 4- 11: SOCS-3 coding sequence synthesis, amplification and purification	239
Figure 4-12: SOCS-3 coding sequence incorporation/orientation analysis	242
Figure 4-13: SOCS-3 coding sequence verification	243
Figure 4-14: Verification of SOCS-3 expression in HaCaT and HECV by RT-PCR and western blotting.....	246
Figure 4-15: Verification of SOCS-3 expression in HaCaT and HECV by q-PCR	248
Chapter V Functional significance of SOCS-4 knockdown in HaCaT and HECV models and potential downstream mechanisms	
Figure 5-1: Diagram of protein microarray plate.....	259
Figure 5-2: ECIS based initial adhesion and migration assay on SOCS-4 mutant HaCaT line	262
Figure 5-3: ECIS based initial adhesion and migration assay on SOCS-4 mutant HECV line.....	263
Figure 5-4: <i>In vitro</i> MTT cell adhesion assay on SOCS-4 mutant HaCaT and HECV lines.....	265
Figure 5-5: <i>In vitro</i> MTT cell proliferation assay on SOCS-4 mutant HaCaT and HECV lines	267
Figure 5-6: <i>In vitro</i> cell migration assay on SOCS-4 mutant HaCaT line.....	270
Figure 5-7: <i>In vitro</i> cell migration assay on SOCS-4 mutant HECV line	271
Figure 5-8: Tubule formation assay on SOCS-4 mutant HECV lines.....	273
Figure 5-9: Kinexus 850 images in comparing proteins from HaCaT pEF6 (bottom, C1) and HaCaT SOCS-4KD (top, C2) cells.....	275
Figure 5-10: Investigation of potential molecular significance in HaCaT SOCS-4 mutant line.....	276
Figure 5-11: Investigation of potential downstream signalling events in HaCaT SOCS-4 mutant line	277
Chapter VI Functional significance of SOCS-3exp on HaCaT and HECV models	
Figure 6-1: ECIS based initial adhesion and migration assay on SOCS-3 mutant HaCaT line	291
Figure 6-2: ECIS based initial adhesion and migration assay on SOCS-3 mutant HECV line.....	292
Figure 6-3: Crystal violet matrigel adhesion assay on SOCS-3 mutant HaCaT and HECV lines	294
Figure 6-4: <i>In vitro</i> MTT cell proliferation assay on SOCS-3 mutant HaCaT and HECV lines by MTT	296
Figure 6-5: <i>In vitro</i> cell migration assay on SOCS-3 mutant HaCaT line.....	298
Figure 6-6: <i>In vitro</i> cell migration assay on SOCS-3 mutant HECV line	299
Figure 6-7: Tubule formation assay on SOCS-3 mutant HECV line	301

List of tables

Chapter I General Introduction

Table 1-1: Four major types of chronic wounds and their potential aetiologies	7
Table 1-2: Key cell types involved in the wound healing process.....	14
Table 1-3 FGF family members involved in wound healing	27
Table 1-4 TGF- β in wound healing	27
Table 1-5 Summary of the association between CIS and key cytokines/growth factors together with the regulatory roles played by CIS.	43
Table 1-6 Summary of the association between SOCS-1 and key cytokines/growth factors together with the regulatory roles played by SOCS-1	46
Table 1-7 Summary of the association between SOCS-2 and key cytokines/growth factors together with the regulatory roles played by SOCS-2	53
Table 1-8 Summary of the association between SOCS-3 and key cytokines/growth factors together with the regulatory roles played by SOCS-3	59
Table 1-9 Summary of the association between SOCS-4 and key cytokines/growth factors together with the regulatory roles played by SOCS-4	74
Table 1-10 Summary of the association between SOCS-5 and key cytokines/growth factors together with the regulatory roles played by SOCS-5	78
Table 1-11 Summary of the association between SOCS-6 and key cytokines/growth factors together with the regulatory roles played by SOCS-6	82
Table 1-12 Summary of the association between SOCS-7 and key cytokines/growth factors together with the regulatory roles played by SOCS-7	85
Table 1-13: SOCS and essential cytokines/growth factors and receptors involved in wound healing (Feng et al., 2016).....	88

Chapter II Methods and materials

Table 2-1: Cell lines used in <i>in vitro</i> study.....	95
Table 2-2: Cells used for SOCS-3 expression profile screening.....	95
Table 2-3: Primers designed and used in this study	97
Table 2-4: Antibodies used for IHC analysis on chronic wound biopsies.....	99
Table 2-5: Antibodies used for verification of SOCS-4 knockdown and SOCS-3 expression	99
Table 2-6: Ingredients for 8% and 10% resolving gel.....	131
Table 2-7: Ingredients for stacking gel.....	131

Chapter III Expression of the suppressor of cytokine signalling (SOCS) family in human chronic wound tissues: potential implications for SOCS in chronic wound healing

Table 3-1: Primers used for detection of SOCS family members and the CK-19 house keeping gene in this study, ACTGAACCTGACCGTACA represents Z sequence	153
Table 3-2: The relationship between expression of SOCS transcript and clinical infection in non-healing chronic wound tissues	161

Chapter IV Establishment of SOCS-3 expression and SOCS-4 knockdown models

Table 4-1: Concentration measured for the ribozyme incorporated plasmids	215
Table 4-2: Concentration measured for the purified SOCS-3 coding sequence product.....	240
Table 4-3: Concentration measured for the SOCS-3 coding sequence incorporated plasmids	242

Abbreviations

ABC: avidin-biotin complex
AC: allergic conjunctivitis
AhR : aryl hydrocarbon receptor
Akt: V-Akt Murine Thymoma Viral Oncogene
Ang: angiopoietin
AP-1: activator protein-1
APS: ammonium persulphate
BMMC: bone marrow derived mast cells
bp: base pair
BSA: bovine serum albumin
bZIP: basic region-leucine zipper
cAMP: cyclic adenosine monophosphate
CCD: coiled-coiled domain
cDNA: complementary deoxyribonucleic acid
C/EBP- β : CCAAT/enhancer-binding protein- β
CIS: Src-homology 2-containing protein
CK-19: cytokeratin-19
c-KIT: KIT Proto-Oncogene Receptor Tyrosine Kinase
CLC: cardiotrophin like cytokine
cm: centimetre
CO₂: carbon dioxide
ConA: concanavalin A
CSF: colony-stimulating factor
CXCL-12: C-X-C Motif chemokine Ligand-12
CXCR-4: C-X-C chemokine receptor- 4
DBD: DNA-binding domain
DCs: dendritic cells
DEPC: diethyl pyrocarbonate
DMEM: Dulbecco's Modified Eagle's Medium
DMSO: dimethylsulphoxide
DNA: deoxyribonucleic acid
DPX: Distyrene Plasticizer Xylene
Duox: dual oxidase
eB: elongin B
eC: elongin C
ECIS: electric cell-substrate impedance sensing
ECM: extracellular matrix
EDTA: ethylene diaminetetraacetic acid
EGF: epidermal growth factor
EGFR: epidermal growth factor receptor
EPO: erythropoietin
ERK: extracellular signal regulated kinase
ESS: extended SH2 sequence
FAK: focal adhesion kinase
FCS: fetal calf serum
FERM: Four-point-one, Ezrin, Radixin, Moesin
FGF: fibroblast growth factor
FLT-3: fms-like tyrosine kinase 3
FLT-3-ITD: internal tandem duplication mutated fms-like tyrosine kinase 3

g: gram
 GAPDH: glyceraldehyde-3-phosphate dehydrogenase
 G-CSF: granulocyte colony-stimulating factor
 G-CSFR: G- granulocyte colony-stimulating factor receptor
 GH: growth hormone
 GHR: growth hormone receptor
 GM-CSF: granulocyte-macrophage colony-stimulating factor
 H₂O₂: hydrogen peroxide
 HCl: hydrochloric acid
 HDMEC: human dermal microvascular endothelial cells
 HGF: hepatocyte growth factor
 HGFR: hepatocyte growth factor receptor
 HIF: hypoxia inducible factor
 HRP: horseradish peroxidase
 HuR: human antigen R
 Hz: hertz
 IEC: intestinal epithelial cell
 IFN- γ : interferon- γ
 IGF-I: insulin-like growth factor-I
 IGF-IR: insulin-like growth factor-I receptor
 IHC: *Immunohistochemistry*
 IKK β : inhibitor of kappa light polypeptide gene enhancer in B-cells, kinase beta
 IL: interleukin
 IR: insulin receptor
 IRS: insulin receptor substrate
 JAB: Janus kinase-binding protein
 JAK: Janus kinase
 JNK: Jun-terminal kinase
 K6: keratin-6
 KD: knockdown
 kDa: kilo-dalton
 KGF: keratinocyte growth factor
 KIR: kinase inhibitory region
 L: litre
 LIF: leukemia Inhibitory Factor
 LIFR: leukaemia inhibitory factor receptor
 LPS: lipopolysaccharide
 LXAR: lipoxin A₄ receptor
 mA: milli-amp
 MAPPIT: mammalian protein-protein interaction trap
 MDH-1: malate Dehydrogenase-1
 mg: milligram
 ml: millilitre
 mM: millimolar
 MMP-2: matrix metalloproteinase-2
 MPD: myeloproliferative disorder
 MTT: thiazolyl blue tetrazolium bromide
 NAP: Nck-, Ash- and phospholipase C gamma-binding protein
 NFAT: nuclear factor of activated T-cells
 NF- κ B: nuclear factor-kappa B
 ng: nano-gram

NH2: amino-terminal domain
 NHE-1: Na⁺/H⁺-exchanger-1
 NK: natural killer
 NKT: natural killer T cell
 nm: nanometre
 Nrf2: NF-E2-related factor 2
 oxLDL: oxidized low-density lipoprotein
 p38 MAPK: protein kinase p38
 PCBP-1: Poly(RC) Binding Protein-1
 PCR: polymerase chain reaction
 PDGF: platelet-derived growth factor
 pERK: phospho extracellular signal regulated kinase
 PI3K: phosphoinositide 3-kinase
 PIAS: protein inhibitors against STATs
 p-NFAT: phospho-nuclear translocation of nuclear factor of activated T-cells
 POMC: pro-opiomelanocortin
 p-Pyk-2: phosphorylated proline-rich tyrosine kinase 2
 PVDF: polyvinylidene difluoride
 q-PCR: real time quantitative polymerase chain reaction
 Ras: rat sarcoma
 RelA: transcription factor p65
 RNA: ribonucleic acid
 RNase: ribonuclease
 ROS: reactive oxygen species
 rpm: revolutions per minute
 RTK: receptor tyrosine kinase
 RT-PCR: reverse transcription polymerase chain reaction
 SCF: stem cell factor
 SD: standard deviation
 SDS: sodium dodecyl sulphate
 SDS-PAGE: sodium dodecyl sulphate polyacrylamide gel electrophoresis
 SFM: serum free medium
 SH2: Src-homology 2
 SHP: SH2-containing phosphatase
 siRNA: small interfering ribonucleic acid
 SLE: systemic lupus erythematosus
 SMAD-2: mothers against decapentaplegic homology-2
 SOCS: suppressor of cytokine signalling
 SREBP: sterol regulatory element-binding protein
 SSI-1: STAT-induced STAT inhibitor-1
 STAT-3: signalling transducer and activators of transcription-3
 TAD: transcriptional activation domain
 TBE: Tris-boric-acid- ethylene diaminetetraacetic acid
 TBS: Tris buffered saline
 TEMED: Tetramethylethylenediamine
 TGF-β: transforming growth factor beta
 TGFβI: transforming growth factor-beta-induced protein
 Tie-2: tyrosine kinase with immunoglobulin-like and EGF-like domains-2
 TIME: general management guidelines
 TLR: Toll-like receptor
 TNF-α: tumour necrosis factor-alpha

TrkA: Tropomyosin-related kinase A
TSLP: thymic stromal lymphopoietin
V: volt
VEGF: vascular endothelial growth factor
VSMCs: vascular smooth muscle cells
W: watt
 α -SMA: alpha-smooth muscle actin
 μ A: micro-amp
 μ g: microgram
 μ l: microlitre
 $^{\circ}$ C: Celsius

Chapter I

General Introduction

1.1 History and background of wound healing

1.1.1 The emergence and development of wound healing treatments

The history of open wound treatment probably dates back to the era when ancient human civilisation began on earth. According to documented evidence, ancient Egyptian and Greeks had their own method to remove pus and to encourage wound healing (Broughton et al., 2006a). However, it was not until the mid-nineteenth century that people began to realise the concept of infection following the first demonstrated use of antiseptics in surgery and the treatment of wounds with dressings. In 1876, the first antiseptic dressing, soaking lint and gauze in carbolic acid, was developed and later on was improved as a nonadherent dressing called 'tulle gras'. It was commonly used in France and became extensively used worldwide in World War I. Silver foil dressings for wounds was also introduced during the mid- to late 1800s, and were extensively used in World War II, later being listed in the *Physician's Desk Reference* in 1955. Additionally, the outbreak of World War II introduced the impetus to develop new and more innovative surgical dressings, which became known as Kerlix sponges and bandages. In the 1880's, several years after the emergence of the antiseptic dressing, skin cleansing was stressed to be of importance in wound care, and the terminology 'debridement' was raised by a Russian military surgeon who considerably reduced the mortality rate of the patients he treated. The modern practice of debridement emerged during World War I in order to cope with contamination from the battlefield (Broughton et al., 2006a). In addition, debridement was defined as the elimination of nonviable material, foreign bodies and poorly healing tissue from a wound (Steed, 2004). More recently, a systematic and relatively comprehensive guideline was proposed by a wound care consensus group in 2003 to address wound management (Schultz et al., 2003),

and is advocated by many medical professionals as well as being of benefit to wound healing management until present day (Powers et al., 2016).

1.1.2 The necessity and importance of study on wound healing

The basic function of skin is to provide a protective barrier against the environment. Wound healing is a dynamic and interactive process which is immediately activated by the damage of skin upon injury. It is one of the important biological process which helps restore the barrier function of skin and regain skin homeostasis after injury. The primary aims of wound treatment are to minimise the healing time and to regenerate scar free tissue without compromising normal skin function.

The process of wound healing is highly complex and requires substantial interaction and co-ordination between different cell types to heal the wound in an orderly and timely manner. Regarding the normal healing process, haemostasis initiates immediately after injury. Inflammatory phase occurs at the same time and normally last for 4 to 6 days (Schreml et al., 2010). Hours following injury, proliferation and re-epithelialisation consisting of epithelialisation, granulation tissue formation and angiogenesis overlaps with inflammation and gradually becomes predominant. This stage normally lasts for approximately a month. Finally, the maturation and remodelling phase begins around day 21 after wounding and continues more than a year (Bryant and Nix, 2015). Issues arising in the co-ordination or regulation of the wound healing process can have severe consequences, in some cases impairing the capacity to complete the process, resulting in wound chronicity.

1.1.2.1 Chronic wounds

Chronic wounds are defined as wounds that fail to follow an orderly and timely reparative process (normal healing process) which in turn disrupts the anatomic and functional integrity of the wound site (Lazarus et al., 1994). Chronic wounds generally are caused by vascular compromise, prolonged inflammation or repetitive insults to the tissues (Bryant and Nix, 2015). The majority of chronic wounds are categorised into three subtypes: pressure ulcers, arterial and venous ulcers and diabetic ulcers, which, despite having diverse aetiologies (Mustoe et al., 2006) share a similar characteristic, namely prolonged inflammation (Powers et al., 2016). In addition, the most common type of chronic wound is lower extremity ulcer, of which 98% are primarily of vascular or diabetic nature (Werdin et al., 2009). To date, general management guidelines concentrating on tissue, infection/inflammation, moisture balance and edge of wound (leading to the TIME acronym), which are critical barriers to wound healing, have been established by the Wound Healing Society in order to address principal elements for the treatment of chronic wounds regardless of the wound type (Powers et al., 2016). Moreover, it has been hypothesised that local tissue hypoxia, bacterial colonisation of the wound, repetitive ischemia-reperfusion injury and an altered cellular and systemic stress response in the aged patient are the four major factors of chronic wound pathogenesis. However, the complexity of chronic wounds has been underestimated due to the limited success of treatment and the lack of successful clinical trials (Mustoe et al., 2006). It has been suggested that the Inflammation stage is the driving force in chronic, non-healing wounds and as such, pro-inflammatory regulators may possess diagnostic and/or prognostic value, in addition to potential as future therapeutic targets (Behm et al., 2012). Therefore, a comprehensive and systematic chronic wound healing model would be beneficial to verify this hypothesis as well as unveiling novel therapeutic

strategies (Menke et al., 2007). However, this requires a better understanding of the basic cellular and molecular traits in the wound healing process than is currently known.

1.1.2.2 Classification of chronic wounds

As primarily mentioned, chronic wounds are primarily categorised into venous, arterial, diabetic and pressure ulcers based on their distinct aetiologies (Table 1-1).

Venous ulcers, which exhibit high recurrence rates, are considered to be the most common type of leg ulcer, comprising an estimated 70-90% of total cases (Snyder, 2005). Venous stasis ulceration is considered to be caused by venous hypertension. A persistently high pressure within the deep vein is attributed to dysfunctional and incompetent valves in the lower extremity (Moreo, 2005). Trauma and a deep vein thrombosis may potentially result in valve damage, subsequently leading to secondary venous hypertension (Valencia et al., 2001). The precise pathophysiology behind venous ulceration still remains to be elucidated, however, such chronic ulcers are hypothesised to be the result of extravasation of red and white blood cells and other macromolecules from the blood vessel into the perivascular tissues caused by the elevated pressure, leading to epithelial cell damage and ulceration (Gohel and Poskitt, 2009).

Arterial ulceration is caused by a reduced arterial blood supply to the lower limb, and is commonly seen in patients with atherosclerotic disease of the medium and large sized arteries (Grey et al., 2006). Inadequately supplied blood products and oxygen subsequently result in local ischemia in the lower extremity, thus, local incidental injuries are unlikely to follow the normal healing process, leading to chronic non-healing wound.

Foot ulceration occurs in 15% of diabetic patients and lead to 84% of lower extremity amputations (Brem and Tomic-Canic, 2007). Ulceration in diabetic

patients generally contributes to non-healing and chronicity and are found to be related to almost all the key components and phases in the wound healing process. Dysregulation of key cell type function, altered cytokine and growth factor production, impaired angiogenic response, imbalanced extracellular matrix (ECM) reorganisation by abnormal collagen accumulation and collagenases activity are all potential pathophysiologic factors leading to diabetic foot ulceration (Galkowska et al., 2006, Goren et al., 2006b, Falanga, 2005, Galiano et al., 2004, Maruyama et al., 2007, Gibran et al., 2002, Lobmann et al., 2002).

Pressure ulcers, in general, occur in patients whose movement ability is severely impaired, such as paralysed patients and coma patients (Moreo, 2005). Patients with spinal cord injuries and the elderly are the two groups at high risk of developing pressure ulcers. These ulcerations are normally found at the sacrum, heels and scapulae as well as positions which experience sustained pressure. Prolonged pressure consequently results in a lack of blood supply, contributing to ischemia and tissue necrosis as well as non-healing ulceration (Yarkony, 1994).

Table 1-1: Four major types of chronic wounds and their potential aetiologies

Chronic ulceration	Aetiology	Potential risk factors
Venous ulcers	Valve failure causes blood reflux, resulting in increased pressures within the deep vein and subsequent venous hypertension which is a direct cause of venous ulceration	Loss of valvular competence
		Calf muscle dysfunction
Arterial ulcers	Critical and acute limb ischemia which cause consistent arterial insufficiency, impaired perfusion and consequently severe tissue ischemia may lead to arterial ulceration	Diabetes
		Tobacco
		Atherosclerotic disease
		Thromboangiitis disease
		Sickle cell disease
Diabetic ulcers	Decreased sympathetic innervation results in a shunting away of blood from the capillary which leads to ischemia and subsequent non-healing ulceration	Peripheral neuropathy
	Inadequate oxygenation and perfusion of tissues caused by peripheral arterial disease impair the healing of ulceration	Peripheral arterial disease
Pressure ulcers	Persistent pressure creates tissue ischemia and edema through capillary damage, and subsequently worsen tissue hypoxia and result in pressure ulceration	Ischemia caused by capillary occlusion
		Reperfusion injury
		Impaired lymphatic function
		Unrelieved pressure

Key reference: (Bryant and Nix, 2015)

1.1.2.3 The impact of chronic wounds

Non-healing wounds in the lower extremities represent major clinical and surgical challenges globally due to the significant cost on healthcare resources and medical professionals. Regarding medical costs, chronic, non-healing wounds are a significant economic burden on public healthcare. According to an investigation into the total (direct and indirect) costs of 22 leading skin disease categories, the expenditure on skin ulcers and wounds in the United States alone was approximately \$12 billion in 2004. Furthermore, regarding direct costs only, skin ulcers and wounds were identified as being the most costly of the 22 skin diseases analysed, accounting for \$9.7 billion of the \$29.1 billion total annual spend (Bickers et al., 2006). An audit covering the population of approximately 590,000 carried out in 2005 indicated that the estimated cost of wound care in 2005-2006 was £15 million to £18 million, accounting for 2%-3% of local NHS healthcare budget (Drew et al., 2007). Moreover, according to a publication on 2008, the estimated annual cost of venous leg ulcers, pressure ulcers and diabetic foot ulcers are £168-198 million, £1.8-2.6 billion and £300 million respectively, suggesting a significant burden to the NHS healthcare budget caused by the diagnosis and treatment of chronic wounds (Posnett and Franks, 2008). Another report indicated that the economic costs associated with diabetic foot care are so considerable that it is even comparable to the expenditure on the treatment of breast and colorectal cancers (Barshes et al., 2013). In addition to the heavy burden on medical costs, due to the high recurrence rate of chronic ulcers, such as venous ulcers (Snyder, 2005), many recovered patients are more likely to go back to hospital and seek medical assistance on more than one occasion. This requires the continuous reoccupation of medical professional resources. Therefore, the establishment of a robust system of multidisciplinary care is of importance to the management of chronic diseases, and this requires an array of

healthcare specialists collaborating together to provide an appropriate primary prevention, and to reduce the delayed recognition as well as improving the management efficiency (Barshes et al., 2013).

Regarding patient impact, chronic non-healing wounds considerably reduce quality of life. A number of studies have demonstrated that chronic ulcers correlate with reduced overall quality of life (Goodridge et al., 2006, Jaksa and Mahoney, 2010, Shanmugam et al., 2010). Diabetic foot ulcers are responsible for the highest proportion of non-traumatic amputations in the United States (Barshes et al., 2013, Snyder, 2005) and compared with other complications associated with diabetes, amputation has been shown to have the greatest negative effect on a person's quality of life (Clarke *et al.*, 2002, Laiteerapong *et al.*, 2011). More than 50% of diabetic foot ulcer patients also suffer from peripheral arterial disease, which may further affect the ability of the ulcer to heal. It is noteworthy that patients with both a diabetic foot ulcer and peripheral arterial disease have a higher risk of cardiovascular morbidity and mortality. However, peripheral arterial disease is salvageable by revascularisation, with limb salvage rates increasing to 85% and more than 60% of ulcers healing within 1 year (Schaper *et al.*, 2012). In addition to amputation, pain is another factor that causes chronic ulcer patients distress and restrains their lower extremity function. In a multinational study of over 2,000 patients, pain was chosen to be the most annoying symptom experienced by chronic ulcer patients rather than the other given choices, such as impaired mobility, difficulties in bathing, leakage, odour and dressing or bandage slippage (Price et al., 2008).

1.1.2.4 Factors leading to non-healing wound and chronic wound management

It has been discovered that the wound healing process can become trapped in either the inflammation or proliferation and re-epithelialisation phases (Bello and Phillips, 2000). Although non-chronic wounds have different aetiologies, all wound types share similar traits to each other, including increased inflammation, continuous extracellular matrix (ECM) degradation, fibroblast, keratinocyte and endothelial cell senescence as well as epidermal arrest, which are partially attributed to the dysregulated production of cytokines and growth factors as well as the imbalanced secretion of proteolytic proteins and their inhibitors (Harding et al., 2002, Telgenhoff and Shroot, 2005). Furthermore, studies examining components present in wound fluids demonstrated that compared to normal acute wounds, chronic wound fluid consists of high levels of proteases which could impair the proliferation of keratinocytes, fibroblasts and endothelial cells, all key cell types involved in the proliferation and re-epithelialisation phase (Bucalo et al., 1993, Trengove et al., 1999, Raffetto et al., 2001, Mendez et al., 1999). It has been found that upregulated inflammatory cytokines contribute to prolonged inflammation, whereas increased proteases, especially matrix metalloproteinases (MMPs) and elastase, and reduced protease inhibitors result in excessive degradation of the ECM (Yager and Nwomeh, 1999, Harding et al., 2002, Lobmann et al., 2002, Ladwig et al., 2002). In addition, dysregulation and relocalisation of growth factor expression, including platelet derived growth factor (PDGF), fibroblast growth factor (FGF)-2, epithelial growth factor (EGF) and transforming growth factor (TGF)- β (Higley et al., 1995), potentially leads to suppressed proliferation, migration and senescence of keratinocytes, fibroblasts and endothelial cells.

Wound bed preparation, removing the barriers to healing and providing active measures that stimulate endogenous healing as well as analysing wound conditions, has been recognised as the global management method and a prerequisite to facilitate the effectiveness of other therapeutic measures (Schultz et al., 2004). Therefore, systematic protocols and treatment guidelines used for the preparation of an adequate wound bed and the assessment of overall health status of the patient are considered to be of the greatest importance (Falanga, 2000). In 2003, a stepwise cyclical approach of 'Wound Bed Preparation', consisting of four components (TIME), was established to standardise the process used by clinicians to assess the status of the wound and in deciding a plan for further intervention (Schultz et al., 2003, Schultz et al., 2004). The establishment of the TIME clinical tool is not only of benefit to the management of chronic wounds, but to the plastic, burns injury and trauma wounds that potentially fail to follow the general healing process. Moreover, it provides clinicians and medical professionals a systematic and standard protocol to evaluate emerging technologies in wound management and assessment (Schultz et al., 2004).

1.2 Cellular and molecular biology of wound repair

In order to seek more cost effective and efficient therapeutic methods and to improve current chronic wound treatments, a better understanding of the molecular and cellular biology behind the chronic wound healing process is of great importance. The normal acute wound healing process has become clearer in terms of key cell types (Table 1-2), regulatory cytokines and growth factors and the involvement of a number of signalling pathways. The wound healing process consists of four highly-orchestrated overlapping stages known as 1) haemostasis, 2) inflammation, 3) proliferation and reepithelialisation, and 4) tissue remodelling

(Behm *et al.*, 2012) (Figure 1-1, Figure 1-2). Dysregulation or prolongation of one or more phases may lead to either delayed healing or non-closure of the wound.

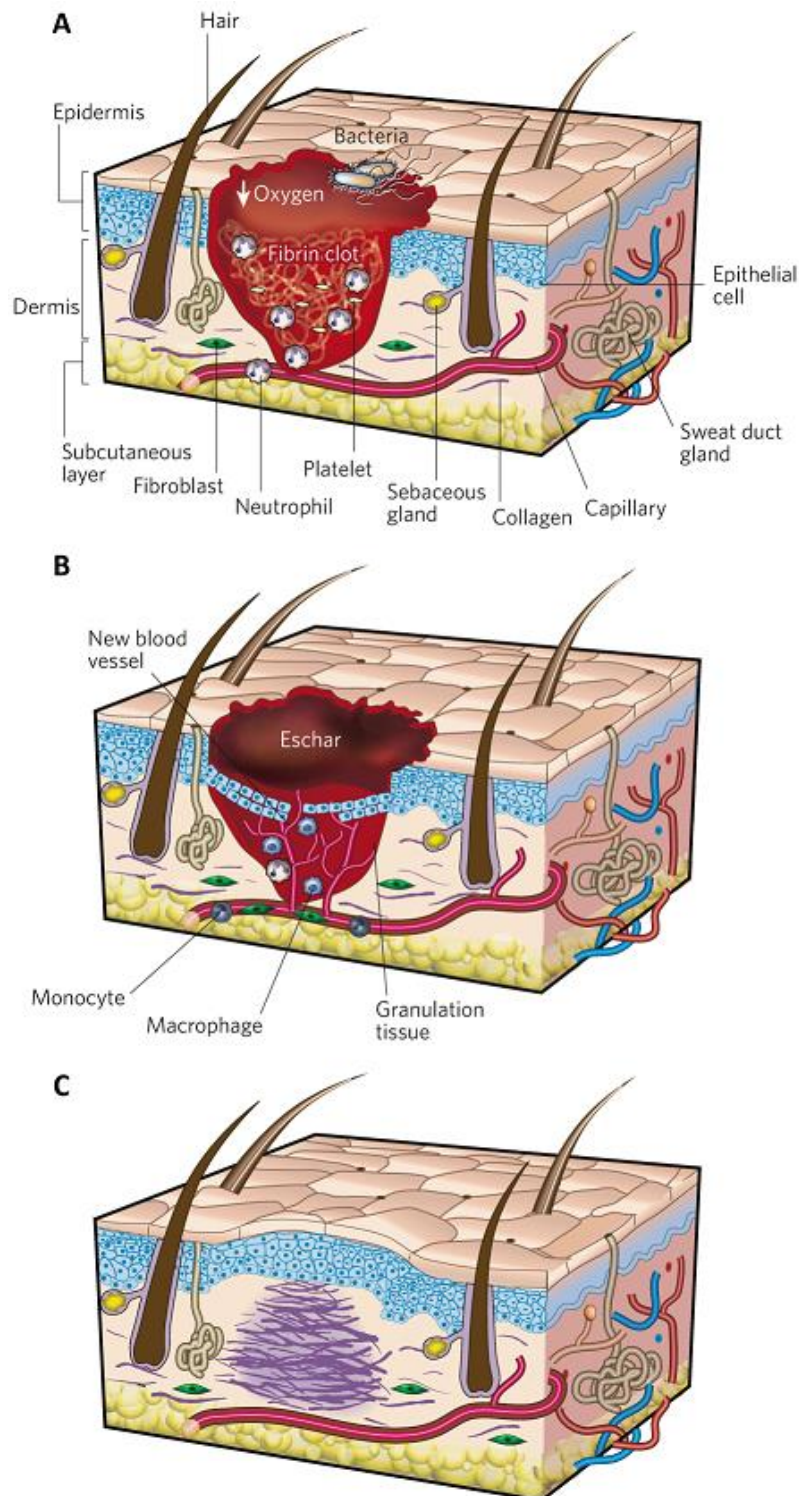


Figure 1-1: Overview of the four overlapping stages during the wound healing process

A. Haemostasis and Inflammation stage; **B.** Proliferation and re-epithelialisation stage; **C.** Tissue remodelling stage. (Gurtner *et al.*, 2008)

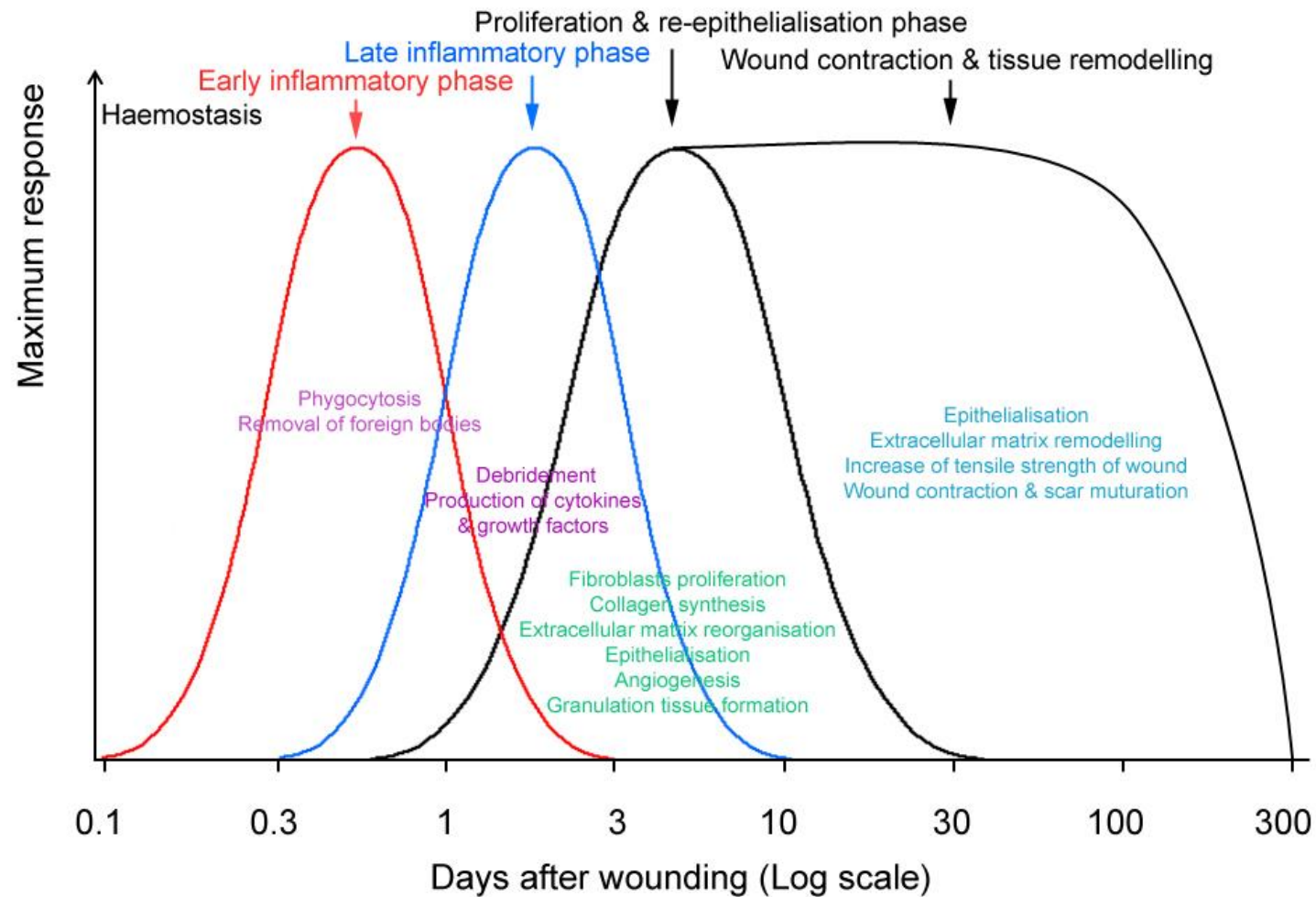


Figure 1-2 The phases of wound healing

Neutrophils are the first cell type attracted to the wound area in the early inflammatory phase, whereas macrophages primarily exert function in the late inflammatory phase; fibroblasts, keratinocytes and endothelial cells are recruited into the wound site and their behaviours are primarily involved in the last two phases of the wound healing process.

Table 1-2 Key cell types involved in the wound healing process

Cell type	Wound healing phase	Functions
Platelet	Haemostasis	Aggregate to plug damaged blood vessel, release cytokines; chemokines and growth factors; initiate entire wound healing cascade
Neutrophil	Inflammation	Removes bacteria and foreign debris by phagocytosis; release growth factors to attract additional leucocytes
Monocyte/macrophage	Inflammation	Debride tissue through phagocytosis and digestion of pathogenic organisms, tissue debris and neutrophils; release growth factors required for angiogenesis, granulation tissue formation and connective tissue formation
T lymphocyte	Inflammation	Remove viral organisms and foreign cells; produce additional cytokines and growth factors necessary for wound healing
Keratinocyte	Proliferation and re-epithelialisation	Migrate and proliferate and differentiate to re-establish epidermal thickness and function; synthesise basement membrane; secrete growth factors required for wound healing
Fibroblast	Proliferation and re-epithelialisation, tissue remodelling	Proliferate, migrate and infiltrate to provisional matrix; synthesise ECM components to promote new connective tissue formation; produce cytokines and growth factors benefit for neovascularisation; transform to myofibroblast and provide tractional forces for wound contraction; synthesis collagens and degrade provisional ECM components for tissue remodelling
Endothelial cell	Proliferation and re-epithelialisation, tissue remodelling	Proliferate, infiltrate to the provisional matrix; establish network of new vessels to achieve neoangiogenesis; reconstruct and remodel newly formed vascular

Key references: (Bryant and Nix, 2015, Clark, 1996)

1.2.1 Haemostasis

Upon injury, blood vessels are damaged resulting in the extravasation of blood constituents. Before healing can commence, haemostasis must be achieved at the wound to minimise blood loss. Blood coagulation and platelet aggregation are immediately initialised to form a cross-linked fibrin-rich clot to plug the damaged blood vessels and thus to achieve haemostasis. This fibrin clot contains adequate molecules such as fibronectin, vitronectin, von Willebrand factor, thrombospondin, plasminogen, plasminogen activator, plasminogen activator inhibitor, thrombin and growth factors, which are required to form a reservoir and scaffold for cell recruitment, migration and proliferation (Clark, 1996). Following haemostasis, numerous mediators and chemotactic factors, such as PDGF, EGF and TGF- β , are secreted by platelets and by damaged cells at the wound site in order to recruit inflammatory cells for further debridement (Darby et al., 2014). The recruited monocytes and fibroblasts migrate over the matrix scaffold aided by the interaction between their integrin receptors and the components present in the provisional clot matrix, such as fibrin, fibronectin and vitronectin. Blood clotting also contributes to the inflammatory response through the attraction of neutrophils and monocytes via secreted mediators from platelets and injured parenchymal cells as well as by stimulating the release of vasoactive mediators from mast cells and granule constituents from neutrophils and macrophages (Clark, 1996).

1.2.2 Inflammation phase

Inflammation starts minutes after injury occurs and generally lasts between 4 and 6 days in the physiological wound healing process (Schreml *et al.*, 2010). The normal function of inflammation in an acute wound is to 1) prepare the wound

bed; 2) remove necrotic tissue, bacteria contaminants, dead cell debris; and 3) recruit and activate fibroblasts at the wound site (Menke et al., 2007). During the inflammatory stage, neutrophils are the first inflammatory cells infiltrating into the wound area, reaching peak numbers at around 24 to 48 hours following injury (Park and Barbul, 2004). After being activated by a variety of chemotactic factors, neutrophils release collagenase molecules to digest the blood vessel basement membrane and infiltrate from the blood vessel to the provisional matrix (Clark, 1996). Upon arrival, neutrophils remove bacteria and foreign material through phagocytosis and subsequent release of enzyme and oxygen radicals. However, tight regulation of the quantity of neutrophils and duration of the infiltration is crucial as they also possess the ability to kill healthy host cells in addition to their major function in removing infectious agents, which may explain the persistent tissue-destroying nature of chronic wounds (Martin and Leibovich, 2005). Neutrophil infiltration ceases within a few days if no substantial contamination occurs and the neutrophils undergo senescence and are subsequently phagocytosed by tissue macrophages (Newman et al., 1982). Whether neutrophils infiltrate resolve or persist, monocytes are subsequently attracted from the circulatory system, through similar mechanisms to neutrophil recruitment, into the wound site by selective monocyte chemoattractants. The increasing accumulation of monocytes differentiate into activated macrophages and then gradually replace the neutrophils as the prominent cell type involved in the removal and degradation of injured tissue debris, apoptotic neutrophils, microorganisms and fragments of ECM via phagocytosis. Importantly, monocytes also act as a source of cytokines and growth factors that subsequently benefit angiogenesis, fibroplasia and ECM reorganisation (Clark, 1996, Singer and Clark, 1999).

1.2.3 Proliferation and re-epithelialisation phase

The start of re-epithelialisation lags hours behind injury and initiate soon after the clot formation (Stenn and Depalma, 1988). Re-epithelialisation involves multiple processes including the migration and proliferation of epidermal keratinocytes, the stratification and differentiation of the neoepithelium, the reorganisation of provisional wound bed matrix (granulation tissue formation), angiogenesis and reconstruction of the basement membrane (Clark, 1996).

1.2.3.1 Epithelialisation

Upon the initiation of epithelialisation, keratinocytes at the wound periphery and damaged epidermal appendages throughout the wound bed alter their integrin and cell adhesion molecule expression profile to reduce adhesion to both neighbouring cells and to the basement membrane, thus enabling their migration to the denuded area. In addition to cell-cell junction (desmosomes) and cell-basement membrane junctions (hemi-desmosomes) being retracted from the plasma membrane to a perinuclear localisation following injury, keratinocytes dramatically change their morphology before migrating, becoming flat and elongated while 'crawling' along the wound bed (Odland and Ross, 1968, Stenn and Depalma, 1988). Since the intact basement membrane is damaged by wounding, provisional matrix, primarily consisting of fibronectin, fibrin and vitronectin, acts as a scaffold and facilitates keratinocyte migration (O'Toole, 2001). The migratory keratinocytes utilise the provisional matrix in the newly formed wound bed to crawl over the interface between moist viable tissue and the protective blood clot scab in order to restore the integrity of epithelium (Clark, 1996). One to two days following injury, neighbouring keratinocytes at the

migratory leading front keratinocytes undergo proliferation to ensure sufficient cells are available for the formation of the epithelial barrier (Martin and Leibovich, 2005, Pastar et al., 2014).

It has been documented that there are various factors that can regulate epithelialisation. Migratory keratinocyte synthesised collagenases have been identified as one of the key factors. For instance, keratinocyte synthesised collagenases degrade types I and IV collagens and enable their migration over the dermal collagen (Woodley et al., 1986). In addition, the connective tissue matrix has also been demonstrated to be of importance to the biological behaviour of epithelial cells. Fibronectin and vitronectin containing an Arg-Gly-D-Asp (RGD) sequence have been demonstrated to facilitate the migration of keratinocyte through the association of $\alpha 5\beta 1$ and $\alpha v\beta 5$ integrin cell receptor, whereas collagen facilitates keratinocyte migration via $\alpha 2\beta 1$ (Clark, 1996). In contrast, laminin, one of the components in connective tissue, uniquely inhibits keratinocytes migration acting as a 'brake' for keratinocyte motility (Woodley et al., 1988). Evidence has shown that fibronectin is degraded into smaller molecular species in non-healing chronic wounds and these can be identified in wound fluid, whereas fibronectin remains in an intact form in normal acute healing wounds (Wysocki and Grinnell, 1990). Therefore, the integrity of fibronectin in provisional matrix and the expression profile of $\alpha 5\beta 1$ integrin in the migratory keratinocytes may potentially predict the healing result. Furthermore, soluble factors, such as interleukin (IL)-1, TGF- α , TGF- β and EGF were also found to promote epithelialisation in both an integrin dependent and independent manner (Brown et al., 1989, Mustoe et al., 1987, Chen et al., 1993, Chen et al., 1995).

1.2.3.2 Granulation tissue formation

Granulation tissue formation, also known as new stroma formation, begins approximately 4 days after injury to re-establish the dermal integrity. Newly formed stroma consists of macrophages, new blood vessels, fibroblasts and loose connective tissue (Clark, 1996). The macrophages recruited into the provisional matrix in earlier phases produce cytokines and growth factors that facilitate fibroplasia and ECM reorganisation by fibroblasts as well as neovascularisation by endothelial cells. After infiltrating into the wound space via the interaction between members of the cell membrane integrin superfamily and the provisional matrix components, dermal fibroblasts gradually move to a profibrotic phenotype and switch their function to collagen synthesis (Welch et al., 1990, Clark, 1996). TGF- β has been demonstrated to be associated with collagen synthesis since it is found highly expressed in profibrotic fibroblasts (Clark et al., 1995). Once an abundant collagen deposition is achieved in the wound area, fibroblasts cease collagen synthesis and undergo programmed cell death, starting approximately 10 days post injury (Williams, 1991). Although the exact mechanism or signals leading to the apoptosis of fibroblasts remains to be elucidated, Interferon (IFN)- γ and collagen matrix has been documented to suppress collagen synthesis by fibroblasts (Duncan and Berman, 1985, Granstein et al., 1987, Grinnell, 1994, Clark et al., 1995).

1.2.3.3 Angiogenesis

In response to a variety of chemotactic and angiogenic signals produced during the inflammatory phase, angiogenesis (the formation of new blood vessels) occurs as a result of endothelial cell migration and proliferation. Microvascular endothelial cells are considered to be the principal parenchymal cells involved in

wound angiogenesis due to their ability to respond to injury through the degradation of the basement membrane, proliferation, migration into the stroma, and the formation of new blood vessels (Marx et al., 1994, Li et al., 2003). After sensing angiogenic signal, endothelial cells from the side of the venule closest to the angiogenic stimuli begin to synthesise and release collagenases followed by degradation of the basement membrane, enabling their migration and penetration through the fragmented basement membrane via projecting pseudopodia. Subsequently, the entire endothelial cell migrates into the perivascular area and the remaining parent vessel initiate proliferation to provide a continuing source of endothelial cells for angiogenesis (Clark, 1996). Being pushed by the proliferative behaviour and pulled by the attractive signals, the migrating endothelial cells start to create new blood vessel sprouts and eventually form new capillary networks (Tonnesen et al., 2000). Angiogenesis leads to the development of new capillary networks and helps restore vascular perfusion, subsequently facilitating the delivery of nutrients and oxygen required to sustain cell metabolism. Thus, the restoration of vascular perfusion by angiogenesis potentially relieves the hypoxic microenvironment of a lesion and hence, any defect capable of interfering with angiogenesis may also lead to delayed or impaired wound healing. Furthermore, insufficient vascularisation, which has been shown to be related to reduced re-epithelialisation and deficient granulation formation can potentially result in the development of chronic, non-healing wounds (Johnson and Wilgus, 2014). Therefore, ensuring the normal function of angiogenesis is essential for the wound healing process and, as such, we may be able to improve wound healing by regulating the behaviour of endothelial cells and the process of angiogenesis (Darby et al., 2014, Senger and Davis, 2011, Folkman and Shing, 1992, Tonnesen et al., 2000).

1.2.4 Tissue remodelling phase

The final stage of wound healing, tissue remodelling, begins 2 to 3 weeks after injury, continuing for a period of several months to a year, potentially even extending to two or three years (Gurtner et al., 2008). At the initiation of tissue remodelling, fibroblasts switch into a myofibroblast phenotype characterised by rich actin-containing microfilaments along the plasma membrane. Such processes promote the establishment of the cell-cell and cell-matrix linkages, contributing to the biomechanics of ECM contraction (Welch et al., 1990). Over the lengthy period of the wound remodelling phase the majority of cell types participating in the former stages, such as endothelial cells, fibroblasts and macrophages, either undergo apoptosis or exit the wound site (Gurtner et al., 2008). As the matrix matures, the early stage components of ECM, such as hyaluronic acid (HA) and fibronectin, which provide a provisional substratum for the infiltrating cells, are gradually replaced by proteoglycans and collagens in order to increase the resilience and strength of the wound. Collagen remodelling also occurs during the transition of granulation tissue to a mature scar, and this process is tightly regulated by a variety of collagenases produced by granulocytes, macrophages, epidermal cells and fibroblasts (Clark, 1996). Normally after 6 months, the newly formed granulation tissue is strengthened by reorganisation of the major type III collagen to the predominant type I collagen (Gurtner et al., 2008). In this stage, granulation tissue gradually converts into mature scar tissue by collagen catabolism (Werner and Grose, 2003). In general, the maturation of the neoepithelium, fibroplasia and neovascularature as well as the reconstitution of the extracellular matrix at wound margin occurs in the same time as the granulation tissue invasion to the centre of the wound space (Kurkinen et al., 1980). Tissue remodelling begins at the wound margin once such an area is readily

covered by neoepidermis and filled with granulation tissue. Meanwhile, this process is accompanied by the newly formed granulation tissue growing toward the centre of the wound site. The composition and structure of the extracellular matrix at the wound margin always differs from the one close to the central wound area (Clark, 1996). Once tissue remodelling is complete, however, unlike uninjured skin, the wound area will never reach a 100 percent organised collagen form and will never return to perfect skin. In addition, hypertrophic and keloid scars may form after healing (Broughton *et al.*, 2006b).

1.3 Role of cytokines / growth factors in wound healing

1.3.1 Cytokines, growth factors and wound healing

Cytokines and growth factors are soluble cell secreted glycoproteins released in response to normal biological signals or environmental stimuli. They bind with cognate cell transmembrane receptors and initiate intracellular signalling cascades followed by regulating fundamental biological processes (Coondoo, 2011).

Cytokines are a class of small proteins involved in both paracrine (mode that cell released molecules affect other cells nearby) and autocrine (mode that molecules affect the cell which produces them) cell signalling. Cytokines include, among others, chemokines (which promote chemotaxis), interferons and interleukins (which are both vital for the function of a healthy immune system) and members of the TNF family (which can induce apoptosis). The cytokines which are produced and released following an immune event can initially dictate whether an immune response is necessary and, if so, whether that response is cytotoxic, humoral, cellular-mediated or allergenic in nature (Borish and Steinke, 2003). Wound healing is tightly regulated by numerous cytokines, growth factors and chemokines released by several cell types (Table 1-2) through various

sophisticated signalling pathways (Barrientos et al., 2008, Behm et al., 2012). Throughout the wound healing process these soluble proteins are extensively produced to mediate the infiltration, migration, proliferation and differentiation of neutrophils, monocytes, keratinocytes, fibroblasts and endothelial cells, contributing to the restoration of an integral skin. Therefore, a tightly spatial and temporal control of these mediators holds the key to a normal wound healing process. There have been extensive studies evaluating the functions of the large pool of these soluble proteins. Among them, the functions of PDGF, VEGF, FGF, EGF-like growth factor and TGF- β families are relatively well documented (Barrientos et al., 2008, Clark, 1996).

1.3.1.1 PDGF

PDGF, which was originally identified as a mitogenic protein, is firstly released by platelets during haemostasis and subsequently involved in mediating cell growth, chemotaxis and matrix production in the following healing process. After injury occurs, large amount of PDGF are secreted and released by platelets and damaged cells, thus, a influx of this chemokine in the wound area initiates the recruitment of fibroblasts (Seppa et al., 1982), smooth muscle cells (Grotendorst et al., 1981), neutrophils and macrophages (Deuel et al., 1982, Siegbahn et al., 1990). In addition, an elevated expression of PDGF- β receptor in conjunction with inflammation has been documented during wound healing, enhancing cell responsiveness to PDGF stimulation (Reuter Dahl et al., 1993, Rubin et al., 1988). Moreover, abundant PDGF secretion is also continuously provided by activated macrophages (Shimokado et al., 1985), fibroblasts (Paulsson et al., 1987), endothelial cells (Harlan et al., 1986) and keratinocytes (Ansel et al., 1993) in an autocrine and paracrine manner, contributing to the later stages of the wound

healing process. In addition to the chemoattractant effect, PDGF was also found to facilitate the production of ECM components, such as fibronectin and HA (Blatti et al., 1988, Heldin et al., 1989), suggesting the regulatory role of PDGF in early matrix formation. Furthermore, *in vitro* studies demonstrated that PDGF could also promote the contraction of collagen matrices (Clark et al., 1989, Gullberg et al., 1990). Such evidence potentially expands the role of PDGF as a wound remodelling mediator in the late stage of wound healing. Regarding angiogenesis, it was found that PDGF had direct and indirect influence in this event (Risau et al., 1992, Sato et al., 1993), however, it was considered to be less effective than other growth factors, such as the FGF family (Folkman and Klagsbrun, 1987).

1.3.1.2 VEGF

A member of VEGF/PDGF group of the cystine-knot superfamily (Holmes and Zachary, 2005), VEGF exerts its function primarily on endothelial cells and plays a potent role in angiogenesis. An early study showed that VEGF acted as a vascular permeability factor (Senger et al., 1983), which is identified that VEGF promoted the mitogenic activity of capillary endothelial cells (Leung et al., 1989) and enhanced endothelial cells survival rate (Gerber et al., 1998), which both contribute to angiogenesis. Additionally, the lethality brought by VEGF deficiency highlighted the importance of VEGF on neovascularisation (Carmeliet et al., 1996). Hypoxia was found to be the critical driver for VEGF upregulation (Shweiki et al., 1992) and upregulation of its receptor, through paracrine induction (Brogi et al., 1996). Evidence at both transcript and protein levels have shown that keratinocytes are an important source of VEGF, which correlates VEGF expression with angiogenesis in the wound healing process (Brown et al., 1992).

1.3.1.3 FGF

FGF, which consists of at least 9 structurally similar but functionally distinct members, is known as a potent growth factor involved in wound healing. FGF was shown to stimulate the proliferation, differentiation, migration, invasion and tubule formation of endothelial cells (Montesano et al., 1986, Kanda et al., 1996), and has also been found to be mitogenic for endothelial cells (Schweigerer et al., 1987). Based on the study by Folkman and colleagues (Folkman and Klagsbrun, 1987), to date, the most extensively studied FGFs are FGF-1 and FGF-2, also known as acidic FGF (aFGF) and basic FGF (bFGF) respectively, regarding their structures and biological functions. FGF-1 and FGF-2 were found to be responsible for angiogenic activities. FGF has been found to be produced and released by several cell types including inflammatory cells, fibroblasts and vascular endothelial cells (Baird et al., 1985, Blotnick et al., 1994, Kandel et al., 1991, Schweigerer et al., 1987, Ross, 1993, Vlodavsky et al., 1987), and these FGFs primarily participate in the proliferation and re-epithelialisation phase as they are capable of stimulating the proliferation and migration of fibroblasts, keratinocytes and endothelial cells, all the essential cell types involved in granulation tissue formation, epithelialisation and angiogenesis (Burgess and Maciag, 1989, Klagsbrun, 1989, Delli Bovi et al., 1987, Zhan et al., 1988, O'Keefe et al., 1988, Shipley et al., 1989, Tsuboi et al., 1993, Lobb et al., 1985). In addition to the regulatory effect on cell types critically involved in the healing process, FGF has also been found to be able to modulate ECM synthesis and collagen degradation by mediating the expression and localisation of proteases (Gross et al., 1983, Buckley-Sturrock et al., 1989, Mignatti et al., 1989, Flaumenhaft and Rifkin, 1991, Sato and Rifkin, 1988). There have been a large number of investigations evaluating the exogenous application of FGF family members in animal models of dermal wound healing utilising a wide

range of different types of wound healing models. Neovascularisation has always been identified after FGF treatment, strongly emphasising the angiogenic role of FGF in wound healing (Clark, 1996). Key roles of FGF in wound healing are summarised in Table 1-3.

Table 1-3 FGF family members involved in wound healing

Isoform	Known producing/secreting cell types	Phases of wound healing	Function	Reference
FGF-1	Monocyte/macrophage, T lymphocyte, endothelial cell, fibroblast	Epithelialisation, granulation tissue formation, angiogenesis	promote endothelial cell migration through stroma; stimulated chemotaxis of fibroblast, facilitate collagenase synthesis; promote the proliferation of keratinocyte and fibroblast	(Mignatti et al., 1989, Buckley-Sturrock et al., 1989, Shipley et al., 1989, O'Keefe et al., 1988, Baird et al., 1985, Blotnick et al., 1994, Vlodavsky et al., 1987, Schweigerer et al., 1987, Kandel et al., 1991)
FGF-2				
FGF-7	fibroblast	Epithelialisation	promote keratinocyte proliferation and migration, increase plasminogen activator activity	(Chedid et al., 1994, Tsuboi et al., 1993)

Table 1-4 TGF- β in wound healing

Isoform	Phases of wound healing	Function	Reference
TGF- β 1	Inflammation, re-epithelialisation, angiogenesis, wound contraction	Recruit inflammatory cells; promote the adhesion and migration of keratinocytes; inhibit the proliferation of keratinocytes; promote endothelial cell proliferation; increase fibronectin expression, urokinase plasminogen activator activity, stimulate collagen production; facilitate fibroblasts contraction	(Sankar et al., 1996, Barrientos et al., 2008, Jeong and Kim, 2004, Sellheyer et al., 1993, Border and Ruoslahti, 1992)
TGF- β 2	Inflammation, re-epithelialisation, granulation formation, angiogenesis	Recruit inflammatory cells and fibroblasts; induce angiogenesis; facilitate the granulation tissue formation; stimulate re-epithelialisation	(Cordeiro et al., 1999, Roberts et al., 1986, Cox et al., 1992)
TGF- β 3	anti-scar formation	Improve the architecture of the neoderms	(Shah et al., 1995)

1.3.1.4 EGFR and TGF- α

TGF- α , an EGF-like growth factor, has been suggested to be a major regulator of keratinocyte proliferation (Coffey et al., 1987, Pittelkow et al., 1993). This is supported by the observation that overexpression of TGF- α in the epidermis results in a hyperproliferative and hyperkeratosis phenotype, indicating the important regulatory role of TGF- α in normal epidermis formation (Dominey et al., 1993). Epidermal growth factor receptor (EGFR) is expressed in the basal layer and the first suprabasal layer of adult epidermis (Nanney et al., 1990). EGFR has been proposed to be a critical mediator of migration, proliferation, differentiation and re-establishment of barrier permeability in keratinocytes during wound healing (Clark, 1996). This was further supported by the evidence that membrane bound EGFR was reduced in chronic wounds, and that keratinocytes at the non-healing edge of chronic wounds were incapable of responding to EGF stimulation due to the cytoplasmic localisation of EGFR (Brem et al., 2007), highlighting an essential role of EGFR in normal keratinocyte function in the wound healing process. In addition, the EGFR pathway is also found to be associated with the production of cytokines and growth factors, reorganisation of the ECM and promotion of endothelial response in dermis. EGFR pathways have therefore been defined as one of the integral pathways affecting nearly all major events of the wound healing process (Clark, 1996).

1.3.1.5 TGF- β

TGF- β has been recognised as the cytokine with the broadest involvement in tissue repair since its extensive association with a variety of cell types participating in the wound healing process (Roberts and Sporn, 1988, Border and Ruoslahti, 1992) (Table 1-4). The unique feature of this cytokine is its auto-

induction property which enables the continuous expression of TGF- β once it is induced either by endogenous release or exogenous application to a wound. To date, three isoforms have been discovered in mammalian cells and exogenous TGF- β 1 and -2 seem to hold similar effects on wound healing outcomes (Ksander et al., 1993), whereas application of TGF- β 3 results in less scarring (Shah et al., 1995). After injury, TGF- β is firstly released by aggregate platelets and damaged parenchymal cells, acting as chemoattractant to stimulate the migration of inflammatory cells, keratinocytes, fibroblasts and endothelial cells to the wound site. Subsequently, TGF- β mediates ECM reorganisation and remodelling by stimulating the recruited cells to produce matrix proteins, matrix-degrading proteases and their inhibitors as well as modulating interactions between matrix components and cells via integrin receptors (Clark, 1996). However, this complex process depends on a cell- and context-specific manner. TGF- β was also identified as a critical mediator of angiogenesis and re-epithelialisation, although the precise effects of TGF- β on these two events still remains unclear due to contrasting results being identified in different models (Sporn et al., 1983, Roberts et al., 1986, Phillips et al., 1992, Flaumenhaft et al., 1993, Mustoe et al., 1991, Chen et al., 1992, Ksander et al., 1990, Jones et al., 1991). Nevertheless, TGF- β has been documented to be involved in the modulation of all phases of the wound healing process. Since initial data demonstrated abnormal growth factor profiles and differential proteolytic balances present in chronic wound fluids (Wysocki et al., 1993) and given that TGF- β has been documented to regulate the ECM reorganisation, clinical trials have investigated the application of TGF- β . Such trials have demonstrated that TGF- β 2 improved the healing outcomes of venous stasis ulcer (Robson et al., 1995), although the specific mechanisms of such effects remain unknown. However, more than a decade later, Pastar *et al.* discovered

that exogenous TGF- β may not be of benefit to non-healing venous ulcers patients since its impact could be minimised by phenotypes which lacked the TGF- β receptor and downstream target genes (Pastar et al., 2010).

1.3.1.6 Other cytokines and growth factors

There are a number of other cytokines and growth factors that may influence the healing process. IFN- γ was found to strongly and specifically induce the expression of Keratin-17 (Jiang *et al.*, 1994), a protein expressed in various healthy epithelia that are characterised as contractile tissue. Thus, IFN- γ was suggested to contribute to the contractile nature of keratinocytes in the later stage of wound healing (Freedberg *et al.*, 2001).

IL-6 derived from fibroblasts, macrophages, endothelial cells and keratinocytes is another essential cytokine which affects granulation tissue formation, reepithelialisation, angiogenesis, cell infiltration and remodelling. Additionally, IL-6 showed enhanced expression in chronic wounds exhibiting aberrant inflammation, suggesting the importance of regulated IL-6 expression patterns in normal wound healing (Behm *et al.*, 2012). The above are a short list of well characterised factors in association with the wound healing process. There exists a long list of soluble factors that are active in physiological and pathological conditions including IL-1, hepatocyte growth factor (HGF), insulin-like growth factor (IGF)-1 and insulin (Behm et al., 2012, Yu et al., 2010, Barrientos et al., 2008), which are not covered by the current literature review.

1.4 SOCS

SOCS are a group of cytokine- and growth factor-induced proteins containing three common structural and functional domains. SOCS proteins negatively

regulate cytokine receptor and receptor tyrosine kinase (RTK) signalling predominantly via inhibition of the JAK/STAT signalling pathway in order to maintain the homeostasis of cell function. The group consists of eight family members; cytokine inducible Src-homology 2-containing protein (CIS) and SOCS-1 to SOCS-7, in mammals (Krebs and Hilton, 2001). Additionally, three family members of SOCS homology have been found in both *Drosophila* and *Ciona intestinalis* (Karsten et al., 2002, Rawlings et al., 2004a, Hino et al., 2003).

1.4.1 Discovery of SOCS

SOCS proteins were discovered separately by three independent groups of scientists. In 1997, Starr *et al* discovered three homologous forms of CIS, namely SOCS-1, SOCS-2 and SOCS-3, and suggested that SOCS-1 plays an important role in the classic negative-feedback loop which regulates cytokine signal transduction (Starr *et al.*, 1997). In the same year, Endo *et al* found that a new JAK-binding protein (JAB), structurally related to CIS and possessing an Src-homology 2 (SH2) domain, acts as a negative regulator in the JAK signalling pathway (Endo *et al.*, 1997). Meanwhile, a new protein, known as STAT-induced STAT Inhibitor-1 (SSI-1), was identified by a third group of scientists, and this protein was also found to be involved in the negative-feedback regulation of cytokine stimulated JAK/STAT signalling (Naka *et al.*, 1997). It was later confirmed that SOCS-1, JAB and SSI-1 all belong to the SOCS family of proteins (Crocker et al., 2008a).

1.4.2 Structure and structural related function

There are three major domains which contribute to the function of SOCS proteins: a conserved central SH2 domain containing an extended SH2 sequence; an N-terminal domain of variable length and divergent sequence and a carboxy-

terminal 40-amino-acid module called the SOCS box (Alexander, 2002, Yasukawa *et al.*, 1999) (Figure 1-3). Due to the proteasomal degradation effect, the SOCS proteins which regulate cytokine signalling are short-live compared to the signalling components such as JAK and STAT proteins (Siewert *et al.*, 1999, Bayle *et al.*, 2006).

1.4.2.1 JAK/STAT signalling

The Janus kinase/signal transducer and activator of transcription (JAK/STAT) pathway is an essential cellular mechanism which responds to a wide array of cytokines by transducing their signals to the nucleus and promoting cell functions such as proliferation, migration, differentiation and apoptosis. Due to the establishment of murine knockout models, the biological significance of the JAK/STAT signalling pathway is extensively recognised (Igaz *et al.*, 2001).

To date, four JAK family members (JAK1, JAK2, JAK3, TYK2) and seven members of STAT (STAT-1, STAT-2, STAT-3, STAT-4, STAT-5a, STAT-5b, STAT-6) are found in mammals (Liongue *et al.*, 2012). Each JAK protein consist of four sturctural domains, namely N-teminal FERM (abbreviation of the first four proteins found in this family: Four-point-one, Ezrin, Radixin, Moesin) (Tepass, 2009), SH2 domain, “pseudo kinase” domain and C- terminal PTK domain (Liongue *et al.*, 2012); while STAT family members possess five functional domains; an amino-terminal domain (NH2); a coiled-coiled domain (CCD); a DNA-binding domain (DBD); an SH2 domain and a carboxy-terminal transcriptional activation domain (TAD) (Kisseleva *et al.*, 2002).

Since the JAK/STAT signalling pathway is utilised by numerous cytokines to transduce signals to nucleus, any mutation which holds the potential to compromise the regular function of the JAK/STAT pathway may also impair the

cytokine stimulated signalling. Additionally, dysregulation of this signalling pathway may cause inflammatory disease, erythrocytosis, gigantism and leukaemia (Rawlings et al., 2004b). Therefore, mechanisms regulating JAK/STAT signalling that can prevent activation beyond the necessary time are of great importance. This is achieved by the use of negative regulators which possess a specific SH2 domain such as SH2-containing phosphatase (SHP), protein inhibitors against STATs (PIAS) and suppressor of cytokine signalling (SOCS) (Wormald and Hilton, 2004). However, compared to SHP and PIAS, which are constitutively expressed (Wormald and Hilton, 2004), SOCS proteins are the only cytokine inducible inhibitors that may have the potential for use as a biomarker for the dysregulation of cell metabolism.

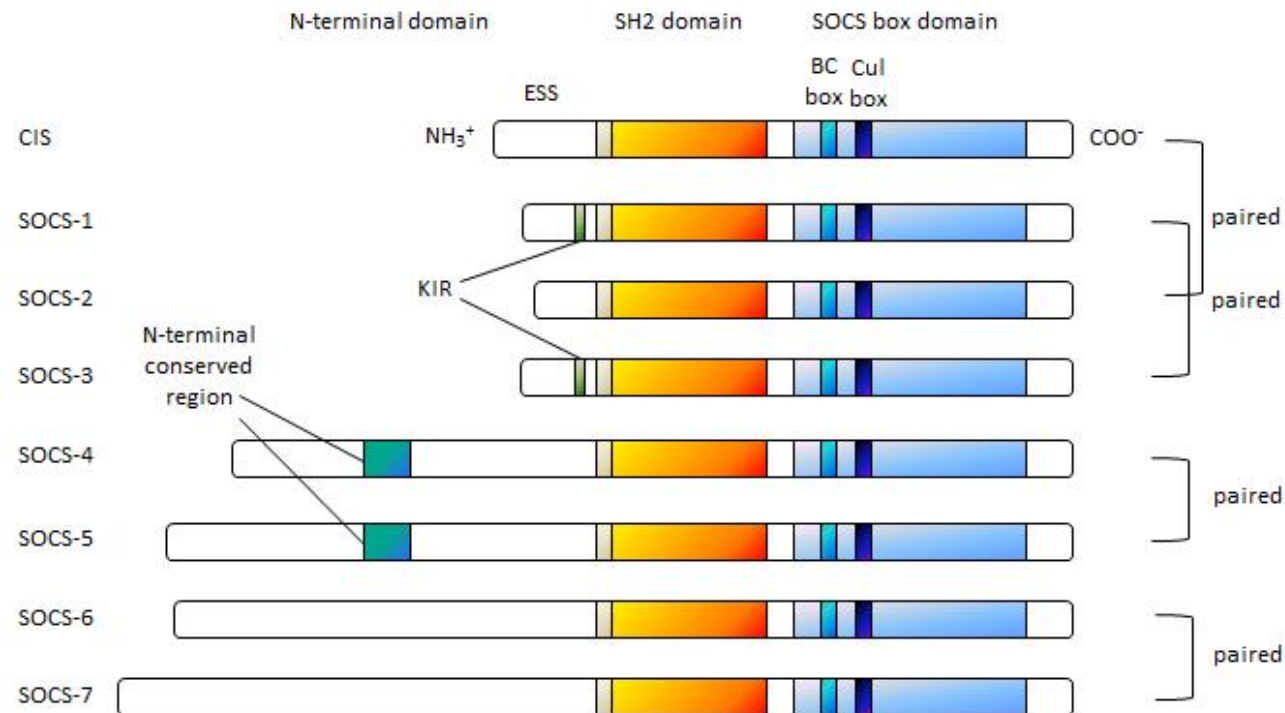


Figure 1-3: Structure of the eight suppressor of cytokine signalling (SOCS) family members

SOCS proteins comprise three structural and functional domains which are **1)** a N-terminal domain with variable length of amino acids sequences, **2)** a central SH2 domain with extended SH2 sequence (ESS) and **3)** a SOCS box domain containing a BC box, a elongin B and C binding domain, and a Cul box, a cullin-5 binding sequence, at the C-terminus. Each two SOCS family members are paired due to their structural and functional similarity. SOCS-1 and SOCS-3 both possess a unique kinase inhibitory region (KIR) which inhibits JAK protein activity. SOCS-4 and SOCS-5 both contain a highly conserved region within their N-terminal domain termed as N-terminal conserved region. SOCS-6 and SOCS-7 share more than 50% amino acid identity in SH2 domain and SOCS box domain. (Feng et al., 2016)

SOCS proteins can be divided into two major sub-families according to the depth and scope of investigation and their structural similarity.

The first sub-family, containing CIS, SOCS-1, SOCS-2 and SOCS-3, has been extensively investigated, whereas scientific study on the other sub-family comprising SOCS-4 to SOCS-7 is still limited. Within each of the two sub-families SOCS proteins can be further paired based on similarities in structure and function. The CIS/SOCS-1 to SOCS-3 sub-family is the most highly investigated and it has been discovered that CIS and SOCS-2 possess similar structures, whereas SOCS-1 and SOCS-3 have similar functions due to their homologous structure. Although investigations on the function of the SOCS-4 to SOCS-7 sub-family are limited and require further elucidation, SOCS-4 and SOCS-5 may be paired since they possess the most similarity with regards to structure, with both proteins containing a highly conserved region within their N-terminal domain, termed the N-terminal conserved region. Similarly, SOCS-6 and SOCS-7, the most homologous among SOCS family members and sharing more than 50% amino acid identity in SH2 and SOCS box domains (Krebs *et al.*, 2002), were proposed to be a pair and they are both involved in nuclear translocation of proteins (Kremer *et al.*, 2007, Hwang *et al.*, 2007).

SOCS family members can also be classified according to their target proteins. CIS/SOCS-1-3 regulate cytokine receptor signalling through the JAK/STAT pathway, whereas SOCS-4 to SOCS-7 are associated with regulation of growth factor receptor signalling (Trengeve and Ward, 2013).

The eight structurally related SOCS family members have been recognised as being able to attenuate cytokine and growth factor signalling by inhibition of JAK tyrosine kinase activity, by blocking signal transduction through competition for the receptor's phosphotyrosine residue, and via the degradation of crucial

molecules, such as JAK and the receptor complex, through a proteasomal pathway (Tregrove and Ward, 2013) (Figure 1-4). To date, the structures of the ternary complex of three SOCS family members (SOCS-2, SOCS-3, SOCS-4-elongin-C-elongin-B) have been established for investigating SOCS function (Bergamin *et al.*, 2006, Babon *et al.*, 2006, Bullock *et al.*, 2006, Bullock *et al.*, 2007, Babon *et al.*, 2008).

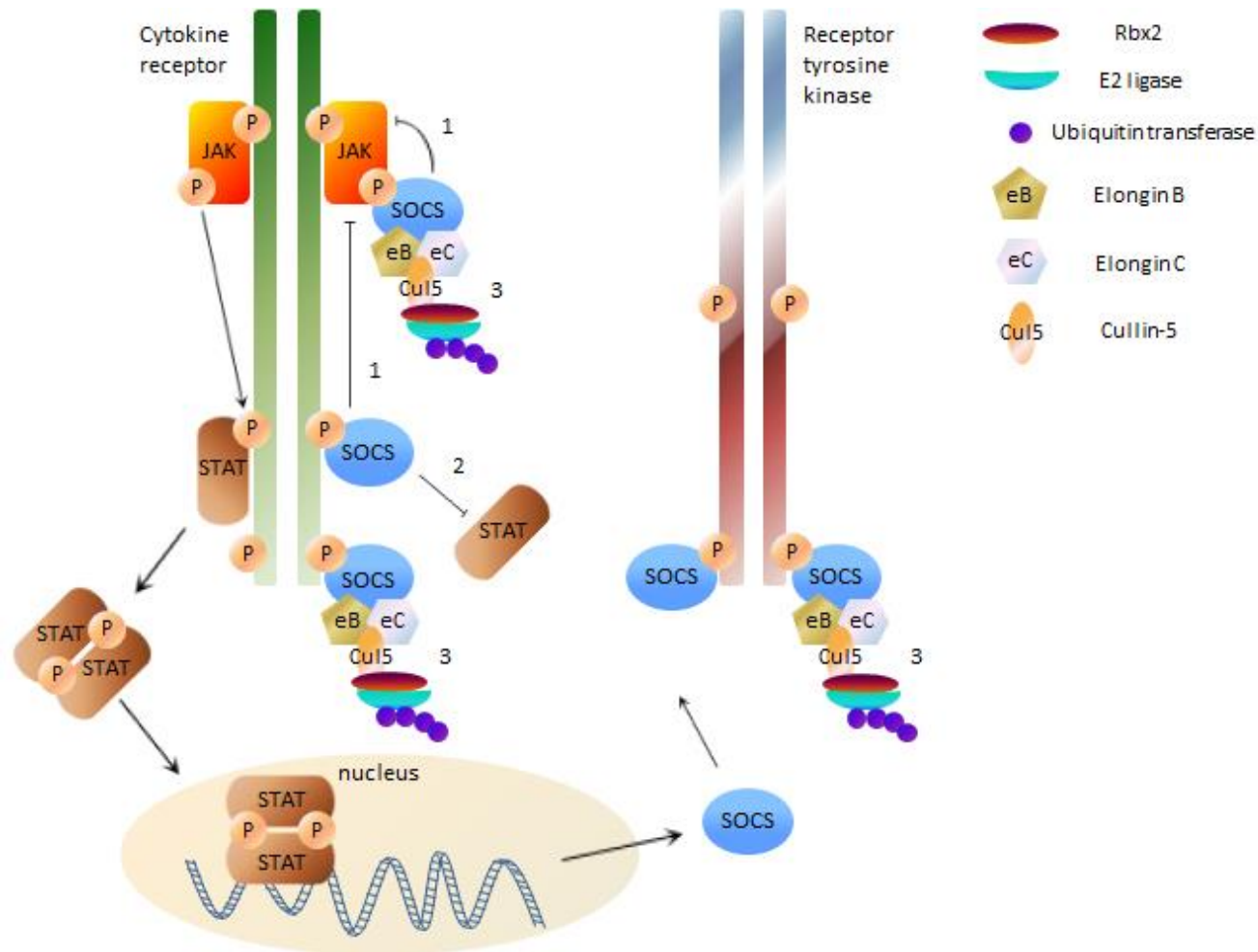


Figure 1-4: Mechanisms of SOCS regulation on cytokine and growth factor signalling

Three mechanisms have been discovered accounting for the negative regulatory role of SOCS on cytokine and growth factor signalling. **1.** SOCS associates with activated JAK protein and inhibit JAK tyrosine kinase activity; **2.** SOCS competes with STAT for the docking site (phosphorylated tyrosine residues) on the cytokine receptor; **3.** SOCS associates with target proteins (JAK and/or cytokine receptors as well as receptor tyrosine kinases) and promote the proteasomal degradation of the SOCS-target protein complex. (JAK: Janus kinase; STAT: signalling transducer and activators of transcription; SOCS: suppressor of cytokine signalling; eB:elongin B; eC: elongin C; Cul5: Cullin-5; Rbx2: RING-box protein-2; P: phosphotyrosine residue)

1.4.2.2 N-terminal region

Although the function of the N-terminal domain in SOCSs has not been fully elucidated, it has been suggested that its helical structure contributes to the stability of the SOCS molecule complex (Greenhalgh *et al.*, 2005). A study showed that SOCS-4 and SOCS-5 both possess a highly conserved N-terminal domain (Feng *et al.*, 2012) and the N-terminal in SOCS-5 was found to be involved in recruiting the EGF and IL-4 receptor complex (Nicholson *et al.*, 2005, Seki *et al.*, 2002). Additionally, the N-terminal of SOCS-6 and SOCS-7, containing more than 350 amino acids, were found to be responsible for transporting proteins into the nucleus (Hwang *et al.*, 2007, Kremer *et al.*, 2007). The short region or kinase inhibitory region (KIR) in the N-terminal domain (amino-terminal region) of SOCS-1 and SOCS-3 have sequence homology with the pseudosubstrate inhibitory region of JAK proteins and show high affinity to JAK proteins. It has been suggested that the interaction between the KIR region of SOCS-1 and JAK activation loop inhibits the catalytic activity of JAK (Yasukawa *et al.*, 1999, Nicholson *et al.*, 1999), therefore partially suppressing cytokine signalling. Further study on the SOCS-3-JAK-2-gp130 crystal structure showed that the KIR region is required for SOCS-3 to block substrate binding of JAK, which leads to the inhibition of JAK's enzymatic activity. Another finding based on this structure is that those residues upstream of the KIR in SOCS-3 act as a JAK-2 pseudosubstrate, a typical characteristic of substrate-blocking inhibitors (Kershaw *et al.*, 2013). The N-terminal domains found in SOCS-4 to SOCS-7, consisting of 300-400 residues, are greatly extended to that of in the other SOCS family members and still remain to be structurally and functionally investigated (Bullock *et al.*, 2007).

1.4.2.3 SH2 domain

The SH2 domain is another essential structure determining target specificity that enable SOCS proteins to exert their function. The SH2 domain of SOCS proteins binds to phosphotyrosine residues on receptor complexes and JAK proteins to regulate the activated JAK/STAT signalling pathway and maintain the balance of cell metabolism. An early study showed that compared to the typical SH2 domain, those present in SOCS proteins contains a extended sub-domain which is required for inhibition of JAK-2 signalling (Yasukawa *et al.*, 1999). Mutation of the SH2 domain in SOCS-1 impaired its inhibitory function on leukemia inhibitory factor (LIF) signal transduction (Nicholson *et al.*, 1999). It was found that CIS utilises the SH2 domain to inhibit cytokine signalling through its competition with STAT for the docking sites present on phosphorylated tyrosine residues of activated cytokine receptors (Matsumoto *et al.*, 1999). Kario *et al* suggested that the SH2 domain in SOCS-5 is necessary for both its interaction with the EGFR and EGFR degradation (Kario *et al.*, 2005).

1.4.2.4 SOCS box domain

The SOCS box domain is a highly conserved motif comprising two functional sub-domains: a BC box recruiting elongin B and C and a Cul box which regulates Cullin-5 binding to RING-box protein-2 (Zhang *et al.*, 1999, Kamura *et al.*, 2004). SOCS box attaches to elongin B/C followed by binding to Cullin-5, a scaffold protein of an E3 ubiquitin ligase, thereby acquiring the ability to terminate cytokine signalling by binding to target molecules and facilitating proteasomal degradation (Zhang *et al.*, 1999). It has been previously established that SOCS proteins are relatively short-lived compared to the signalling components they affect, such as the JAK and STAT proteins, and such phenomenon was thought to be attributable

to proteasomal degradation through association with their SOCS box (Bayle *et al.*, 2006). Babon *et al.* (Babon *et al.*, 2009) discovered a correlation between the affinity of SOCS for Cullin-5 and the importance of the SOCS box, and predicted that SOCS-4 and SOCS-6 are likely to be strong SOCS box-dependent molecules due to their high affinity for Cullin-5. Interestingly, tyrosine residues 204 and 211 at the carboxy terminal in SOCS-3 were discovered to be able to sustain SOCS-3 stability through the association with elongin C and phosphorylation of either residue resulted in loss of elongin-C binding, leading to the acceleration of SOCS-3 turnover (Haan *et al.*, 2003).

The establishment of the crystal structure of SOCS-2 and SOCS-4-elongin-B/elongin-C complex aided in the understanding and identification of the distinct functions of the SOCS box in both CIS/SOCS-1 to SOCS-3 and SOCS-4 to SOCS-7 sub-families (Bullock *et al.*, 2006, Bullock *et al.*, 2007).

It seems that not all eight SOCS members primarily take advantage of the SOCS box structure to exert their negative regulatory functions. Despite higher efficiency of cytokine signalling suppression compared to other SOCS family members, the SOCS box in SOCS-1 and SOCS-3 showed a distinctly lower affinity for Cullin-5 compared to other homologues (Babon *et al.*, 2009), indicating another possible unique functional domain present in both SOCS members. So far, the only discovered structural domain in SOCS-1 and SOCS-3 is KIR, which demonstrated direct interaction with JAK protein (Sasaki *et al.*, 1999) and inhibited JAK kinase activity (Yasukawa *et al.*, 1999). Therefore, SOCS box may not be the only functional domain contributing to the negative feedback regulatory function of SOCS-1 and SOCS-3. This hypothesis was further supported by *in vivo* investigation in *Drosophila* and mouse. SOCS box depletion in SOCS36E, a SOCS member in *Drosophila*, only results in a partial reduction of SOCS36E activity

(Callus and Mathey-Prevot, 2002). *In vivo* studies on SOCS-1 and SOCS-3 using SOCS box knock out mice both showed similar results, demonstrating that SOCS box-null mice had a milder phenotype than SOCS-null mice, and SOCS box-null mice expressed intermediate responses between wild type and SOCS-null mice to cytokine stimulation (Boyle et al., 2007, Zhang et al., 2001). Therefore, SOCS box, along with the other two major domains in SOCS family members, mediate cytokine signalling complementarily and synergistically. Although most of the functions and structure of the SOCS-4 to SOCS-7 subfamily still remain unclear, it was found that the SOCS box was required for the inhibitory function of SOCS-5 on EGF stimulation (Kario *et al.*, 2005, Nicholson *et al.*, 2005).

1.4.3 Biological functions of SOCS family members

SOCS proteins have been primarily classed as negative regulator of cytokine signalling. However, due to the structural variance and the different expression profile in different tissues and cell types, they were found to play a diverse role in a variety of physiology and pathology conditions.

1.4.3.1 CIS

CIS is expressed in a variety of tissues and is able to associate with tyrosine phosphorylated molecules. CIS was found to be strongly expressed in the kidney, lung and liver in mice, whereas lower expression of CIS was observed in the heart, stomach, testis, spleen and thymus (Yoshimura et al., 1995, Starr et al., 1997). It was suggested that CIS is a negative regulator of cytokine induced signalling for growth as well as a tumour suppressor gene (Yoshimura et al., 1995). CIS has been discovered to be induced by a number of cytokines and growth factors and primarily acts as a negatively feedback regulator to growth hormone (GH)

signalling via inhibition of JAK-2 and STAT-5 activation (Verdier et al., 1998, Matsumoto et al., 1999, Ram and Waxman, 1999, Ram and Waxman, 2000). The relationship between CIS and a variety of cytokines, capable of bringing about CIS expression, together with the key regulatory roles played by CIS in related downstream signalling pathways are summarised in Table 1-5.

Table 1-5 Summary of the association between CIS and key cytokines/growth factors together with the regulatory roles played by CIS.

Cytokines /growth factors that induce CIS	Regulatory role of CIS in signalling pathway	Reference
Erythropoietin (EPO)	Associate with tyrosine-phosphorylated EPO receptor, inhibit EPO signalling by downregulating STAT-5 activation	(Matsumoto et al., 1997, Yoshimura et al., 1995)
IL-2	Impair IL-2 signalling through the association with IL-2R β chain	(Aman et al., 1999, Yoshimura et al., 1995)
IL-3	Associate with IL-3R β chain	(Yoshimura et al., 1995, Matsumoto et al., 1997)
Prolactin (PRL)	Inhibit PRL signalling through the association with PRLR, thus suppressing the activation of STAT-5	(Dif et al., 2001, Pezet et al., 1999, Tonko-Geymayer et al., 2002)
Growth hormone (GH)	Suppress GH signal by binding to GHR phosphor-tyrosine site, competing with STAT-5b, facilitating proteosomal degradation of (GHR-JAK2)-CIS complex	(Ram and Waxman, 1999, Ram and Waxman, 2000, Adams et al., 1998)
EGF		(Tonko-Geymayer et al., 2002)
Granulocyte-macrophage colony-stimulation factor (GM-CSF)		(Yoshimura et al., 1995)
Ciliary neurotrophic factor (CNTF)		(Bjorbaek et al., 1999)
IL-9		(Lejeune et al., 2001)
Thrombopoietin (TPO)		(Starr et al., 1997, Okabe et al., 1999)
IL-6, IFN- γ , Tumor necrosis factor (TNF- α)		(Starr et al., 1997)
Granulocyte colony-stimulating factor (G-CSF)		(Hunter et al., 2004)
IL-10		(Shen et al., 2000)
Thymic stromal lymphopoietin (TSPL)		(Isaksen et al., 1999)
IFN- α		(Brender et al., 2001b)
	Inhibit IGF-1-induced STAT-3 activation	(Zong et al., 2000)
	Interact with leptin receptor on Y985 and Y1077	(Lavens et al., 2006)

1.4.3.1.1 *In vivo* role of CIS

CIS transgenic mice have been generated and show a decreased body weight compared to wild-type mice, although they developed normally. However, lactation failure, reduction of gamma delta T cells and natural killer cells and an alteration of helper T1 (Th1)/Th2 differentiation were found in this phenotype (Matsumoto et al., 1999).

1.4.3.1.2 CIS and wound healing

With regards to wound healing, an early study discovered that CIS could inhibit IL-2 signalling by associating with the β -chain of the IL-2 receptor and by suppressing the IL-2 dependent activation of STAT-5 (Aman et al., 1999). In addition, IL-2 was found to be able to enhance fibroblast infiltration and metabolism *in vitro*, and was suggested to be beneficial for an immunocompromised wound (Efron and Moldawer, 2004). Therefore, CIS may potentially act as a negative regulator in granulation tissue formation.

1.4.3.2 SOCS-1

SOCS-1 has been found to be highly expressed in thymus and spleen both in human and mouse, whereas high expression was also observed in human placenta (Hilton et al., 1998, Starr et al., 1997, Kato et al., 2006). Moderate expression of SOCS-1 was observed in lung and testis in both species, as well as in adipose, ovary and the uterus in humans and the colon in mice (Starr et al., 1997, Kato et al., 2006, Hilton et al., 1998). Studies have shown that SOCS-1 could be induced by a variety of cytokines and growth factors and primarily acts as a negative feedback regulator to proinflammatory cytokines such as IL-6, TNF- α and IFN- γ (Table 1-6). SOCS-1 is found to be able to mediate inflammation by

regulating the cell growth, survival, apoptosis and differentiation of innate immune cells as well as non-immune cells, and is essential for the balance of IFN-mediated Th1/Th17 cell differentiation (Tanaka et al., 2008).

Table 1-6 Summary of the association between SOCS-1 and key cytokines/growth factors together with the regulatory roles played by SOCS-1

Cytokines /growth factors that induce SOCS-1	Regulatory role of SOCS-1 in signalling pathway	Reference
GH	Inhibit the GHR-dependent tyrosine phosphorylation of JAK-2 directly; inhibit GH-induced STAT-5 activation; suppress GH-induced transactivation effect	(Ram and Waxman, 1999, Hansen et al., 1999, Sporri et al., 2001, Adams et al., 1998)
IL-2	Inhibit IL-2 by suppressing STAT-5 activation; associate with JAK-1, JAK-2 and JAK-3 to reduce their tyrosine-kinase activity; bind to IL-2R β chain; reduce IL-2-induced <i>c-fos</i> promoter activation by inhibiting JAKs activity	(Sporri et al., 2001, Endo et al., 1997)
IL-4	Inhibit the activation of JAK-1 and STAT-6 in response to IL-4	(Sporri et al., 2001, Naka et al., 1997, Losman et al., 1999, Hebenstreit et al., 2003, Egwuagu et al., 2002)
IL-6	Inhibit IL-6-induced tyrosine-phosphorylation of gp130 and STAT-3; associate with JAK-2 and Tyk-2; reduce the inhibitory effect of β -casein by IL-6	(Sporri et al., 2001, Endo et al., 1997, Naka et al., 1997, Motta et al., 2004)
IL-10	Potentially inhibit IL-10-induced signalling by suppressing the activation of STAT-3	(Niemand et al., 2003)
IL-13	Attenuate IL-13-induced signalling	(Hebenstreit et al., 2003)
IFN- α	Inhibit IFN- α -dependent STAT-1 tyrosine phosphorylation and nuclear translocation; suppress the anti-proliferative and antiviral effect of IFN- α	(Crespo et al., 2000, Wang et al., 2000, Song and Shuai, 1998)
IFN- β	Attenuate IFN- β chemokine-related inflammation	(Crespo et al., 2000, Qin et al., 2008)
IFN- γ	Inhibit IFN- γ -dependent STAT-1 tyrosine phosphorylation and nuclear translocation;	(Sporri et al., 2001, Song and Shuai, 1998, Starr et al., 1997, Tanaka et al., 2008, Alexander et al., 1999,

	suppress antagonistic effect of IFN- γ on STAT-3 and Smads, neutralise IFN- γ -dependent inhibition of Th17 differentiation; inhibit the anti-proliferative and antiviral effect of IFN- γ ; suppress the IFN- γ -mediated STAT1 phosphorylation at Y701 and the association of STAT-1 and DNA	Zhang et al., 2001, Park et al., 2000)
EPO	Inhibit EPO-induced EPOR activation	(Sporri et al., 2001, Endo et al., 1997)
G-CSF		(Naka et al., 1997)
Leukemia inhibitory factor (LIF)	Inhibit LIF-mediated cell apoptosis and differentiation; suppress LIF-induced STAT-3 activation	(Naka et al., 1997, Nicholson et al., 1999)
PRL	Suppress PRL-stimulated signal through the association with JAK-2 and inhibition of STAT-5-mediated transcription; inhibit PRLR-mediated signalling	(Sporri et al., 2001, Pezet et al., 1999, Motta et al., 2004, Helman et al., 1998)
Ciliary neurotrophic factor (CNTF)		(Bjorbaek et al., 1999)
leptin		(Motta et al., 2004)
Steel factor	Promote steel factor-dependent cell survival	(De Sepulveda et al., 1999)
	Suppress TNF- α -mediated cell apoptosis via sustaining the activation of p38 mitogen-activated protein kinase (MAPK); reduce the inhibitory effect of β -casein by TNF- α	(Morita et al., 2000, Motta et al., 2004)
	Reduce IL-3-induced <i>c-fos</i> promoter activation by inhibiting JAKs activity	(Endo et al., 1997)
	Interfere with IL-7-stimulated-pre-TCR activation	(Trop et al., 2001)

	Negatively regulate IL-12-induced IL-12R and STAT-4 activation	(Eyles et al., 2002)
	Reduce IL-15-induced STAT-5 phosphorylation	(Ilangumaran et al., 2003)
	Suppress thrombopoietin(TPO)-induced signalling	(Starr et al., 1997, Wang et al., 2000)
	Inhibit thymic stromal lymphopoietin (TSLP)-mediated signalling	(Isaksen et al., 1999)
	Surppress oncostatin M (OSM)-mediated cell differentiation; inhibit OSM-induced STAT-3 activation	(Starr et al., 1997, Song and Shuai, 1998)
	Negatively regulate insulin signalling through the association with IRS-1 and by the inhibition of JAK; associate with IRS-1 and IRS-2 for ubiquitin-mediated degradation; inhibit insulin-dependent dostream signalling, extracellular signal-regulated kinase (ERK), protein kinase B, phosphatidylinositol 3-kinase (PI3K)/Akt activation	(Kawazoe et al., 2001, Rui et al., 2002, Mooney et al., 2001, Liu et al., 2008a)
	Associate with IGF-1R to inhibit IGF-1-induced STAT-3 activation	(Zong et al., 2000, Dey et al., 1998)
	Sustain ERK activated anti-inflammatory pathways; maintain RAS through facilitating degradation of RAS inhibitor, p120 RasGAP	(Madonna et al., 2008)
	Associate with receptor tyrosine kinase KIT, FIL-3 and suppress their mitogenic signals	(De Sepulveda et al., 1999)

1.4.3.2.1 *In vivo* role of SOCS-1

SOCS-1 deficient mice exhibited complex diseases in a diverse range of organs and could not survive beyond weaning, indicating that SOCS-1 is required for various cell types and is essential for normal postnatal growth and survival (Starr et al., 1998, Naka et al., 1998, Metcalf et al., 1999, Marine et al., 1999b). Additionally, SOCS-1 and IFN- γ double knockout mice expressed other aberrant phenotypes including polycystic kidneys, chronic inflammatory lesions (Metcalf et al., 2002), perturbed T cell development (Cornish et al., 2003, Lee et al., 2009) and enhanced sensitivity to lipopolysaccharide (LPS) (Kinjyo et al., 2002). In order to investigate the function of SOCS-1 in individual tissue, a thymocyte/T cell specific SOCS-1 expression mouse model was established. Apart from multiple lymphoid abnormalities, such mice did not develop lethal multiorgan inflammatory pathologies seen in SOCS-1 deficient mice, indicating that thymocyte/T cell specific SOCS-1 deficiency alone is insufficient to cause neonatal lethality (Chong et al., 2003). It was suggested that SOCS-1 plays a regulatory role in the activation of macrophages through Toll-like receptor (TLR) signaling (Kinjyo et al., 2002, Nakagawa et al., 2002), indicating the potential role of SOCS-1 in regulating innate immunity through inhibition of macrophage activation. Investigation on a SOCS-1 and IFN- γ double knockout mouse model demonstrated that dendritic cells were hyperactive and hyperresponsive to IFN- γ in SOCS-1 deficient conditions. Therefore, a mouse model which expressed SOCS-1 only in T and B cells was established to further investigate the regulatory role of SOCS-1 on dendritic cells *in vivo*. Such phenotype expressed accumulated dendritic cells in the thymus and spleen as well as developing skin lesions, glomerulonephritis, and auto-antibody production, which are similar symptoms to systemic lupus erythematosus (SLE). Thus, it was suggested that SOCS-1 is essential to the normal function of dendritic

cells and the suppression of systemic autoimmunity. Moreover, the reduction of SOCS-1 expression could be a risk factor for SLE (Hanada et al., 2003). Hepatocyte specific-SOCS-1 deficient mice exhibited enhanced concanavalin A (ConA)-induced hepatitis. Such phenotypes expressed enhanced apoptosis signals after being treated with ConA, showing induced hyperactivation of STAT-1 and TNF- α -mediated-Jun-terminal kinase (JNK), an proapoptotic kinase, as well as higher cell surface accumulation of Fas protein which mediates hepatocyte apoptosis. On the contrary, overexpression of SOCS-1 in mice prevented ConA-induced liver injury by repressing the induction of proinflammatory cytokines. Taken together, SOCS-1 plays a negative regulatory role in acute hepatitis (Torisu *et al.*, 2008). SOCS-1 transgenic mice have also been generated using the *lck* proximal promoter, and the SOCS-1 transgene was strongly expressed in T cell lineage. This phenotype exhibited decreased phosphorylation of STATs induced by cytokines, and expressed defects in the development of T cells, which resembled the phenotype of mice lacking JAK-1, JAK-3 and common gamma-chain. This may indicate the inhibitory role of SOCS-1 in regulating downstream signalling of JAKs and common gamma-chain-using cytokines (Fujimoto et al., 2000).

1.4.3.2.2 SOCS-1 and wound healing

A *in vitro* study in human keratinocytes demonstrated that SOCS-1 exerts its inhibitory function against the pro-inflammatory effects of IFN- γ by not only inhibiting STAT-1 but also via maintenance of ERK-1/2-dependent anti-inflammatory pathways (Madonna et al., 2008), indicating a direct anti-inflammatory role of SOCS-1 on human epidermal keratinocytes. Since IFN- γ was found to contribute to the enhancement of tissue remodelling and the reduction of re-epithelialisation and wound contraction, regulation of IFN- γ is considered

crucial to wound healing (Efron and Moldawer, 2004). Therefore, further investigation of the regulatory role of SOCS-1 on IFN- γ during the re-epithelialisation stage of wound healing may identify new potential therapeutic targets.

Similar to CIS, SOCS-1 was also discovered to negatively regulate IL-2 signalling through inhibition of JAK-1 and STAT-5 activity as well as associating with the IL-2 receptor. Additionally, SOCS-1 suppresses the signalling of IL-4, an anti-inflammatory cytokine, through inhibition of JAK-1 and STAT-6 (Egwuagu et al., 2002). Therefore, due to the fact that IL-2 and IL-4 are involved in fibroblast infiltration, proliferation and collagen production, SOCS-1 may hold the potential to mediate granulation tissue formation.

A previous study showed that SOCS-1 inhibits TNF- α induced cell apoptosis via regulation of p38 MAPK, indicating an important regulatory role for SOCS-1 in TNF- α signalling (Morita et al., 2000). TNF- α was found to be up-regulated in chronic wounds and was suggested to result in prolonged inflammation through degradation of the ECM, growth factors and cell receptors by inducing MMPs production (Barrientos et al., 2008). Thus, SOCS-1 may have the potential to maintain homeostasis of the inflammation phase of chronic wounds through regulation of TNF- α .

It was discovered that SOCS-1 could inhibit HGF-induced STAT-3 activation (Seki et al., 2008), indicating its regulatory role in HGF-dependent signalling. HGF, which can be induced by TNF- α , IL-1 and IL-6, was considered to promote granulation tissue formation and angiogenesis in wound healing. HGF exerts its function by binding to its receptor tyrosine kinase, HGFR. Chronic wounds were suggested to be attributable to HGF/HGFR pathway dysregulation, and topical application of HGF was recommended as a potential treatment for chronic

wounds (Behm et al., 2012). Therefore, the precise control of HGF signalling by the implementation of SOCS-1 may hold potential as another therapeutic option for chronic wounds.

Upon insulin treatment, instead of direct inhibition of insulin receptor (IR) auto-phosphorylation SOCS-1 is more likely to inhibit insulin-dependent activation of ERK-1/2 (Mooney et al., 2001). During the wound healing process, ERK has been considered as an important regulator of wound contraction (Hirano et al., 2002) and an *in vivo* study in mice showed that the inhibition of ERK activation led to delayed wound healing (McFarland-Mancini et al., 2010). Taken together, SOCS-1 may also mediate wound healing by regulating the activation of ERK.

1.4.3.3 SOCS-2

SOCS-2 has been discovered to be the most abundant in human fetal kidney as well as adult heart, liver, pancreas and skeletal muscle, whereas moderate expression was also observed in adult kidney, thymus, prostate, testis, small intestine and colon (Dey et al., 1998, Minamoto et al., 1997). In addition, similar expression profiles were found in mice which showed prominent expression of SOCS-2 in lung, liver, salivary gland, testis, muscle and kidney (Metcalf et al., 2000). SOCS-2 has been extensively studied and found to be involved in regulating a variety of a cytokine induced signalling pathways where the imbalance of SOCS-2 is also considered to be related to a broad range of pathologies (Rico-Bautista *et al.*, 2006) (Table 1-7).

Table 1-7 Summary of the association between SOCS-2 and key cytokines/growth factors together with the regulatory roles played by SOCS-2

Cytokines /growth factors that induce SOCS-2	Regulatory role of SOCS-2 in signalling pathway	Reference
GH	Associate with GHR on on Y487 and Y595; inhibit the GHR-dependent tyrosine phosphorylation of JAK-2 via the association with GHR for GHR degradation; suppress the activation of STAT-5; negatively regulate GH signal through proteasomal degradation; interfere with the inhibitory effect of SOCS proteins on GH signalling; block the GH-mediated inhibition of neuronenin-1 expression to promote neuronal differentiation	(Adams et al., 1998, Greenhalgh et al., 2002a, Vesterlund et al., 2011, Dogusan et al., 2000, Piessevaux et al., 2006, Ram and Waxman, 1999, Miller et al., 2004, Turnley et al., 2002, Uyttendaele et al., 2007, Greenhalgh et al., 2002b, Favre et al., 1999)
Estrogen	Inhibit GH signalling vis GH/JAK/STAT pathway upon estrogen stimulation	(Leung et al., 2003)
EPO		(Starr et al., 1997, Wang et al., 2004)
PRL	Associate with PRLR; supress the activation of STAT-5; restore PRL signalling through the inhibitory effect of SOCS-1	(Pezet et al., 1999, Harris et al., 2006, Dogusan et al., 2000)
IL-1- β		(Dogusan et al., 2000)
IL-2	Enhance IL-2-induced STAT activation through the association with SOCS-3 for degradation	(Minamoto et al., 1997, Tannahill et al., 2005, Brender et al., 2001b)
IL-3	Enhance IL-2-induced STAT activation through the association with SOCS-3 for degradation	(Minamoto et al., 1997, Tannahill et al., 2005)
IL-6		(Dogusan et al., 2000)
IL-9		(Lejeune et al., 2001)
IL-10		(Shen et al., 2000)
IL-15	Regulate human NK cell effector function through the interaction with phosphorylated proline-rich tyrosine kinase 2 on Y402 to facilitate its degradation in a IL-15-dependent	(Lee et al., 2010)

	manner	
G-CSF		(Minamoto et al., 1997)
GM-CSF		(Faderl et al., 2003)
CNTF		(Bjorbaek et al., 1999)
IFN- α	Interfere with the inhibitory effect of SOCS proteins on IFN signalling; inhibit IFN- α -induced reporter activity	(Brender et al., 2001b, Piessevaux et al., 2006, Shen et al., 2000)
IFN- γ	Interfere with the inhibitory effect of SOCS proteins on IFN signalling	(Dogusan et al., 2000, Piessevaux et al., 2006)
LIF	Suppress the apoptotic effect of LIF	(Minamoto et al., 1997)
Insulin		(Sadowski et al., 2001)
lipoxin	Participate in lipoxin-induced IL-12 suppression to regulate inflammation	(Machado et al., 2006)
	Associate with EGFR and sustain phosphorylation of Y845 of EGFR to regulate neurite outgrowth	(Goldshmit et al., 2004)
	Interfere with the inhibitory effect of SOCS proteins on leptin signalling; associate with leptin receptor on Y1077, and block interaction of CIS with STAT-5 at this site	(Piessevaux et al., 2006, Lavens et al., 2006)
	Associate with activated IGF-1R	(Dey et al., 1998)
	Negatively regulate IGF-1 to inhibit cell proliferation; associate with IGF-1 and inhibit IGF-1-induced STAT-3 activation	(Horvat and Medrano, 2001, Metcalf et al., 2000, Miller et al., 2004, Dey et al., 1998, Zong et al., 2000)
	Associate with Tropomyosin-related kinase A (TrkA) expression upon neurotrophin binding, and increase TrkA expression on cell surface to promote neuronal survival and neurite outgrowth potentially through sustained activation of pAkt and pERK1/2	(Uren et al., 2014)

	Interact with fms-like tyrosine kinase 3 (FLT-3) on Y589 and Y919 for degradation and negatively regulate internal tandem duplication mutated FLT-3 (FLT-3-ITD)-dependent STAT-5 activation to regulate cells proliferation	(Kazi and Ronnstrand, 2013)
	Negatively regulate the mutant JAK-2 (JAK2V617F-activating mutation)-induced STAT-5 activation	(Quentmeier et al., 2008)

1.4.3.3.1 *In vivo* role of SOCS-2

SOCS-2 deficient mice were found to display gigantism symptoms following weaning, although most organs were shown to be histologically normal. Such phenotypes resembled those shown in both GH and IGF-1 transgenic mice (Metcalf et al., 2000). Further investigation on the same SOCS-2 deficient mouse model and primary cells generated from this demonstrated that SOCS-2 could regulate neural progenitor cells differentiation (Turnley et al., 2002). Interestingly, in contrast to the hypothesis that overexpression of SOCS-2 in mice could lead to growth defects, SOCS-2 overexpression mice showed a hypergrowth phenotype which resembled that observed in SOCS-2 deficient mice, indicating the positive role of SOCS-2 in GH signalling. Therefore, SOCS-2 has been suggested to have a dual effect on GH signalling .

1.4.3.3.2 SOCS-2 and wound healing

It has been suggested that SOCS-2 is an important anti-inflammatory regulator and is required for immune responses in diverse pathologies (Machado et al., 2006). Therefore, SOCS-2 holds the potential to play regulatory roles in the inflammatory phase in the wound healing process. It was found that SOCS-2 increased IL-2-dependent STAT phosphorylation via the association with SOCS-3 to facilitate its proteasomal degradation as well as blocking the interaction of CIS with STAT-5 (Tannahill et al., 2005, Lavens et al., 2006), a inverse function to CIS, SOCS-1 and SOCS-3 on IL-2 regulation. Together with that evidence that IL-2 elevated fibroblast infiltration during wound healing (Efron and Moldawer, 2004), it appears that SOCS-2 may help to restore the balance of IL-2 signalling regulated by other SOCS family members.

SOCS-2 was also found to be able to associate with EGFR at the Y845 Src binding site and to decrease STAT-5b phosphorylation stimulated by EGF, indicating its negative regulatory role on EGF-induced signalling (Goldshmit et al., 2004). Upon EGF binding, EGFR is activated and facilitates re-epithelialisation by inducing the proliferation and migration of keratinocytes (Barrientos et al., 2008). Thus, SOCS-2 may potentially suppress the re-epithelialisation via suppression of EGFR activation.

1.4.3.4 SOCS-3

1.4.3.4.1 SOCS-3, a diverse regulatory factor

SOCS-3 is expressed in the spleen, thymus and lung in mice (Starr et al., 1997), whereas in humans, SOCS-3 is expressed in a greater number of tissues. The highest expression of SOCS-3 was observed in adipose, lung ovary and aortic tissue, and moderate expression of SOCS-3 is found in blood leucocyte, placenta, trachea and colon (Kato et al., 2006). The expression pattern of SOCS-3 in normal human tissues indicates that SOCS-3 is predominantly expressed in macrophages, immature myeloid DCs and endothelial cells, whereas moderately positive expression of SOCS-3 was found in neutrophils and some B and T-lymphocytes. Additionally, SOCS-3 is found to be occasionally expressed in natural killer cells and many types of epithelium (White et al., 2011). SOCS-3 has been documented to be induced by a wide range of cytokines and growth factors, and acts as negative feedback inhibitor to these molecules to maintain the homeostasis of the activated signalling pathway, thus regulating cell behaviour and metabolisms. (Table 1-8) SOCS-3 holds the greatest sequence homology to SOCS-1 and similarly but not identically to SOCS-1, the inhibitory mechanism of SOCS-3 on the catalytic activity of JAK proteins mainly depends on its binding to the activated receptors

rather than directly interacting with JAK proteins or competing for the docking site with STAT proteins (Alexander, 2002). SOCS-3 has been shown to be an important mediator of insulin and pro-inflammatory cytokines.

Table 1-8 Summary of the association between SOCS-3 and key cytokines/growth factors together with the regulatory roles played by SOCS-3

Cytokines /growth factors that induce SOCS-3	Regulatory role of SOCS-3 in signalling pathway	Reference
IL-1 β	Prevent IL-1 β -induced toxicity through the inhibition of inducible nitric oxide synthase (iNOS) expression	(Boisclair et al., 2000)
IL-2	Associate with JAK-1 and inhibit its phosphorylation through the interaction with IL-2R β chain; suppress the STAT-5b activation; inhibit IL-2-mediated lymphocyte proliferation; associate with Ras inhibitor, p120 RasGAP, to maintain ERK activation upon tyrosine phosphorylation by IL-2 on Y211	(Cohney et al., 1999, Cacalano et al., 2001)
IL-3	Inhibit IL-3-mediated lymphocyte proliferation; block STAT-3 activation to contribute to the inhibitory effect of IL-3 on IL-11 signalling	(Cohney et al., 1999, Magrangeas et al., 2001a)
	Inhibit IL-4-induced STAT-6 activation and gene transcription	(Losman et al., 1999)
IL-6	Inhibit phosphorylation of IL-6-induced STAT-1 and STAT-3; inhibit IL-6-induced macrophage differentiation; regulate IL-6 signalling via the association with JAK-gp130 to block substrate binding of JAK and facilitate JAK ubiquitination; suppress IL-6-stimulated migration and proliferation of vascular smooth muscle cells by blocking STAT-3 activation	(Crocker et al., 2003, Nicholson et al., 1999, Brender et al., 2007, Song and Shuai, 1998, Starr et al., 1997, Xiang et al., 2013, Yasukawa et al., 2003, Kershaw et al., 2014, Niemand et al., 2003)
IL-9	Inhibit the IL-9-induced STAT-1, -3, -5 activation; suppress IL-9-mediated anti-apoptotic effect	(Lejeune et al., 2001)
IL-10	Partially attenuate IL10-triggered biological response; involved in the attenuation of oxidized low-density lipoprotein (oxLDL)-induced apoptosis by IL-10 through inhibition of p38 MAPK and c-Jun N-terminal kinase (JNK) activation	(Shen et al., 2000, Berlatto et al., 2002, Yin et al., 2013)
IL-11	Negatively regulate IL-11-mediated adrenocorticotrophic hormone	(Auernhammer and Melmed,

	(ACTH) production	1999)
	Inhibit IL-12-induced STAT-4 activation through the association with IL-12R β 2 Y800	(Egwuagu et al., 2002, Yamamoto et al., 2003, Seki et al., 2003)
IL-22		(Kotenko et al., 2001)
	Inhibit IL-23-mediated STAT-3 activation; inhibit generation of Th17 cell	(Chen et al., 2006, Li et al., 2006)
	Negatively regulate IL-27-mediated mitogenic signals to T cells	(Brender et al., 2007)
IFN- α	Inhibit IFN- α -dependent STAT-1 tyrosine phosphorylation and nuclear translocation; inhibit the anti-proliferative and antiviral effect of IFN- α ; inhibit IFN- α -induced reported activity	(Song and Shuai, 1998, Shen et al., 2000, Hong et al., 2001)
IFN- β	Attenuate IFN- β chemokine-related inflammation	(Qin et al., 2008)
IFN- γ	Inhibit the anti-proliferative and antiviral effect of IFN- γ ; suppress the IFN- γ -mediated STAT1 phosphorylation at Y701 and the association of STAT-1 and DNA; suppress the IFN- γ -stimulated migration and proliferation of vascular smooth muscle cells by blocking STAT-3 activation	(Song and Shuai, 1998, Park et al., 2000, Xiang et al., 2013)
TGF- β	Negatively regulate TGF- β 1/Smad-3 signalling through the association with Smad-3 to suppress its nuclear translocation and transcription activity	(Liu et al., 2008b)
EPO	Associate with EPOR Y401 and JAK-2 to inhibit STAT-5 activation and EPO-mediated proliferation; associate with Ras inhibitor, p120 RasGAP, to maintain ERK activation upon tyrosine phosphorylation by EPO on Y211	(Sasaki et al., 2000, Cacalano et al., 2001, Marine et al., 1999a)
GH	Block the GH-induced transactivation effect; inhibit GH-induced STAT-5 activation; inhibit JAK-2 activity in a GHR-dependent manner	(Adams et al., 1998, Hansen et al., 1999)
PRL	Suppress PRL-stimulated signal through the association with JAK-2	(Pezet et al., 1999, Helman et al.,

	and inhibit STAT-5-mediated transcription; inhibit PRLR-mediated signalling	1998)
Leptin	Suppress leptin-mediated signal transduction	(Bjorbaek et al., 1998)
Angiotensin II (Ang II)	Attenuate Ang II-induced JAK-2/STAT-1 activation through the association with JAK-2	(Calegari et al., 2003)
GM-CSF		(Faderl et al., 2003)
CNTF	Inhibit CNTF-induced signal transduction in astrocytes	(Bjorbaek et al., 1999)
TPO		(Wang et al., 2000)
TNF- α	Contribute to the inhibitory effect of TNF- α on IFN- α signalling and TNF- α mediated degradation of IRS-1 and IRS-2	(Hong et al., 2001, Shi et al., 2004)
OSM	Inhibit OSM-induced STAT-3 activation and nuclear translocation; attenuate OSM-mediated ERK1/2 activation	(Song and Shuai, 1998, Magrangeas et al., 2001b)
EGF	Associate with Ras inhibitor, p120 RasGAP, to maintain ERK activation upon tyrosine phosphorylation by EGF on Y211; contribute to the inhibitory effect of EGF on PRL-induced STAT-5 activation	(Cacalano et al., 2001, Tonko-Geymayer et al., 2002)
PDGF (induce SOCS-3 phosphorylation)	Associate with Ras inhibitor, p120 RasGAP, to maintain ERK activation upon tyrosine phosphorylated by EGF on Y211	(Cacalano et al., 2001)
basic fibroblast growth factor (bFGF)		(Terstegen et al., 2000)
LIF	Inhibit LIF-induced macrophage differentiation; suppress LIF-mediated STAT-3 tyrosine phosphorylation	(Nicholson et al., 1999, Adams et al., 1998)
TSH	Associate with JAK-1 and JAK-2 upon TSH stimulation	(Park et al., 2000)
resistin	Help resistin antagonise insulin signalling	(Steppan et al., 2005)
insulin	Inhibit insulin-induced STAT-5b activation via the competition to IR binding motif Y960; attenuate insulin signalling through the association with IRS-1 and IRS-2 for proteasomal degradation; inhibit	(Sadowski et al., 2001, Emanuelli et al., 2000, Rui et al., 2002, Liu et al., 2008a)

	insulin-induced PI3K/Akt activation	
LPS	Inhibit LPS-mediated IL-6 production and suppress CCAAT/enhancer-binding protein- β (C/EBP- β) activity via N-terminal KIR, SH2 domain Y204 and SOCS box; attenuate LPS-induced STAT-1 α and STAT-3 activation	(Yan et al., 2010, Qin et al., 2006)
	Inhibit C-X-C Motif chemokine Ligand-12 (CXCL-12) signalling through the association with C-X-C chemokine receptor- 4 (CXCR-4); attenuated CXCL-12 induced CXCR-4-dependent focal adhesion kinase (FAK) signalling by enhancing the FAK ubiquitination for proteasomal degradation	(Soriano et al., 2002, Le et al., 2007)
G-CSF	Suppress G-CSF-mediated STAT-3 activation; negatively regulate G-CSF-driven signalling in myeloid cells; negatively regulate G-CSF-induced STAT-5 activation; associate with G-CSFR on Y729 for ubiquitination	(Croker et al., 2004, van de Geijn et al., 2004, Irandoust et al., 2007)
	Inhibit IGF-1-induced STAT-3 activation; interact directly with activated IGFIR	(Zong et al., 2000, Dey et al., 2000)
	Negatively regulate IL-2 production by CD28 through the association with phosphorylated CD28	(Matsumoto et al., 2003)
	Associate with DP-1 on amino acids 156 and 172 to regulate cell cycle through the inhibition of E2F/DP-1 transcriptional activity	(Masuhiro et al., 2008)
	Disrupt cell apoptosis by sustaining the activation of PI3K/Akt for the activation of nuclear factor-kappa B (NF- κ B) as well as inhibiting BAD	(Madonna et al., 2012)
	Suppress TCR-mediated IL-2 production by preventing dephosphorylation of activated nuclear factor of activated T-cells (NFAT); inhibit calcineurin-mediated signalling through the association with its catalytic subunit	(Banerjee et al., 2002)

1.4.3.4.2 *In vivo* role of SOCS-3

SOCS-3 knockout mice express fatal placental defects and embryonic lethality (Roberts et al., 2001). Although this phenotype could be temporarily rescued by leukaemia inhibitory factor receptor (LIFR) deficiency (Takahashi et al., 2003), the dual deficient SOCS-3 and LIFR mice exhibited fatal inflammatory disease and high neonatal mortality (Robb et al., 2005). Additionally, absence of SOCS-3 in mice led to lethal inflammatory response, however, IL-6 deficiency extended the survival time of this phenotype, suggesting the anti-inflammatory role of SOCS-3 in IL-6-mediated signalling (Crocker et al., 2012). Mice lacking SOCS-3 in macrophages or hepatocytes helped to demonstrate the complementary role of SOCS-3 and SOCS-1 on regulating cytokine signalling (Crocker et al., 2003). Hematopoietic-specific SOCS-3 knockout mice developed a range of inflammatory pathologies after young adulthood (Crocker et al., 2004). The progenitor cells of such mice exhibited skewed differentiation from neutrophils toward macrophages, indicating the maintenance role of SOCS-3 on cell differentiation specificity in response to cytokine signalling (Crocker et al., 2008b). T cell conditional knockout mice were generated and such mice displayed no significant difference in thymus or spleen as well as the proportions of CD4⁺ and CD8⁺ cells, except for enlarged lymph nodes. However, such phenotypes displayed increased responses to TCR engagement and was hypersensitive to gp130 cytokine stimulation (Brender et al., 2007). Another neural cell-specific SOCS-3 deficient mouse model displayed enhanced leptin response, resulting in body weight loss and suppression of food intake (Mori et al., 2004), suggesting the regulatory role of SOCS-3 in leptin signalling. Such evidence emphasised the importance of SOCS-3 in T cell activity and differentiation. Furthermore, a keratinocyte-specific SOCS-3 knockdown mouse model exhibited a severe skin inflammation phenotype along with epidermal

hyperplasia, suggesting an essential regulatory role of SOCS-3 in proinflammatory responses (Uto-Konomi et al., 2012).

The establishment of a SOCS-3 constitutive expression mouse model resulted in embryonic lethality due to fetal erythropoiesis blockage, which is similar to the phenotype seen in JAK-2 or erythropoietin receptor deficient mouse models and suggests a regulatory role of SOCS-3 in fetal liver hematopoiesis, possibly through JAK-2 or erythropoietin receptor-dependent signalling (Marine et al., 1999a). Another study on SOCS-3 transgenic mice and heterologous mice demonstrated that SOCS-3 impaired CD28-mediated IL-2 production and NF- κ B activation in primary T cells (Matsumoto et al., 2003). In addition, SOCS-3 transgenic mice exhibited increased Th2 responses and Th2-related allergic disease phenotypes (Seki et al., 2003). Moreover, SOCS-3 overexpression in mice showed suppressed Th17 differentiation due to inhibition of STAT-3 activation (Tanaka et al., 2008). These evidences emphasised the important role of SOCS-3 in T cell activation and differentiation. Furthermore, the keratinocyte-specific SOCS-3 overexpression mice displayed prolonged inflammation and severe impairment of wound closure, interfering with the proliferation and migration of keratinocytes in the epidermis (Linke et al., 2010b, Linke et al., 2010a).

1.4.3.4.3 SOCS-3 and wound healing

Many studies have shown that SOCS-3 is a regulator of a pool of pro-inflammatory cytokines, such as IL-2, IL-6, TNF- α , IFN- α , - β , - γ (Table 1-8). Enhanced expression of IL-6, a pro-inflammatory cytokine, was observed during the inflammatory phase of wound healing. In addition, IL-6 is considered to be an essential initiator of the wound healing process due to its mitogenic and proliferative effect on keratinocytes and the chemoattractive function of neutrophils (Barrientos et al.,

2008). Moreover, evidence showed that SOCS-3 inhibits IL-1 β induced signalling (Karlsen et al., 2001) and that IL-1 β exhibited similar expression patterns and synergistic roles to TNF- α in chronic wounds. Taken together, SOCS-3 may play an important role in regulating the homeostasis of cytokine signalling in the inflammation phase of wound healing.

Another study, investigating the downstream mechanism of psoriasis, unveiled that the anti-apoptotic mechanism utilised by SOCS-3 in keratinocytes was through the sustained activation of PI3K/Akt, which in turn activates nuclear factor-kappa B (NF- κ B), an apoptosis protector, and in parallel, inhibits the pro-apoptotic function of BAD (Madonna et al., 2012), thus, SOCS-3 may potentially be involved in mediating keratinocytes survival in chronic wound, another pathological condition in wound healing.

A previous study has demonstrated a positive regulatory role of SOCS-3 in toll-like receptor-4 (TLR-4) response in macrophages, and SOCS-3 negatively mediates endogenous TGF- β 1-induced Smad-3 signalling to restore the production of TNF- α and IL-6 (Liu et al., 2008b). One of the key functions of TGF- β 1 is the production of cytokines and inflammatory mediators during wound healing (Border and Ruoslahti, 1992). Therefore, SOCS-3 may indirectly modulate wound healing by regulating the cytokine production of TGF- β 1. Similar to SOCS-1, SOCS-3 could also suppress HGF-induced STAT-3 activation. Since SOCS-1 and SOCS-3 have the closest sequence homologies, they may compensate for each other on the regulation of HGF signalling during wound healing.

1.4.3.4.4 Implication of SOCS-3 in a variety of diseases and cancer

1.4.3.4.4.1 SOCS-3 in immune diseases

Clinical investigation of ulcerative colitis biopsies showed that the transcript expression level of SOCS-3 correlated with grade assessment using both endoscopic and histologic techniques (Miyataka et al., 2007). An investigation of polytraumatised patients indicated significantly elevated expression levels of SOCS-3 mRNA in neutrophil granulocytes immediately after the traumatic event, and those who died within 90 days displayed significant higher SOCS-3 mRNA expression compared to those who survived (Brumann et al., 2014). This might suggest that the overexpression of SOCS-3 impaired normal immune function which then lead to fatality. An additional study on the intestinal T cells from patients with Crohn's disease demonstrated constitutive expression of both SOCS-3 and STAT-3 compared to healthy volunteers. Due to the negative regulatory role of SOCS-3 on the stimulation of various cytokines, this constitutive expression of SOCS-3 may cause resistance to exogenous cytokines for Crohn's disease patients (Lovato et al., 2003).

Introduction of SOCS-3, by injection of recombinant adenovirus carrying SOCS-3 cDNA, markedly repressed the symptoms of arthritis in an arthritic mouse model and the inhibitory role of SOCS-3 on STAT-3 activity was suggested as a potential therapeutic strategy for the treatment of rheumatoid arthritis (Shouda et al., 2001). Another study on using SOCS-3 deleted mouse models in hematopoietic and endothelial cells demonstrated severe IL-1-dependent inflammatory arthritis with increased neutrophil synovium infiltrate and elevated osteoclast generation as well as bone destruction, suggesting a negative regulatory role of SOCS-3 in inflammatory joint disease (Wong et al., 2006).

Further *in vivo* study demonstrated that SOCS-3 could skew T cells differentiation to Th2 cells (Li et al., 2006). Additionally, given that Th2 cells are considered to have important pathogenetic roles in immune dysfunction which characterises atopic dermatitis (Leung, 1995), and that the expression level of SOCS-3 transcript was found significantly elevated in patients with atopic dermatitis compared to healthy controls (Arakawa et al., 2004), it suggested that SOCS-3 could potentially contribute to atopic dermatitis pathogenesis by enhancing Th2 cells differentiation. Another study also suggested a correlation between SOCS-3 expression and the severity of atopic dermatitis and asthma. Therefore, a transgenic SOCS-3 mouse model and dominant-negative SOCS-3 mutant mouse models were established for further investigation into the regulatory role of SOCS-3 in Th2 cell related pathogenesis, indicating that SOCS-3 has an essential role in the maintenance of Th2-regulated allergic diseases (Seki et al., 2003). Further investigation was implemented by Moriwaki and colleagues, which demonstrated that suppression of SOCS-3 in CD4⁺ T cells helped relieve the development of allergic inflammation in an allergic mouse model of asthma, indicating a potential therapeutic approach for allergic diseases (Moriwaki et al., 2011).

A new approach utilising intranasal treatment with SOCS-3-small interfering RNA (siRNA) to achieve SOCS-3 silencing in the whole lung environment in chronic asthmatic mouse models was examined afterwards, leading to an improvement in chronicity and remodelling and, demonstrating an alternative and easily administered potential therapeutic for asthma patients (Zafra et al., 2014). Another study on an allergen-induced allergic conjunctivitis (AC) mouse model showed that overexpression of SOCS-3 in T cells led to the deterioration of AC, whereas, T cell specific SOCS-3 deletion could rescue the AC

phenotype. This evidence further indicates that SOCS-3 could be a potential target for therapeutic intervention in allergic disease (Ozaki et al., 2005).

1.4.3.4.4.2 SOCS-3 in vascular inflammatory diseases

SOCS-3 is believed to be involved in atherosclerosis due to the fact that significantly higher expression of SOCS-3 in vascular smooth muscle cells (VSMCs) and macrophages was found in the inflammatory region in human plaques as well as in aortic lesions from atherosclerosis development mouse models. Further study demonstrated that SOCS-3 depletion in mice increased the presence of VSMCs, CD4⁺ T lymphocytes and macrophages in the aortas, suggesting the inhibitory role of SOCS-3 in leukocyte infiltration and VSMCs proliferation in atherosclerosis (Ortiz-Munoz et al., 2009). Consistent results were observed in a study focusing on a T cell specific-SOCS-3 depletion mouse model which induced an anti-inflammatory effect on macrophages.

Additionally, the correlation between the expression profile of IL-17, phosphorylated STAT-3 in dissected human atherosclerotic plaques and the stability of the plaque phenotype was consistent with the finding in SOCS-3 deficient mice models. However, SOCS-3 overexpression models exhibited increased lesion size, and was found to promote atherosclerotic lesion development, possibly via the suppression of IL-17, leading to increased T cell infiltration and vascular inflammation. Given that *in vivo* administration of IL-17 reduced the vascular T cell infiltration and atherosclerotic lesion development, SOCS-3 seems to accelerate the development of atherosclerosis (Taleb et al., 2009). Regardless of this controversy and diversity, SOCS-3 has been demonstrated to be an important regulatory factor in atherosclerosis.

SOCS-3 has also been linked to heart disease. The markedly decreased gp130 protein level and the enhanced gp130/SOCS-3 protein expression ratio in human heart failure myocardial tissues comparing to control donors heart samples suggest the inactivation of gp130 signalling pathway (Zolk et al., 2002). This is in agreement with the proposal that SOCS-3 could potentially be a pharmaceutical target to cardiac disease due to its regulatory role in gp130-dependent pathways, a important receptor in cardiac hypertrophy and heart failure (Yasukawa et al., 2001).

1.4.3.4.4.3 SOCS-3 in metabolic diseases

SOCS-3 has also been linked to a number of metabolic diseases and disorders and has been suggested to mediate glucose homeostasis regulated by metabolic hormones such as lepin and insulin. This was implicated through a study on heterozygous SOCS-3 deficient mice which showed enhanced sensitivity to exogenous leptin administration and resistance to the development of diet-induced obesity (Howard et al., 2004). Such phenotypes were also exhibited in neural cell-specific SOCS-3 knockout mouse models. Neural cell specific SOCS-3 knockout mouse models were generated to elucidate the function of SOCS-3 on leptin signalling. These demonstrated that leptin resistance could be rescued by SOCS-3 deficiency in the brain, and leptin-induced STAT-3 phosphorylation was elevated, leading to significant body weight loss as well as a reduction of food intake. Such evidence indicates that SOCS-3 plays negative regulatory roles in lepin signalling, and highlights the concept of a potential therapeutic method of targeting SOCS-3 in the brain for the treatment of leptin resistance (Mori et al., 2004).

Similar to the effect on leptin, insulin resistance was found in SOCS-3 overexpression mouse models and evidence demonstrated that SOCS-3 regulated insulin resistance by antagonising STAT3-mediated inhibition of sterol regulatory element-binding protein (SREBP)-1c promoter activity (Ueki et al., 2004). It was later demonstrated by *in vivo* study that SOCS-3 could regulate leptin sensitivity in pro-opiomelanocortin (POMC) expressing neurons (Kievit et al., 2006), and POMC neurons are important to the regulatory role of SOCS-3 in metabolic abnormalities, however, it seems that this regulatory role of SOCS-3 could only be effective in specific cell types (Reed et al., 2010). Adipose tissue-specific SOCS-3 overexpression mouse models suppressed insulin signalling in adipocyte, and exhibited resistance to diet-induced obesity partially by suppressing lipogenesis and increasing lipolysis, although this was not sufficient to systemic insulin resistance (Shi et al., 2006). Mouse models with SOCS-3 deficiency in liver showed enhanced insulin sensitivity in the liver at a young age, whereas, systemic insulin resistance was found in such aged mice due to the hyperactivation of STAT-3 which produces acute-phase proteins, leading to dysregulation of lipid and glucose metabolism (Torisu et al., 2007). Another study exhibited that liver specific SOCS-3 deletion only enhanced the insulin sensitivity of chow diet mice, whereas, the high fat diet contributed to greater hepatic insulin resistance in this genotype (Sachithanandan et al., 2010).

The phenotype of skeletal muscle-specific SOCS-3 overexpression exhibited the blockage of both insulin and leptin-dependent signalling, indicating the antagonistic role of SOCS-3 in insulin-dependent glucose disposal (Yang et al., 2012). However, study on the skeletal muscle-specific deletion of SOCS-3 mice demonstrated that skeletal muscle SOCS-3 was not required for regulating whole-body energy expenditure and the SOCS-3 knockout genotype did not protect from

diet-induced obesity but prevented from obesity-induced glucose intolerance and insulin resistance (Jorgensen et al., 2013). Taken together,

SOCS-3 is considered to be an important contributing factor for obesity associated leptin and insulin resistance as well as type 2 diabetes.

1.4.3.4.4.4 SOCS-3 in cancer

Since a variety of inflammatory mediators are of importance and utilise JAK/STAT signalling to exert their function in cancer associated inflammation, the role of SOCS-3, a negative feedback regulator of cytokine signalling, primarily mediated through regulation of JAK/STAT signalling, has been investigated in cancer initiation and progression. Lower or non-expression of SOCS-3 was found in lung cancer cells and this SOCS-3 silencing results from hypermethylation in the *SOCS-3* promoter region. Furthermore, restoration of SOCS-3 expression led to decreased STAT-3 activation and growth suppression of lung cancer cells, indicating the inhibitory role of SOCS-3 in lung cancer pathogenesis (He et al., 2003). A study on SOCS-3 overexpression in intestinal epithelial cell (IEC) and Caco-2 cell lines indicated an anti-proliferative role of SOCS-3 in colon cancer cells. Further study on IEC specific SOCS-3 knockout mice models demonstrated that SOCS-3 inhibits crypt proliferation and hyperplasia in the colon upon acute injury. Additionally, SOCS-3 was proposed to be a tumour suppressor as increased tumour size and number was found in IEC-selective SOCS-3 deleted mice compared to that of in wild-type littermates after chronic inflammatory treatment, SOCS-3 was proposed to be a tumour suppressor (Rigby et al., 2007).

It has been suggested that IL-6 trans-signalling as well as the STAT-3/SOCS-3 pathway were involved in pancreatic intra-epithelial neoplasias progression and pancreatic ductal adenocarcinoma development and SOCS-

deficient Kras^{G12D} mice increased the progression of pancreatic cancer (Lesina et al., 2011), which is in agreement with the results found in lung and colon cancer. Gastrointestinal epithelial cell-specific SOCS-3 conditional knockout mice expressed enhanced lepin production and STAT-3 hyperactivation, and the phenotype of such SOCS-3 deficient mice resembled the pathology and molecular alterations found in human intestinal-type gastric tumours, although inflammatory responses were not required for this gastric tumorigenesis. This demonstrated the anti- tumorigenic role of SOCS-3 in gastric tumours (Inagaki-Ohara et al., 2014). However, the regulatory role of SOCS-3 in cancer seems to be more complicated and might be cell type specific.

SOCS-3 has also been suggested to be unlikely to possess tumour suppressive effects on breast cancer and ovarian cancer tissues (Sutherland et al., 2004). Investigation of prostate cancer cells suggested that SOCS-3, acting as a tumour cell protector against growth inhibition, was induced by the cAMP derivative and could antagonise the inhibitory function of cyclic adenosine monophosphate (cAMP) on the proliferation and apoptosis of prostate cancer cells (Bellezza et al., 2006). Another study showed that increased expression of SOCS-3 correlated with the development and progression of prostate cancer (Puhr et al., 2009). Further *in vitro* study on prostate cancer cell lines exhibited that SOCS-3 knockdown increased IL-6 induced cell apoptosis via activation of STAT-3 (Puhr et al., 2009). In a separate study, macrophage specific-SOCS-3 deleted mice exhibited increased survival rate after being challenged with melanoma cells, indicating a potential protective role of SOCS-3 in tumour metastasis (Hiwatashi et al., 2011).

SOCS-3 was also found to be constitutively expressed in T cell lymphoma cell lines, and this phenotype accounts for the prolonged IFN- α -induced STAT-3

activation (Brender et al., 2001a). Additionally, constitutive expression of SOCS-3 was detected in the majority of chronic myelogenous leukaemia cell lines, which conferred such cell lines with resistance to IFN- α therapy (Sakai et al., 2002). Moreover, tumour cells generated from cutaneous T cell lymphoma patients exhibited constitutive expression of SOCS-3 through the constitutive activation of STAT-3, leading to the attenuation of IFN- α -dependent growth inhibition (Brender et al., 2005).

1.4.3.5 SOCS-4

SOCS-4 is the least investigated member of the SOCS family. Study on the expression profile of SOCS family members in porcine tissue demonstrated that the highest expression of SOCS-4 was found in the small intestine, large intestine and thymus, although little variation in expression between different tissues was observed (Delgado-Ortega et al., 2011). To date, there are not many studies available to fully recognise the function of SOCS-4. Fortunately, the establishment of the SOCS-4-elongin-C-elong-B model has helped to aid in the elucidation of structural aspects of SOCS-4. SOCS 4 adapts an alternative packaging structure to that of earlier members of the family, CIS/SOCS1–3. This alternative packaging solution stabilises the SH2 region enabling SOCS-4 to be more stable and rigid than the alternative packaging structure seen in the CIS/SOCS-1–SOCS-3 sub-family (Bullock et al., 2007, Bullock et al., 2006). These initial studies have highlighted structural differences within SOCS-4 in comparison to other family members, though much work remains to fully elucidate its full biological significance. Table 1-9 summarises known cytokine/growth factor interactions and regulatory roles of SOCS-4.

Table 1-9 Summary of the association between SOCS-4 and key cytokines/growth factors together with the regulatory roles played by SOCS-4

Cytokines /growth factors that induce SOCS-4	Regulatory role of SOCS-4 in signalling pathway	Reference
EGF	Negatively mediate EGFR activity; highly associate with EGFR on Y1092 to compete with STAT-3	(Kario et al., 2005, Bullock et al., 2007, Scheitz et al., 2012)
LIF	Interact with cardiotrophin-like cytokine (CLC, a IL-6 cytokine), poly(rC) binding protein 1 (Pcbp1, affecting STAT-3 activation) and cytosolic malae dehydrogenase (Mdh1, influencing cell cycle), contributing to ovarian follicular development	(Sutherland et al., 2012)
	Inhibit STAT-3 and STAT-6 phosphorylation	(Hu et al., 2010)
	Potentially modulates TLR2 signalling; modulate EGFR/STAT-3 signalling and IL-6 production	(Arts et al., 2015)

1.4.3.5.1 *In vivo* role of SOCS-4

SOCS-4 deficient mice, compared with control wild type littermates, exhibited increased susceptibility to infection with influenza A, showing delayed viral clearance, dysregulation of proinflammatory cytokines and chemokines, and impaired trafficking of virus-specific CD8 T cells to the infection site. This evidence suggests a regulatory role for SOCS-4 in the inflammatory response to influenza. Moreover, *in vitro* study on CD8 T cell from this mouse model has indicated the potential role of SOCS-4 in regulating TCR stimulation and signalling, a novel function of SOCS-4 (Kedzierski et al., 2014).

1.4.3.5.2 SOCS-4 and wound healing

The expression of SOCS-4 was found to be induced by *Cryptosporidium parvum* (a protozoan parasite) through the decrease of microRNA-98 and *let-7* which normally function to target the SOCS-4 3' untranslated region resulting in downregulation of SOCS-4 expression (Hu et al., 2010). In addition, an investigation seeking the link between genetic alteration and autoimmune disorder on a Turkish family highlighted that a *SOCS-4* mutation which impairs the function of SOCS-4 protein may hold the potential to modulate EGFR/STAT-3 signalling as well as IL-6 production (Arts et al., 2015). These data imply a possible mechanism of SOCS-4 in regulating autoimmunity. Moreover, convergence evaluation studies on animals which adapt to live in high-altitude environment suggested that SOCS-4 potentially acts as a regulator to hypoxia inducible factor (HIF)-1 α , a mediator required for adaptation to hypoxia, indicating the involvement of SOCS-4 in the regulation of hypoxia (Wang et al., 2015). Therefore, SOCS-4 may potentially have regulatory role in haemostasis and inflammation, the two early phases in the wound healing process.

SOCS-4 was also found to be induced by the stimulation of EGF and to be able to markedly reduce the expression of EGFR and EGFR-mediated signalling (Kario *et al.*, 2005). It was also discovered that SOCS-4 decreased STAT-3 activation by EGFR via enhanced EGFR degradation as well as through competing for the docking site with STAT-3 for the phosphorylated tyrosine residue Y1092 on EGFR (Bullock *et al.*, 2007). Moreover, SOCS-4 has been implicated in maintaining the homeostasis of keratinocyte proliferation via regulation of EGFR and STAT-3 activation since repressed SOCS-4 expression, brought about by Runx1, exhibited a hypergrowth phenotype (Scheitz *et al.*, 2012). Based on the importance of EGFR signalling and keratinocyte behaviour during the proliferation and re-epithelialisation phase in wound healing, SOCS-4 may act as a modulator to keep the balance of EGF-like protein signal transduction as well as epidermal cell function.

1.4.3.5.3 The involvement of SOCS-4 in cancer

Since inflammation and angiogenesis are both critical properties in wound healing and cancer, investigation on the involvement of SOCS-4 in cancer may also give clues to potential functions of SOCS-4 in wound healing. In breast cancer biopsies, higher mRNA expression of SOCS-4 were found to associate with better overall survival, and inversely correlated with TNM classification (Sasi *et al.*, 2010). A different study, investigating human gastric cancer biopsies showed attenuated expression of SOCS-4 compared to the control tissues, both in mRNA and protein level. In addition, the promoter hypermethylation of the *SOCS-4* gene, which impaires SOCS-4 expression, correlated with poor prognosis of gastric cancer patients (Kobayashi *et al.*, 2012). Another *in vitro* study on thyroid cancer cell lines indicated that the expression of SOCS-4 was attenuated by IL-23, a

proinflammatory cytokine, through up-regulation of the expression of microRNA-25 which targets the 3' untranslated region of *SOCS-4* gene, leading to elevated cell migration and invasion (Mei et al., 2015). These evidence suggested the role of *SOCS-4* in cancer may be tissue-dependent and may potentially hold different effects in distinct microenvironments.

1.4.3.6 SOCS-5

SOCS-5 is the most structurally similar member of the *SOCS* family to *SOCS-4*. It is expressed widely in murine tissues. The highest expression was found in the brain, lung, spleen and colon, whereas bladder, testis, eye and mesenteric lymph node (primarily in T and B cells) exhibited moderate expression (Hilton et al., 1998, Brender et al., 2004). Additionally, *SOCS-5* was found to be constitutively expressed in retina cells from mouse (Takase et al., 2005). The expression profile in human tissues indicated a variety of expression of *SOCS-5* in the spleen, lymph node, thymus, bone marrow, skeletal muscle, heart, brain, placenta and fetal liver (Magrangeas et al., 2000). Similarly to *SOCS-4*, *SOCS-5* is one of the more poorly studied members of *SOCS* proteins, although it has been documented to be able to negatively regulate cytokine and growth factor signalling. (Table 1-10)

Table 1-10 Summary of the association between SOCS-5 and key cytokines/growth factors together with the regulatory roles played by SOCS-5

Cytokines /growth factors that induce SOCS-5	Regulatory role of SOCS-5 in signalling pathway	Reference
EGF	Suppresses EGF mitogenic effect through the association with EGFR and use SOCS box to recruit E3 ubiquitin ligase to promote EGFR degradation	(Nicholson et al., 2005, Kario et al., 2005)
	Associate with IL-4R α chain to inhibit IL-4-mediated activation of STAT-6, resulting in skewed Th cell differentiation from Th2 to Th1	(Seki et al., 2002)
	Partially reduce IL-6 and LIF signalling	(Nicholson et al., 1999)

1.4.3.6.1 *In vivo* role of SOCS-5

A SOCS-5 overexpression mouse model was found to alleviate the symptoms of allergic conjunctivitis, a Th2 cell-mediated allergic disease (Ozaki et al., 2005). Moreover, enhanced bacterial clearance activity was found in a T cell specific-SOCS-5 overexpression mouse model compared to control littermates and this was found to be due to the alteration of cytokine balance in such phenotypes, indicating the importance of SOCS-5 in T cell related innate immunity (Watanabe et al., 2006). In contrast, a completely SOCS-5 deficient mouse model was also generated to investigate the regulatory role of SOCS-5 on lymphocytes since it has been found that SOCS-5 is expressed in primary B and T cells in wild-type mice. However, unexpected results were found, indicating that SOCS-5 deficient mice shown normal B and T cell development and no obvious phenotype deficiency comparing to the control littermates, suggesting that the function and the development of B and T cells seemed to be SOCS-5-independent (Brender et al., 2004). One potential explanation is due to the possible functional redundancy of SOCS-5 and other SOCS family members in lymphocytes modulation, since the expression of other SOCS members in primary T cells has been previously reported (Egwuagu et al., 2002).

1.4.3.6.2 SOCS-5 and wound healing

The constitutive expression of SOCS-5 and the increased SOCS-5 expression during experimental autoimmune uveitis suggested a negative regulatory role in the inflammatory response (Takase et al., 2005), raising the possibility that SOCS-5 acts as a mediator during wound healing.

It has been suggested that SOCS-5 specifically interacts with the IL-4 receptor α -chain and may functionally affect IL-4-induced STAT activation

regardless of receptor tyrosine phosphorylation status (Seki et al., 2002). During the wound healing process, IL-4, secreted by T lymphocytes, basophils and mast cells, is able to induce fibroblast proliferation, collagen production and arginase activity to promote wound healing (Efron and Moldawer, 2004). Taken together, SOCS-5 may affect the re-epithelialisation phases of wound healing through modulation of IL-4 signalling.

Similarly to SOCS-4, SOCS-5 can be induced by EGF stimulation and inhibited the activation of EGFR levels via proteasomal degradation (Kario et al., 2005, Nicholson et al., 2005). Upon injury, EGF, derived from platelets, macrophages and fibroblasts, accelerates re-epithelialisation via the activation of EGFR, and subsequently promotes the proliferation and migration of keratinocytes (Barrientos et al., 2008). Since SOCS-5 has the ability to interact with EGFR, and to promote the degradation of EGFR, investigation into the interaction between SOCS-5 and EGFR in wound healing models may hold the potential for the discovery of new therapeutic targets.

1.4.3.7 SOCS-6

SOCS-6 is another ubiquitously expressed SOCS protein whose distribution was found in many tissues and organs. However, relatively high expression of SOCS-6 has been found in spleen, lung, kidney, large intestine and salivary gland in comparison to testis, liver, bone marrow, heart and thymus in the adult mouse (Krebs et al., 2002). In addition, constitutive expression of SOCS-6 was also observed in human, mouse and rat retinal cells (Liu et al., 2008a). SOCS-6 was initially documented to be an insulin signal regulator (Krebs et al., 2002, Mooney et al., 2001, Li et al., 2004). However, further investigation uncovered that SOCS-6 is also involved in mediating cell proliferation signals, T cell receptor signals,

neuronal differentiation and potentially modulating the negative regulatory effect of SOCS proteins themselves (Table 1-11).

Table 1-11 Summary of the association between SOCS-6 and key cytokines/growth factors together with the regulatory roles played by SOCS-6

Cytokines /growth factors that induce SOCS-6	Regulatory role of SOCS-6 in signalling pathway	Reference
Insulin	Associate with IR in an insulin dependent manner; inhibit insulin-mediated activation of ERK1/2 and protein kinase B as well as IRS phosphorylation; interact with p85 PI3K in an insulin dependent manner to suppress the negative effects of p85 on glucose metabolism; associate with IRS-2, IRS-4 and p85 PI3K; promote retina cell survival through the maintenance of insulin-induced Akt signalling	(Mooney et al., 2001, Li et al., 2004, Krebs et al., 2002, Liu et al., 2008a)
IGF-1	Inhibit IGF-1 signalling through the association with IGFR and JAK-2 to inhibit STAT-5 activation	(Gupta et al., 2011)
Stem cell factor (SCF)	Associate with KIT substrate peptide residues 564-574, particularly Y567 and Y568, to reduce SCF-induced activation of ERK1/2 and p38 to reduce cell proliferation	(Bayle et al., 2004, Zadjali et al., 2011)
	Associate with FLT-3 Y591 and Y919 for internalisation and degradation of FLT-3 to inhibit FLT-3 activation as well as downstream ERK signalling pathway	(Kazi et al., 2012)
	Associate with activated p56(lck) F505 for subsequent degradation to repress T cell receptor (TCR) signalling	(Choi et al., 2010)
	Interact with the SOCS box of all members of SOCS to compromise their negative regulatory role	(Piessevaux et al., 2006)
	Localise in the nucleus via N-terminal region, and degrade nuclear STAT-3 through C-terminal region	(Hwang et al., 2007)
	Interact with Pim3 and inhibit ERK1/2 activity in response to glucose stimulation	(Vlacich et al., 2010)

1.4.3.7.1 *In vivo* role of SOCS-6

Transgenic mice overexpressing SOCS-6 developed normally despite increased glucose metabolism and insulin tolerance (Li et al., 2004). However, SOCS-6 deficient mice did not show significant differences in blood glucose and plasma insulin levels compared to the wild-type littermates. No glucose and insulin tolerance was found in such phenotype (Krebs *et al.*, 2002). The fact that no abnormalities were seen in SOCS-6 deficient mice compared to wild-type littermates may be due to the functional redundancy of SOCS-6 and SOCS-7 since they share more than 50% similarity in their functional domains at the protein level (Banks *et al.*, 2005). It has also been proposed that the redundancy of the other SOCS family members may compensate for the defects caused by lack of SOCS-6 (Trenkove and Ward, 2013).

1.4.3.7.2 SOCS-6 and wound healing

It has been suggested that SOCS-6 facilitates proteasomal degradation of target proteins to which the SH2 domain of SOCS-6 binds (Krebs et al., 2002). As with SOCS-2, SOCS-6 also has the ability to interact with other SOCS family members in a SOCS box dependent manner and acts as a negative regulator of SOCS protein activity (Piessevaux et al., 2006). Based on the above mentioned possible link between SOCS proteins and critical wound healing molecules, SOCS-6 may have a dual effect on modulating different stages of the wound healing process either via, similar to other SOCS members, its regulatory role on cytokine and growth factor signalling or through the unique ability to associate with their own family members, resulting in proteasome-dependent degradation.

1.4.3.8 SOCS-7

Studies on two mouse strains both demonstrated that SOCS-7 expression is distributed across a variety of tissues including brain, muscle, liver, pancreas, fat, skin and spleen (Krebs et al., 2002, Banks et al., 2005). It was previously discovered that Nck-, Ash- and phospholipase C gamma-binding protein (NAP)-4, also known as SOCS-7, contains a putative nuclear localisation signal and a motif specific to nuclear proteins (Matuoka et al., 1997, Martens et al., 2004). SOCS-7 has been documented to be induced by a number of cytokines and growth factors and primarily acts as a mediator to insulin, prolactin and growth hormone signalling (Table 1-12).

Table 1-12 Summary of the association between SOCS-7 and key cytokines/growth factors together with the regulatory roles played by SOCS-7

Cytokines /growth factors that induce SOCS-7	Regulatory role of SOCS-7 in signalling pathway	Reference
GH	Inhibit GH signalling through STAT-5	(Dogusan et al., 2000)
PRL	Interact with activated STAT-3 and STAT-5 to attenuate their DNA binding ability; inhibit PRL signalling through STAT-5	(Dogusan et al., 2000, Martens et al., 2005)
Insulin	Associate with INSR; bind to IRS-1 for proteasomal degradation to negatively regulate insulin signalling	(Banks et al., 2005)
IL-6		(Dogusan et al., 2000)
IL-1 β		(Dogusan et al., 2000)
	Inhibit leptin-induced STAT-3 translocation	(Martens et al., 2005)
	associate with IRS-4 and p85 PI3K in response to IGF-I stimulation	(Krebs et al., 2002)
	Associate with phosphorylated EGFR; contains nucleus-connection sequence for protein transportation	(Matuoka et al., 1997)
	Negatively regulate thymic stromal lymphopoietin (TSLP)	(Knisz et al., 2009)

1.4.3.8.1 *In vivo* role of SOCS-7

A SOCS-7 deficient mouse model, using C57BL/6 mice, was established to examine the regulatory role of SOCS-7 in cytokine and growth factor signalling. No abnormalities in blood glucose and serum insulin levels were observed between SOCS-7 deficient mice and wild-type littermates when they were born, however, mild retardation and reduced body weight and organ size was shown in SOCS-7 deficient mice. Thus, it was proposed that other SOCS family members, such as SOCS-6, may compensate for SOCS-7 function due to their structural similarity and the resemblance of in phenotypes of their deficient mouse models (Krebs et al., 2004). However, fatal hydrocephalus developed in half of the SOCS-7 deficient mice between 3-15 weeks of age. This phenotype was suggested to be related to the disorganisation of subcommissural organ, which is the only specific abnormality detected in the brain of all SOCS-7 deficient mice. Additionally, in agreement with the SOCS-7 deficient mouse phenotype, the expression profile of *SOCS-7* gene, prominently expressed in brain, also indicated its important functional role in brain tissue (Krebs et al., 2004). Interestingly, mixed 129S6xC57BL genetic background SOCS-7^{-/-} mice did not show abnormalities in length, weight, and body composition compared to wild-type littermates within 6 month of age. This indicated that the genetic background plays an important role in the establishment of SOCS-7 deficient mouse models (Banks et al., 2005). Another study on the mixed 129S6xC57BL genetic background SOCS-7^{-/-} mice showed that approximately half of such phenotypes exhibited severe cutaneous inflammation, showing degranulated mast cells and elevated inflammatory infiltrate by 16 months of age. In addition, the significantly increased IgG₁ and the elevated trend of IgE in such mixed 129S6xC57BL genetic background SOCS-7^{-/-}

mice resembled the phenotype of the thymic stromal lymphopoietin (TSLP) overexpression mouse model (Knisz et al., 2009).

1.4.3.8.2 SOCS-7 and wound healing

Study using a SOCS-7 deficient mouse model demonstrated severe cutaneous inflammation phenotype and elevated production of pro-inflammatory cytokines, such as IL-6, IL-13 and TNF- α by mast cells (Knisz et al., 2009). Therefore, SOCS-7 may potentially negatively regulate the inflammatory phase of wound healing.

An early study demonstrated that SOCS-7 is able to bind to activated EGFR via SH2 domain, therefore, it may exert similar function to SOCS-2, -4 and -5 to negatively regulate EGF-like signalling during the wound healing process (Matuoka et al., 1997).

1.4.3.9 A summary of SOCS proteins and key molecules in wound healing

Previous sections have highlighted the involvement of SOCS family members in wound healing. However, to date, studies focusing deeper roles of SOCS proteins in wound healing are limited. It is known that there are many cytokines and growth factors which are mediated by SOCS proteins and these themselves have key roles in the wound healing process (Table 1-13). Further investigation of the regulatory roles of SOCS on such cytokines/growth factors and their receptors may provide novel routes for further establishment of SOCS in wound healing and their potential therapeutic applications.

Table 1-13: SOCS and essential cytokines/growth factors and receptors involved in wound healing (Feng et al., 2016)

Cytokine/ growth factor/ receptor	Target components in wound healing	Functions in wound healing	SOCS member induced by cytokine/ growth factor	SOCS member known tonegatively/ <i>positive</i> ly regulates downstream signalling	Downstream pathway/molecule by which cytokine/receptor are negatively/ <i>positively</i> regulated by SOCS
IL-1 β	Endothelial cells, macrophages, leukocytes, keratinocytes, fibroblasts	Inflammation, angiogenesis, re-epithelialisation, tissue remodelling, induces keratinocyte, neutrophil and fibroblast chemotaxis, induce neutrophil activation	SOCS-2	SOCS-3/negative	
			SOCS-3		
IL-2	Fibroblast	Increase fibroblast infiltration and enhance fibroblast metabolism	CIS	CIS/negative	IL-2R via STAT-5
			SOCS-1	SOCS-1/negative	
			SOCS-2	<i>SOCS-2/positive</i>	<i>Through association with SOCS-3 and degradation</i>
			SOCS-3	SOCS-3/negative	Association with JAK-1 and IL-2R/ Binding to Calcineurin
IL-4	Macrophages, fibroblasts	Enhance collagen synthesis, induces fibroblast proliferation	SOCS-1	SOCS-1/negative	Inhibition of activated JAK-1 and STAT-6
			SOCS-2		
IL-4R			SOCS-5	SOCS-5/negative	Inhibition of STAT-6
IL-6	Endothelial cells, macrophages, keratinocytes,	Inflammation, angiogenesis, re-epithelialisation, collagen deposition, tissue remodelling, induce fibroblast	CIS	SOCS-3/negative	
			SOCS-1		
			SOCS-3	SOCS-5/negative	

	leukocytes, fibroblasts	proliferation	SOCS-5		
IL-10	Macrophages	Inhibits macrophage activation and infiltration, inhibits TNF- α , IL-1 and IL-6 expression	CIS		
			SOCS-3		
IFN- γ	Macrophages, keratinocytes	Induces collagenase activity, preventing collagen synthesis and crosslinking	CIS	SOCS-1/negative	
			SOCS-1		
			SOCS-2	SOCS-3/negative	
			SOCS-3		
TNF- α		Regulates collagen synthesis and degradation, increases vascular permeability and homeostasis, provides metabolic substrates	CIS		
			SOCS-1	SOCS-1/negative	
			SOCS-3		
EGF			CIS		
			SOCS-2	SOCS-2/negative	Association with activated EGFR
			SOCS-3		
			SOCS-4	SOCS-4/negative	Competing for docking site with STAT-3
			SOCS-5		
EGFR	Keratinocytes, fibroblast	Re-epithelialisation, increases fibroblast collagenase secretion, inhibits fetal wound contraction	SOCS-4	SOCS-4/negative	Association with activated EGFR and degradation
			SOCS-5	SOCS-5/negative	Association with activated EGFR and degradation
			SOCS-7	SOCS-7/negative	Association and degradation
PDGF	Leukocytes, macrophages,	Inflammation, re-epithelialisation, collagen deposition, tissue remodelling, recruits fibroblasts	SOCS-3		

	fibroblasts	and macrophages, induces collagen synthesis			
HGF	Endothelial cells, keratinocytes	Suppression of inflammation, granulation tissue formation, angiogenesis, re-epithelialisation	SOCS-1	SOCS-1/negative	Inhibition of STAT-3 activation
			SOCS-3	SOCS-3/negative	
TGF- β	Fibroblasts, keratinocytes, macrophages, leukocytes, endothelial cells, ECM	Inflammation, angiogenesis, granulation tissue formation, collagen synthesis, tissue remodelling, leukocyte chemotactic function	SOCS-3	SOCS-3/negative	

1.5 Aims of the thesis

Studies have emerged on the investigation of SOCS protein in diverse pathologies, especially in cancer related disease, since the discovery of such proteins in 1997 and it has been recognised that SOCS are a cytokine inducible negative feedback inhibitor to cytokine and growth factor signalling. In addition, many downstream molecules have been discovered to be modulated by SOCS and the mechanisms of SOCS regulating certain cytokine and growth factor signalling are under investigation for further verification.

However, there are few studies focusing on the impact of SOCS on wound healing, and the role of SOCS in the wound healing process remains unclear. Our hypothesis are 1) SOCS may hold the potential to predict healing results and; 2) may potentially play regulatory roles in functions of key cell types involved in wound healing process.

The aim of the thesis is therefore to investigate the importance of the SOCS family in the wound healing process.

Specific aims of the thesis are

- i. to investigate and define the expression profile of SOCS members in clinical chronic wound samples to explore their potential to differentiate between those chronic wounds that show healing potential and those which do not. Two chronic wound cohorts were collected and grouped based on the same criteria;
- ii. to identify the cellular impact of SOCS-3 and SOCS-4, which showed a significant difference in gene expression between two chronic wound subgroups, in both keratinocyte and endothelial *in vitro* cell models;
- iii. to investigate the potential role of SOCS-3 and SOCS-4 in the key wound healing cellular function;

iv. to explore potential pathway(s) that connect SOCS-3 and SOCS-4 with keratinocyte and endothelial cell functions that are involved in the wound healing process.

Chapter II

Methods and materials

2.1 Cells

Two cell lines were used for *in vitro* model generation and functional assay investigation in this study (Table 2-1). The immortalised human keratinocyte cell line (HaCaT) (Boukamp *et al.*, 1988) was purchased from the German Cancer Research Centre (Heidelberg, Germany). The human HECV endothelial cell line was purchased from Interlab Cell Line Collection (Genova, Italy).

HaCaT, a spontaneously transformed human epithelial cell line, is the first permanent epithelial cell line whose DNA fingerprint pattern is unaffected by long-term cultivation and this cell line exhibits normal differentiation despite the unlimited growth potential (Boukamp *et al.*, 1988). In addition, investigation on wound healing has shown HaCaT as a competent *in vitro* cell model for transfection study (Goren *et al.*, 2006a). HECV is a human vascular endothelial cell line originated from human umbilical cord, and this cell line has been utilised as *in vitro* models for the investigations on endothelial cell function in both cancer and wound healing (Tan *et al.*, 2015, Liu *et al.*, 2013). Hence, in order to evaluate the potential regulatory role of SOCS-3 and SOCS-4 in wound healing, keratinocyte (HaCaT) and endothelial cell (HECV) were chosen for the further *in vitro* cell function study.

Both HaCaT and HECV cell lines were routinely cultured in DMEM/Ham's F12 with L-Glutamine medium (Sigma-Aldrich, Inc., Dorset, UK), supplemented with antibiotic antimycotic solution (Sigma-Aldrich, Inc. Dorset, UK), and 10% fetal calf serum (Sigma-Aldrich, Inc., Dorset, UK), and incubated at 37.0°C, 5% CO₂ and 95% humidity. Another 10 cell lines were used for SOCS-3 expression profile screening (Table 2-2).

Table 2-1: Cell lines used in *in vitro* study

Cell line	Organism	Morphology	Ethnicity	Gender	Sources and features	Growth Conditions
HaCaT	<i>Homo sapiens</i>	Epithelial	Caucasian	Male	<i>In vitro</i> spontaneously transformed keratinocytes from histologically normal skin	Grown in DMEM supplemented with 10% FCS and antibiotics at 37°C in 5% CO ₂
HECV	<i>Homo sapiens</i>	Endothelial	Caucasian	Female	Umbilical cord	Grown in DMEM supplemented with 10% FCS and antibiotics at 37°C in 5% CO ₂

Table 2-2: Cells used for SOCS-3 expression profile screening

Tissue type	Cell line name	Origin	Tissue type	Cell morphology	Other information
Liver	PLC-PRF-5		Hepatoma	Epithelial	Hepatitis virus B surface antigen positive expression
Lung	SKMES	65 year-old Caucasian male	Squamous cell carcinoma	Epithelial	Derived from Metastatic Site: pleural effusion
	A549	58 year-old Caucasian male	Carcinoma	Epithelial	
	MRC-5	14-weeks gestation Caucasian male	Normal lung fibroblast cell line	Fibroblast	Foetal
Colon	CaCo-2		Adenocarcinoma	Epithelial	
Prostate	CA-HPV-10	63 year-old Caucasian male	Non-tumourigenic cell line derived from prostatic adenocarcinoma, transformed through HPV18 transfection	Epithelial	HPV-18 transformed
	PC-3	62 year-old Caucasian male	Grade IV adenocarcinoma	Epithelial	
	PZ-HPV-7	70 year-old Caucasian male	Non-tumourigenic epithelial cell line transformed through HPV18 transfection	Epithelial	HPV-18 transformed
	DU-145	69 year-old Caucasian male	Carcinoma	Epithelial	
	hFOB 1.19	Fetus	“Normal” foetal	Osteoblast	SV40 large T antigen transfected

2.2 Primers

Specific primers were designed using Beacon designer software (PREMIER Biosoft International, Palo Alto CA, USA) and synthesised by Sigma (Dorest, UK). Details of the primers are outlined in Table 2-3.

Table 2-3: Primers designed and used in this study

Function	Target gene/sequence	Name of Primer	Sequence of Primer
Screening of clinical samples and cell lines by q-PCR and conventional PCR	SOCS-1	SOCS-1 F1	5'-GATGGTAGCACACAACCAG
		SOCS-1 ZR1	5'- <i>ACTGAACCTGACCGTAC</i> AGAGGAAGAGGAGGAAGGTT
	SOCS-2	SOCS-2 F8	5'-GTCAGACAGGATGGTACTGG
		SOCS-2 R8	5'-CTGGAATTTATATTCTTCCA
		SOCS2 F1	5'-GGATGGTACTGGGGAAGTAT
		SOCS2 ZR1	5'- <i>ACTGAACCTGACCGTAC</i> TGGGAGCTATCTCTAATCAA
	SOCS-3	SOCS-3 F8	5'-AAGACCTTCAGCTCCAAGA
		SOCS-3 R8	5'-GTCTCCGACAGAGATGCT
		SOCS3 F2	5'-TCAAGACCTTCAGTCCA
		SOCS3 ZR2	5'- <i>ACTGAACCTGACCGTAC</i> GTCACTGCGCTCCAGTAG
	SOCS-4	SOCS-4 F8	5'-CAGCTGTTTCATCCATTGAG
		SOCS-4 R8	5'-CCATTGGGTTTGTCTT
		SOCS-4 F1	5'-GGCAGTGTTTTCCAATAAAG
		SOCS-4 ZR1	5'- <i>ACTGAACCTGACCGTAC</i> AAGGTGGGAAAGGACACTTAT
	SOCS-5	SOCS-5 F1	5'-AGTCAAAGCCTCTCTTTCC
		SOCS-5 ZR1	5'- <i>ACTGAACCTGACCGTAC</i> ACATTTTGGGCTAAATCTGA
	SOCS-6	SOCS-6 F1	5'-CCTTACAGAGGAGCTGAAAA
		SOCS-6 ZR1	5'- <i>ACTGAACCTGACCGTAC</i> ACGAAAAGAAAAGAACCATC
	SOCS-7	SOCS-7 F9	5'-AGACTAACAGCTGCTCGGAA
		SOCS-7 R9	5'-CCCACTGATATCATCTAGGAGGC
		SOCS7 F1	5'-CAGGCCCTGAATTACCTC
		SOCS7 Zr1	5'- <i>ACTGAACCTGACCGTAC</i> AGAGGTTGCTGCTGCTGCT
	Cytokeratin-19 (CK-19)	CK-19 F8	5'-AGCCACTACTACACGACCAT

		CK-19 ZR8	5'- <i>ACTGAACCTGACCGTACAT</i> TCGATCTGCAGGACAATC	
Ribozyme synthesis	SOCS-4	SOCS-4 rib F1	5'-CTGCAGTAAAGGCTAAATCTGATCGAGGTGGCTGATGAGTCCGTGAGGA	
		SOCS-4 rib R1	5'-ACTAGTGAACTCATGTTAGATTAGTGTCTTTTTTCGTCCTCACGGACT	
		SOCS-4 rib F2	5'-CTGCAGTTCACTGATATGAATTTTCCTTTTAGACGCTGATGAGTCCGTGAGGA	
		SOCS-4 rib R2	5'-ACTAGTCGGCACTCTTCAGGGCTTTTCGTCCTCACGGACT	
Knockdown verification by q-PCR		SOCS-4 F2	5'-GAGACTCAGCACAGGAGGAC	
		SOCS-4 ZR2	5'- <i>ACTGAACCTGACCGTACAG</i> TCAGTGCATCAAAGCTAA	
Overexpression verification by q-PCR	SOCS-3	SOCS-3 F2	5'-TCAAGACCTTCAGCTCCA	
		SOCS-3 ZR2	5'- <i>ACTGAACCTGACCGTACAG</i> TCACTGCGTCCAGTAG	
SOCS-3 coding sequence amplification	SOCS-3 coding sequence	SOCS-3 exp F1	5'-ATGGTCACCCACAGCAAGTTTCCCGC	
		SOCS-3 exp F2	5'-ATGGTCACCCACAGCAAGTTTCCC	
		SOCS-3 exp F3	5'-ATGGTCACCCACAGCAAGTTTC	
		SOCS-3 exp F4	5'-ATGGTCACCCACAGCAAGTT	
		SOCS-3 exp F5	5'-ATGGTCACCCACAGCAA	
		SOCS-3 exp R	5'-TTAAAGCGGGGCATC	
Screening on cell lines by PCR	Glyceraldehyde-3-phosphate dehydrogenase (GAPDH)	GAPDH F8	5'-GGCTGCTTTTAACTCTGGTA	
		GAPDH R8	5'-GACTGTGGTCATGAGTCCTT	
Knockdown and overexpression verification by q-PCR		β-Actin	GAPDH F2	5'-CTGAGTACGTCGTGGAGTC
			GAPDH ZR2	5'- <i>ACTGAACCTGACCGTACAC</i> AGAGATGATGACCCTTTTG
		β-Actin F10	5'-CATTAAGGAGAAGCTGTGCT	
		β-Actin ZR10	5'- <i>ACTGAACCTGACCGTACAG</i> CTCGTAGCTCTTCTCCAG	
Transgene/Coding sequence insertion and orientation check	T7F promoter	T7F	5'-TAATACGACTCACTATAGGG	
	Ribozyme common sequence	RbBMR	5'-TTCGTCCTCACGGACTCATCAG	
		RbToPF	5'-CTGATGAGTCCGTGAGGACGAA	
	BGHR site	BGHR	5'-TAGAAGGCACAGTCGAGG	

- Z Sequence '*ACTGAACCTGACCGTACA*' is highlighted in green colour and italic font

2.3 Antibodies

Full details of the antibodies used in this study are outlined in Table 2-4 and Table 2-5 as follows:

Table 2-4: Antibodies used for IHC analysis on chronic wound biopsies

Antibody name	Host species	Antibody concentration	Supplier and catalogue number
SOCS-1 (H93)	Rabbit	2µg/ml	Santa cruz biotechnology, SC-9021
SOCS-2 (H74)	Rabbit		Santa cruz biotechnology, SC-9022
SOCS-3 (H103)	Rabbit		Santa cruz biotechnology, SC-9023
SOCS-4 (H-20)	Goat		Santa cruz biotechnology, SC-68827
SOCS-5 (31-L)	Mouse		Santa cruz biotechnology, SC-100858
SOCS-6 (H-251)	Rabbit		Santa cruz biotechnology, SC-5608
SOCS-7 (C-19)	Goat		Santa cruz biotechnology, SC-8291
SOCS-7 (E-8)	Mouse		Santa cruz biotechnology, SC-137241

Table 2-5: Antibodies used for verification of SOCS-4 knockdown and SOCS-3 expression

Antibody name	Host species	Molecular Weight (kDa)	Antibody concentration	Supplier and catalogue number
SOCS-4	Mouse	51	0.1µg/ml	R&D Systems MAB5628
SOCS-3	Rabbit	30	1:1,000	Abcam, Ab53984
GAPDH (6C5)	Mouse	37	1:4,000	Santa cruz biotechnology, SC-32233
GAPDH (FL-335)	Rabbit	37	1:4,000	Santa cruz biotechnology, SC-25778
Actin (I-19)	Goat	43	1:4,000	Santa cruz biotechnology, SC-1616
Anti-Mouse IgG	Rabbit		1:100,000	Sigma-aldrich, A9044
Anti-Rabbit IgG	Goat		1:100,000	Sigma-aldrich, A0545

2.4 General reagents and solutions

2.4.1 Reagents and chemicals

2.4.1.1 Solutions and reagent for cell culture

Ethylene Diaminetetraacetic Acid (EDTA) trypsin

10X Trypsin-EDTA Solution (Product number T4174) was purchased from Sigma-Aldrich, Inc. (Dorset, UK) and was diluted with distilled water to 1X. This solution was then aliquoted into 25ml aliquots and stored at -20°C until further use.

Phosphate buffered saline (PBS)

10X Phosphate buffered saline (P5943) was purchased from Sigma-Aldrich, Inc. (Dorset, UK) and was diluted with distilled water to 1X. This solution was then aliquoted into 25ml aliquots and stored at room temperature until further use.

Antibiotics

100X Antibiotic Antimycotic Solution (A5955) was purchased from Sigma-Aldrich, Inc. (Dorset, UK) and was aliquoted into 5ml aliquots and stored at -20°C until further use. Each of the aliquots was added into a 500ml bottle of medium to obtain a final 1X concentration.

Fetal Calf Serum (FCS)

Fetal Calf Serum was purchased from Sigma-Aldrich, Inc. (Dorset, UK). Such stocks were divided into 25ml aliquots and stored at -20°C for further use.

2.4.1.2 Solutions and reagent for molecular biology

Tris-Boric-Acid-EDTA (TBE)

TBE buffer 10X concentrate (T4415) was purchased from Sigma-Aldrich, Inc. (Dorset, UK), diluted with distilled water into 1X stock and stored at room temperature for further use.

Diethyl Pyrocarbonate (DEPC) Water

250ml of DEPC (Sigma-Aldrich, Inc., Dorset, UK) was added to 4.75L of distilled water. This solution was subsequently autoclaved, and stored at room temperature for further use.

Loading buffer (used for DNA electrophoresis)

25mg of bromophenol blue (Sigma-Aldrich, Inc., Dorset, UK) and 4g sucrose (Fisons Scientific Equipment, Loughborough, UK) were dissolved in 10ml of distilled water and stored at 4°C.

2.4.1.3 Solutions and reagent for cloning

LB Broth

8g LB Broth low salt granulated powder (Melford Laboratories Ltd., Suffolk, UK) was dissolved in 400ml distilled water, and the pH value was adjusted to 7.0 before being autoclaved. This solution was then stored at room temperature for further use.

LB Agar

LB agar was made by dissolving 10g of LB Broth low salt granulated powder (Melford Laboratories Ltd., Suffolk, UK) and 7.5g of agar (A1296) (Sigma-Aldrich, Inc., Dorset, UK) in 500ml of distilled water before adjusting the pH value to 7.0 followed by autoclaving. This solution was then stored at room temperature in

the form of a solid gel for further use. Upon usage, the gel was heated by microwave until completely melted.

Ampicillin

Ampicillin was prepared by dissolving 1g of ampicillin (Melford Laboratories Ltd., Suffolk, UK) in 10ml of sterile PBS to give a concentration of 100mg/ml.

2.4.1.4 Solutions and reagent for western blotting

Lysis Buffer

8.76g of NaCl (150mM), 6.05g of Tris (50mM), 200mg Sodium azide (0.02%, w/v) and 5g Sodium deoxycholate (0.5%, w/v) was dissolved in 1L distilled water followed by the addition of 15ml Triton X-100 (1.5%, v/v) to make a 1L stock of protein lysis buffer and stored at 4°C. 50ml of the lysis buffer was then used to dissolve one of the cOmplete™, EDTA-free protease inhibitor cocktail tablet (Roche Diagnostics, Mannheim, Germany) followed by division to 1ml aliquots before being stored at -20°C for further use. If required, 100mM of Na₃VO₄ was added into the pre-made lysis buffer at the working concentration of 1mM upon the usage of lysis buffer.

10% (w/v) Ammonium Persulphate (APS)

1g Ammonium Persulphate (Melford Laboratories Ltd., Suffolk, UK) was dissolved in 10ml distilled water and stored at 4°C for further use.

10% (w/v) Sodium Dodecyl Sulphate (SDS)

50g Sodium Dodecyl Sulphate (Melford Laboratories Ltd., Suffolk, UK) was dissolved in 500ml distilled water and stored at room temperature for further use.

Tris Buffered Saline (TBS)

1L of Tris Buffered Saline 10X solution (T5912) (Sigma-Aldrich, Inc., Dorset, UK) was diluted in 9L of distilled water and stored at room temperature for further use.

Running buffer (for SDS-PAGE)

1L of Tris-Glycine-SDS Buffer 10X concentrate (T7777) (Sigma-Aldrich, Inc., Dorset, UK) was diluted in 9L of distilled water and stored at room temperature for further use.

Transfer buffer

1L of Tris-Glycine Buffer 10X concentrate (T4904) (Sigma-Aldrich, Inc., Dorset, UK) was diluted in 9L of distilled water containing 2L methanol (Fisher Scientific UK, Loughborough, UK) and stored at room temperature for further use.

Ponceau S stain

Ponceau S staining solution was made by dissolving 0.1% Ponceau S (P3504) (Sigma-Aldrich, Inc., Dorset, UK) in 5% acetic acid (w/v), and was subsequently stored at room temperature for further use.

2.4.1.5 Solutions and reagent for microarray protein lysis

100mM Tris buffer was made by dissolving 6.0g of Tris powder in 1.5L distilled water. One of the cOmplete™, EDTA-free protease inhibitor cocktail tablet (Roche Diagnostics, Mannheim, Germany), 5ml of 2-mercaptoethanol (10%, v/v), nonident P-40 (1%, v/v) and 5ml of 500mM NaF (50mM) were added to 50ml of

the Tris buffer, mixed and divided into 1ml aliquots before being stored at -20°C for further use.

2.4.1.6 Solutions and reagents for immunohistochemical staining

Avidin-biotin complex (ABC)

The ABC complex was prepared using a VECTASTAIN® ABC Kit (Vector Laboratories, Inc., CA, USA). 4 drops of each reagent A and reagent B were added into 20ml of wash buffer and mixed thoroughly, and such combined solution was left for at least 30 minutes at 4°C before use.

2.5 Cell culture, maintenance, storage and revival

2.5.1 Preparation of growth medium and cell maintenance

Cell culture medium (normal medium) was made by adding 10% heat inactivated FCS (inactivate the complement protein and kill mycoplasma) (Sigma-Aldrich, Inc., Dorset, UK) and antibiotics in Dulbecco's Modified Eagle's Medium (DMEM) Nutrient Mixture F-12 Ham with 15mM HEPES, NaHCO₃, pyridoxine and L-glutamine (Sigma-Aldrich, Inc., Dorset, UK). This medium was used for routine cell culture.

Normal medium containing 5µg/ml blasticidin (Melford Laboratories Ltd., Suffolk, UK) (selection medium) were used to select the cell lines transfected with the pEF6/His plasmid or transgene incorporated plasmid vectors for 8-14 days. Subsequently, the transfectants were then cultured in normal medium supplemented with and 0.5µg/ml blasticidin (maintenance medium) for cell maintenance.

Cell lines were cultured in 25cm² (T25) and 75cm² (T75) culture flasks (Greiner Bio-One Ltd., Gloucestershire, UK), and the flasks were loosely capped and incubated at 37°C, 5% CO₂ and 95% humidity.

2.5.2 Trypsinisation (detachment) of adherent cells and cell counting

When cells reached 80-90% confluency, they are growing exponentially (near the end of the log phase) and maintain healthy status. This confluency also improves overall cell viability. Therefore once cells reached 80-90% confluency, the medium was aspirated by a glass aspirator and rinsed and washed with sterile PBS to remove excess serum which could influence the efficiency of trypsin. Appropriate amounts of trypsin (1ml for T25 flask, 2ml for T75 flask) was pipetted into the flask and incubated at 37°C, 5% CO₂ and 95% humidity for approximately 15 minutes until cell detachment could be visually confirmed under the microscope.

Once the cells were detached, equal amount of medium was pipetted into the flask to neutralise the excess trypsin, and the cell suspension was then transferred into a sterile 30ml universal centrifuge container (Greiner Bio-One Ltd., Gloucestershire, UK) followed by being centrifuged at 1,700rpm for 5 minutes to obtain a cell pellet.

The supernatant was aspirated by a glass aspirator, and the cell pellet was re-suspended with an appropriate amount of medium based on the pellet size. Cell number was then counted and calculated with a Neubauer haemocytometer counting chamber (Mod-Fuchs Rosenthal, Hawksley, UK) using an Olympus CKX31 microscope at a objective magnification of X10 (Olympus, Tokyo, Japan).

2.5.3 Storage and revival of cells

Cells were detached, centrifuged to form a pellet and re-suspended in an appropriate volume, as described above. Cell suspensions were then divided into 900µl aliquots and pipetted into pre-labelled 1ml CRYO.S™ tube (Greiner Bio-One Ltd., Gloucestershire, UK) before the addition of 100µl of Dimethylsulphoxide (DMSO) (Sigma-Aldrich, Inc., Dorset, UK) followed by screwing and tightening the cap of the CRYO.S™ tube. These tubes were then wrapped in protective tissue paper and stored at -80°C or subsequently transferred to liquid nitrogen stores for long term storage.

In order to revive the cells, the pre-stored CRYO.S™ tube was removed from the -80°C freezer or liquid nitrogen stocks and thawed rapidly before being transferred into a universal container containing 4ml pre-warmed medium. Such universal containers were then centrifuged at 1700rpm for 5 minutes to obtain a cell pellet. The supernatant was aspirated by a glass aspirator to remove the medium containing DMSO, and the cell pellet was re-suspended with 5ml growth medium before being transferred into a pre-labelled fresh flask for further incubation.

2.6 Tissue collection and processing

Two wound cohorts were used for this study. For transcript analysis, the cohort used was came from a prospective study to investigate potential diagnostic/prognostic indicators of chronic wound healing in venous leg ulcer patients (Cohort 1) (Ref CT0101). Tissues were collected from patients who entered this study from 1990 to 1995, attending the University Hospital of Wales wound healing clinic. For the IHC analysis, tissues used were from another study that aimed to develop a diagnostic platform and novel therapies for non-healing

chronic wounds based on impaired keratinocyte re-epithelialisation (Cohort 2) (Ref 09/wse02/51). Tissues for this cohort were also collected from patients who attended the same wound clinics between 2010 and 2013 with chronic venous leg ulcer wounds. For both studies, ethical approval was granted by the Local Research Ethics Committee and written informed patient consent was obtained, before wound edge tissues were collected from the chronic venous leg ulcers.

Venous disease was diagnosed by Duplex ultrasonography, and all wounds had been present for a minimum of 3 months. Other inclusion criteria included: no evidence of other diagnosis and no evidence of infection, as judged by the leading clinical physician. Where required, swabs were taken to confirm this.

Following the application of a local anaesthetic (1% Lidocaine) and using an aseptic technique, a 6mm punch biopsy was taken at the wound margin, so that the resulting biopsy incorporated both epidermis and dermis at the wound edge and the adjacent distal tissue. Sample biopsies were frozen immediately to prevent morphological distortions and damage. The tissue was orientated onto a cork board by rotating the biopsy 90° in order to obtain a full section of both epidermis and dermis at the wound edge and distal to the wound edge, and then OCT medium (Optimal Cutting Temperature compound) was applied. The sample biopsy was then snap frozen in iso-pentane that had been pre-cooled and floated on liquid nitrogen, in order to prevent ice crystal formation that would damage the architecture of the tissue. The biopsies were then stored at -80°C before being placed for long term storage in liquid nitrogen prior to processing. Samples were sectioned on a cryostat (Leica Microsystems Ltd., Milton Keynes, UK) at 7µm thickness for immunohistochemical staining, and multiple sections cut at 20µm thickness were processed for RNA extraction, reverse transcription and transcript expression analysis using q-PCR.

The patients' wounds were subsequently treated for 12 weeks as per best medical treatment. Specifically, this consisted of regular wound care with appropriate dressings and compression. The compression was produced with 3 layers of Tubigrip™ bandages (Mölnlycke Health Care, Dunstable, UK) at an appropriate size to deliver 40 mmHg of pressure.

At the end of the 12 week treatment period, the wounds were assessed and remeasured. The biopsies from patients whose wounds had reduced in size over this period or completely re-epithelialised were termed as "healing/healed" chronic wounds (Cohort 1 n = 20, Cohort 2 n=45) and those which remained static or grew in size were termed as "non-healing" chronic wounds (Cohort 1 n = 51, Cohort 2 n=45)). For the IHC part of the study, ten biopsies from each group (healing and non-healing) were chosen from Cohort 2 based on the quality of tissues as determined by H&E staining, and also the completeness of clinical information. The cohort has been described previously (Bosanquet et al., 2012, Jones et al., 2016), (Aravindan *et al.*, 2017 in press).

2.7 Total RNA isolation

RNA was isolated using TRI-reagent (Sigma-Aldrich, Inc., Dorset, UK) under the manufacturer's instructions both for the multiple sections from the patient biopsies and the cells.

Tissue lysate:

Multiple sections from the same patient sample biopsy were combined and homogenised in 1ml of ice-cold TRI-reagent using a handheld homogeniser (Cole-Parmer, London, UK) with the lysate was then transferred into a 1.5ml microfuge tubemicrofuge tube.

Cell lysate:

Once cells reached 80-90% confluency, the medium was removed by glass aspirator and 1ml of TRI-reagent (1ml TRI-reagent is sufficient for 80-90% confluent cells grown in T25 flask) was added to the cell monolayer. A 28cm length Cell Scraper (Greiner Bio-one, Frickenhausen, Germany) was used to maximise the harvest of the cell lysate, and the cell lysate was transferred into a 1.5ml microfuge tube. Once lysate was obtained from cells or tissues the following procedure was undertaken:

The homogenate was kept at room temperature (20-22°C) for 5 minutes before the addition of 100µl of 1-bromo-3-chloropropane (Sigma-Aldrich, Inc., Dorset, UK) and subjected to vigorous shaking for 15 seconds. The mixture of the lysate and 1-bromo-3-chloropropane was kept for 5-10 minutes at room temperature until the formation of two separate layers. Following centrifugation at 4°C and 12,000g for 15 minutes, the upper aqueous phase (clear transparent layer) containing RNA was carefully transferred into a fresh 1.5ml microfuge tube. An equal volume of isopropanol to the extracted upper aqueous phase was added into the microfuge tube followed by being shaken vigorously for 10 seconds to mix thoroughly. The microfuge tube was then centrifuged at 4°C and 12,000g for 10 minutes to obtain the RNA pellet which was visible in the bottom of the microfuge tube. The supernatant was discarded and the RNA pellet was washed twice with 75% ethanol DEPC water (prepared by mixing absolute ethanol with DEPC water in 1:3 ratio). The wash stage consisted of adding 1ml of 75% ethanol DEPC water, vortexing and subsequent centrifugation at 7,500g for 5 minutes. After the final wash, as much ethanol as possible was removed through pipette aspiration and the microfuge tube was put into a Techne, Hybrdiser HB-1D drying oven at 50°C to

briefly dry out the remaining liquid. The RNA pellet was then dissolved in 20-100µl of DEPC water depending on the pellet size followed by being stored at -80°C for further use. DEPC water was used to minimise the effects of RNases by the inhibition of histidine active sites.

2.8 Reverse transcription polymerase chain reaction (RT-PCR)

The isolated RNA sample was quantified using a NanoPhotometerTM (IMPLEN; GeneFlow Ltd., Lichfield, UK) and standardised before undertaking reverse transcription using the GoScriptTM Reverse Transcription System kit (Promega Corporation, Madison, WI, USA) to generate cDNA. The reverse transcript protocol is outlined as follows:

A sufficient volume of the quantified RNA sample containing 500ng RNA was mixed with 1µl of Oligo(dT)₁₅ and was topped up to 5µl by DEPC water in a thin-walled 200µl tube. Such RNA and Oligo(dT)₁₅ solution was heated in a 2720 Thermal Cycler (Applied Biosystems, Paisley, UK) at 70°C for 5 minutes followed by immediately being placed in ice for 5 minutes. After this initial step, the tube was removed from the thermal cycler and added with 15µl of reaction mix containing the following:

- GoScriptTM 5X Reaction Buffer - 4µl
- MgCl₂ – 1.2µl
- PCR Nucleotide Mix - 1µl
- Recombinant RNasin Ribonuclease Inhibitor – 0.5µl
- GoScriptTM Reverse Transcriptase - 1µl
- Nuclease-Free Water – 7.3µl

The 20µl reaction mix was centrifuged at 1000rpm for 20 seconds and was placed back to the thermal cycler to be heated under the condition outlined as follows:

- Step 1: Annealing stage - 25°C for 5 minutes
- Step 2: Extending stage - 42°C for 60 minutes
- Step 3: Inactivating reverse transcriptase stage - 70°C for 15 minutes

The generated cDNA sample was diluted 1 in 4 by PCR water and was stored at - 20°C for further use.

2.9 Polymerase chain reaction (PCR)

Conventional PCR was carried out using GoTaq Green master mix (Promega, Madison, USA) and specific primers were designed using Beacon designer software (PREMIER Biosoft International, Palo Alto CA, USA) and synthesised by Sigma-Aldrich, Inc. (Dorset, UK). The primer was diluted to a concentration of 10pM before being added into the reaction mix. The reaction mix was briefly centrifuged and placed in a 2720 Thermal Cycler (Applied Biosystems, Paisley, UK). The 16µl reaction mix and the general PCR conditions that were used for cDNA amplification are shown as follows:

PCR Reaction mix:

- GoTaq Green master mix - 8µl
- Specific forward primer - 1µl
- Specific reverse primer - 1µl
- PCR H₂O - 5µl
- Prepared cDNA sample - 1µl

General PCR conditions:

- Step 1: Initial denaturing period - 94°C for 5 minutes
- Step 2: Denaturing stage - 94°C for 30 seconds
- Step 3: Annealing stage - 54°C for 40 seconds
- Step 4: Extension stage - 72°C for 1 minutes

- Step 5: Additional extension stage - 72°C for 10 minutes
- Hold at 4°C

Step 2 - 4 were repeated for 30-36 cycles depending on different experiments. The predicted size of the PCR product was determined by Primer Blast, and the negative control reaction mix in all cases consisted of PCR water instead of cDNA samples.

2.10 Agarose gel electrophoresis

The cDNA samples amplified from the 2720 Thermal Cycler (Applied Biosystems, Paisley, UK) were separated by gel electrophoresis on a 0.8% or 2% agarose gel, and the gel concentration was determined by the predicted size of cDNA samples. The agarose gel was made by adding an appropriate amount of agarose (Melford Chemicals, Suffolk, UK) into 1X TBE buffer which was diluted from 10X stock (Sigma-Aldrich, Inc., Dorset, UK). The mixed buffer was heated thoroughly to fully dissolve the powder, forming a clear and transparent agarose solution, and was stained with SYBR safe DNA gel stain (Invitrogen, Paisley, UK) at a 1:10,000 dilution in keeping with the manufacturers guidance. For example, for a typical 150ml 0.8% gel, 1.2g of agarose was dissolved in 150ml 1X TBE buffer and, once cooled, 15µl of SYBR safe added and mixed. Such stained agarose TBE solution was poured into the electrophoresis tank assembled with plastic combs (SCIE-PLAS, Cambridge, UK)(Figure 2-1) which enable the formation of loading wells. Once cooled down and polymerised, the agarose gel was submerged in 1X TBE buffer, and 4µl of PCR Ranger 100bp DNA Ladder/ Ranger 1000bp DNA Ladder (Geneflow, Fradely, Staffordshire, UK) and 8µl of amplified cDNA samples were loaded into designated wells followed by being electrophoretically separated at 110V, 50mA and 50W for a sufficient amount of time (20-50 minutes). A EV243

power consort (Topac Inc., Cohasset, MA, USA) was utilised for agarose gel electrophoresis. Upon completion of electrophoresis, images were acquired, visualised and captured using Syngene gel doc system (Syngene, Cambridge, UK) on a blue light trans-illuminator.

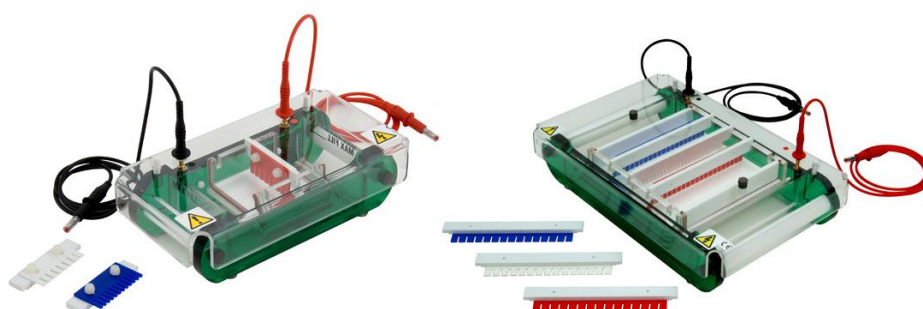


Figure 2-1: Agarose gel electrophoresis apparatus

2.11 Generation of mutant HaCaT and HECV cell lines

2.11.1 Discovery and the catalytic mechanism of ribozymes

In order to achieve SOCS-4 knockdown, hammerhead ribozyme transgenes that specifically target GUC or AUC sites of SOCS-4 mRNA and cleave SOCS-4 transcripts were designed according to the predicted secondary structure of SOCS-4 mRNA (Figure 2-2) by Zuker's RNA mFold software (Zuker, 2003). The hammerhead ribozyme was first discovered by Forster and Symons in 1987 as a self-cleaving domain in the RNA genome in a variety of plant viroids and virusoids (Forster and Symons, 1987). Such hammerhead motifs are able to form short synthetic oligonucleotides, acting as multiple turnover catalysts which are capable of cleaving RNA targets (Uhlenbeck, 1987, Haseloff and Gerlach, 1988). A general univesal secondary structure which is integrated by several invariant nucleotides and consists of three helical stems (I, II and III) could be found in all hammerhead motifs. Stem II is incorporatated intramolecularly in such secondary structure,

whereas stem I and III are formed by hybridisation based on the complementary sequences of the targeted substrate. Moreover, the best cleavage sites were discovered to be AUC, GUC and UUC (Figure 2-3).

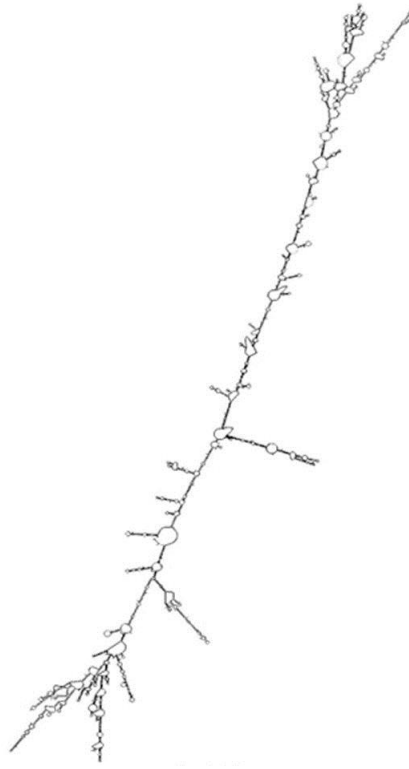


Figure 2-2: Diagram of the predicted secondary structure of human SOCS-4 mRNA

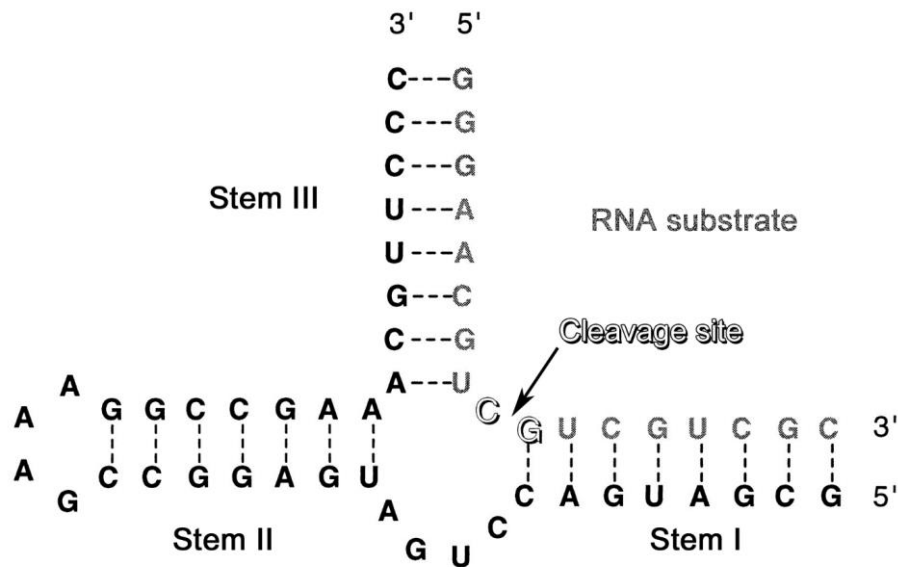


Figure 2-3: Diagram of hammerhead ribozyme secondary structure

Hammerhead ribozymes consist of three helices. Stem II, containing highly conserved sequences, is flanked by stem I and III that are adjacent to the cleavage site and are base-paired to the RNA substrate. Dash line indicates the Watson-Crick base pairs.

2.11.2 TOPO TA gene cloing and generation of stable transfectants

The pEF6/V5-His TOPO® TA expression system (Invitrogen, Paisley, UK) provides a highly efficient one-step cloning technique which does not require ligase, post-PCR procedures, or PCR primers containing specific sequences. Such an approach allows the direct insertion of *Taq* polymerase-amplified PCR products into a plasmid vector for constitutive expression in mammalian cells after transfection.

The linearised pEF6/V5-His TOPO® vector in the kit consists of single, overhanging 3' deoxythymidine (T) residues which allows *Taq* polymerase-amplified PCR products, containing a single deoxyadenosine (A) at the 3' ends, to ligate efficiently (Figure 2-4). The EF-1 α promoter in pEF6/V5-His TOPO® then enables the constitutive expression of the PCR product after the transfection of the plasmid.

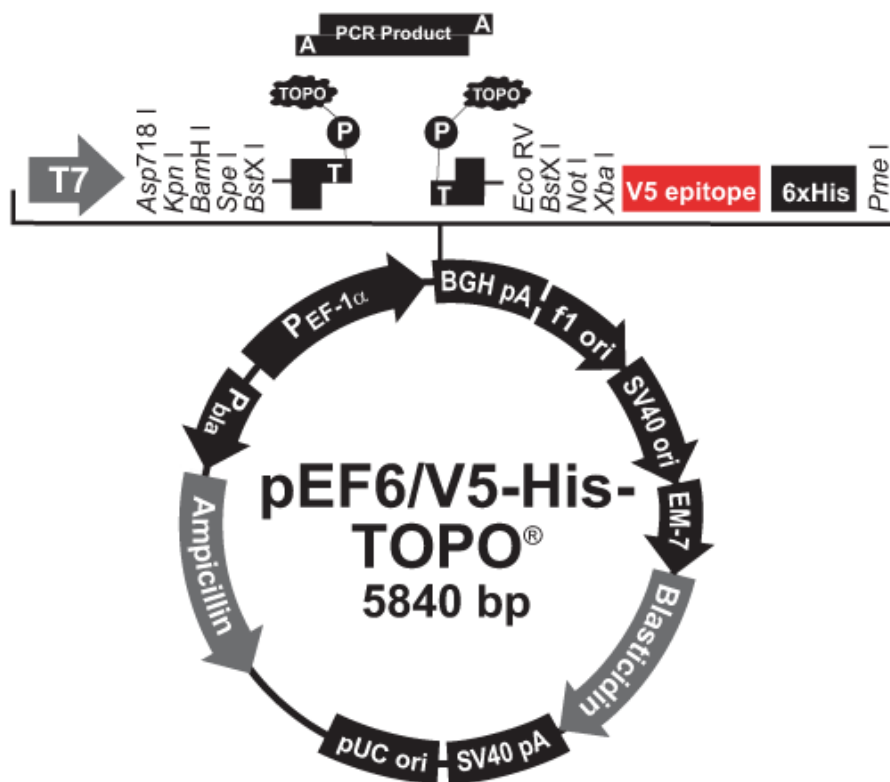


Figure 2-4: Diagram of the pEF6/V5-His TOPO[®] vector feature (from pEF6-His TOPO[®] TA Expression Kit manual)

The PCR products were cloned into pEF6/V5-His TOPO[®] plasmid, and the total 6μl cloning reaction was mixed and stored on ice in advance to the One Shot Chemical Transformation (Invitrogen, Paisley, UK). The condition used for TOPO cloning reaction was as follows:

- PCR product - 4μl
- Salt solution - 1μl
- TOPO vector - 1μl

5μl of TOPO cloning reaction was added into each vial of One Shot TOP10 Chemically Competent *Escherichia coli* (*E. coli*) (Invitrogen, Paisley, UK) and mixed gently by stirring using the pipette tip. The vial was stored on ice for 5-30 minutes (based on the product size) before heat-shocking at 42°C for 30 seconds followed by immediately transferring into ice. To each vial, 250μl of room temperature

S.O.C medium was added and the tubes shaken at a 45° angle at 225rpm on a horizontal orbital shaker (Bibby Stuart Scientific, UK) at 37°C for 1 hour.

After the incubation period, the transformed products from each vial were spread in different seeding density on a pre-warmed agar petri dish containing 100µg/ml ampicillin followed by incubating overnight at 37°C.

Several colonies from each petri dish were randomly picked and the PCR product insertion and orientation of the incorporated PCR product was checked by PCR using primer combination of T7F vs BGHR and T7F vs specific forward or reverse primer respectively. The reaction mix is outlined as follows:

PCR product insertion primer pair mix (used for overexpression sequences)

- GoTaq Green master mix - 8µl
- T7F plasmid specific forward primer - 1µl
- BGHR plasmid specific reverse primer - 1µl
- PCR water -6µl

Correct orientation primer pair mix

- GoTaq Green master mix - 8µl
- T7F plasmid specific forward primer - 1µl
- PCR product specific reverse primer - 1µl
- PCR water -6µl

Incorrect orientation primer pair mix

- GoTaq Green master mix - 8µl
- T7F plasmid specific forward primer - 1µl
- PCR product specific forward primer - 1µl
- PCR water -6µl

For ribozyme transgene insertion and orientation checking, the molecule specific forward and reverse primer were replaced in the above mixtures with forward (RbToPF) and reverse (RbBMR) sequences to the common region of the ribozyme transgene.

Each colony was inoculated into both reaction mixes using a sterile pipette tip, and the reaction mixes were placed in a 2720 Thermal Cycler (Applied Biosystems, Paisley, UK). The PCR reaction conditions were used as follows: 94°C for 5 minutes, followed by 30 cycles of 94°C for 30 seconds, 55°C for 40 seconds and 72°C for 1 minute with a final extension step of 72°C for 10 minutes. Gel electrophoresis on a 2% agarose gel stained with SYBR safe DNA gel stain were utilised to visualise the conventional PCR reaction products.

Colonies with correctly orientated PCR product inserts were inoculated into universal tubes containing 5ml of selective LB broth (containing 100µg/ml ampicillin) followed by being incubated overnight at 37°C whilst being shaken with 45° angle at 225rpm.

2.11.3 Plasmid amplification and extraction

Plasmid extraction was undertaken using the Sigma GenElute Plasmid MiniPrep Kit (Sigma, Dorset, UK) based on the protocol provided. The overnight incubated universal tubes containing the chosen colonies were centrifuged at 5,000RCF to acquire a bacterial pellet. The supernatant in each tube was discarded and the bacterial pellet was re-suspended thoroughly using 200µl Resuspension Solution containing RNase A and transferred into a 1.5ml microfuge tube. To the microfuge tube was added 200µl of Lysis Solution followed by 8 gentle inversions. This lysis stage was conducted within 5 minutes to avoid permanent plasmid denaturation. Then, 350µl of Neutralisation Solution was added and the microfuge tube was

gently inverted 6 times followed by centrifugation at 12,000g for 10 minutes to pellet the cell debris. The clear lysate in the microfuge tube was transferred into a Miniprep Binding Column which was placed into a Microcentrifuge Tube. Such Miniprep Binding Column was washed with Column Preparation Solution in advance to maximise plasmid binding capacity. The clear lysate added Microcentrifuge Tube was then centrifuged for 1 minute at 12,000g to enable the plasmid binding to Miniprep Binding Column. Flow-through liquid was discarded and 700µl of Wash Solution (containing ethanol) was added into the Miniprep Binding Column followed by centrifugation at 12,000g for 1 minute before discarding the flow-through liquid. The Microcentrifuge Tube was then centrifuged again at 12,000g for 1 minute to remove the remaining Wash solution before the Miniprep Binding Column was transferred into a fresh Collection Tube. Plasmid was eluted by adding 50µl of Elution Solution followed by spinning the fresh Collection Tube at 12,000g for 1 minute and was stored at -20°C for further use.

2.11.4 Plasmid transfection via electroporation into HaCaT and HECV cell lines

Wild type HaCaT and HECV cells were grown in T75 culture flasks until reaching approximately 80% confluency. Cells were trypsinised and transferred into a universal container which was subsequently centrifuged to obtain a cell pellet. The cell pellet was then re-suspended in normal medium and cell number was determined before preparing a suspension containing 1,000,000 cell/ml. 800µl of cell suspension was pipetted into a 4mm cuvette followed by the addition of 8µg of plasmid. The mixture of cell suspension and plasmid was gently mixed by finger flipping before electroporation. Transfection conditions consisted of 310V and 1500µA. Transfected cell solutions were then transferred into a T25 flask

containing pre-warmed normal medium. Another 800µl of cell suspension was added into a different fresh cuvette without adding any plasmid followed by electroporation transfection at the same condition. Such electroporated cell suspension was transferred into a separate pre-warmed flask to act as a selection control. Both flasks were incubated overnight at 37.0°C, 5% CO₂ and 95% humidity. On the following day, flasks were placed into selection medium (normal medium containing 5µg/ml blasticidin) for approximately 8 - 14 days until no viable cells remained in the selection control flask. Then, transfected HaCaT cells were placed into maintenance medium (normal medium containing 0.5µg/ml blasticidin), whereas, HECV cells remained in selection medium for further culture.

2.11.5 siRNA transfection via DharmaFECT transfect reagent 1 into HaCaT and HECV cell lines

Cells were trypsinised and transferred into a universal container followed by centrifugation to obtain a cell pellet. Complete medium (antibiotic-free DMEM plus 10% FCS) was used to re-suspend the cell pellet, and cell number was counted to make a cell suspension with appropriate cell density before seeded into a 24-well plate and an overnight incubation at 37.0°C, 5% CO₂ and 95% humidity.

ON-TARGETplus Non-targeting Pool (Non-targeting siRNA) and ON-TARGETplus Human SOCS-4 (122809) siRNA (SOCS-4-targeting siRNA), purchased from the manufacturer (GE Healthcare Dharmacon Inc., UK), was centrifuged and re-suspended using 1x RNase-free siRNA Buffer to make 20µM stock before aliquoting into separate 0.5ml microfuge tubes, and were stored at -20°C for further experimentation.

The siRNA and DharmaFECT 1 transfect reagent (transfect reagent) (GE Healthcare Dharmacon Inc., UK) was diluted separately to 25nM and 1µl/well, in serum and antibiotic-free medium, was gently mixed by pipetting carefully up and down followed by 20 minutes incubation at room temperature to obtain a ready-to-use transfection medium.

Once the pre-seeded cell reached 80% confluency, the medium was aspirated and replaced by ready-to-use transfection medium followed by an appropriate period of incubation at 37.0°C, 5% CO₂ and 95% humidity. Transfection medium was removed and replaced by normal medium after 24 hours incubation to minimise the cytotoxicity of the transfect reagent.

2.12 Real time quantitative polymerase chain reaction (q-PCR)

q-PCR was undertaken to analyse the transcript expression level of target genes. Such technique is more sensitive than conventional RT-PCR and capable of detecting small quantities of cDNA and providing a more reliable value of the template copy number in each sample. This method requires a sequence specific DNA based fluorescent reporter probe which only quantifies the target transcript containing such probe sequence in order to greatly improve the specificity of the detection.

Amplifluor™ Uniprimer™ Universal system (Intergen company®, New York, USA) was used in this study. The amplifluor probe consists of a 3' region specific to the Z-sequence, ACTGAACCTGACCGTACA, which presents on the target specific primers and a 5' hairpin structure labelled with a fluorescent tag (FAM). Whilst in the hairpin structure, such fluorescent tag is linked to an acceptor moiety (DABSYL) which effectively quenches the fluorescence and produces no fluorescence signal. Primers were designed to the specific target transcript using

Beacon Designer Software. To each of the primer pairs specific to the target sequence, a Z-sequence was added to allow incorporation of the amplifluor uniprimer probe during PCR. Such Z-sequence incorporated DNA transcript acts as a template for the amplifluor uniprimer probe, and the hairpin structure in the probe is subsequently degraded and unfolded by DNA polymerase, therefore, disrupting the stable structure between fluorophore and quencher to enable sufficient fluorescence emission to be detected. The principle of this process is demonstrated in Figure 2-5. Pre-prepared cDNA samples were amplified and detected on a StepOne plus Real-Time PCR System (Applied Biosystems, Paisley, UK), using Precision FAST 2X q-PCR MasterMix (Primerdesign Ltd, Chandler's Ford, UK), specific forward primer (10pM), reverse primer containing the Z sequence (1pM) and the FAM-tagged Uniprimer probe (10pM). Each sample was loaded into a 96-well plate and the reaction mixed. The q-PCR conditions used are shown below:

q-PCR Reaction mix:

- Precision FAST 2X q-PCR MasterMix - 5µl
- Specific forward primer - 0.3µl
- Specific reverse primer with Z-sequence - 0.3µl
- Amplifluor probe – 0.3µl
- PCR H₂O – 3.1µl
- Prepared cDNA sample - 1µl

q-PCR conditions:

- Step 1: Initial denaturation - 94°C for 10 minutes
- Step 2: Denaturation - 94°C for 10 seconds
- Step 3: Annealing - 55°C for 30 seconds
- Step 4: Extension - 72°C for 10 minutes

Step 2 - 4 were repeated for 100 cycles.

The fluorescent signal was detected at the annealing stage, and the fluorescent signal emitted during PCR correlates to the amount of DNA template that has been incorporated with Z- sequence. The geometric increase of the fluorescent signal directly correlates to the exponential increase of DNA template, which is used to determine a threshold cycle for each reaction. The transcript copy number could be determined by the time/cycle number when fluorescent signal reaches a specific threshold. Expression of the target sequence was detected in conjunction with a range of standards of known transcript, PDPL, that are used to generate a standard curve to enable the calculation of transcript copy number in each unknown sample (Figure 2-6). Finally, the transcript copy number was normalised by the detected copy number of β -Actin and/or GAPDH.

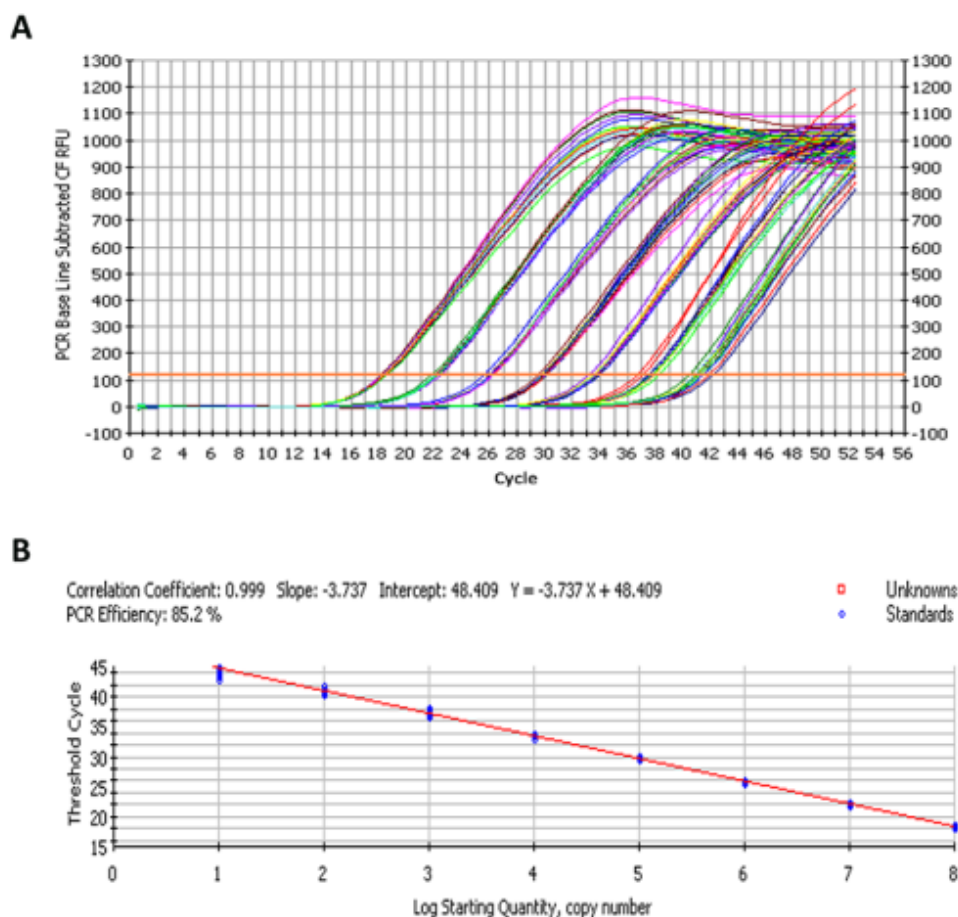


Figure 2-6: Diagram of standard curve generation

A. Reaction curves for serial diluted standard samples (10^8 to 10 copy number) using StepOne plus Real-Time PCR System; **B.** The standard curve generated based on the threshold cycle and copy number of the serial diluted standard samples. Red line indicates the standard curve generated and blue dots stand for different standard samples with known copy number.

2.13 Immunohistochemistry (IHC)

Primary antibodies: Anti-SOCS-1 (sc-9021, polyclonal antibody), anti-SOCS2 (sc-9022, polyclonal antibody), anti-SOCS3 (sc-9023, polyclonal antibody), anti-SOCS4 (sc-68827, polyclonal antibody), anti-SOCS5 (sc-100858, monoclonal antibody), anti-SOCS6 (sc-5608, polyclonal antibody) and anti-SOCS7 (sc-8291, polyclonal antibody and sc-137241, monoclonal antibody) were purchased from Santa Cruz

(or Insight Biotechnology, UK). All antibodies were used at a final concentration of 2µg/ml.

Histological analysis was performed using a standard streptavidin-biotin peroxidase technique. The frozen sections were fixed for 15 minutes in dried acetone (10162180) (Fisher Scientific UK, Loughborough, UK) and then air dried for 15 minutes. The sections were then washed three times in TBS for 5 minutes each. This was then followed by a 30 minute permeabilisation wash with 0.1% Saponin/TBS (Sigma-Aldrich, Inc., Dorset, UK). Since this reaction is reversible all subsequent washes were performed with 0.1% saponin/TBS. The sections were then incubated with a blocking solution in a humidified box at room temperature for 1 hour. The blocking solution, which contained 0.1% bovine serum albumin (BSA)/0.1% saponin/10% horse serum (horse serum was used to minimise the background since secondary antibody was raised in horse) in TBS, was also used to dilute all subsequent reagents. Excess blocking solution was removed and the sections were then incubated with the relevant, previously optimised, primary antibody for 1 hour. Following washing with 0.1% saponin/TBS, the sections were then incubated for 30 minutes with the biotinylated secondary antibody raised in horse (Vector Laboratories, UK), followed by a 30 minute incubation with ABC reagent in VECTASTAIN® ABC Kit (Vector Laboratories, Inc., CA, USA). 3'3 diaminobenzidine (DAB) substrate (5mg/ml) was used to develop the final reaction product, the sections were rinsed in tap water, counterstained with Gill's haematoxylin (Vector Laboratories, UK), and rehydrated through a series of graded alcohols, cleared in xylene (Fisher, UK) and mounted in Distyrene Plasticizer Xylene (DPX) (Merck, UK). Negative controls were performed where primary antibody was replaced with wash buffer.

Staining was visualised with a Leica DM1000LED microscope equipped with a MC120 HD camera and Leica Application Suite version 3.0.0 software (Leica Microsystems, Milton Keynes, UK), and the localisation and intensity of staining for each antibody was assessed by myself and a senior wound healing technician at both the wound edge and area distal to the wound edge.

2.14 Cellular lysis and protein extraction

Upon reaching sufficient confluency, cells were harvested through two different methods as follows dependent on future experimental application.

- Method 1. Cells were washed with 4°C sterile PBS twice and scraped from the flask using a sterile cell scraper in 5ml sterile PBS. The cell suspension was transferred to a 30ml universal container using a sterile pipette, followed by being centrifuged at 2500 rpm for 10 minutes to pellet the cells. The cell pellet was then lysed in 150-300µl (based on the pellet size) lysis buffer and transferred to a 1.5 ml microfuge tube using a sterile pipette.
- Method 2. Cells were trypsinised before being collected and centrifuged to obtain a pellet. PBS was used to wash the cell pellet twice through re-suspending followed by centrifugation. 100µl of protein lysis buffer was used to re-suspend the pellet, and the protein lysate was transferred into a 1.5ml microfuge tube using a sterile pipette.

The microfuge tube was subsequently placed on a Labinoco rotating wheel (Wolf laboratories, York, UK) (25rpm and 4°C) for no less than 40 minutes for sufficient extraction. After 15 minutes centrifugation at 13,000rpm,

supernatant (protein lysate) was transferred into a fresh 1.5ml sterile microfuge tube using a sterile pipette before being stored at -20°C.

2.15 Protein sample quantification, denaturisation and normalisation

A Bio-Rad *DCTM* protein assay kit (Bio-Rad, Laboratories, Hemel-Hempstead, UK) was used to determine the concentration of the extracted protein samples as outlined. Standard bovine serum albumin (BSA) protein samples (stock concentration of 10mg/ml) was made by dissolving BSA powder (Sigma-Aldrich, Inc., Dorset, UK) in PBS. Eight serially diluted BSA standard samples, ranging from 10mg/ml to 0.078mg/ml, was made by mixing the appropriate amount of BSA original stock and PBS. 5µl of each serially diluted BSA standard samples and the protein extraction samples were aliquoted into a 96-well plate in triplicates. Sufficient amount of working reagent A' was made by combining 1 portion of reagent S with 50 portions of reagent A. To the 5µl serially diluted standard BSA and extracted protein aliquots, 25µl of working reagent A' was added before the addition of 200µl of reagent B. The plate was transferred onto a shaker and was left for 30 minutes to allow the completion of the colorimetric reaction. The absorbance of the serial concentration BSA standard protein and extracted protein samples were then detected at 630nm using an ELx800 plate reading spectrophotometer (Bio-Tek, Wolf laboratories, York, UK).

A standard curve was generated based on the absorbance and the concentration of the serial diluted BSA standard protein samples. Subsequently, the concentration of the unknown concentration protein samples were calculated according to the standard curve before being normalised to the desired concentration of 2mg/ml through the addition of an appropriate amount of lysis buffer. Subsequently, such 2mg/ml samples were further diluted in a 1:1 ratio

with 2x Lamelli sample buffer to obtain a final concentration of 1mg/ml sample, and were denatured by being boiled at 100°C for 5 minutes before being stored at -20°C for further use.

2.16 Protein extraction and fluorometric protein quantification for Kinexus™ antibody microarrays

In order to acquire high concentration protein lysate, each cell type was cultured in two T75 flask until reaching 80% confluency followed by serum starvation for 24 hours before protein extraction. Upon protein extraction, cells were washed with 4°C sterile PBS twice and scraped from the flask using a sterile cell scraper in 5ml sterile PBS. The cell suspension from two flasks was combined and transferred to a 30ml universal container using a sterile pipette, followed by being centrifuged at 2500 rpm for 10 minutes to pellet the cells. The cell pellet was then lysed in 600µl lysis buffer and transferred to a 1.5 ml microfuge tube using a sterile pipette. The microfuge tube was subsequently placed on a Labinoco rotating wheel (Wolf laboratories, York, UK) (25rpm and 4°C) for no less than 40 minutes for sufficient extraction. After 15 minutes centrifugation at 13,000rpm, the supernatant (protein lysate) was transferred into a fresh 1.5ml sterile microfuge tube using sterile pipette before being stored at -20°C for further use.

A fluorescence assay using fluorescamine was applied to quantify total protein since the Bio-Rad DC™ protein assay kit is not compatible with 2-mercaptoethanol, one of the ingredients in the lysis buffer. Fluorescamine acetone was made by dissolving 15mg of fluorescamine (F9015)(Sigma-Aldrich, Inc., Dorset, UK) in 5ml absolute acetone (10162180) (Fisher Scientific UK, Loughborough, UK) in a glass vial and stored at 4°C for further use. Eight serially diluted BSA standard samples, ranging from 10mg/ml to 0.078mg/ml, was made

by mixing the appropriate amount of BSA original stock and PBS. The extracted protein samples were diluted 1 in 10 by adding 50µl of protein sample in 450µl of PBS. Then, 150µl of each serially diluted BSA standard samples and the 10X diluted protein extracted samples were aliquoted into a 96-well plate in triplicates before the addition of 50µl of fluorescamine acetone followed by being shaken for 1 minute. The fluorescence signal was then determined using a GloMax®-Multi Microplate Multimode Reader (Promega Biosystems Inc., Sunnyvale, CA, USA) with a 365nm excitation and 410-460nm emission filter. The concentration of the extracted protein samples were calculated based on the standard curve before being normalised to the desired concentration of 4mg/ml through the addition of an appropriate amount of lysis buffer to make 300µl stock followed by being stored at -20°C and sent for Kinexus™ antibody microarray analysis (Kinexus Bioinformatics, Vancouver, British Columbia, Canada).

2.17 Tris-glycine sodium dodecyl sulphate polyacrylamide gel electrophoresis (SDS-PAGE) and western blotting

2.17.1 Gel preparation and gel running

Tris-glycine SDS-PAGE was undertaken using an OmniPAGE VS10DSYS vertical electrophoresis system (OmniPAGE, Cleaver Scientific Ltd., Rugby, UK)(Figure 2-7). The vertical electrophoresis system was properly assembled according to the protocol provided by the manufacturer. 8% or 10% resolving gels and stacking gels were prepared in 15ml and 5ml aliquots respectively (enough for two gels) based on the size of the target protein. Ingredients used in the preparation of the stacking gel and resolving gel are outlined as follows (Table 2-6 and Table 2-7):

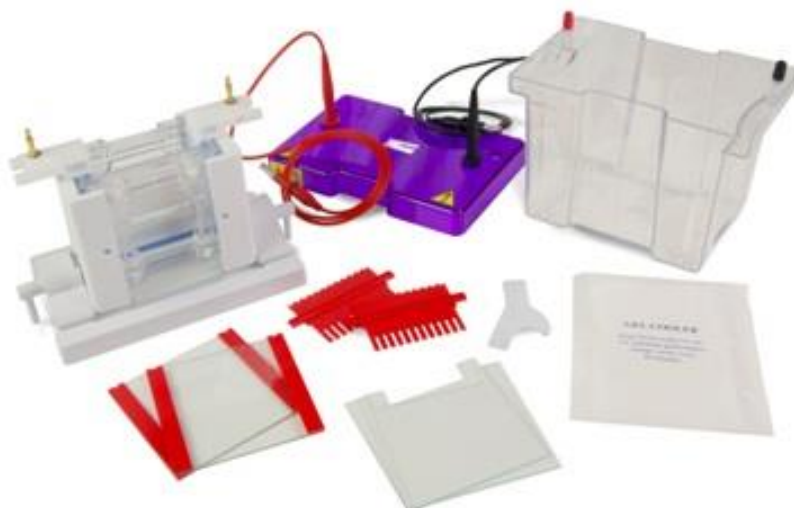


Figure 2-7: Acrylamide gel electrophoresis apparatus

Table 2-6: Ingredients for 8% and 10% resolving gel

Component	8% Resolving gel	10% Resolving gel
Distilled water	6.9ml	5.9ml
30% acrylamide mix (Sigma-Aldrich, Inc., Dorset, UK)	4.0ml	5.0ml
1.5M Tris-HCl buffer pH8.8 (Bio-Rad Laboratories, Hammel Hempstead, UK)	3.8ml	3.8ml
10% SDS	0.15ml	0.15ml
10% Ammonium persulphate	0.15ml	0.15ml
TEMED (Sigma-Aldrich, Inc., Dorset, UK)	0.009ml	0.006ml

*8% gel was used to separate proteins with molecular weight higher than 100kDa, whereas 10% gel was used when protein size was less than 100kDa

Table 2-7: Ingredients for stacking gel

Component	Stacking gel
Distilled water	3.4ml
30% acrylamide mix (Sigma-Aldrich, Inc., Dorset, UK)	0.83ml
0.5M Tris-HCl buffer pH6.8 (Bio-Rad Laboratories, Hammel Hempstead, UK)	0.63ml
10% SDS	0.05ml
10% Ammonium persulphate	0.05ml
TEMED (Sigma-Aldrich, Inc., Dorset, UK)	0.005ml

Once prepared and mixed thoroughly, the polyacrylamide resolving gel was immediately loaded into the two glass plates until it reached a level approximately 2cm below the top edge of the smaller plate. Ethanol was used to gently top up to ensure the formation of a smooth gel surface. The resolving gel was then left at room temperature for approximately 30 minutes to polymerase. The ethanol was then discarded by inverting the cassette after a clear interface was visible between the top ethanol layer and the bottom resolving gel layer. Subsequently, the stacking gel was prepared and loaded immediately on top of the polymerised resolving gel until it reached the top edge of the smaller plate. Well forming Teflon combs were subsequently inserted into the stacking gel without generating any air bubbles. After polymerisation of the stacking gel, the loading cassette was equipped into the electrophoresis tank. The central reservoir of the cassette and the electrophoresis tank was then filled with 1X running buffer to the appropriate level before the comb was removed. 20µl of the pre-prepared protein sample along with 8µl of the diluted Geneflow BLUEye Prestained Protein Ladder (Geneflow Limited, Fradley, Staffordshire, UK) were loaded into wells before gel running. EV243 power consort (Topac Inc., Cohasset, MA, USA) was used for acrylamide gel electrophoresis, and the electrophoresis condition used during the stacking gel running stage was 110V, 50mA and 50W, whereas the voltage was increased to 120V once the protein samples reached to the top edge of the resolving gel. The electrophoresis was undertaken for various length of time according to protein size and gel percentage.

2.17.2 Preparation and operation of gel transfer

One piece of Immobilon-P PVDF transfer membrane (EMD Millipore Corporation, Billerica, MA, USA) and six sheets of filter paper (Sigma-Aldrich, Inc., Dorset, UK) for each gel was prepared in advance to the gel transfer stage. PVDF transfer membrane was cut into the dimensions of 7.5cm x 7.5cm, and was soaked in 100% methanol then distilled water both for 30 seconds followed by being immersed in 1X transfer buffer for at least 5 minutes. Filter paper was cut into the dimensions of 8cm x 8cm followed by immersion in 1X transfer buffer for 10-20 minutes.

Mini Trans-Blot cell (Bio-Rad, Laboratories, Hamel-Hempstead, UK) (Figure 2-8 A) was used for protein transfer. Upon the completion of the electrophoresis, the power supply was disconnected and the gel running apparatus was disassembled. The glass plates were pried open using the spacer to expose the gel and the top portion of the gel, containing the stacking gel, was removed using the sharp edge of the spacer. The resolving gel, containing the fractionated protein samples, was carefully transferred on top of the pre-prepared polyvinylidene difluoride (PVDF) transfer membrane. Along with the filter paper and fibre pad, gel and membrane were assembled in a 'sandwich' shape and were tightened by the gel holder cassette (Figure 2-8 B). Such apparatus was then placed into the electrode assembly in the buffer tank along with a chilled pad, and 1X transfer buffer was then used to fill the buffer tank to the top edge of the gel holder cassette before being covered with lid.

Subsequently, the assembled buffer tank was placed into an ice box or cold room at 4°C, and EV202 power consort (Topac Inc., Cohasset, MA, USA) was utilised for protein transfer at the conditions of 100V, 200mA, 50W for 1-2 hours depending on the protein molecular weight (longer time for larger molecular

weight proteins). Transfer verification was undertaken by lifting one corner of the membrane and visualising if the gel was clear and transparent.

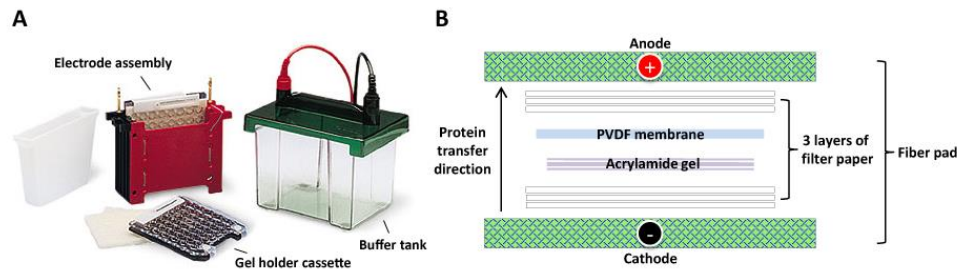


Figure 2-8: Western blotting protein transfer equipment

A. Mini Trans-Blot cell was used for protein transfer; **B.** Diagram of 'sandwich' protein transfer layout.

2.17.3 Protein staining and immunoprobing

2.17.3.1 Membrane staining

In order to verify the successful protein transfer, Ponceau S, a reversible and reusable protein stain that does not interfere with any subsequent immunoprobing, was utilised to stain the membrane. After gel transfer was completed, the membrane was separated from the gel transfer apparatus and was immersed in Ponceau S in a weighing tray with the protein side up on a shaker for a few minutes at room temperature. The membrane was then washed with distilled water until the emergence of the protein bands. If required, the membrane was cut into several pieces using a dry sterile blade, and subsequently the remaining stain was washed off for further immunoprobing.

2.17.3.2 Immunoprobing

After the washing stage, the membrane was rolled into a 50ml centrifuge tube (Nunc, Fisher-Scientific, Leicestershire, UK) containing

10ml of blocking solution (5% low fat milk and 0.1% Tween 20 in TBS), and incubated for one hour at room temperature on a roller mixer (Stuart, Wolf-Laboratories, York, UK). The membrane surface that contacted with the gel was ensured to face the inside of the centrifuge tube with the other side in contact with the inner-surface of the tube.

Once the blocking was complete, the primary antibody, prepared in blocking solution was pipetted into the centrifuge tube, and the tube was incubated on roller mixer at 4°C overnight. On the next day, the primary antibody was discarded and 10ml of wash solution (0.1% Tween 20 in TBS) was added into the tube before being rolled for 10 minutes to wash away the unbound primary antibody. Such wash stages were repeated three times. The membrane was then transferred into a fresh centrifuge tube containing 10ml of blocking solution with horseradish peroxidase (HRP) conjugated secondary antibody, and was incubated for two hours at room temperature on roller mixer followed by three washing steps (as above).

Subsequently, the membrane was treated with EZ-ECL Chemiluminescent Detection Kit (Biological industries, Kibbutz Beit-Haemek, Israel) as outlined. The EZ-ECL solution A and B were mixed in equal volumes and incubated in the dark at room temperature for at least for 5 minutes to equilibrate. The volume of each solution was calculated according to the protocol (0.1ml of the mixed EZ-ECL solution was used to sufficiently cover 1cm² membrane). Following the last wash, the excess wash solution on the membrane was drained off, and the membrane was placed on a clean weighing tray with the protein side facing up. The mixed EZ-ECL solution was then gently added on the membrane using a pipette in a 'S' shape followed by incubation for 1 minute in the dark at room temperature.

The excess EZ-ECL mixed solution was drained off from the membrane, and the chemiluminescent signal was then detected using a G:BOX Chemi XRQ imaging system (Syngene, Cambridge, UK) according to the protocol provided by the manufacturer.

2.17.3.3 Semi-quantitative analysis on western blot results by densitometry

Image J v1.50c was utilised for the semi-quantitative analysis of Western blot results. The rectangular selection tool was used to select a set area for each band on the Western blot image and the value of the integrated density for the selected area was then measured. The integrated density of the protein of interest was then normalised by the equation outlined:

- Normalised integrated density = normalising factor x integrated density of the protein of interest
- Normalising factor = GAPDH or Actin of control sample / GAPDH or Actin of treated sample

2.18 Cell functional assays

2.18.1 Electric cell-substrate impedance sensing (ECIS) based initial attachment and spreading, and migration assay

Electric cell-substrate impedance sensing (ECIS) instruments (Applied Biophysics Inc., NJ, USA) were applied to investigate cell behaviour based on the impedance parameter detected from gold electrodes coated on the bottom of a 96-well array (Applied Biophysics Inc., NJ, USA). ECIS is an *in vitro* assay used to quantify cell behaviour through detection of impedance variation based upon the current flow change on the electrode that is cultured with cells. Such a technique enables the

measurement of impedance over a range of frequencies to study different functional and structural cell properties, based on cell-cell junctional contacts and cell-substrate interactions, during the same period of time. Moreover, there are two parameters, resistance and capacitance, derived from impedance measurements. Resistance, consisting para- and trans-cellular current flow (Figure 2-9), is more likely to represent the quality and function of the cell barrier, whereas capacitance stands for the overall coverage of the electrodes (Szulcek et al., 2014). In this project, resistance measured in 4,000Hz were chosen to analyse cell function due to its best sensitivity to the current flow variation caused by cell behaviour change (Wegener et al., 2000).

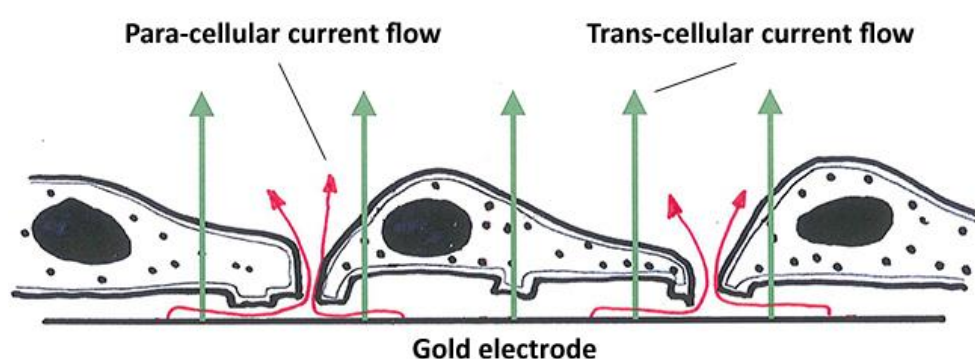


Figure 2-9: Diagram of current flow following cell attachment to the gold electrode

The 96-channel array station was connected to ECIS instruments pre-warmed at 37°C, 5% CO₂ and 95% humidity in an incubator (Figure 2-10 A). 200µl of normal medium was pipetted into each well of the 96-well array in a biosafety cabinet, and the 96-well array was connected to the 96-channel array station followed by connection check and stabilisation using Applied BioPhysics-ECIS Software V1.2.135 (Applied Biophysics Inc., NJ, USA).

During the time required to complete stabilisation, the cell suspension solution with appropriate cell density was prepared based on the cell type. Once the array stabilisation was completed, the 96-well array was removed from the

array station and transferred into a biosafety cabinet where the medium was aspirated using a glass aspirator and replaced with 200µl of prepared cell suspension solution with appropriate cell density (HaCaT: 8×10^4 cells/well; HECV: 4×10^4 cells/well). Each sample was seeded in six replicates. After the cell seeding, the 96-well array was equipped in the array station in the incubator.

Following inoculation at time zero, resistance increases as the cells attach to the electrode and begin spreading (Koo and Yun, 2016, Szulcek et al., 2014, Wegener et al., 2000) and the resistance will continue to increase until the cells reach confluence (Figure 2- 11). For the initial functional analysis of our cells, the resistance was measured at multiple frequencies, and the first four hours of data, obtained at 4,000Hz was taken to analyse the initial adhesion and spreading in line with the study by Wegener *et al.* (Wegener et al., 2000).

In normal ECIS measurements, a current of less than 1µA is normally used. This is undetected by the cells, and, in its measurement mode, ECIS essentially eavesdrops on cell behaviour electrically. When the current is boosted 1000 fold to 1mA, the resulting voltages across the cell membranes result in electroporation. When this high current is applied for more than several seconds, cell death ensues due to severe electroporation and possible local heating effects. Therefore, wound migration assay could be performed once the resistance curve reached plateau (Figure 2-12, Figure 2- 13) (Koo and Yun, 2016, Szulcek et al., 2014). A lethal electroporation (electrical wounding) was applied to the cells covering the gold electrodes for 20 seconds at the conditions of 3000µA and 60,000Hz to generate a uniformed lesion (250 µm diameter). The resistance was measured following electrical wounding and used to analyse cell migratory function over a four hour period following wounding. The electrical wounding and the subsequent measurements were repeated twice. The resistance obtained for each hour was

used to subtract the initial value at hour zero to display the resistance change which represents the cell recoverage of the electrodes from the starting point. Experiments were repeated for at least three times.

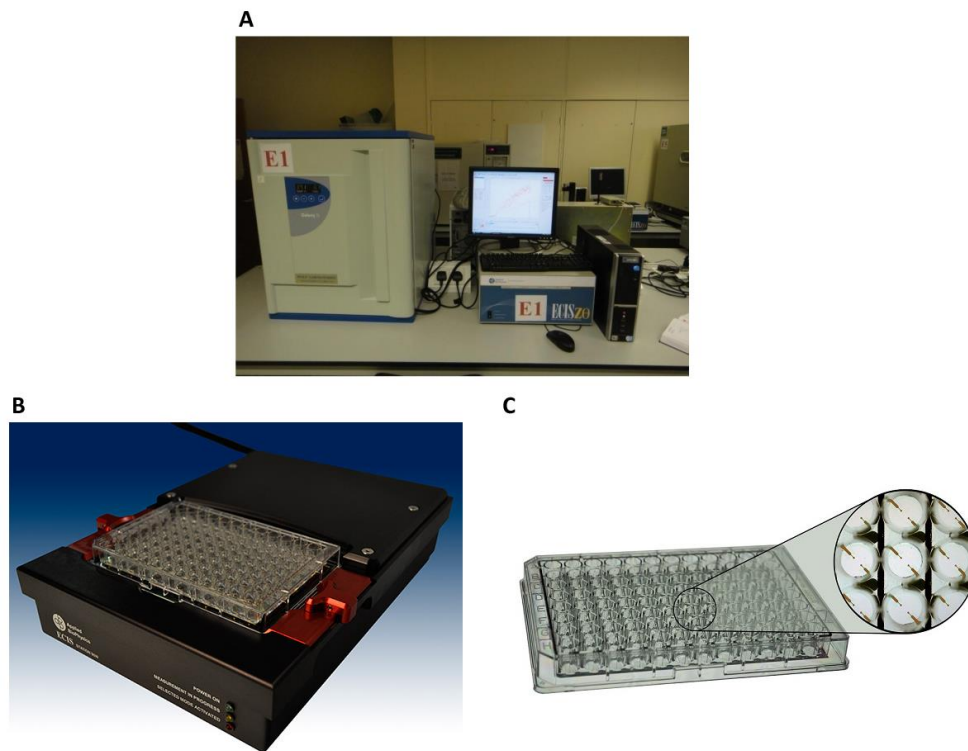


Figure 2-10: Electric cell-substrate impedance sensing (ECIS) system and cultureware

A. ECIS Z theta instrument connected to a 96-channel array station that was placed in a incubator; **B.** 96-channel array station equipped with a 96-well array; **C.** A 96W1E+ disposable electrode array coated with two electrodes on the bottom of each well.

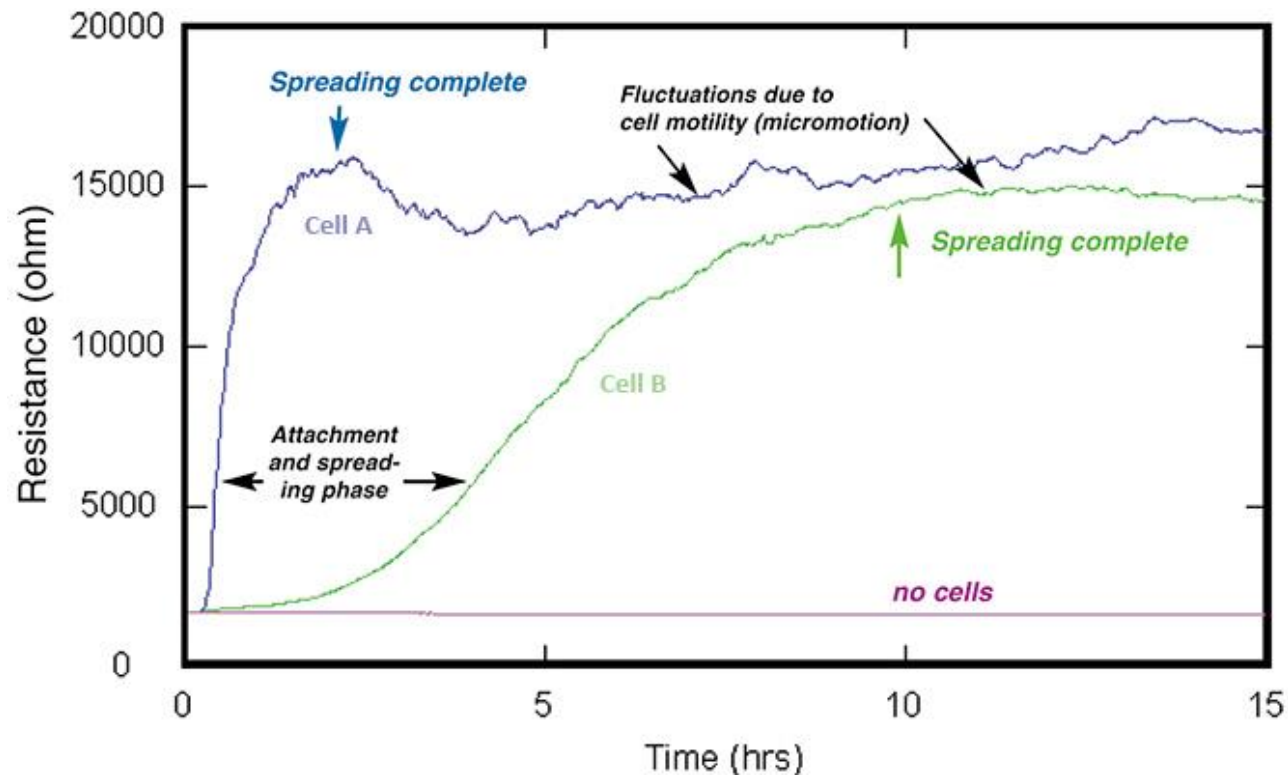


Figure 2- 11: Diagram of ECIS based cell attachment and spreading assay-resistance trace following inoculation

Following inoculation, resistance increases as the cells attach to the electrode and begin spreading. The resistance continues to increase until the cells reach confluence at the 2nd hours for cell A (blue curve) and the 10th hours for cell B (green curve). The small fluctuations in the curves are due to micromotion from the constant movement of the monolayer of cells on the electrode.

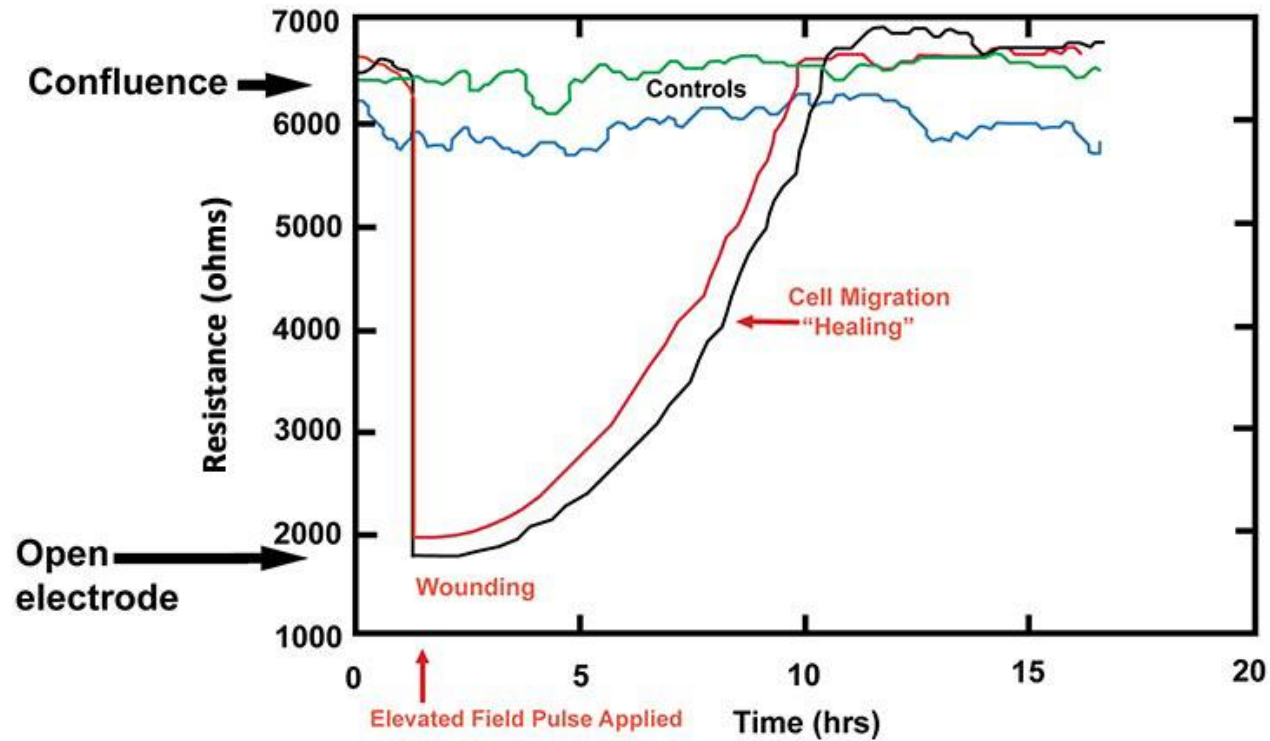


Figure 2-12: Diagram of ECIS based cell migration assay-resistance trace following lethal electroporation (electrical wounding)

Cells were first grown as complete monolayers and the resistance traces from four confluent wells can be seen as different colours (control: green and blue; wounded: black and red). At the red arrow timepoint, an elevated lethal electroporation was applied to two of the wells (black and red), wounding the cells on the electrode (250 μ m diameter) and resulting in the drop of resistance to that of an open electrode. As the time flows, these two traces gradually return to control values, as the healthy cells outside of the electrode migrate inward to recover the wounded area (healing).

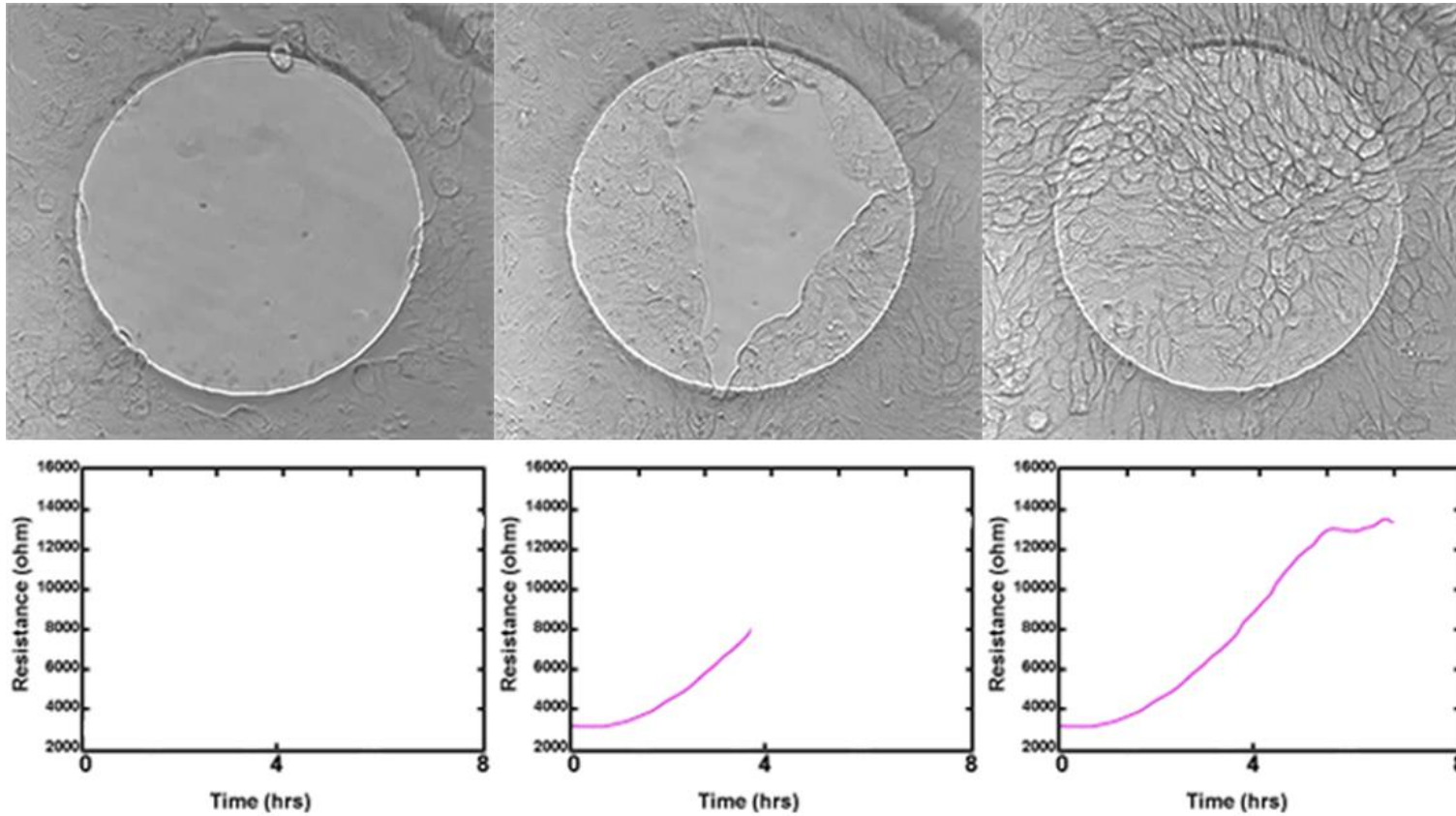


Figure 2- 13: Diagram of the relationship between cell migration and resistance trace following electrical wounding

Following electrical wounding, the resistance starts to increase as the cells outside of the electrode migrate to the open space until the wound has healed.

2.18.2 *In vitro* thiazolyl blue tetrazolium bromide (MTT) cell proliferation assay

MTT (3-(4,5-dimethylthiazol-2-yl)-2,5-diphenyltetrazolium bromide) tetrazolium has been widely adopted in a variety of cell functional assays, especially cell viability assay. MTT could be converted into a purple coloured formazan product with absorbance near 570nm by viable cells with active metabolism. Such formazan product, soluble in DMSO, accumulates as precipitate and distributes inside the cell as well as the culture medium near the cell surface. The amount of formazan product corresponds to the number of viable cells following linearity. Thus, the absorbance of formazan solution is comparable to the number of viable cells (Riss et al., 2004). MTT stock solution (5.5mg/ml) was made by adding 110mg thiazolyl Blue tetrazolium bromide powder (MTT) (Sigma-Aldrich, Inc., Dorset, UK) in 20ml PBS into a foil wrapped 30ml universal container, and the tube was then placed on a roller mixer (Stuart, Wolf-Laboratories, York, UK) until the powder was dissolved thoroughly. Once the powder was dissolved completely, the solution was filtered through a 0.2µm filter on top of a fresh foil wrapped sterile universal tube in a biosafety cabinet and stored at 4°C in fridge for further use.

Once 80% confluency was obtained, cells were trypsinised, centrifuged and re-suspended with normal medium. Cell number was then counted manually and an appropriate amount and cell density of cell solution was prepared for cell seeding. 200µl of the cell suspension (2000 cells/200µl) was then pipetted into three 96-well plates in six replicates followed by incubation for 24 (1 day), 72 (3 days) and 120 hours (5 days) at 37.0°C, 5% CO₂ and 95% humidity respectively. 20µl of sterile MTT stock solution was added at 24, 72 and 120 hours after cell seeding (working concentration of 0.5mg/ml MTT) and the plates were incubated at 37°C, 5% CO₂ and 95% humidity for 4 hours. The MTT medium solution was then aspirated gently, using a glass aspirator, followed by the addition of 200µl of

DMSO. After 10 minutes incubation at 37.0°C, 5% CO₂ and 95% humidity, the plate was taken out and tapped gently to thoroughly mix the DMSO solution.

The absorbance of each well was read at 540nm using an ELx800 plate reading spectrophotometer (Bio-Tek, Wolf laboratories, York, UK). Experiments were repeated for a minimum of three times. The cell number in each well was determined by the absorbance and a percentage increase at each time point was calculated as follows:

$$\text{Percentage increase} = \frac{[(\text{day 3 or day 5 absorbance} - \text{day 1 absorbance}) / (\text{day 1 absorbance} - \text{background absorbance})] \times 100\%}$$

2.18.3 *In vitro* MTT cell adhesion assay

Cell adhesion assays were used to examine cell initial adhesive ability to matrigel matrix. Matrigel® Basement Membrane Matrix (Corning Incorporated, Flintshire, UK) was diluted with serum free medium (SFM) to 50µg/ml and 5µg of matrigel was added to the wells of 96-well plate under sterile conditions followed by dehydration at 55°C for 1 to 2 hours. The matrigel matrix coated wells were rehydrated by gently pipetting 100µl SFM and incubating at room temperature for at least 30 minutes before aspirating the SFM. Cells (40,000 cells in 200µl normal medium) were seeded on the rehydrated matrigel matrix in six replicates and the plate was incubated for 45 minutes. Subsequently, the medium was gently aspirated by glass aspirator and 100µl of PBS was used to gently wash the wells twice. MTT in 200µl normal medium (0.5mg/ml working concentration) was added to each well and the plate was incubated at 37.0°C, 5% CO₂ and 95% humidity for 4 hours. The medium containing MTT was then aspirated followed by the addition of 200µl DMSO. After 10 minutes of incubation in DMSO at 37.0°C, 5%

CO₂ and 95% humidity, the plate was taken out and tapped gently to let the DMSO solution mix thoroughly.

The absorbance of each well was detected at 540nm using ELx800 plate reading spectrophotometer (Bio-Tek, Wolf laboratories, York, UK). Initially attached cell numbers in each well was determined by the absorbance. Experiments were repeated a minimum of three times.

2.18.4 *In vitro* cell migration assay (wound healing assay)

A EVOS® FL Auto Imaging System (Life technologies, CA, USA) equipped with EVOS® Onstage Incubator (Life technologies, CA, USA) (Figure 2-14) were used the *in vitro* cell migration assay. Such a system was used to capture images at certain time intervals at the same location in each monitored well and continuously maintain culture conditions for the cells being investigated.

Cells in 1ml of normal medium were pre-seeded with appropriate density (HaCaT: 600,000 cells/well, HECV: 400,000 cells/well) in a 24-well plate and incubated until the formation of a monolayer on the next day. The cell monolayer was scraped by a 200µl pipette tip producing an approximately straight wound. The medium was aspirated by glass aspirator and the well was washed by pipetting and aspirating PBS twice to remove the detached cell debris. 2ml of normal medium was then gently pipetted into the well followed by 10 minutes of incubation at 37°C, 5% CO₂ and 95% humidity for cell recovery. The 24-well plate was then placed in an EVOS® Onstage Incubator (Life technologies, CA, USA) equipped in an EVOS® FL Auto Imaging System (Life technologies, CA, USA). Integrated EVOS® FL Auto Imaging System Software was used to set up and adjust the chamber environment condition at 37°C, 5% CO₂ and 80% humidity. Three views on each wound were set up to be captured in 30 minutes interval until the

15th and 20th hour for HaCaT and HECV respectively. The distance between two wound edges was measured using Image J v1.50c in pixels, and the distance change at every time interval was calculated by wound edge distance at minute zero subtracting wound edge distance at each time point. The mean and standard deviation was calculated using the three measurements per each wound, and was plotted on a scatter line chart. Experiments were repeated a minimum of three times.



Figure 2-14: EVOS® FL Auto Imaging System installed with EVOS® Onstage Incubator

2.18.5 Tubule formation assay

Matrigel® Basement Membrane Matrix (Corning Incorporated, Flintshire, UK) was used in the tubule formation assay to investigate the vascular regeneration ability of endothelial cells on matrigel matrix. 50µl of neat matrigel matrix was gently pipetted into the bottom of each well in 96-well plate without generating any bubbles. The plate was kept in sterile condition for at least 40 minutes until polymerisation. Cells (40,000 cells in 200µl normal medium) were gently seeded on the polymerised matrigel matrix in six replicates and the plate was incubated

at 37°C, 5% CO₂ and 95% humidity. The plate was then taken out, and images of each well was visualised and captured at X5 objective magnification at 2 hour intervals until the 10th hour, using a Leica DMI1 microscope equipped with a MC120 HD camera and Leica Application Suite version 3.0.0 software (Leica Microsystems, Milton Keynes, UK). The total perimeter of each formed tubule in every image was measured using Image J v1.50c, and mean and standard deviation was then calculated according to the values from each replicate. Results were subsequently plotted as a bar chart. Experiments were repeated a minimum of three times.

2.19 Statistical analysis

Statistical analysis was undertaken using the SigmaPlot 11 and Graphpad Prism 6 statistical software packages. Data was analysed using t-test or Mann Whitney test, depending on data parameters. Values of $p < 0.05$ (*), $p < 0.01$ (**), $p < 0.001$ (***) and $p < 0.0001$ (****) were regarded as statistically significant.

Chapter III

Expression of the suppressor of cytokine signalling (SOCS) family in human chronic wound tissues: potential implications for SOCS in chronic wound healing

3.1. Introduction

The area of chronic wound healing has drawn much attention from many healthcare professionals due to the high cost of healthcare resources for patients seeking appropriate treatment combined with the complexity of its underlying mechanisms. It has been demonstrated that a reduction in tissue growth factors, a proteinase / inhibitor imbalance, and the presence of senescent cells contribute to the pathophysiology in chronic wounds (Harding *et al.*, 2002). A variety of treatments, such as dressings, topical growth factor application, autologous skin grafting and bioengineered skin equivalents have been applied to treat certain types of chronic wounds in addition to the basic treatments (Harding *et al.*, 2002). However, the specific mechanisms of a number of these treatment remain unclear and are currently under investigation. Therefore, additional insight into the mechanisms responsible are required to gain a better understanding of the wound-healing process. Further clarification of this complex system may contribute to the emergence of a prognostic marker to predict the healing potential of chronic wounds which could benefit the management of patients suffering with this clinical problem.

Chronic wounds have been defined as wounds that fail to follow the normal healing process in a timely and orderly manner, which severely disrupt the anatomic and functional integrity of the skin (Lazarus *et al.*, 1994). Chronic wound such as venous leg ulcers are constantly trapped within the inflammatory phase since the normal mechanisms responsible for switching off inflammation are disrupted by their pathological status (Trentham *et al.*, 2000). Studies have shown that the imbalance of MMP/tissue inhibitors of MMP (TIMP) is one of the key factors leading to non-healing chronic wounds (Trentham *et al.*, 1999, Yager *et al.*, 1996). Elevated pro-inflammatory cytokines, IL-1, IL-6 and TNF- α , were also found

in non-healing chronic wound compared to healing ones (Trentham et al., 2000). In addition, previous *in vitro* study has proved that the expression of MMP and TIMP was regulated by IL-1 and TNF- α (Ito et al., 1990). Moreover, the abnormal distribution of growth factors was also found in chronic ulceration (Higley et al., 1995). Therefore, the dysregulation of a range of pro-inflammatory cytokines and growth factors play critical roles in the pathophysiology of wound healing.

As discussed in the general introduction section of this thesis, the SOCS family of proteins are known to play key roles in the regulation of a range of growth factors and cytokines, and this regulation will likely have further implications in the process of wound healing (Feng et al., 2016). Indeed members of this family have been linked to wound healing, for example SOCS-1 and SOCS-3 are induced by a number of pro-inflammatory cytokines including IL-2, IL-4 and IL-6 and IFN, and subsequently act as a feedback negative regulator to suppress their inflammatory response and hence, have potential to alleviate the exacerbated inflammation in chronic wounds in order to restore the normal reparative process. In contrast to the inhibitory effect of SOCS-1 and SOCS-3 on IL-2 signalling, SOCS-2 was found to restore IL-2 signalling through association and degradation of SOCS-3 (Tannahill et al., 2005). Additionally, SOCS-2 and SOCS-6 have been found to associate with other SOCS family members (Piessevaux et al., 2006), suggesting a potential role in coordination of other SOCS proteins to maintain the balance of cytokine signalling during wound healing. Other members of the SOCS family have been poorly characterised in this context though SOCS-4 and SOCS-5 are known to be induced by EGF and negatively regulate EGF signalling through the interaction with EGFR (Kario et al., 2005). Additionally, SOCS-7 can be induced by pro-inflammatory cytokines such as IL-1 β and IL-6, and associate with EGFR (Matuoka et al., 1997). Given the role of EGF-like growth factor in the proliferation and re-

epithelialisation phase (Clark, 1996) of wound healing these, more poorly characterised members, may also play important roles.

Given the potential significance of this family in the wound healing process, the scale of healthcare issues caused by chronic wounds and the need to seek novel biomarkers or therapeutics to identify or treat non-healing chronic wounds, the current chapter aimed to explore the expression of SOCS-1 – SOCS-7 in two clinical cohort of chronic wounds. Firstly, differences in gene expression of SOCS members was explored between healing/healed (n=20) and non-healing wounds (n=51) and subsequently a subset of an additional cohort of chronic healing/healed (n=45) and non-healing (n=45) wounds was used to explore protein distribution and expression.

3.2. Materials and methods

3.2.1 Primers

Specific primers were designed using Beacon designer software (PREMIER Biosoft International, Palo Alto CA, USA) and synthesised by Sigma (Dorest, UK). Details of the primers are outlined in Table 3-1.

Table 3-1: Primers used for detection of SOCS family members and the CK-19 house keeping gene in this study, *ACTGAACCTGACCGTACA* represents Z sequence

Primer	Forward	Reverse
SOCS 1	5'-GATGGTAGCACACAACCAG	5'- <i>ACTGAACCTGACCGTACA</i> GAGGAGGAGGAGGAAGGTT
SOCS 2	5'-GGATGGTACTGGGGAAGTAT	5'- <i>ACTGAACCTGACCGTACA</i> TGGGAGCTATCTCTAATCAA
SOCS 3	5'-TCAAGACCTTCAGCTCCA	5'- <i>ACTGAACCTGACCGTACA</i> GTCAGTCACTGCGCTCCAGTAG
SOCS 4	5'-GGCAGTGTTTTCCAATAAAG	5'- <i>ACTGAACCTGACCGTACA</i> AGGTGGGAAAGGACACTTAT
SOCS 5	5'-AGTCAAAGCCTCTCTTTCC	5'- <i>ACTGAACCTGACCGTACA</i> CATTTTGGGCTAAATCTGA
SOCS 6	5'-CCTTACAGAGGAGCTGAAAA	5'- <i>ACTGAACCTGACCGTACA</i> CGAAAAGAAAAGAACCATC
SOCS 7	5'-CAGGCCCTGAATTACCTC	5'- <i>ACTGAACCTGACCGTACA</i> GAGGTTGCTGCTGCTGCT
CK-19	5'-AGCCACTACTACACGACCAT	5'- <i>ACTGAACCTGACCGTACA</i> TCGATCTGCAGGACAATC

3.2.2 RNA extraction and reverse transcription

RNA extraction was undertaken in accordance with the manufacturers instructions and as described in section 2.7 of chapter II before being resuspended in DEPC water, quantified using a NanoPhotometerTM (IMPLEN; Geneflow Ltd., Lichfield, UK), standardised and reverse transcribed to generate cDNA, as described in section 2.8 of chapter II.

3.2.3 q-PCR

Primers were designed to each of the SOCS family members using the Beacon Designer Software (Bio-Rad, Hercules, CA, USA) and transcript expression in each of the wound samples quantified using qPCR. This method uses a Molecular Beacon / Amplifluor system as described in full in section 2.12 of chapter II

SOCS family members were detected in conjunction with the CK-19 housekeeping gene and values were normalised against this gene. Details of primers used in this section of the thesis are outlined in Table 3-1.

3.2.4 IHC

Immunohistochemical analysis was undertaken to explore the staining pattern and intensity of the SOCS family members in the chronic wound cohort biopsies. Primary antibodies used were indicated in Table 2-4 Chapter II. All antibodies were purchased from Insight Biotechnologies (Wembly, England, UK) and were used at a final concentration of 2µg/ml.

IHC analysis was performed, as described in section 2.13 of chapter II, on a subset of chronic wound tissues that included healing/healed (n=10) and non-healed (n=10) biopsies using a standard avidin-biotin peroxidase technique.

Staining was visualised with a microscope under a range of magnifications. The localisation and staining intensity for each antibody was assessed at both the wound edge and areas distal to the wound edge. Staining intensity was qualitatively graded as strong, moderate or negative. Full details regarding tissue collection, processing and the clinical cohorts are outlined in section 2.6 of Chapter II.

3.2.5 Statistical analysis

Statistical analysis was undertaken using the SigmaPlot 11 statistical software package (Systat Software Inc, London, UK). Data was analysed using Mann Whitney test as the data was not normally distributed. Values of $p < 0.05$ were regarded as statistically significant.

3.3. Results

3.3.1 Gene expression levels of SOCS family members in healing/healed and non-healing chronic wounds

The transcript expression levels of seven SOCS family members were quantified, using q-PCR, in a cohort of venous leg ulcer patients and compared between those chronic wounds defined as healed/healing (n=20) and those defined as non-healing (n=51) (Figure 3-1, Figure 3-2). Compared to healing/healed chronic wounds, the non-healing chronic wound tissues had significantly enhanced level of SOCS-3 gene expression, showing an 81% increase in expression ($p = 0.0284$). Similarly, significantly higher levels of SOCS-4 were also seen in non-healing chronic wounds compared to healing/healed chronic wounds, with a 93% increase in SOCS-4 gene expression ($p = 0.0376$).

Similarly, enhanced gene expression levels of SOCS-1, 2, 5 and 6 were also observed in the non-healing chronic wounds compared to the healing/healed chronic wounds, accounting for 50%, 43%, 93% and 87% increases respectively. However, the results did not reach statistical significance ($p > 0.05$). Somewhat in contrast to this general trend, the expression levels of SOCS-7 transcript was found to be elevated 43% in the healing/healed chronic wounds when compared to that of the non-healing chronic wounds, though again, the results were not found to be statistically significant ($p > 0.05$).

Patients were also assessed for signs of clinical and microbiological infection. In the cohort, one of the 20 patients who are defined as healing/healed had signs of infection, whereas, 7 out of 51 non-healing patients had signs of infection. We further compared the levels of gene expression of all the seven SOCS members in the non-healing cohort. As shown in Table 3-2, there were no difference in all the gene expression levels of SOCSs when the respective

subgroups were compared. Thus there did not appear to be a link between the infection of wound tissue and the expression levels of SOCSs.

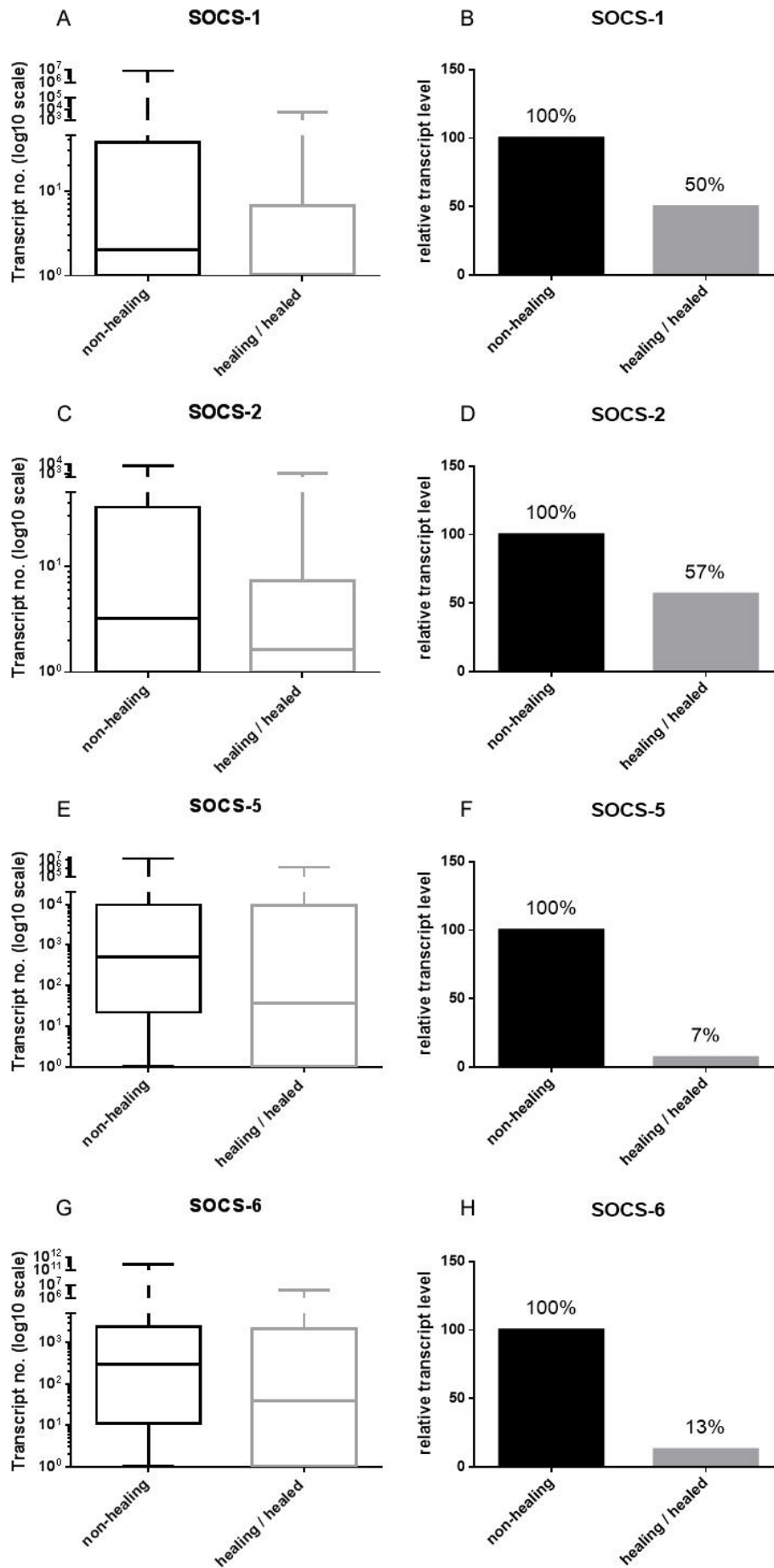


Figure 3-1: The gene expression profile of SOCS-1, -2, -5 and -6 in clinical chronic wound biopsies

A, C, E, G Gene expression levels of SOCS-1, -2, -5 and -6 in chronic wound tissues (healing/healed n=20, non-healing n=51) are presented on a log scale as box plot; **B, D, F, H** Relative gene expression levels (median) of SOCS-1, -2, -5 and -6 as percentage of non-healing group. The expression of each SOCS family member is normalised by the expression of CK-19; data was analysed using a Mann Whitney test (non parametric t test).

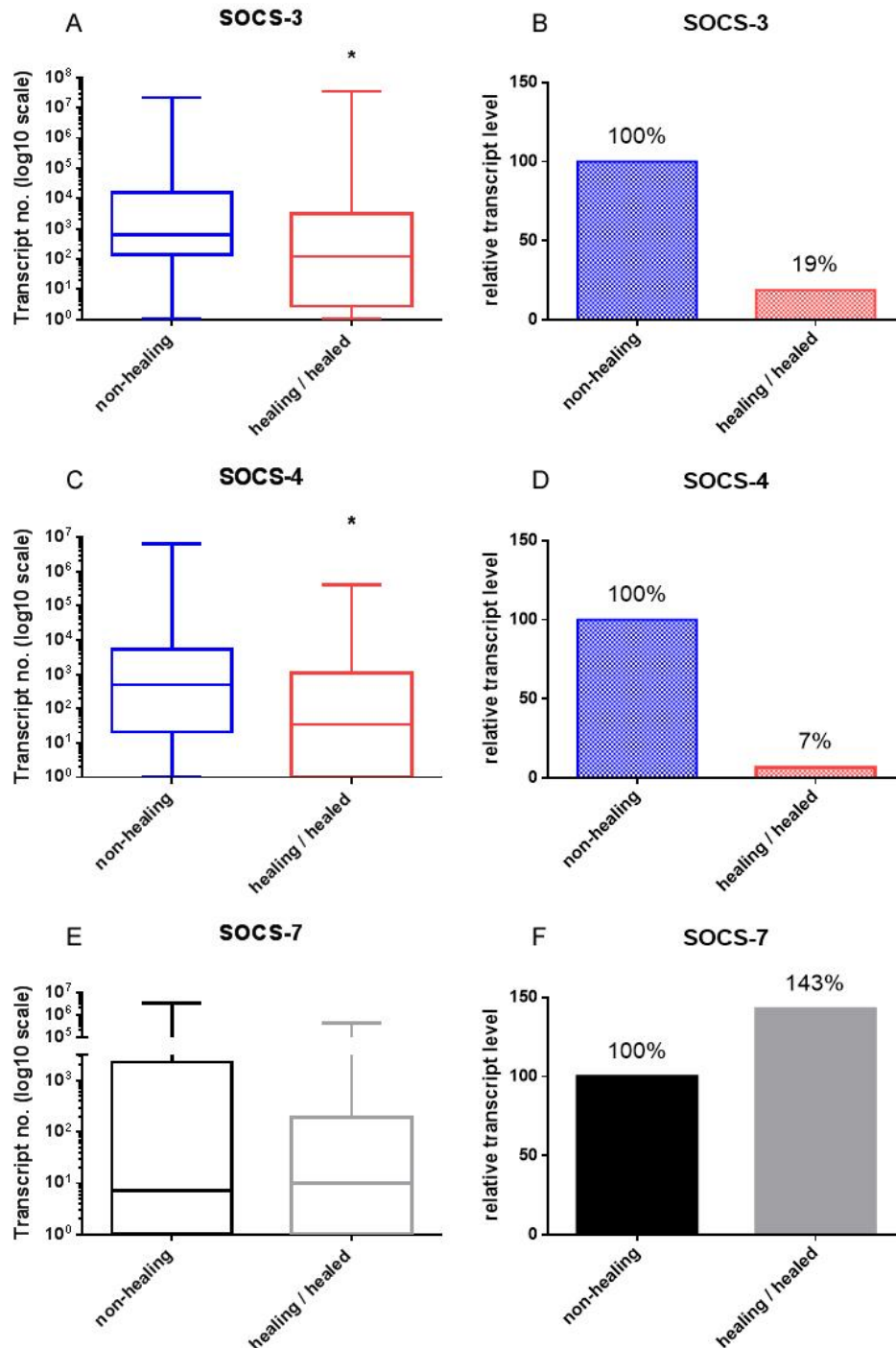


Figure 3-2: The gene expression profile of SOCS-3, -4 and -7 transcript in clinical chronic wound biopsies

A, C, E Gene expression levels of SOCS-3, -4 and -7 in chronic wound tissues (healing/healed n=20, non-healing n=51) are presented on a log scale as box plot; **B, D, F** Relative gene expression levels (median) of SOCS-3, -4 and -7 as percentage of non-healing group. The expression of each SOCS family member is normalised by the expression of CK-19; * represents $p < 0.05$, data was analysed using a Mann Whitney test (non parametric t test).

Table 3-2: The relationship between expression of SOCS transcript and clinical infection in non-healing chronic wound tissues

SOCS	Infected (n=7)		Non-infected (n=44)		P value *
	Median	IQR	Median	IQR	
SOCS-1	2	0.25-25.5	3	0-47.5	0.966
SOCS-2	1.37	0.448-52.148	3.865	0.375-31.36	0.816
SOCS-3	363	31.25-12173.75	659	159-15168	0.632
SOCS-4	478	59-10378	606	15-3907	0.742
SOCS-5	764	89.25-16537.5	475	21-8786	0.722
SOCS-6	822.223	126.272-2088713.923	257.845	10.636-1901.7	0.268
SOCS-7	0	0-53889.25	20.5	0-1356.5	0.898

* Mann-Whitney U test was used for the statistical analysis

3.3.2 Protein expression levels of seven SOCS family members in chronic tissues

Another clinical cohort (Cohort 2) of healing/healed (n = 45) and non-healing (n = 45) chronic wound samples were used for IHC analysis. A subset of 10 healing/healed and 10 non-healing chronic wound samples, taken from this cohort, were used to explore the protein expression and localisation of SOCS-1 to SOCS-7 within these two chronic wound sub-families.

3.3.2.1 Negative staining in chronic tissues

IHC analysis was performed on the chronic wound tissues from Cohort 2, detecting the distribution and expression levels of seven SOCS proteins. Negative control staining was precessed along with the experiment to testify the specificity of the secondary antibody. As shown in Figure 3-3 and Figure 3-4, there was no positive staining observed in all the negative controls in either non-healing chronic wound biopsies or healing/healed wound biopsies, suggesting correct secondary antibody specificity to the relative primary antibody used in this study.

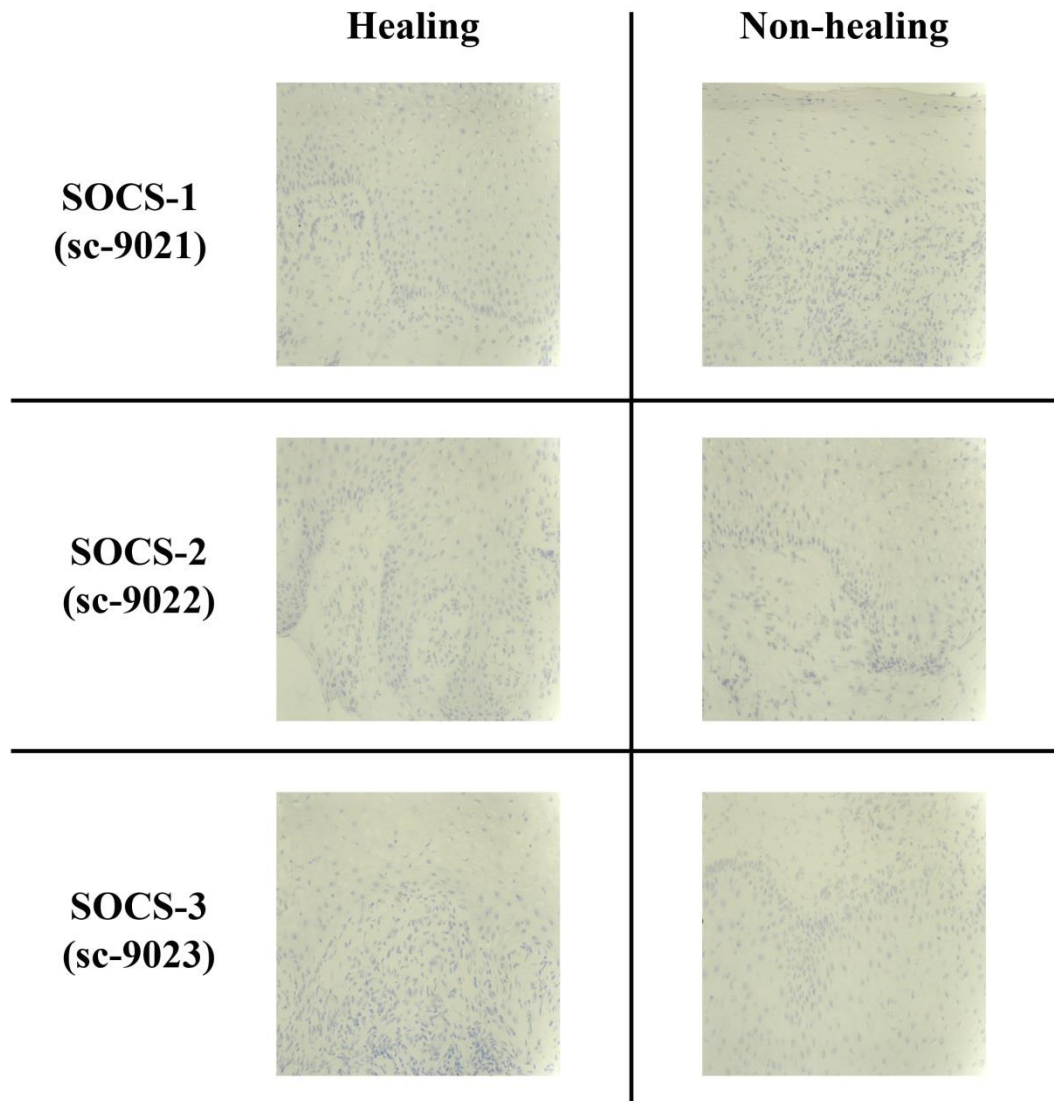


Figure 3-3: Negative control staining in SOCS-1, -2 and -3 primary antibody group

Pictures were captured at x10 objective magnification; representative images of healing/healed (n = 10) and non-healing (n = 10) chronic wound sections are shown.

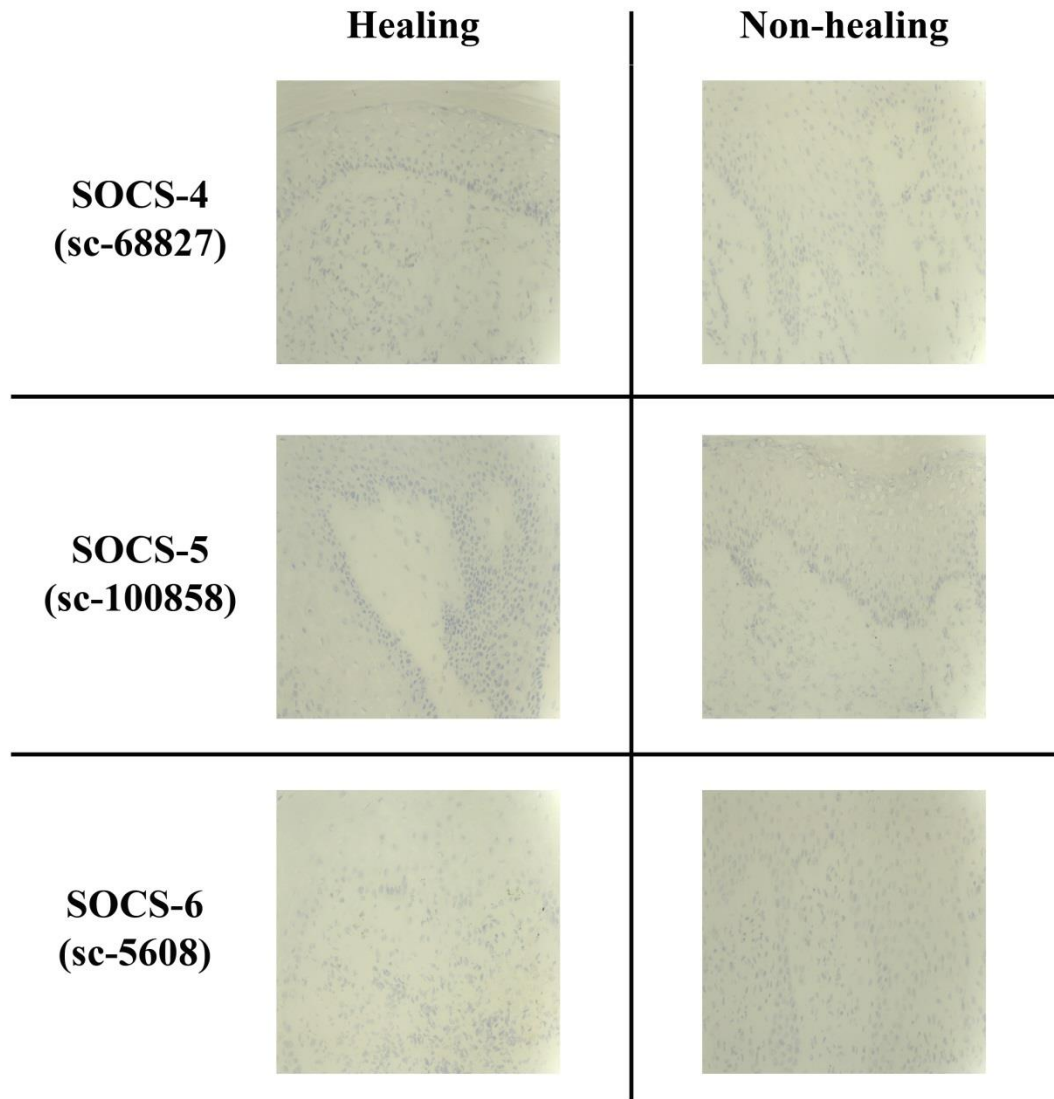


Figure 3-4: Negative control staining in SOCS-4, -5 and -6 primary antibody group

Pictures were captured at x10 objective magnification; representative images of healing/healed (n = 10) and non-healing (n = 10) chronic wound sections are shown.

3.3.2.2 SOCS-1 staining in chronic tissues

IHC analysis revealed that the majority of chronic wounds tested stained positively for SOCS-1 protein (15/20 chronic wounds). The expression of SOCS-1 was observed in 7/10 healing/healed and 8/10 non-healing chronic wounds, and therefore there was no distinct differences between the two groups. The majority of the positive biopsies expressed moderate levels of SOCS-1, with the exception of one non-healing chronic wound where the expression was defined as strong (Figure 3-5, Figure 3-6).

A comparison of SOCS-1 expression at the wound edge to that observed distal to the wound (towards normal tissue) revealed that 6/20 biopsies demonstrated an increased expression of SOCS-1 distal to the wound edge, although no difference was evident between the healing/healed and non-healing groups (3/10 healing/healed and 3/10 non-healing).

Generally in these chronic wounds, diffuse cytoplasmic staining was observed in the mature keratinocytes of the epidermis, although increasing nuclear and cytoplasmic intensity was seen in the basal layer distal to the wound edge. Most blood vessels were found to be weakly positive for SOCS-1 in all the biopsies analysed. Positive staining was also observed in the dermal inflammatory infiltrate of some biopsies.

According to the IHC results, SOCS-1 was predominantly expressed in epidermis, and weakly expressed in dermis in both healing/healed and non-healing chronic wound biopsies, although no difference was observed on either the expression intensity or the distribution patterns of SOCS-1 between the two groups.

SOCS-1 expression at the wound edge

Healing/healed

Non-healing

Moderate

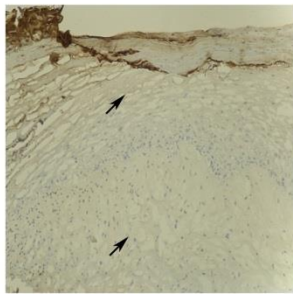
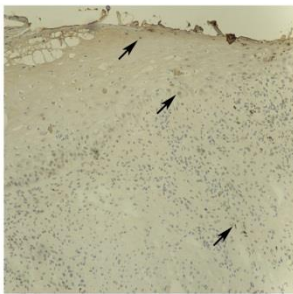
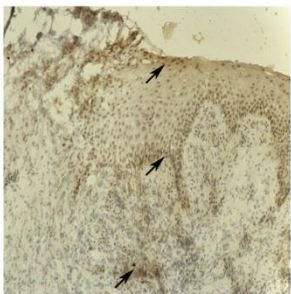
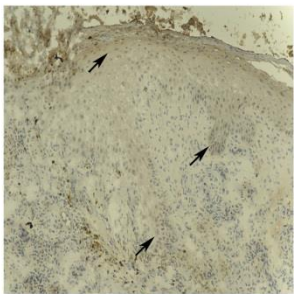
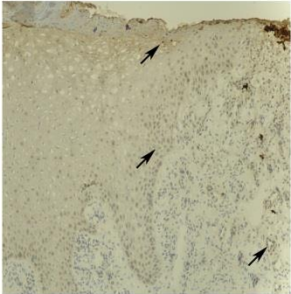
Distribution

Strong

Moderate

Distribution

X10



X20

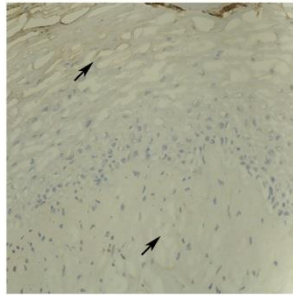
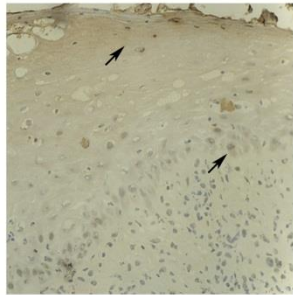
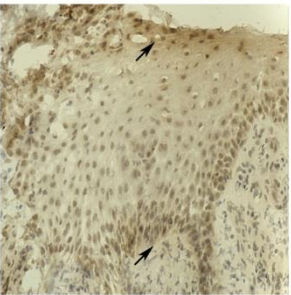
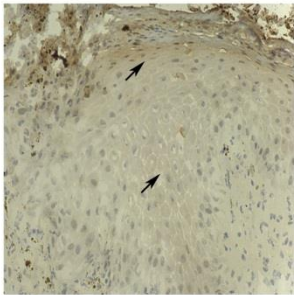
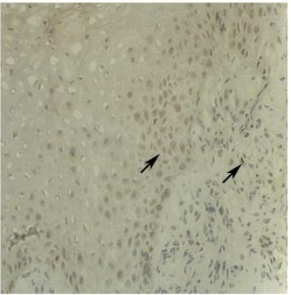


Figure 3-5: The expression pattern of SOCS-1 at the wound edge of clinical chronic wound biopsies

IHC evaluation of the SOCS-1 protein at the wound edge of healing/healed wounds (left two panels) and non-healing wounds (right three panels), with 'distribution' panels indicating the expression pattern of SOCS-1 in the two groups. Overall, non-healing sections demonstrate areas of strong and moderate staining as well as protein distribution (right three panels), whereas healing/healed wound biopsies only indicate moderate staining and protein distribution (left panels). Pictures were captured at two objective magnifications (x10 and x20); representative images of healing/healed (n = 10) and non-healing (n = 10) chronic wound sections are shown; arrows indicate positive staining.

SOCS-1 expression distal to the wound edge

Healing/healed

Moderate

Distribution

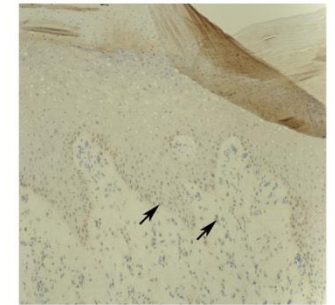
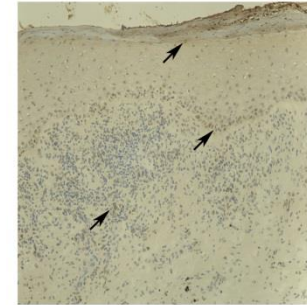
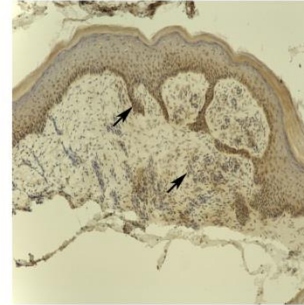
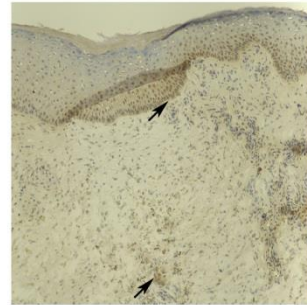
Non-healing

Strong

Moderate

Distribution

X10



X20

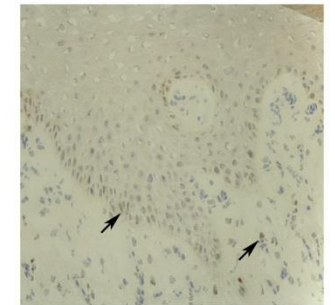
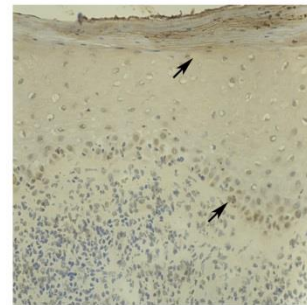
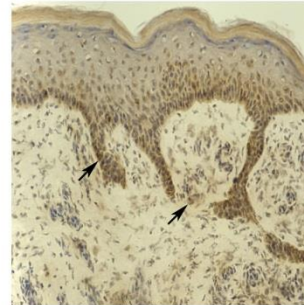
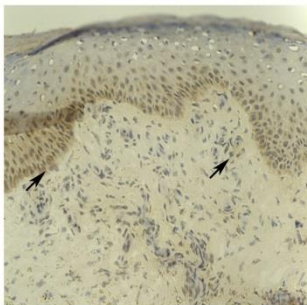
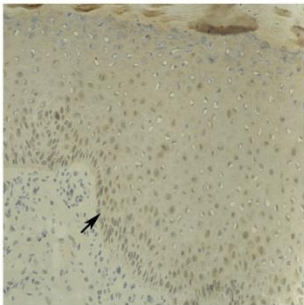


Figure 3-6: The expression pattern of SOCS-1 distal to the wound edge in clinical chronic wound biopsies

IHC evaluation of the SOCS-1 protein distal to the wound edge of healing/healed wounds (left two panels) and non-healing wounds (right three panels), with 'distribution' panels indicating the expression pattern of SOCS-1 in the two groups. Overall, non-healing sections demonstrate areas of strong and moderate staining as well as protein distribution (right three panels), whereas healing/healed wound biopsies only indicate moderate staining and protein distribution (left panels). Pictures were captured at two objective magnifications (x10 and x20); representative images of healing/healed (n = 10) and non-healing (n = 10) chronic wound sections are shown; arrows indicate positive staining.

3.3.2.3 SOCS-2 staining in chronic wound tissues

Positive SOCS-2 staining was identified in 17/20 chronic wound biopsies, 8/10 healing/healed and 9/10 non-healing biopsies respectively. The majority of these positively stained biopsies exhibited SOCS-2 expression of moderate intensity, albeit 3/20 revealed stronger intensity (2/10 healing/healed, 1/10 non-healing) (Figure 3-7, Figure 3-8). Three of the positively stained biopsies showed SOCS-2 expression in the dermal cell infiltrate, while no expression was observed in the epidermis.

SOCS-2 protein expression was uniform throughout the whole biopsy, with only four chronic wounds showing differences between the wound edge and distal to the wound (3/10 healing/healed, 1/10 non-healing). Within the healing/healed subset, two of these biopsies showed an increased expression distal to the wound edge, whereas the other subset demonstrated an increased SOCS-2 in the dermal infiltrate directly below the leading migratory epidermis (which was negatively stained).

Expression of SOCS-2 protein was generally observed as diffuse cytoplasmic in mature keratinocytes, or nuclear in the lower keratinocytes of the basal layer. Membranous staining was observed in the very mature keratinocytes of some biopsies. SOCS-2 protein was also found in dermis.

In summary, SOCS-2 was observed in both the nucleus and cytoplasm of keratinocyte in the epidermis, whereas relatively lower expression of SOCS-2 was seen in dermis in both healing/healed and non-healing chronic wound biopsies. However, no expressional difference of SOCS-2 was found between healing/healed or non-healing wounds and likewise there was no preference of SOCS-2 to the wound edge location.

SOCS-2 expression at the wound edge

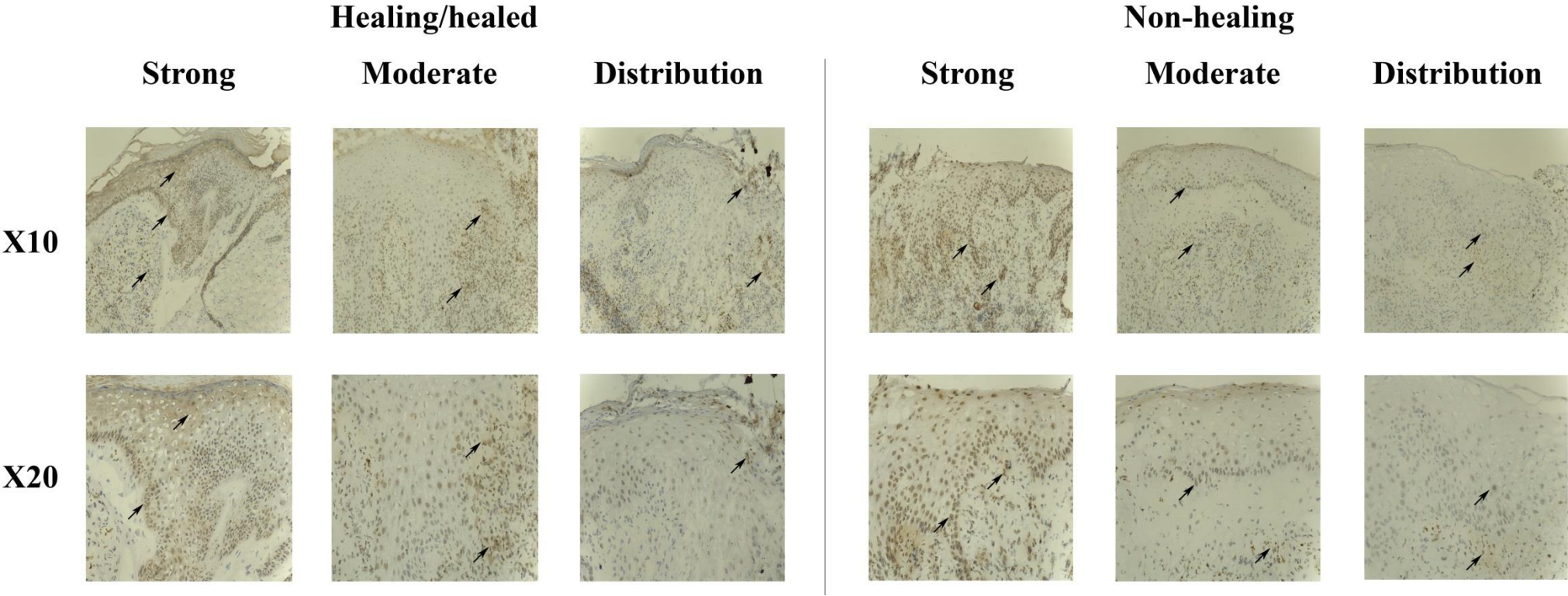


Figure 3-7: The expression pattern of SOCS-2 at the wound edge in clinical chronic wound biopies

IHC evaluation of the SOCS-2 protein at the wound edge of healing/healed wounds (left three panels) and non-healing wounds (right three panels), with 'distribution' panels indicating the expression pattern of SOCS-2 in the two groups. Overall, both healing/healed and non-healing sections demonstrate areas of strong and moderate staining as well as protein distribution. Pictures were captured at two objective magnifications (x10 and x20); representative images of healing/healed (n = 10) and non-healing (n = 10) chronic wound sections are shown; arrows indicate positive staining.

SOCS-2 expression distal to the wound edge

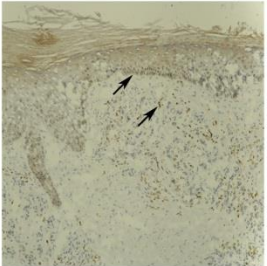
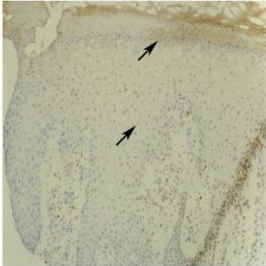
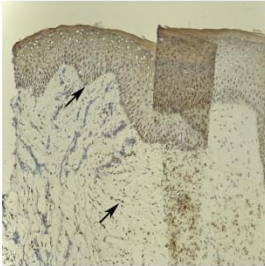
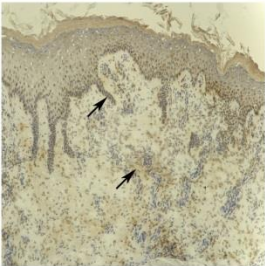
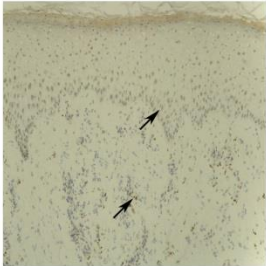
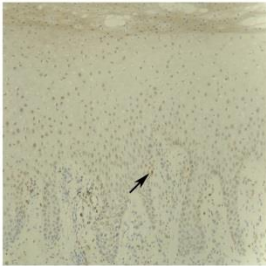
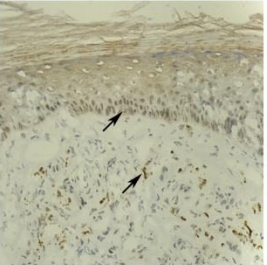
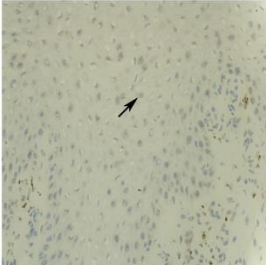
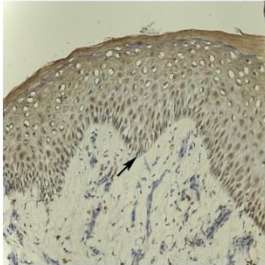
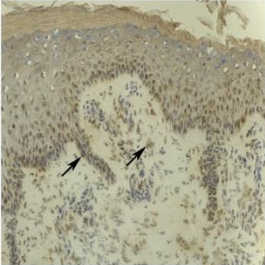
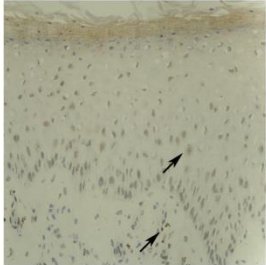
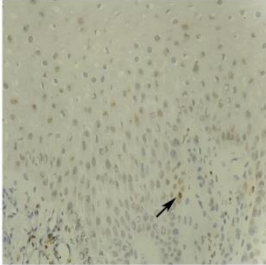
	Healing/healed			Non-healing		
	Strong	Moderate	Distribution	Strong	Moderate	Distribution
X10						
X20						

Figure 3-8: The expression pattern of SOCS-2 distal to the wound edge in clinical chronic wound biopsies

IHC evaluation of the SOCS-2 protein distal to the wound edge of healing/healed wounds (left three panels) and non-healing wounds (right three panels), with 'distribution' panels indicating the expression pattern of SOCS-2 in the two groups. Overall, both healing/healed and non-healing sections demonstrate areas of strong and moderate staining as well as protein distribution. Pictures were captured at two objective magnifications (x10 and x20); representative images of healing/healed (n = 10) and non-healing (n = 10) chronic wound sections are shown; arrows indicate positive staining.

3.3.2.4 SOCS-3 staining in chronic wound tissues

Positive SOCS-3 staining was observed in all of the non-healing chronic wounds (10/10) tested, and in the majority of healing/healed chronic wounds (8/10). Most of the positively stained biopsies exhibited SOCS-3 staining of a moderate intensity (5/10 healing/healed, 8/10 non-healing), but strong staining was observed in 3/10 healing/healed and 2/10 non-healing wounds (Figure 3-9, Figure 3-10).

Five of the chronic wounds studied showed increased expression of SOCS-3 protein in the epidermis distal to the wound edge, and interestingly the majority of these were non-healing chronic wounds (1/10 healing/healed, 4/10 non-healing), suggesting a potential trend of enhanced expression and relocalisation of SOCS-3 in the non-healing wound environment. The remaining 15/20 chronic wounds studied had uniform epidermal staining throughout the biopsies.

SOCS-3 expression was seen as diffuse cytoplasmic staining in the mature keratinocytes or nuclear in the lower basal and suprabasal layers, particularly distal to the wound edge. Many inflammatory cells within the dermis also expressed SOCS-3, particularly below the leading wound edge (migratory epidermis) and around blood vessels.

Therefore, SOCS-3 was expressed in all of the non-healing biopsies and 80% of the healing/healed tissues, and was primarily expressed in epidermis and several parts of dermis. Uniformed distribution of SOCS-3 was observed in majority (13/18) of the positively stained biopsies, whereas 5 samples (4 non-healing versus 1 healing/healed) demonstrated elevated SOCS-3 expression in the epidermis distal to the wound edge.

SOCS-3 expression at the wound edge

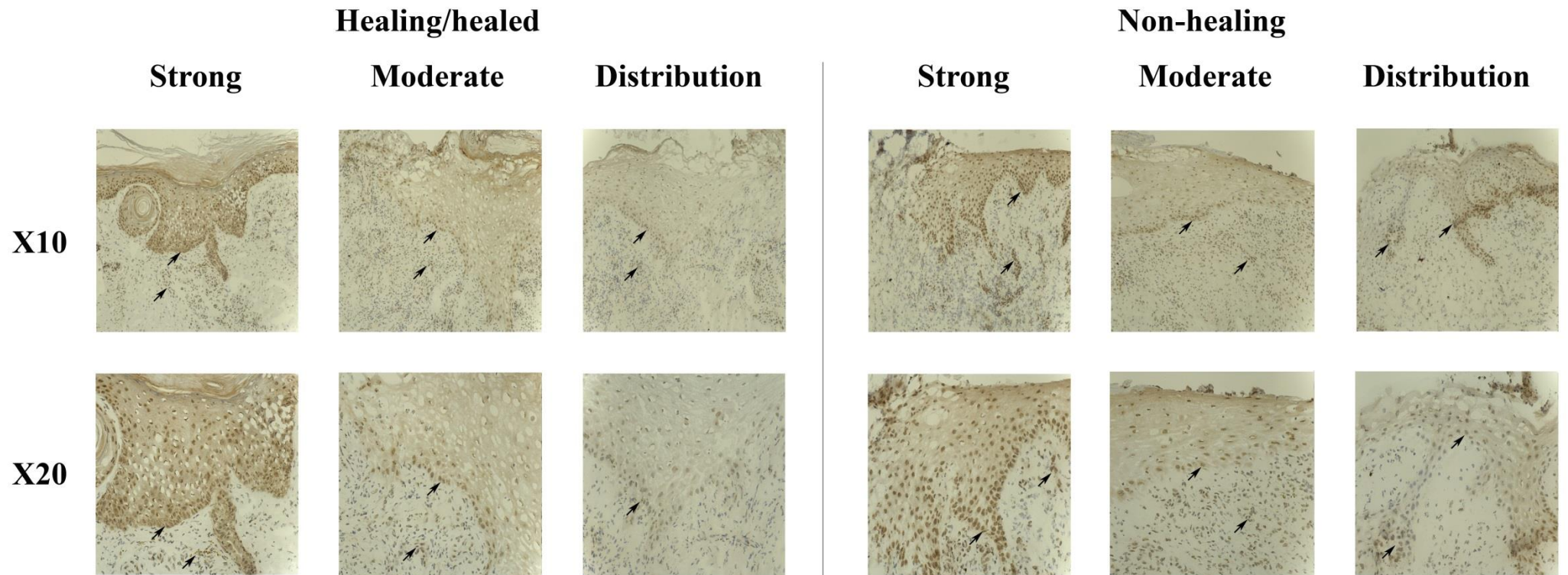


Figure 3-9: The expression pattern of SOCS-3 at the wound edge in clinical chronic wound biopies

IHC evaluation of the SOCS-3 protein at the wound edge of healing/healed wounds (left three panels) and non-healing wounds (right three panels), with 'distribution' panels indicating the expression pattern of SOCS-3 in the two groups. Overall, both healing/healed and non-healing sections demonstrate areas of strong and moderate staining as well as protein distribution. Pictures were captured at two objective magnifications (x10 and x20); representative images of healing/healed (n = 10) and non-healing (n = 10) chronic wound sections are shown; arrows indicate positive staining.

SOCS-3 expression distal to the wound edge


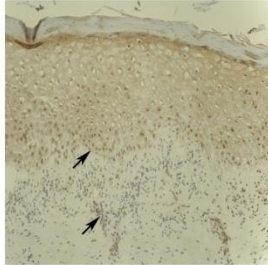
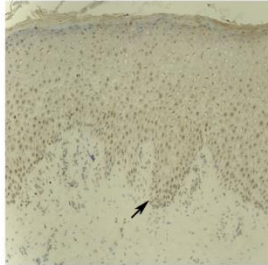
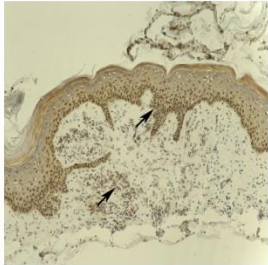
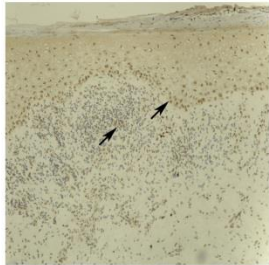
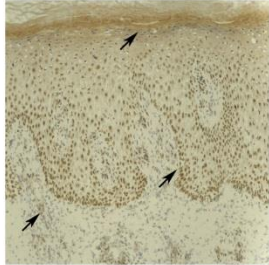
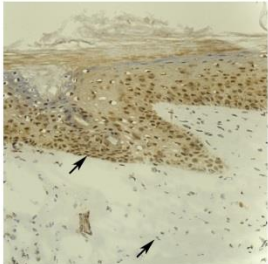
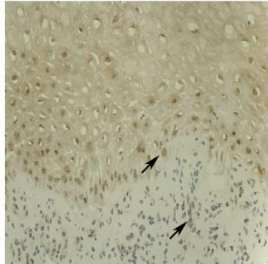
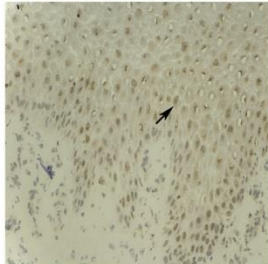
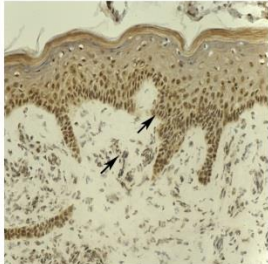
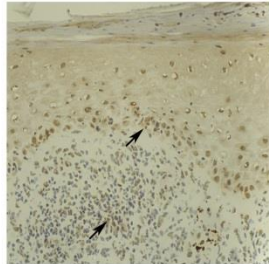
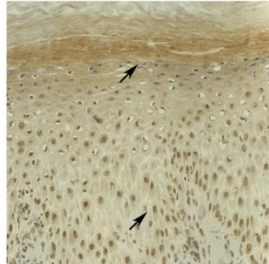
	Healing/healed			Non-healing		
	Strong	Moderate	Distribution	Strong	Moderate	Distribution
X10						
X20						

Figure 3-10: The expression pattern of SOCS-3 distal to the wound edge in clinical chronic wound biopsies

IHC evaluation of the SOCS-3 protein distal to the wound edge of healing/healed wounds (left three panels) and non-healing wounds (right three panels), with 'distribution' panels indicating the expression pattern of SOCS-3 in the two groups. Overall, both healing/healed and non-healing sections demonstrate areas of strong and moderate staining as well as protein distribution. Pictures were captured at two objective magnifications (x10 and x20); representative images of healing/healed (n = 10) and non-healing (n = 10) chronic wound sections are shown; arrows indicate positive staining.

3.3.2.5 SOCS-4 staining in chronic wound tissues

SOCS-4 protein expression was observed in almost all of the chronic wound biopsies studied (18/20), and no distinct differences were evident between the two subsets (9/10 healing/healed, 9/10 non-healing). The majority of chronic wounds had uniform staining of moderate intensity throughout the biopsies (16/20), and only two samples exhibited increased (strong) staining for SOCS-4 (1/10 healing/healed, 1/10 non-healing) (Figure 3-11, Figure 3-12).

Increased expression of SOCS-4 distal to the wound edge was evident in 5/10 chronic wounds examined, and this was observed in the healing and non-healing wounds (3/10 healing/healed, 2/10 non-healing).

SOCS-4 expression was mostly localised to the nucleus of the lower basal and suprabasal cells of the epidermis, but diffuse cytoplasmic staining was also observed in the very mature upper keratinocyte layers. SOCS-4 protein was also located in dermis.

In summary, SOCS-4 was expression in the epidermis in 90% of each healing/healed and non-healing chronic wounds, however, no difference was observed between the two groups regarding expression levels or distribution patterns.

SOCS-4 expression at the wound edge

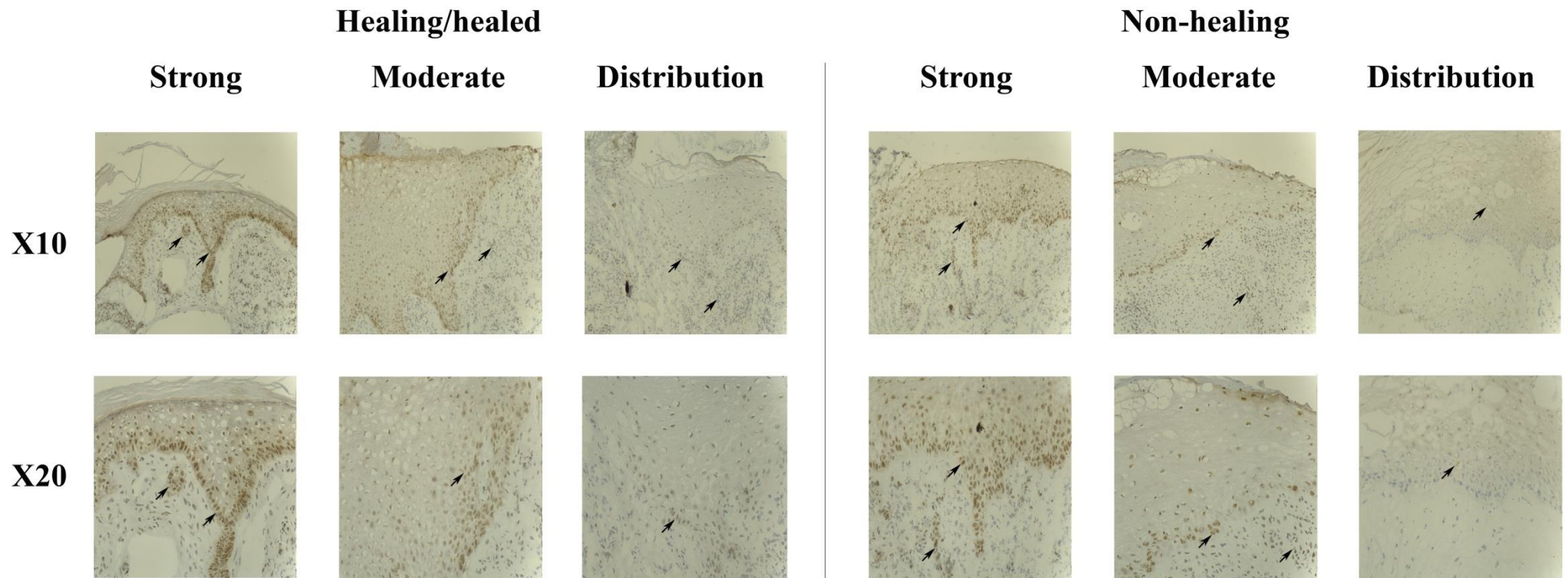


Figure 3-11: The expression pattern of SOCS-4 at the wound edge in clinical chronic wound biopies

IHC evaluation of the SOCS-4 protein at the wound edge of healing/healed wounds (left three panels) and non-healing wounds (right three panels), with 'distribution' panels indicating the expression pattern of SOCS-4 in the two groups. Overall, both healing/healed and non-healing sections demonstrate areas of strong and moderate staining as well as protein distribution. Pictures were captured at two objective magnifications (x10 and x20); representative images of healing/healed (n = 10) and non-healing (n = 10) chronic wound sections are shown; arrows indicate positive staining.

SOCS-4 expression distal to the wound edge

Healing/healed

Non-healing

Strong

Moderate

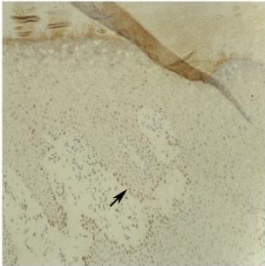
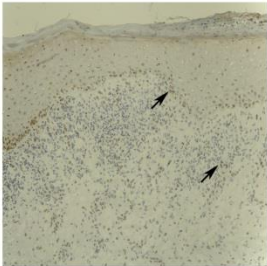
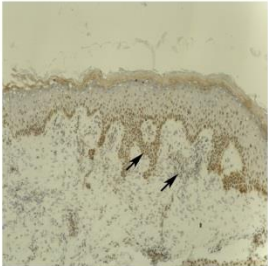
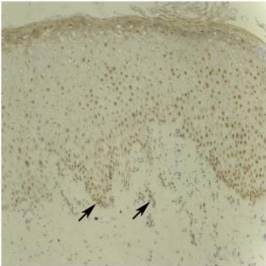
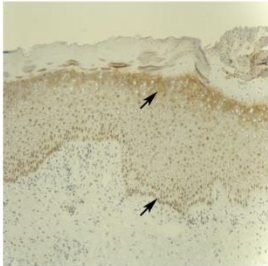
Distribution

Strong

Moderate

Distribution

X10



X20

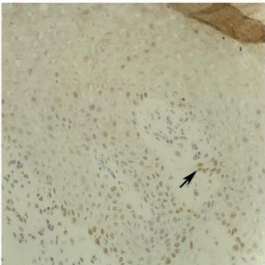
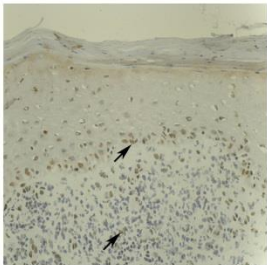
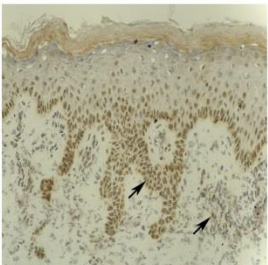
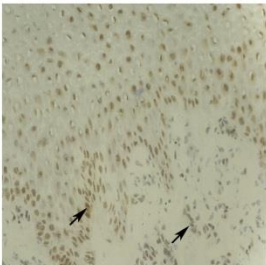
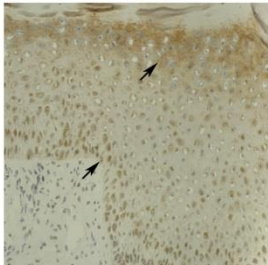
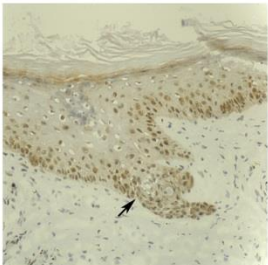


Figure 3- 12: The expression pattern of SOCS-4 distal to the wound edge in clinical chronic wound biopies

IHC evaluation of the SOCS-4 protein distal to the wound edge of healing/healed wounds (left three panels) and non-healing wounds (right three panels), with 'distribution' panels indicating the expression pattern of SOCS-4 in the two groups. Overall, both healing/healed and non-healing sections demonstrate areas of strong and moderate staining as well as protein distribution. Pictures were captured at two objective magnifications (x10 and x20); representative images of healing/healed (n = 10) and non-healing (n = 10) chronic wound sections are shown; arrows indicate positive staining.

3.3.2.6 SOCS-5 staining in chronic tissues

A generally weaker staining intensity of SOCS-5 protein was observed compared to that seen for the other SOCS proteins, but was still identified in almost all the chronic wounds studied (8/10 healing/healed, 8/10 non-healing) (Figure 3-13, Figure 3-14). Uniform expression was observed in both subsets, albeit 2/10 non-healing biopsies showed an increased SOCS-5 expression distal to the wound edge. SOCS-5 staining was mainly cytoplasmic, and observed in all layers of the epidermis, whereas, distribution of SOCS-5 was also found in dermis.

SOCS-5 expression at the wound edge

Healing/healed

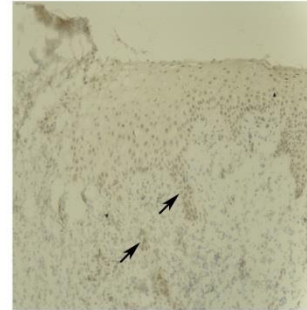
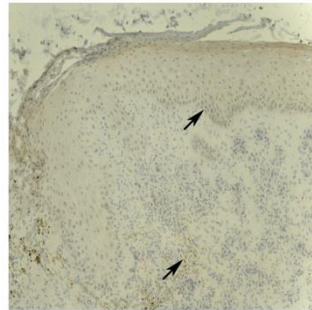
Non-healing

Moderate

Moderate

Distribution

X10



X20

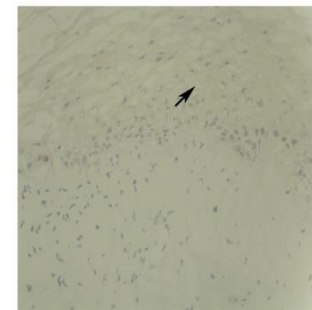
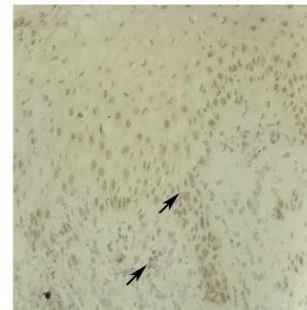
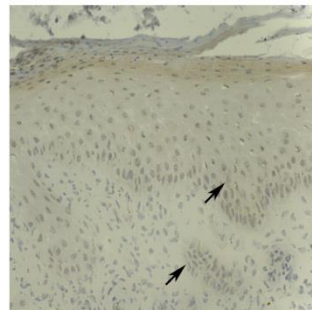


Figure 3-13: The expression pattern of SOCS-5 at the wound edge in clinical chronic wound biopsies

IHC evaluation of the SOCS-5 protein at the wound edge of healing/healed wounds (left panel) and non-healing wounds (right two panels), with 'distribution' panels indicating the expression pattern of SOCS-5 in the non-healing wounds. Overall, the healing/healed sections demonstrate areas of moderate staining, whereas non-healing biopsies display moderate staining of SOCS-5, as well as showing its protein distribution. Pictures were captured at two objective magnifications (x10 and x20); representative images of healing/healed (n = 10) and non-healing (n = 10) chronic wound sections are shown; arrows indicate positive staining.

SOCS-5 expression distal to the wound edge

Healing/healed

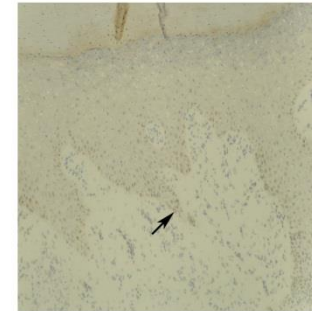
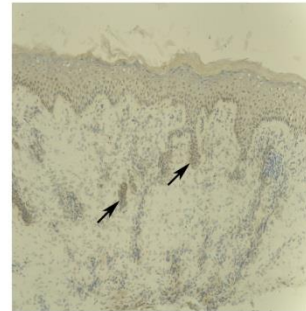
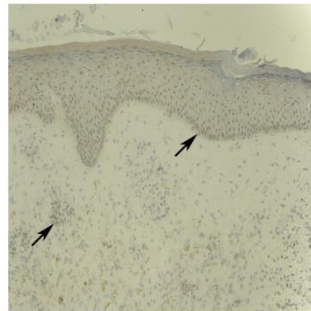
Non-healing

Moderate

Moderate

Distribution

X10



X20

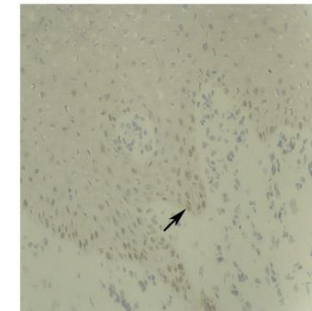
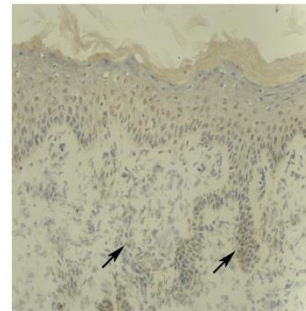
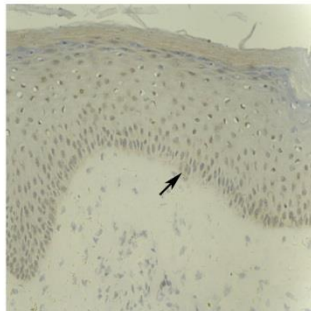


Figure 3-14: The expression pattern of SOCS-5 distal to the wound edge in clinical chronic wound biopsies

IHC evaluation of the SOCS-5 protein distal to the wound edge of healing/healed wounds (left panel) and non-healing wounds (right two panels), with 'distribution' panels indicating the expression pattern of SOCS-5 in the non-healing wounds. Overall, the healing/healed sections demonstrate areas of moderate staining, whereas non-healing biopsies display moderate staining of SOCS-5, as well as showing its protein distribution. Pictures were captured at two objective magnifications (x10 and x20); representative images of healing/healed (n = 10) and non-healing (n = 10) chronic wound sections are shown; arrows indicate positive staining.

3.3.2.7 SOCS-6 staining in chronic tissues

SOCS-6 protein expression was observed in 12/20 chronic wounds, equally in the healing/healed (6/10) and non-healing chronic wounds (6/10). The IHC analysis revealed the staining to be of moderate intensity in most biopsies (5/10 healing/healed, 5/10 non-healing), with only two biopsies showing particularly stronger expression of SOCS-6 (1/10 healing/healed, 1/10 non-healing (Figure 3-15, Figure 3-16)).

Increased SOCS-6 expression was identified in the epidermal layers distal to the wound edge in 4/20 biopsies examined (2/10 healing/healed, 2/10 non-healing), although the remaining biopsies showed uniform staining throughout the tissue samples.

The nucleus of basal and suprabasal keratinocytes were particularly positive for SOCS-6. However, cytoplasmic staining in other layers was also observed. In addition, dermal expression of SOCS-6 was also observed.

Although SOCS-6 was observed in both epidermis and dermis in both healing/healed and non-healing chronic wounds, there was no difference between the two groups in terms of either the expression levels or distribution patterns of SOCS-6.

SOCS-6 expression at the wound edge

Healing/healed

Non-healing

Strong

Moderate

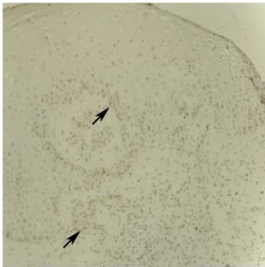
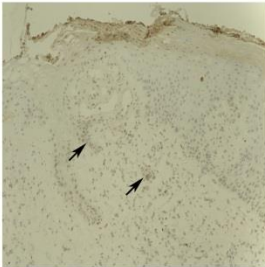
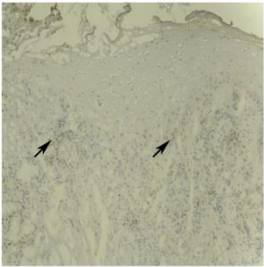
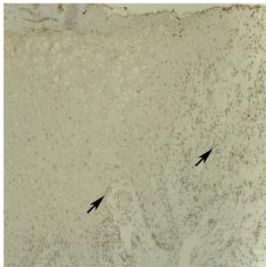
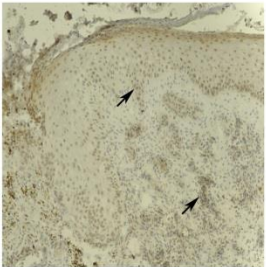
Distribution

Strong

Moderate

Distribution

X10



X20

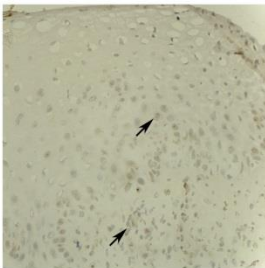
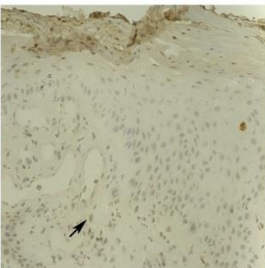
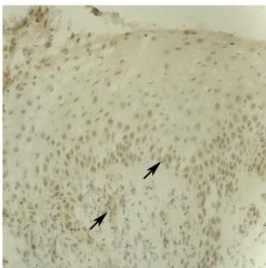
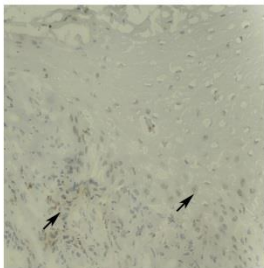
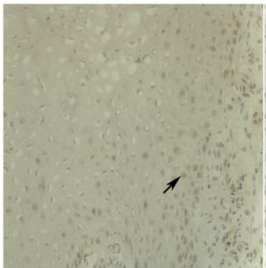
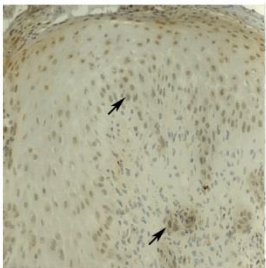


Figure 3-15: The expression pattern of SOCS-6 at the wound edge in clinical chronic wound biopies

IHC evaluation of the SOCS-6 protein at the wound edge of healing/healed wounds (left three panels) and non-healing wounds (right three panels), with 'distribution' panels indicating the expression pattern of SOCS-6 in the two groups. Overall, both healing/healed and non-healing sections demonstrate areas of strong and moderate staining as well as protein distribution. Pictures were captured at two objective magnifications (x10 and x20); representative images of healing/healed (n = 10) and non-healing (n = 10) chronic wound sections are shown; arrows indicate positive staining.

SOCS-6 expression distal to the wound edge

Healing/healed

Non-healing

Strong

Moderate

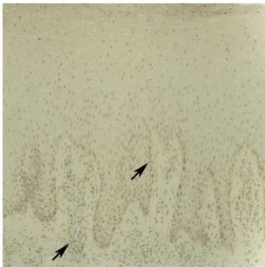
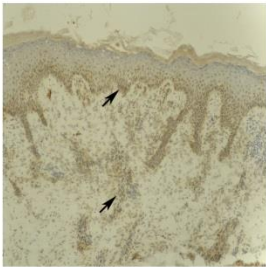
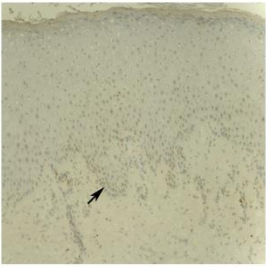
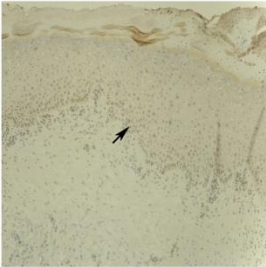
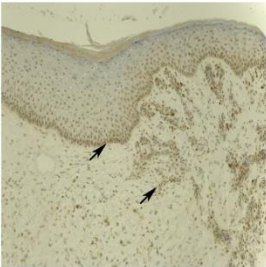
Distribution

Strong

Moderate

Distribution

X10



X20

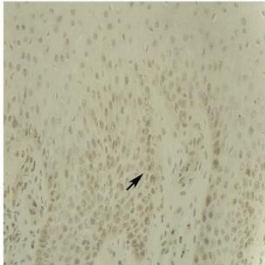
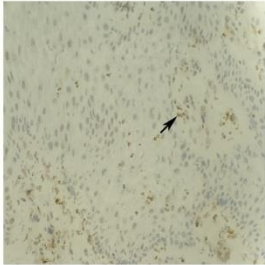
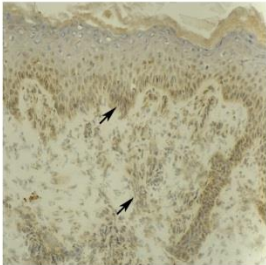
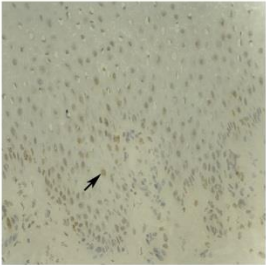
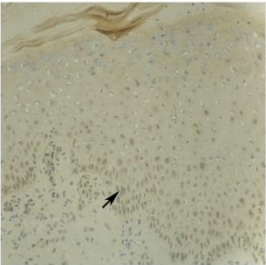
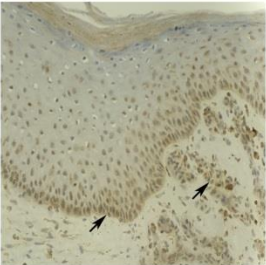


Figure 3-16: The expression pattern of SOCS-6 distal to the wound edge in clinical chronic wound biopsies

IHC evaluation of the SOCS-6 protein distal to the wound edge of healing/healed wounds (left three panels) and non-healing wounds (right three panels), with 'distribution' panels indicating the expression pattern of SOCS-6 in the two groups. Overall, both healing/healed and non-healing sections demonstrate areas of strong and moderate staining as well as protein distribution. Pictures were captured at two objective magnifications (x10 and x20); representative images of healing/healed (n = 10) and non-healing (n = 10) chronic wound sections are shown; arrows indicate positive staining.

3.3.2.8 SOCS-7 staining in chronic tissues

SOCS-7 expression was examined throughout the healing/healed and the non-healing chronic wound tissue sections. The sections demonstrated no significant staining profiles when tested with either of the two antibodies available within our laboratories. Thus, this molecule appears to demonstrate weak to no expression in the tissues tested in the present study. Typical negative staining patterns obtained for this molecule using one of the antibodies (sc-8291) are shown in Figure 3-17.

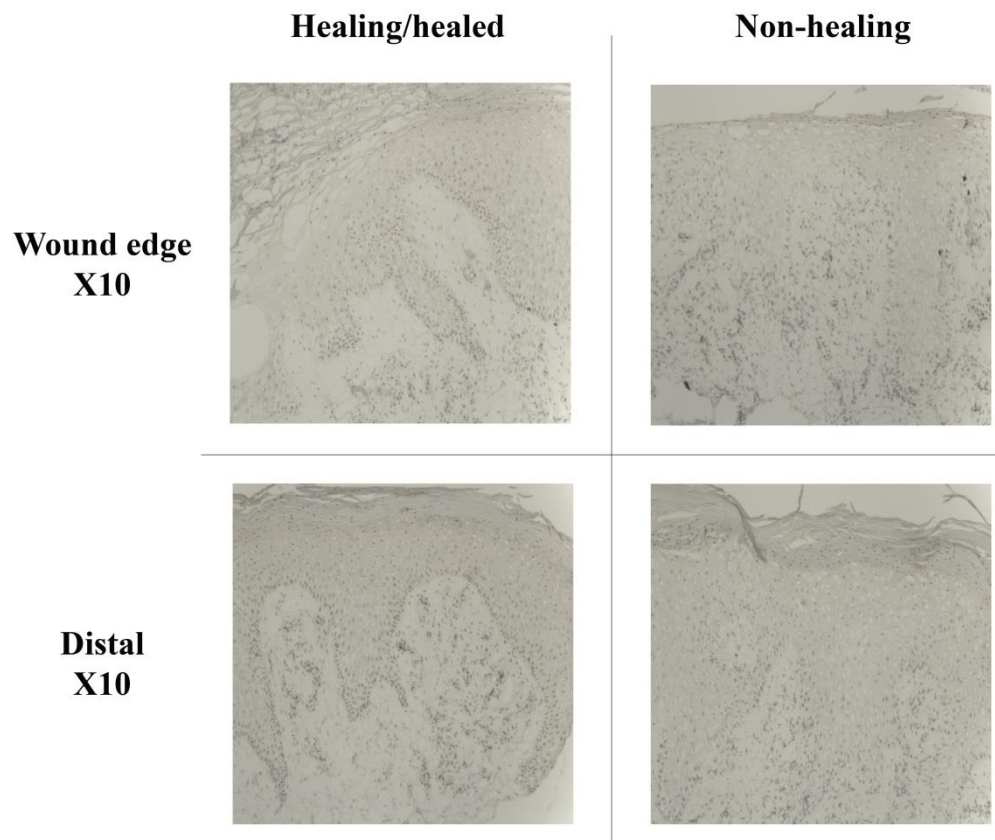


Figure 3-17: The expression pattern of SOCS-7 in clinical chronic wound biopies

IHC evaluation of the SOCS-7 protein in healing/healed wounds (left panel) and non-healing wounds (right panel). Negative staining was seen throughout the cohort tested. Representative images of healing/healed (n = 10) and non-healing (n = 10) chronic wound sections are shown.

3.4. Discussion

The present data highlighted differences in gene expression of SOCS family members between the healing/healed and non-healing chronic wounds. Notably, significant differences were obtained for the gene expression of SOCS-3 and -4 between these two groups, accounting for 81% and 93% decreases in the healing/healed group. In addition, gene level screening performed in this study demonstrated 50%, 43%, 93% and 87% higher, albeit not significant, expression of SOCS-1, 2, 5 and 6 respectively in non-healing chronic venous leg ulcer patients, whereas a 43% decreased gene expression of SOCS-7 was observed in this group, yet not statistically significant either. Hence, the gene expression profiles suggests an association between SOCS-3 and SOCS-4 and the healing potential of chronic wounds. In order to examine the protein expression and localisation of SOCS family members IHC analysis was undertaken. However, the significance of the gene expression data was not supported by the protein level and the IHC analysis did not reveal any obviously distinct differences in SOCS expression between the non-healing and healing/healed chronic wounds. This is contradictory to the transcript analysis, though such differences between transcript and IHC analysis may be partially explained by the smaller subset of samples used in the IHC analysis than in the q-PCR analysis resulting to the more finite availability and suitability of clinical sections for staining in comparison to the relative ease of generating large amounts of cDNA for gene expression analysis. This discrepancy may also have arisen due to the qualitative nature of the IHC study or may be some aspect of post-transcriptional regulation. Additional clarification of this observation is required in a larger cohort of chronic wounds and is also warranted within cohorts of acute and chronic wounds, though such resources were not available for this study.

In the current study, SOCS-1 to SOCS-6 were all found to be expressed in both epidermal keratinocytes and dermal area. This suggested the extensive expression of the SOCS proteins in several cell types involved in wound healing. Moreover, this finding potentially suggested that SOCS proteins may play distinct regulatory roles in different cells in the healing process, although further investigation is required to identify the specific molecule(s) or downstream signalling pathway(s) which may be regulated by SOCS. Efforts to elucidate aspects of this will be undertaken in two such cell types, keratinocytes and endothelial cells, within the remainder of this study.

Regarding the expression patterns of SOCS protein in different cell types in chronic wounds, SOCS-1 was observed in mature keratinocytes and dermal inflammatory infiltrate cells, and surrounding blood vessels despite the weak expression level. SOCS-2 was found expressed in cytoplasm of mature keratinocytes in the epidermis and the nuclear compartment of lower differentiated keratinocytes in the basal layer. Of note, SOCS-3 was found extensively expressed in all layers of keratinocytes of the epidermis, inflammatory infiltrate cells and surrounding blood vessels in dermis in all positive stained chronic wounds, whereas SOCS-4, SOCS-5 and SOCS-6 were only expressed in all layers of keratinocytes of epidermis. The positive expression of SOCS-1 to 6 in keratinocytes suggested the existence of the cytokine receptors which could lead to the synthesis of SOCS-1 to 6 in this cell type, as well as the potential regulatory role of these SOCS proteins in the epidermis of chronic wound. For example, a previous study has demonstrated that human keratinocytes are highly susceptible to IFN- γ , and following induction SOCS-1 acts as a feedback negative regulator to protect keratinocytes from excessive IFN- γ stimulation (Madonna et al., 2008). This is in agreement with our finding, and may imply that the positive expression

of SOCS-1 in the epidermis of the chronic wounds in our study may in part due to the IFN- γ stimulation.

SOCS family members have been previously linked to inflammation due to their regulatory roles in pro-inflammatory cytokine signalling. For example, studies suggested that SOCS-1 negatively regulates the pro-inflammatory cytokine IFN- γ , and inhibits IFN- γ -dependent STAT-1 activation (Alexander et al., 1999, Tanaka et al., 2008). Another SOCS protein, SOCS-3, acting as a anti-inflammatory regulator, mediates IL-6-gp130 signalling by preventing the activation of STAT-3 (Crocker et al., 2003, Lang et al., 2003). In addition, SOCS-3 was also found to be a negative regulator of IFN- γ -induced STAT-1 activation (Song and Shuai, 1998). Therefore, the expression of SOCS-1 and SOCS-3 in the dermal infiltrate may suggest that they are induced in the recruited infiltrating cells to regulate pro-inflammatory cytokine signalling. However, dual fluorescent staining would be required to identify whether these positive stained cells were T-lymphocytes, macrophages, fibroblasts or other cells. Furthermore, direct evidence indicates that SOCS proteins may hold the potential to influence the wound-healing process by regulating the function of wound site resident cells. A study by Linke *et al.* has shown that keratinocyte proliferation and migration are strongly disturbed by the presence of SOCS-3, which contributes to impaired wound healing (Linke et al., 2010b). Other study demonstrated that the exacerbated inflammation which characterises chronic wounds is shown to be associated with overexpression of SOCS-3 (Linke et al., 2010a). These data may explain the significantly increased gene expression of SOCS-3 transcript levels in the non-healing chronic wound biopsies compared to that in the healing/healed chronic wound biopsies, suggesting that the upregulation of SOCS-3 correlated with impaired keratinocyte migration and proliferation as well as poor healing results. In addition, according

to the SOCS-3 IHC staining pattern, the distinct proportion (1 : 4) of increased SOCS-3 protein expression in the epidermis distal to the wound edge throughout 20 chronic wound biopsies (1/10 healing/healed, 4/10 non-healing) are noteworthy. This suggest the loss of SOCS-3 expression on the leading migratory epidermis in the healing/healed chronic wound or/and the relocation of SOCS-3 protein between healing/healed and non-healing chronic wounds. Taken together, SOCS-3 may potentially act as biomarkers and/or potential therapeutics to manage chronic wounds, although additional study is required to fully elucidate this role. Thus, establishment of a larger cohort of these tissues, as well as exploring SOCS function and expression across acute and chronic wound tissue and normal skin would be of interest and benefit.

SOCS-4 has been previously demonstrated to be induced by EGF and inhibit the EGFR signalling by competing for the binding motif on EGFR with STAT-3 (Kario et al., 2005, Bullock et al., 2007). According to the IHC staining results, SOCS-4 was found to be expressed in 18 chronic wounds biopsies out of 20, and the expression of SOCS-4 primarily localised in the nucleus of the lower basal and suprabasal layers in epidermis. This is in agreement with the distribution of EGFR which is located in the basal layer and first suprabasal layer of adult epidermis (Nanney et al., 1990). Taken together, this may represent a link where SOCS-4 expression in these chronic wounds could potentially be induced by EGF stimulation, and subsequently negatively regulate EGFR signalling and STAT-3 activation, contributing to the modulation of keratinocyte behaviour, though further study is needed to fully explore this link. Although SOCS-5, the greatest sequence homolgy to SOCS-4, is also documented to be induced by EGF as a feedback negative suppressor of EGFR signalling (Kario et al., 2005), the expression pattern, diffuse cytoplasmic expression in almost all layers of

epidermis, in the chronic wound biopsies was different from SOCS-4. This result may suggest an alternative role of SOCS-5 to SOCS-4 in keratinocytes in chronic wounds.

In summary, this initial chapter explored the expression profiles of SOCS-1 to SOCS-7 in chronic healing/healed and non-healing samples. Whilst many of these members do not appear to be differentially expressed or localised between these two chronic sub-types, it does support a differential gene expression of SOCS-3 and -4. There is also evidence to suggest that SOCS-3 may undergo relocalisation between the two chronic subtypes. Thus, whilst limited by cohort size, this early data suggests involvement of SOCS-3 and -4, either functionally or as potential genetic biomarkers, in these chronic samples. To follow on from this, further characterisation of the cellular role of SOCS-3 and SOCS-4 in human keratinocytes and endothelial cells will be undertaken throughout the remainder of the thesis to support or clarify the potential of SOCS-3 and SOCS-4 in chronic wounds highlighted in this chapter.

Chapter IV

Establishment of SOCS-3 expression and SOCS-4 knockdown models

4.1 Introduction

SOCS-3 is one of the most extensively studied SOCS family members. A previous *in vivo* study has indicated that knockdown of SOCS-3 in epithelial basal keratinocytes contributes to severe skin inflammation, indicating its important role in skin homeostasis (Uto-Konomi *et al.*, 2012). However, the basal keratinocyte-specific overexpression of SOCS-3 also led to impaired wound healing due to the suppression of keratinocyte proliferation and migration in a transgenic mouse overexpressing SOCS-3 (Linke *et al.*, 2010b). Moreover, in addition to disrupting acute wound healing, mice overexpressing SOCS-3 also exhibits a prolonged inflammation phenotype that resembled the characteristics of chronic wounds (Linke *et al.*, 2010a). Taken together, these data demonstrate the important regulatory role of SOCS-3 in the wound healing process, and highlight the importance of maintaining the balance of SOCS-3 expression in wound healing.

SOCS-4 is the most poorly investigated member of the SOCS family. Studies have indicated that SOCS-4 plays a regulatory roles in inflammation caused by influenza and parasite infection (Kedzierski *et al.*, 2014, Hu *et al.*, 2010), suggesting its regulatory potential in inflammation, and hence a potential link to inflammatory stage of wound healing. Another investigation on genetic alteration and evolution in animals which *live in* high-altitude environments suggested that SOCS-4 may hold the potential to regulate HIF-1 α , a mediator involved in the adaptation to hypoxia (Wang *et al.*, 2015). Since hypoxia occurs in the early wound stages, such evidence provides another clue as to the potential role of SOCS-4 in the early stage of wound healing.

Keratinocytes are of importance to injury response and are involved in secreting cytokines for the recruitment of other cells, producing growth factors to

improve collagen formation and angiogenesis, and undergoing migration and proliferation to fully enable epithelialisation (Pastar *et al.*, 2008). Endothelial cells are another key cell type that is involved in the wound healing process, especially in angiogenesis. In response to a variety of chemotactic and angiogenic signals, the proliferation and migration of endothelial cells occurs, and various tube-like structures and new capillary networks are formed to supply sufficient nutrient and oxygen to the surrounding environment involved in the wound healing process, therefore relieving the hypoxic pressure of the lesion.

The previous chapter has highlighted the differential gene expression of SOCS-3 and SOCS-4 between chronic healing/healed and non-healing wounds and also indicated potential relocalisation of SOCS-3 between these wound types, though, contrastingly, IHC analysis does not suggest any differential expression. Whilst the initial chapter raises a number of questions, when the results are viewed in conjunction with the literature there appears potential for SOCS-3 and SOCS-4 to influence the process of wound healing.

The distribution of SOCS-3 and SOCS-4 in the chronic wounds biopsies from the IHC results in Chapter III indicated that SOCS-3 and SOCS-4 were predominantly expressed in keratinocytes of epidermis, whereas the positive expression of SOCS-3 and -4 in dermis suggested their potential expression in endothelial cells. In addition, previous studies has shown that knockdown and overexpression of SOCS-3 in keratinocytes resulted in severe disruption of inflammation homeostasis and skin repair (Linke *et al.*, 2010a, Linke *et al.*, 2010b, Uto-Konomi *et al.*, 2012). Therefore, SOCS-3 and -4 may hold the potential to regulate function of keratinocytes and endothelial cells, subsequently contributing to the wound healing process.

To investigate the potential biological and regulatory role of SOCS-3 and SOCS-4 in wound healing, human epithelial keratinocytes (HaCaT) and endothelial cells (HECV) were chosen to establish *in vitro* models to explore the cellular importance of SOCS-3 and SOCS-4. The current chapter focuses on establishment of *in vitro* models using both ribozyme and siRNA SOCS-4 knockdown techniques, as well as SOCS-3 expression, through coding sequence synthesis and transfection. Successful established models will subsequently be used to characterise and discuss the functional importance of SOCS-3 and SOCS-4 in later chapters.

4.2 Methods and materials

4.2.1 Synthesis of SOCS-4 targeting ribozyme by touchdown PCR

Touchdown PCR was carried out using REDTaq® Ready Mix™ PCR Reaction Mix (Sigma-aldrich, Dorset, UK) with $MgCl_2$ and two specific primer pairs, SOCS-4 rib F1 vs rib R1 and SOCS-4 rib F2 vs rib R2, to synthesise two different transgene, labelled as ribozyme 1 and ribozyme 2, which target different specific GUC or AUC sites to the mRNA of SOCS-4. PCR reaction conditions were used as follows:

- Step 1: Initial denaturing period - 94°C for 5 minutes
- Step 2: Denaturing stage - 94°C for 20 seconds
- Step 3: Series of annealing stages - 70°C for 30 seconds, 60°C for 30 seconds, 58°C for 30 seconds, 54°C for 30 seconds, 50°C for 30 seconds
- Step 4: Extension stage - 72°C for 30 seconds
- Step 5: Additional extension stage - 72°C for 10 minutes
- Step 2 - 4 were repeated over 40 cycles with 8 cycles for each 5 different annealing temperature.

2% agarose gel stained with SYBR safe DNA gel stain was used for gel electrophoresis to verify the presence of the synthesised transgene. GenScript PCR DNA Ladder (Range 100-2000bp) was used as ladder.

4.2.2 TOPO TA cloning of SOCS-4 targeting ribozyme into the pEF6/V5-His-TOPO plasmid vector and incorporated transgene orientation check

This methodology is described in section 2.11.2 of Chapter II.

Specifically for orientation analysis of SOCS-4 ribozyme plasmid colonines, there are 90bp between the T7F promoter and the beginning of the transgene insert. Primer RbBMR and RbToPF, holding complementary sequences, recognise and bind to a central catalytic region of each ribozyme transgene sequences that

are common in both ribozymes used. Reactions utilising the T7F vs RbBMR primer pairs with the predicted size of 143bp (ribozyme 1) and 147bp (ribozyme 2) was used to verify the correct orientation for each inserted transgene, whereas the reaction containing the combination of T7F vs RbToPF primers with the predicted size of 144bp (ribozyme 1) and 136bp (ribozyme 2), was used to identify incorrect orientation. The absence of a band from both reactions indicated a closed plasmid configuration with no ribozyme insert, whereas the presence of a band in both reactions indicated a mixed orientation of the ribozyme.

4.2.3 Amplification of complete coding sequence of SOCS-3 using PCR

4.2.3.1 SOCS-3 coding sequence primer pair specificity check and annealing

temperature confirmation

Five primer pairs, SOCS-3 exp F1 vs exp R, exp F2 vs exp R, exp F3 vs exp R, exp F4 vs exp R and exp F5 vs exp R, that correspond to the SOCS-3 coding sequence were used to amplify PLC-PRF-5 and SKMES cDNA samples at the same PCR condition to initial screening stage in order to test their specificity.

Furthermore, primer pairs of SOCS-3 exp F4 vs exp R and SOCS-3 exp F4 vs exp R were used following similar conditions to the initial PCR screen but over a range of four differing annealing temperature, each reaction corresponding to either 52°C, 54°C, 56°C or 58°C annealing, to determine the optimal annealing temperature.

4.2.3.2 Secondary screening of SOCS-3 on normal cell lines/tissues and SOCS-3

coding sequence amplification with high fidelity enzyme mix kit

Eight RNA reverse transcribed cDNA samples from different normal tissue and cell lines (Table 2-2) were amplified using SOCS-3 F8 vs R8 primer pair to detect the

expression of SOCS-3. The PCR conditions were the same as those used for SOCS-3 initial screening.

A High fidelity enzyme mix kit (Fisher Scientific UK, Loughborough, UK) was used to amplify SOCS-3 coding sequence. The reaction mix and PCR conditions were used as follows:

PCR reaction mix:

- 10x High Fidelity PCR Buffer with $MgCl_2$ - 2.5 μ l
- dNTP Mix 2.5nM - 2.5 μ l
- Forward Primer: SOCS-3 exp F4 - 2.5 μ l
- Reverse Primer: SOCS-3 exp R- 2.5 μ l
- High Fidelity PCR Enzyme Mix - 1.3 μ l
- MRC-5 cDNA - 1 μ l
- Nuclease-free water - 12.7 μ l

PCR reaction conditions:

- Step 1: Initial denaturing period - 94°C for 3 minutes
- Step 2: Denaturing stage - 94°C for 30 seconds
- Step 3: annealing stage - 58°C for 30 seconds
- Step 4: Extension stage - 72°C for 1 minutes
- Step 5: Additional extension stage - 72°C for 10 minutes

Step 2 - 4 were repeated for 35 cycles.

4.2.4 Extraction of PCR product from agarose gel

The extraction of PCR product was undertaken using GenElute™ Gel Extraction Kit (Sigma-aldrich, Dorset, UK). The excised gel slice containing PCR product was weighted as 220mg. After calculation, 660 μ l of Gel Solubilisation Solution was added into the PCR product containing microfuge tube before incubation at 60°C

for 10 minutes to completely dissolve the gel. Then, 220µl of absolute isopropanol was mixed with the gel dissolved solution until homogenous. GenElute Binding Column was placed into a 2ml collection column followed by the addition of 500µl Column Preparation Solution. The collection column was then centrifuged for 1 minute, and the flow-through liquid was removed. The mixture of isopropanol and gel dissolved solution was then loaded into the pre-prepared binding column followed by centrifuging for 1 minute, and the flow-through liquid was discarded. 700µl of Wash Solution was added into the binding column, and the flow-through liquid was again discarded after 1 minute of centrifuging. Such wash step was repeated once, without the addition of any Wash Solution to remove the excess liquid completely. The binding column was then transferred into a fresh collection column. 50µl of Elution Solution was pre-warmed at 65°C and was added into the binding column before centrifuging for 1 minute to obtain the purified SOCS-3 coding sequence product. The concentration of the extracted DNA product was measured using a NanoPhotometerTM (IMPLEN; GeneFlow Ltd., Lichfield, UK).

4.2.5 TOPO TA cloning of SOCS-3 coding sequence into the pEF6/V5-His-TOPO plasmid vector and incorporated transgene orientation check

The total 5µl cloning reaction was mixed and stored on ice for 20 minutes in advance to One Shot Chemical Transformation, and the condition used for TOPO cloning reaction was as follows:

- Purified SOCS-3 coding sequence - 3µl
- Salt solution - 1µl
- TOPO vector - 1µl

5µl of TOPO cloning reaction was added into one vial of One Shot TOP10 Chemically Competent *E. coli*. and mixed gently by stirring using pipette tip. The

vial was stored on ice for 30 minutes before heat-shocking at 42°C for 30 seconds followed by immediately transferring to ice. To the vial was added 250µl room temperature SOC medium and shaken at a 45° angle at 225rpm at 37°C for 1 hour.

After the incubation period, the transformed products from the vial were spread in two seeding density on a pre-warmed agar petri dish containing 100µl/ml ampicillin followed by incubating overnight at 37°C.

Ten colonies from the petri dish were randomly picked and the SOCS-3 coding sequence insertion and the orientation of the incorporated SOCS-3 coding sequence was checked by RT-PCR reaction using primer combination of T7F vs BGHR (predicted size of 942bp, indicative of product insertion), T7F vs SOCS-3 exp F4 (predicted size of 768bp, indicative of incorrect orientation) and T7F vs SOCS-3 exp R (predicted size of 768bp, indicative of correct orientation). The details of the PCR reaction mix was as follows:

SOCS-3 coding sequence incorporation check mix

- GoTaq Green master mix - 8µl
- T7F plasmid specific forward primer - 1µl
- BGHR plasmid specific reverse primer - 1µl
- PCR water -6µl

Correct orientation primer pair mix

- GoTaq Green master mix - 8µl
- T7F plasmid specific forward primer - 1µl
- SOCS-3 coding sequence specific reverse primer (SOCS-3 exp R) - 1µl
- PCR water -6µl

Incorrect orientation primer pair mix

- GoTaq Green master mix - 8µl
- T7F plasmid specific forward primer - 1µl

- SOCS-3 coding sequence specific forward primer (SOCS-3 exp F4) - 1µl
- PCR water -6µl

Each colony was inoculated into all reaction mixes using a sterile pipette, and the reaction mixes were placed in a thermal cycler. The PCR reaction conditions were used as follows: 94°C for 5 minutes, followed by 30 cycles of 94°C for 30 seconds, 55°C for 40 seconds and 72°C for 1 minute with a final extension step of 72°C for 10 minutes. Gel electrophoresis on a 0.8% agarose gel stained with SYBR safe DNA gel stain was used to separate the RT-PCR reaction products, and the gel was visualised under UV light followed by image capture.

There are 264bp between the first base pair of T7F promoter to the last base pair of the BGHR site in the empty plasmid. Since the full length of SOCS-3 coding sequence is 678bp, the predicted product size that the T7F vs BGHR primer pair amplified from the SOCS-3 coding sequence incorporated plasmid is 942bp. Based on the length of 90bp between the T7F promoter and the beginning of the incorporated transgene as well as 678bp of SOCS-3 coding sequence, the primer pair of T7F vs SOCS-3 exp R and T7F vs SOCS-3 exp F4, both amplifying the product with the predicted size of 768bp, were used to verify the correct and incorrect orientation for the inserted transgene.

4.2.6 Statistical analysis

Statistical analysis was undertaken using the SigmaPlot 11 and Graphpad Prism 6 statistical software packages. Data was found to be normalised as was therefore analysed using t-test. Values of $p < 0.05$ (*), $p < 0.01$ (**), $p < 0.001$ (***) and $p < 0.0001$ (****) were regarded as statistically significant.

4.3 Results

4.3.1 Expression profile of seven SOCS family members (SOCS-1 to SOCS-7) in epithelial and endothelial cell line candidates

The expression levels of SOCS-3 and -4 were examined along with the other five SOCS members (SOCS-1, -2, -5, -6 and -7) to determine the strategy for the establishment of *in vitro* models. RNA was isolated from HaCaT and HECV wild-type cells followed by reverse transcription to cDNA. Such cDNA samples were used as templates for amplification using GoTaq Green Master Mix and the primer pairs of SOCS-1 F1 vs ZR1, SOCS-2 F8 vs R8, SOCS-3 F8 vs R8, SOCS-4 F8 vs R8, SOCS-5 F1 vs ZR1, SOCS-6 F1 vs ZR1, SOCS-7 F9 vs R9 and GAPDH F8 vs R8 (Table 2-3). The PCR products were loaded on 0.8% agarose gel, and were separated by gel electrophoresis followed by being visualised under blue light and image capture (Figure 4-1).

SOCS-2, SOCS-4, SOCS-5 and SOCS-6 were expressed in both HaCaT and HECV cell, furthermore, the gene expression levels of such four SOCS family members exhibited higher expression in HECV cells to that of in HaCaT cells. However, there was no expression of SOCS-1, SOCS-3 and SOCS-7 in either HaCaT or HECV cells.

Following the gene expression profile of SOCS-3 and -4 in the clinical cohort in Chapter III and the expression levels of these two molecules in HaCaT and HECV cells, it was decided to establish knockdown and expression strategies for SOCS-4 and SOCS-3 respectively to further explore the significance of these SOCS members in HaCaT and HECV cell wound model systems.

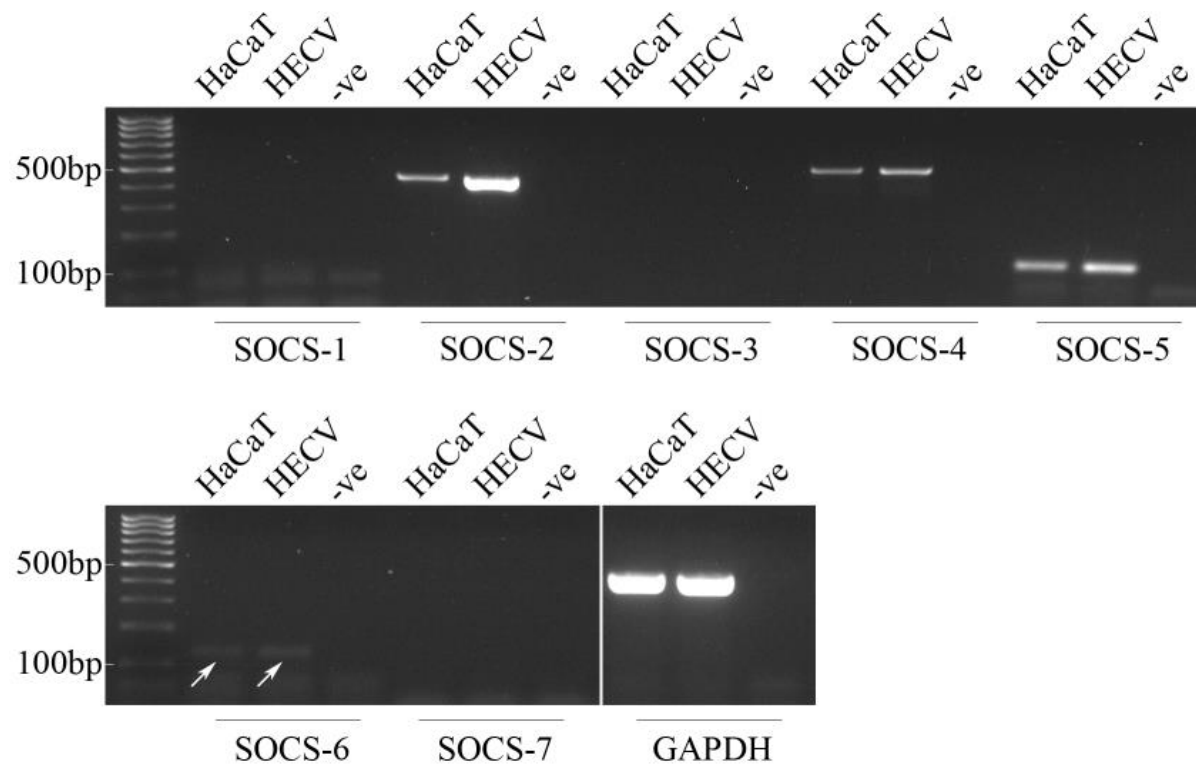


Figure 4-1: Screening of SOCS-1 to SOCS-7 in HaCaT and HECV cell lines

HaCaT and HECV cDNA samples were screened for seven SOCS family members and GAPDH. The predicted product size of each PCR product is: SOCS-1 (108bp), SOCS-2 (461bp), SOCS-3 (521bp), SOCS-4 (541bp), SOCS-5 (117bp), SOCS-6 (131bp), SOCS-7 (590bp) and GAPDH (475bp), -ve represents amplification of PCR water instead of cDNA

4.3.2 Generation of SOCS-4 knockdown models and SOCS-3 expression models

4.3.2.1 Generation of SOCS-4 knockdown models using ribozyme transgene

Touchdown PCR was carried out to synthesise two different transgenes, labelled as ribozyme 1 and ribozyme 2. Two products were visualised below 100bp which is in agreement with the size of the two transgene, ribozyme 1 (85bp) and ribozyme 2 (81bp) (Figure 4-2 A).

The synthesised transgenes (ribozyme 1 and ribozyme 2) were cloned into a pEF6/V5-His-TOPO plasmid vector, and the transgene orientation was checked using PCR and a combination of plasmid specific and ribozyme specific primers as previously described in the methodology sections (Figure 4-2 B, C). Colony 1, 2, 7 and 8 from the 'Ribozyme 1 petri dish' and colony 4 and 8 from the 'Ribozyme 2 petri dish' showed positive expression following amplification with the incorrect orientation (T7F vs RbToPF) primer pair rather than the correct orientation pair (T7F vs RbBMR), indicating that the transgene was mostly incorporated into those colonies in the incorrect orientation. Moreover, colony 3 from 'Ribozyme 1 petri dish' showed positive expression with both primer pairs, demonstrating a mixture of correct and incorrect transgene inserts in such colony, whereas no expression was found in both lanes for colony 3 picked from 'Ribozyme 2 petri dish', suggesting no desired transgene was incorporated into the plasmid. However, colony 4 and 5 from the 'Ribozyme 1 petri dish' and colony 1, 2, 5, 6 and 7 from the 'Ribozyme 2 petri dish' exhibited positive expression following amplification with the correct orientation primer pair and negative expression following amplification with the incorrect orientation primer pair. This showed that the majority of the plasmids in those colonies were incorporated with the correct orientation of the transgene inserts.

Two of the eight randomly picked colonies with correctly orientation transgene inserts from each petri dish were chosen for further incubation. Thus, colony 4 and 5 from the 'Ribozyme 1 petri dish' and colony 1 and 2 from the 'Ribozyme 2 petri dish' were inoculated into two universal tubes containing 5ml of selective LB broth (containing 100µg/ml ampicillin) before plasmid extraction was undertaken. Following this, the extracted plasmid was run on a 0.8% agarose gel to confirm the presence and the size of the plasmid (Figure 4-2 D). The predicted sizes of ribozyme 1 and ribozyme 2 incorporated into plasmids are 5925bp and 5921bp respectively which was indicated for all samples. The concentration of each plasmid sample was measured and shown as follows (Table 4-1):

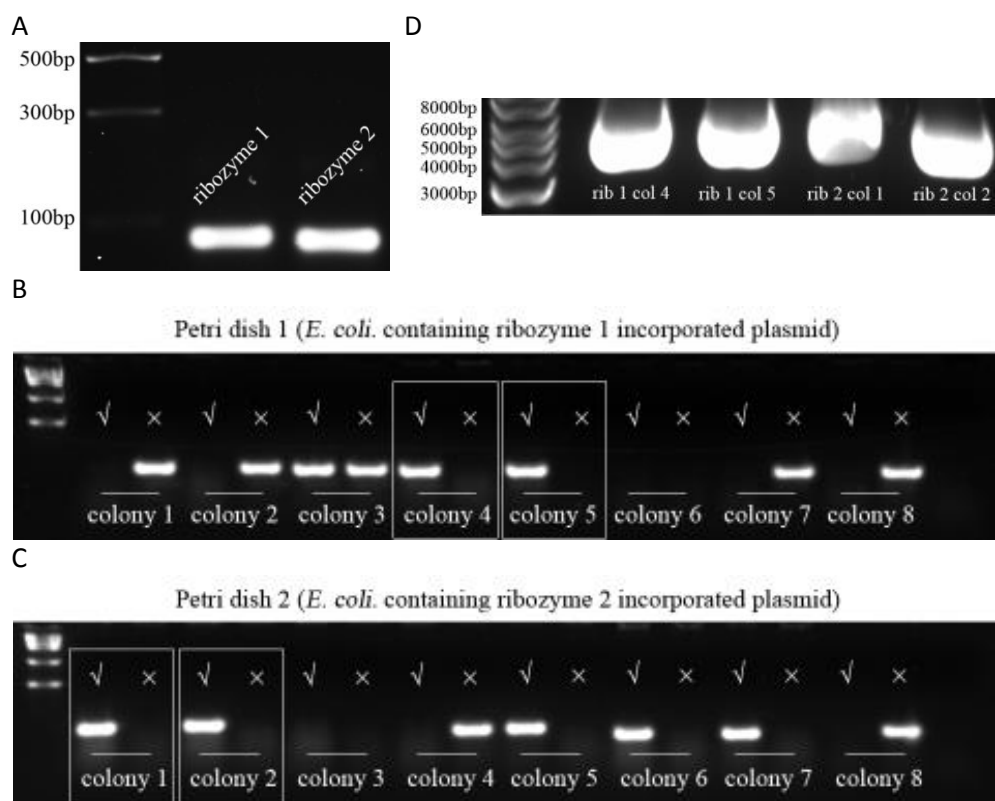


Figure 4-2: Ribozyme transgene synthesis, incorporation and plasmid extraction

A. Ribozyme transgenes, synthesised by touchdown PCR, were loaded on 2% agarose gel and separated by gel electrophoresis and two bands were visualised below 100bp marker. The predicted size of ribozyme 1 and ribozyme 2 transgene are 85bp and 81bp respectively; **B, C.** Colonies picked from petri dishes spread with *E. coli.* that had been transfected with ribozyme 1 and 2 incorporated plasmid were inoculated into PCR reaction mix for transgene orientation check. The '✓' mark represents correct orientation that was verified by primer combination of T7F vs RbBMR (143bp for ribozyme 1 and 147bp for ribozyme 2), whereas, 'X' indicates the incorrect orientation which was confirmed by primer pair of T7F vs RbToPF (144bp for ribozyme 1 and 136bp for ribozyme 2). The '□' mark was used to indicate colonies which were chosen for further plasmid amplification; **D.** The extracted plasmid containing ribozyme 1 or ribozyme 2 were mixed with loading buffer and loaded on 0.8% agarose gel for gel electrophoresis. The predicted size of ribozyme 1 incorporated plasmid (rib 1 col4, rib1 col5) is 5925bp, whereas, the predicted size of the plasmids inserted with ribozyme 2 (rib2 col1, rib2 col2) is 5921bp.

Table 4-1: Concentration measured for the ribozyme incorporated plasmids

No.	Plasmid	A260/280	Concentration (ng/μl)
1	Ribozyme 1 colony 4	1.862	540
2	Ribozyme 1 colony 5	1.914	550
3	Ribozyme 2 colony 1	1.873	665
4	Ribozyme 2 colony 2	1.895	540

4.3.2.2 Verification of SOCS-4 knockdown by ribozyme transgene in epithelial and endothelial cell models through RT-PCR, q-PCR and western blotting

SOCS-4 targeting ribozyme transgene incorporated plasmids and control plasmids (pEF6) were transfected via electroporation. After the blasticidin selection period, RT-PCR, q-PCR and western blot were used to verify knockdown of SOCS-4 in HaCaT and HECV. RNA was isolated from HaCaT and HECV cells transfected with control plasmid (pEF6) and ribozyme incorporated plasmids before reverse transcription to obtain cDNA samples respectively. SOCS-4 and GAPDH transcripts were amplified through RT-PCR in such cDNA samples, and the amplified products were loaded on a 0.8% agarose gel for gel electrophoresis followed by being visualised and images captured. Primer combination of SOCS-4 F8 vs R8, SOCS-4 F2 vs ZR2, GAPDH F8 vs R8, GAPDH F2 vs ZR2 and Actin F10 vs ZR10 were used for RT-PCR and q-PCR amplification.

SOCS-4 knockdown was achieved using ribozyme transgene technology in both epithelial and endothelial cell models (HaCaT and HECV). Transcript expression levels of SOCS-4 in the transfected cells were examined using RT-PCR (Figure 4-3 A, B). The expression of SOCS-4 in two of the four transfected HaCaT cell lines (rib1 col4, rib2 col1) was reduced 36% and 51% respectively comparing to the respective control cells (transfected with empty pEF6 plasmids alone), whereas all four of the transfected HECV cell line (rib1 col4, rib1 col5, rib2 col1, rib2 col2) showed a 30%, 33%, 18% and 23% decreased expression of SOCS-4 in compared to the control cells (transfected with empty pEF6 plasmids alone). SOCS-4 knockdown in the cells which were transfected with ribozyme 2 colony 1 plasmid were further verified using q-PCR (Figure 4-3 C, D, E, F) and western blotting (Figure 4-3 G, H) to explore transcript and protein level respectively. Transfected HaCaT and HECV cells containing the ribozyme transgene plasmids

were routinely tested to confirm continued knockdown of SOCS-4 expression in comparison to control cells. HaCaT and HECV cells transfected with control and transgene plasmid (rib2 col 1) were designated as HaCaT pEF6, HaCaT SOCS-4KD, HECV pEF6, HECV SOCS-4KD.

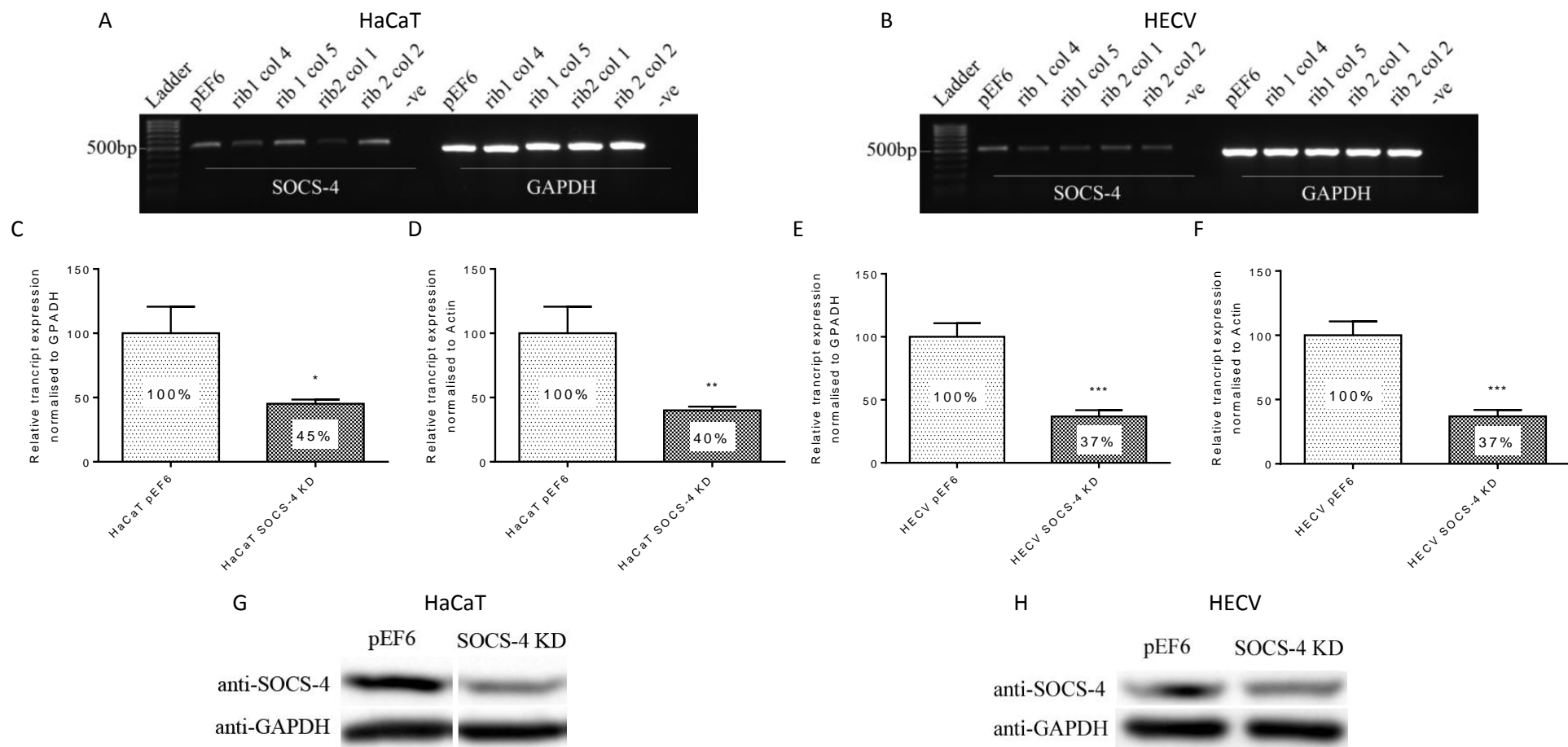


Figure 4-3: Verification of SOCS-4 knockdown in HaCaT and HECV by RT-PCR, q-PCR and western blotting

A, B. The transcript expression levels of GAPDH and SOCS-4 from different plasmid transfected cells was detected and displayed. The size of the sequences that SOCS-4 and GAPDH primer pairs amplified is 541bp and 475bp respectively. Representative images shown (n=3); **C, D, E, F.** The transcript level of SOCS-4 in HaCaT and HECV cells transfected with control plasmid and ribozyme sequence transgene incorporated plasmids were detected by q-PCR and normalised by the expression level of GAPDH and Actin respectively (*: $p < 0.05$, **: $p < 0.01$, ***: $p < 0.001$, error bars represent standard deviation). Representative data is shown (n=3); **G, H.** The protein expression level of SOCS-4 and GAPDH in HaCaT and HECV cells transfected with control plasmid and ribozyme transgene incorporated plasmids were detected by western blotting. Representative images are shown (n=3).

4.3.2.3 Generation of SOCS-4 knockdown cell models by siRNA

4.3.2.3.1 Initial investigation on SOCS-4 knockdown in HaCaT and HECV by

siRNA

The transfection efficacy of siRNA transfection technique was firstly tested on gene level expression. The expression levels of SOCS-4 in wild type, transfect reagent-treated only, non-targeting siRNA and SOCS-4-targeting siRNA transfected cells were examined using q-PCR, and normalised by the expression of GAPDH and Actin respectively. Primer pairs of SOCS-4 F2 vs ZR2, GAPDH F2 vs ZR2 and Actin F10 vs ZR10 were used for the cDNA product amplification.

As shown in Figure 4-4 A, B, following normalisation with GAPDH and Actin expression, the expression of SOCS-4 in SOCS-4-targeting siRNA transfected HaCaT was found to be decreased by more than 60% compared to the non-targeting siRNA transfected control (GAPDH normalisation $p < 0.01$, Actin normalisation $p < 0.01$), whereas the transcript levels of SOCS-4 in SOCS-4-targeting siRNA transfected HECV showed downregulation by approximately 85% in comparison with the non-targeting siRNA control cell (GAPDH normalisation $p < 0.0001$, Actin normalisation $p < 0.0001$)(Figure 4-4 C, D). There was no significant change of SOCS-4 expression between transfect reagent-treated only cell and non-targeting siRNA transfected cells for both HaCaT and HECV (Figure 4-4 A, B, C, D). No significant difference in SOCS-4 expression was found between wild type HaCaT and transfect reagent-treated only or non-targeting transfected HaCaT cells following normalisation with the expression of Actin (Figure 4-4 B), whereas, once normalised by GAPDH expression, SOCS-4 expression decreased significantly both in those transfect reagent-treated only and non-targeting siRNA transfected HaCaT compared to the wild type (WT vs transfect reagent $p < 0.01$, WT vs non-targeting $p < 0.01$), though expression levels were much more substantially

decreased in the HaCaT SOCS-4 siRNA group (Figure 4-4 A). However, SOCS-4 expression in HECV cells normalised by GAPDH demonstrated no significant changes between wild type and transfection reagent-treated only and non-targeting siRNA transfected cells (Figure 4-4 C). Moreover, interestingly, SOCS-4 expression normalised by Actin in transfect reagent-treated only and non-targeting siRNA transfected HECV were both upregulated to that of wild type cells (WT vs transfect reagent $p < 0.05$, WT vs non-targeting $p < 0.05$; 48 hour of treatment of 25nM siRNA and 1 μ l transfect reagent per well) (Figure 4-4 D).

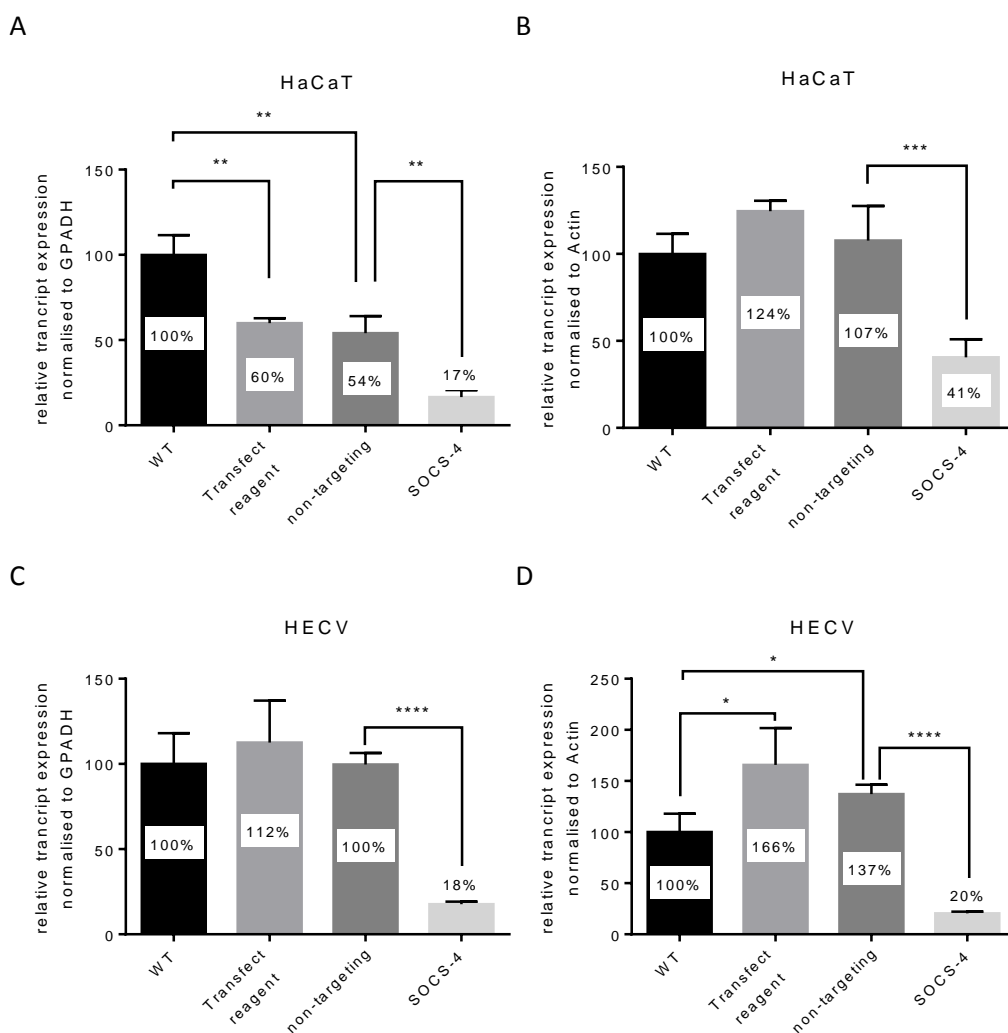


Figure 4-4: Initial investigation on SOCS-4 knockdown in HaCaT and HECV by siRNA

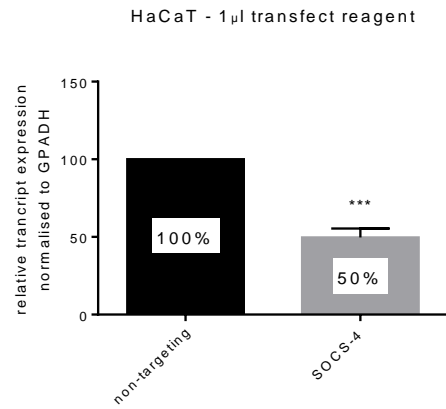
A, B. The transcript levels of SOCS-4 in wild type HaCaT, transfect reagent-treated only HaCaT and 25nM of non-targeting and SOCS-4-targeting siRNA transfected HaCaT cells were detected by q-PCR and were normalised to the expression of GAPDH and Actin respectively; **C, D.** The transcript levels of SOCS-4 in wild type HECV, transfect reagent-treated only HECV and 25nM of non-targeting and SOCS-4-targeting siRNA transfected HECV were examined by q-PCR and were normalised to the expression of GAPDH and Actin respectively. (****: $p < 0.0001$, ***: $p < 0.001$, **: $p < 0.01$, *: $p < 0.05$, error bar represent standard deviation, representative data is shown, $n=3$)

4.3.2.3.2 Transfect reagent concentration optimisation on HaCaT and HECV

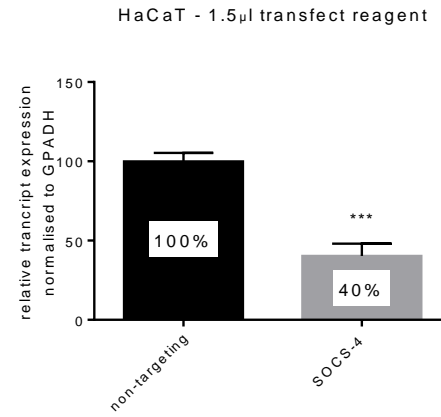
Optimisation of transfect reagent concentration allows more efficient SOCS-4 knockdown. Therefore, experiments were designed to seek an optimal transfect reagent concentration for siRNA transfection in HaCaT and HECV. Transfection medium was made by mixing 25nM of either non-targeting or SOCS-4 targeting siRNA and serial concentration of transfect reagent using serum free and antibiotic-free medium. Different transfect reagent concentration was used for HaCaT (1µl/well, 1.5µl/well, 2µl/well) and HECV (0.5µl/well, 0.75µl/well, 1µl/well) based on the sensitivity of the cells towards the transfect reagent observed previously (data now shown).

After normalised by the expression of GAPDH and Actin, significantly decreased SOCS-4 expression was detected in the SOCS-4-targeting siRNA transfected HaCaT cells compared to the non-targeting siRNA control in all different transfect reagent concentration treated groups (GAPDH normalisation $p < 0.001$, Actin normalisation 1µl/well, 1.5µl/well: $p < 0.01$, 2µl/well: $p < 0.001$)(Figure 4-5 A-F). Moreover, the transfect reagent concentration of 2µl/well group showed a greater knockdown efficiency than the other two groups, which held an approximately 80% knockdown ratio. As indicated in Figure 4-6 A-F, in HECV cells, significant decreases in SOCS-4 expression were found from only one (0.75µl/well) of all three different transfect reagent concentration treated groups once normalised to both GAPDH and Actin expression in HECV ($p < 0.01$), and the knockdown ratio was approximately 85%.

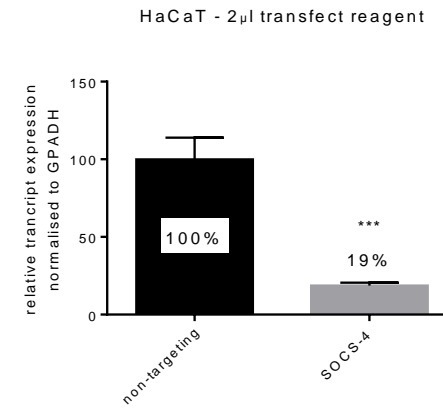
A



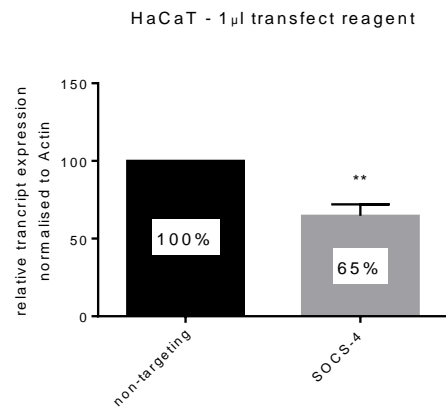
B



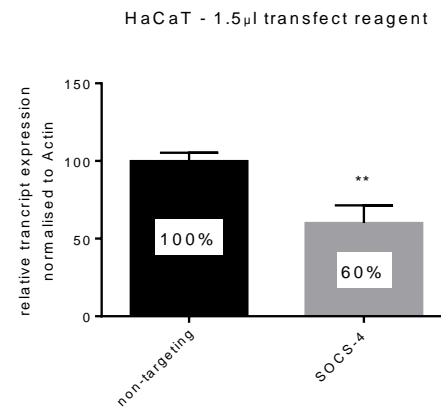
C



D



E



F

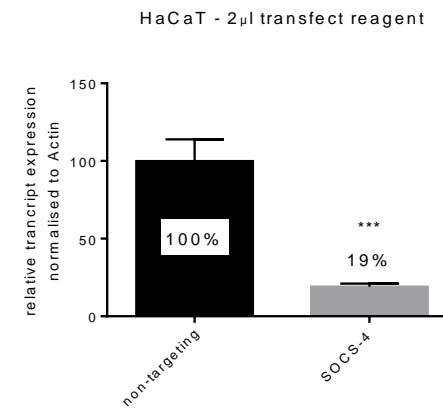
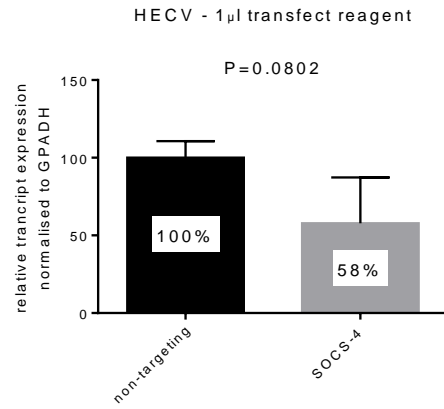


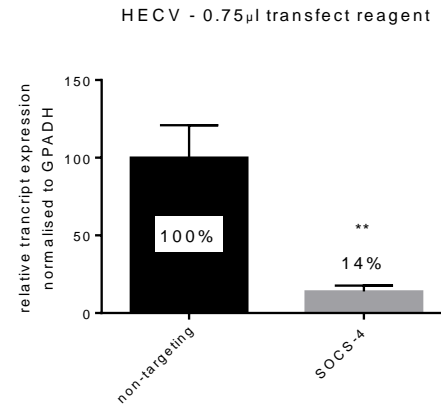
Figure 4-5: Transfect reagent concentration optimisation for HaCaT

A, B, C. The expression levels of SOCS-4 in non-targeting and SOCS-4-targeting siRNA with different concentrations (1µl/well, 1.5µl/well and 2µl/well) of transfect reagent transfected HaCaT were examined by q-PCR and normalised to the transcript levels of GAPDH; **D, E, F.** The expression levels of SOCS-4 in non-targeting and SOCS-4-targeting siRNA with different concentrations (1µl/well, 1.5µl/well and 2µl/well) of transfect reagent transfected HaCaT were detected by q-PCR and normalised to the transcript levels of Actin; (***: $p < 0.001$, **: $p < 0.01$, error bar stands for standard deviation, representative data is shown, n=3)

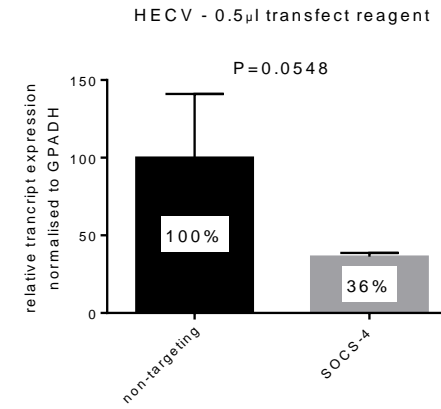
A



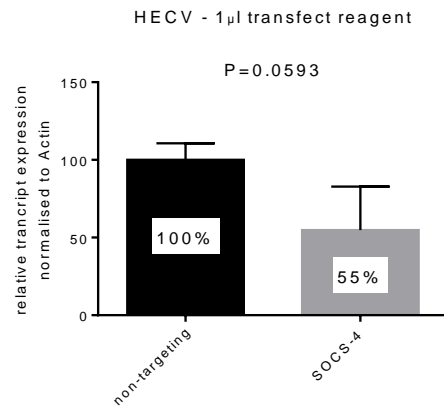
B



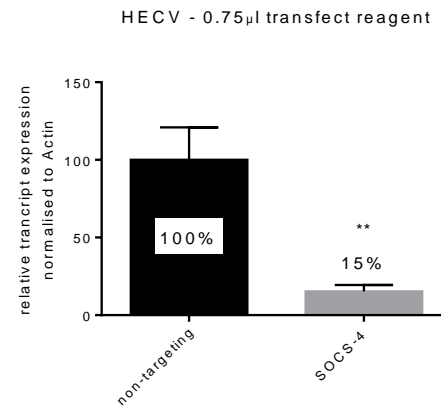
C



D



E



F

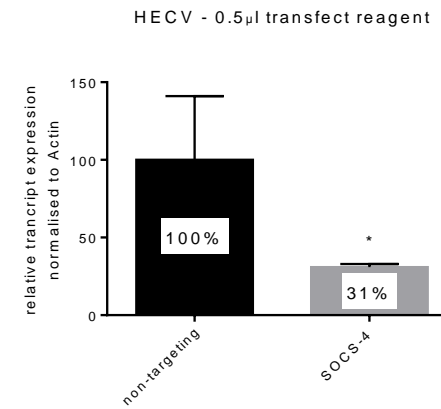


Figure 4-6: Transfect reagent concentration optimisation for HECV

A, B, C. The expression levels of SOCS-4 in non-targeting and SOCS-4-targeting siRNA with different concentrations (1µl/well, 0.75µl/well and 0.5µl/well) of transfect reagent transfected HECV were examined by q-PCR and normalised to the transcript levels of GAPDH; **D, E, F.** The expression levels of SOCS-4 in non-targeting and SOCS-4-targeting siRNA with different concentrations (1µl/well, 0.75µl/well and 0.5µl/well) of transfect reagent transfected HECV were detected by q-PCR and normalised to the transcript levels of Actin. (**: $p < 0.01$, *: $p < 0.05$, error bar stands for standard deviation, representative data is shown, n=3)

4.3.2.3.3 Time point evaluation on siRNA generated SOCS-4 knockdown

siRNA has been recognised as a transient method to temporarily downregulate gene expression levels in mammalian cells. Therefore, the detection of the effective duration of SOCS-4 knockdown by siRNA would be essential for the further functional assay design. Hence, the gene level expression of SOCS-4 after siRNA treatment in HaCaT and HECV were tested at the time of 48 hour and 72 hour following transfection.

HaCaT and HECV cells were treated with transfection medium containing 25nM of siRNA and 2 μ l/well or 0.75 μ l/well transfect reagent respectively and were incubated at 37.0°C, 5% CO₂ and 95% humidity for 48 hours and 72 hours before undertaking RNA extraction and reverse transcription according to the respective protocols.

SOCS-4 expression normalised to GAPDH was decreased by approximately 50% in SOCS-4-targeting siRNA treated HaCaTs compared to the non-targeting siRNA treated controls after 48 hours ($p < 0.05$)(Figure 4-7 A), whereas no significant change on SOCS-4 was found between wild type, transfect reagent-treated only and non-targeting siRNA transfected cells (Figure 4-7 A). However, once normalised by Actin, there was no significant change between any paired groups after 48 hours siRNA treatment (Figure 4-7 B). Furthermore, no significant change on SOCS-4 expression level was detected after 72 hours of siRNA treatment to HaCaT (Figure 4-7 C, D).

The transcript level of SOCS-4 was downregulated in SOCS-4-targeting siRNA transfected HECV in comparison with the non-targeting siRNA transfected cells following normalisation against both GAPDH and Actin expression (GAPDH normalisation $p < 0.001$, Actin normalisation $p < 0.001$) after 48 hour of siRNA transfection, accounting for approximately 70% decrease in both cases (Figure 4-8

A, B). Although the GAPDH and Actin normalised SOCS-4 expression was found to be significantly decreased between SOCS-4-targeting siRNA to non-targeting siRNA transfected HECV (GAPDH normalisation $p < 0.01$, Actin normalisation $p < 0.001$), the knockdown ratio dropped down to around 40 - 50% reduction after 72 hours of siRNA treatment (Figure 4-8 C, D). Moreover, the transcript level of SOCS-4 in transfect reagent-treated only and non-targeting siRNA transfected HECV were both significantly higher than the wild type cells once normalised to GAPDH expression, representing a respective 67% and 27% increase in comparison to the wild type (WT vs transfect reagent $p < 0.0001$, WT vs non-targeting $p < 0.01$) (Figure 4-8 C), whereas, transfect reagent-treated only HECV cells had a 46% increase in SOCS-4 expression compared to wild type cells following normalisation against Actin, which was found to be significant (WT vs transfect reagent $p < 0.001$, WT vs non-targeting $p > 0.05$) (Figure 4-8 D). Interestingly, SOCS-4 expression in non-targeting siRNA transfected HECV cells was decreased by 32% and 43 % respectively compared to transfect reagent-treated only HECV cells when SOCS-4 expression was normalised to both GAPDH and Actin (GAPDH normalisation $p < 0.01$, Actin normalisation $p < 0.01$) (Figure 4-8 C, D).

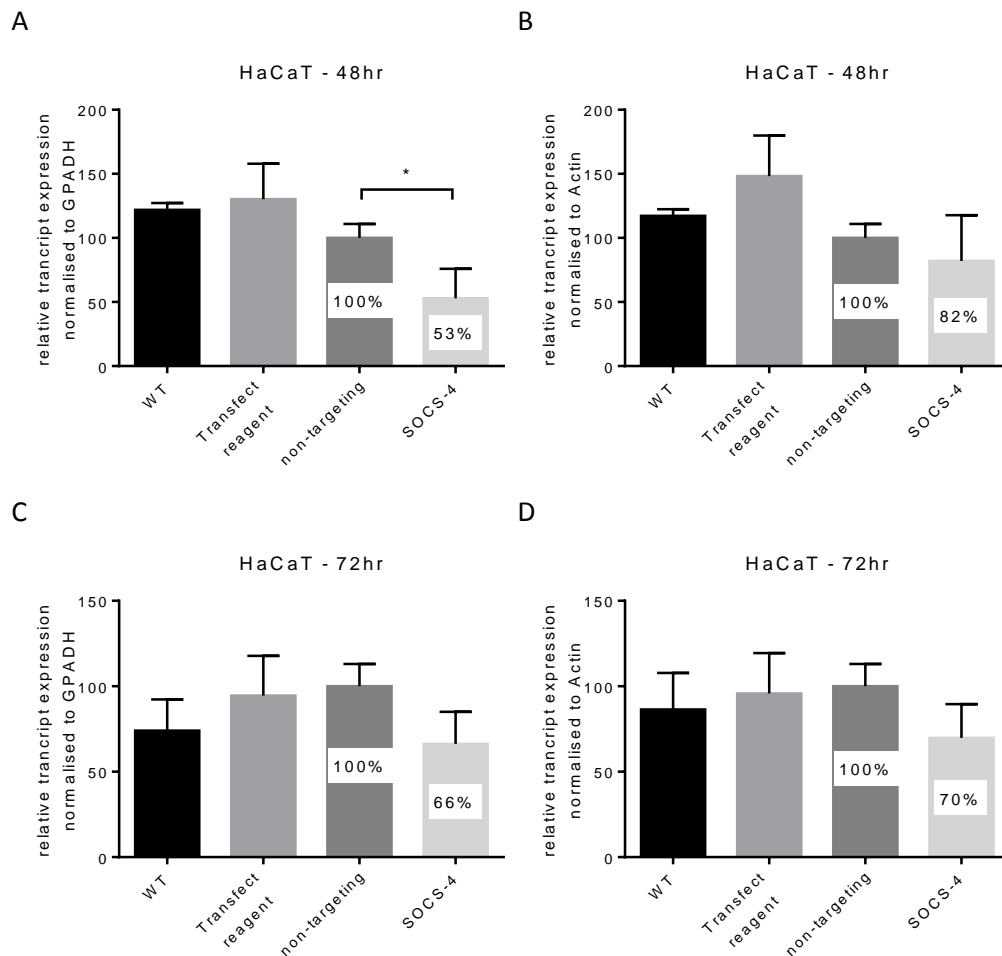


Figure 4-7: Time point evaluation of siRNA generated SOCS-4 knockdown in HaCaT

A, B, C, D. RNA was isolated and reverse transcribed to cDNA from wild type HaCaT, transfect reagent-treated only HaCaT, 25nM of non-targeting and SOCS-4-targeting siRNA transfected HaCaT cells after 48 and 72 hours. The transcript levels of SOCS-4 in these cDNA samples was detected by q-PCR and normalised to the expression of GAPDH and Actin respectively; (*: $p < 0.05$, error bar stands for standard deviation, representative data is shown, $n=3$)

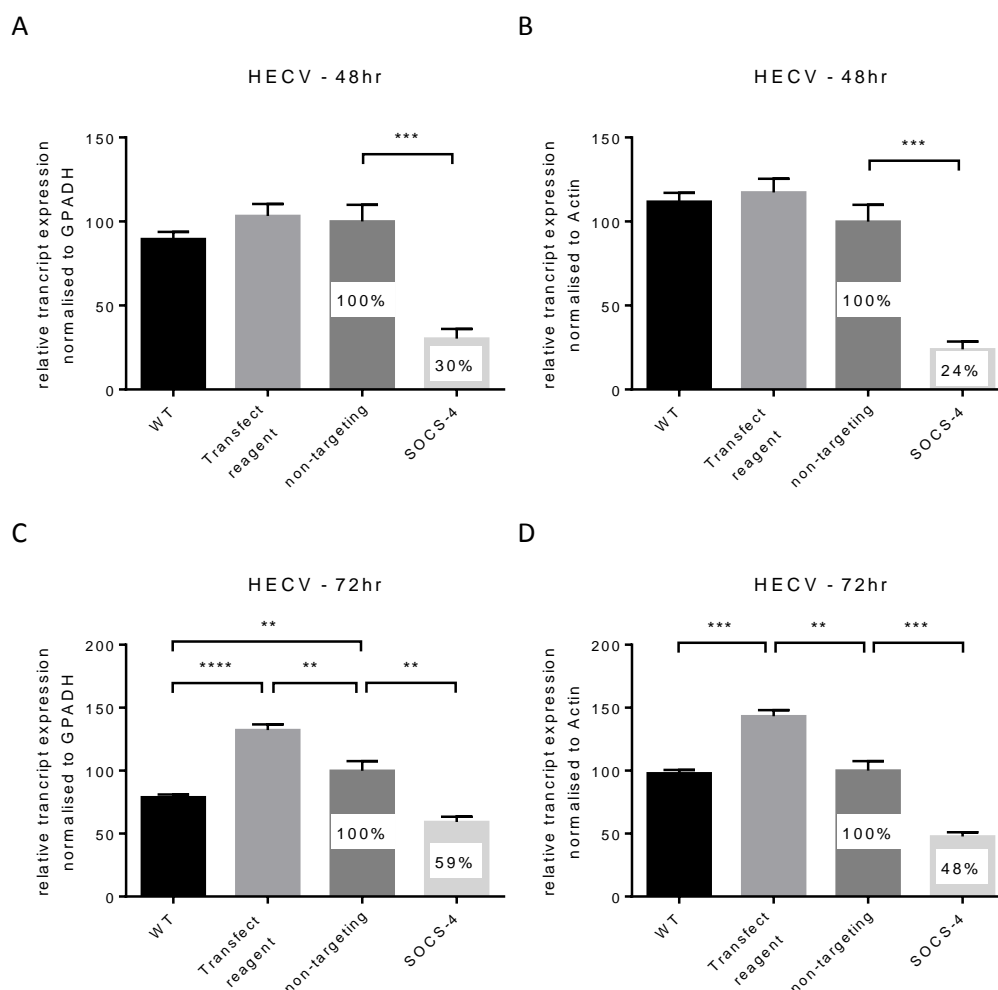


Figure 4-8: Time point evaluation of siRNA generated SOCS-4 knockdown in HECV

A, B, C, D. RNA was isolated and transcribed to cDNA from wild type HECV, transfect reagent treated only HECV, 25nM of non-targeting and SOCS-4-targeting siRNA transfected HECV after 48 and 72 hours. The transcript levels of SOCS-4 in these cDNA samples was examined by q-PCR and normalised to the expression of GAPDH and Actin respectively. (*: $p < 0.05$, **: $p < 0.01$, ***: $p < 0.001$, ****: $p < 0.0001$, error bar stands for standard deviation, representative data is shown, $n=3$)

4.3.2.3.4 Protein expression detection via western blotting on siRNA

transfected HaCaT and HECV

In previous sections, the gene level expression of SOCS-4 in HaCaT and HECV was decreased by approximately 50% and 70% respectively after 48 hours siRNA transfection. Subsequently, the protein expression level was detected in both siRNA transfected cell lines using western blotting following 48 hour transfection. The siRNA transfection medium consisted of 25nM of siRNA and 2µl/well or 0.75µl/well of transfect reagent in serum and antibiotic-free medium for HaCaT and HECV respectively. After 24 hours of incubation at 37.0°C, 5% CO₂ and 95% humidity, the medium containing transfect reagent was replaced by normal medium, and the plate was incubated for another 24 hours before protein extraction.

Equal amount of samples were loaded on the stacking gel and western blotting was undertaken to detect the total protein expression of SOCS-4, GAPDH and Actin. The protein expression level of SOCS-4, GAPDH and Actin in wild type and siRNA transfected HaCaT and HECV cells was detected through western blotting (Figure 4-9 A, B). Semi-quantitative analysis was undertaken using image J to measure the integrate-density of each protein band indicating the protein expression level of the specific protein probed (Figure 4-9 C, D, E, F).

There was more than 40% increase on the protein expression of SOCS-4 in SOCS-4-targeting siRNA transfected HaCaT cells compared to the non-targeting siRNA transfected samples once normalised to GAPDH (Figure 4-9 C), whereas, Actin normalised SOCS-4 expression demonstrated less than 5% downregulation (Figure 4-9 D). However, the SOCS-4 protein expression in non-targeting siRNA transfected HaCaT, normalised to both GAPDH and Actin, was increased approximately 10% compared to wild type HaCaT cells (Figure 4-9 C, D). The

protein level of SOCS-4 in SOCS-4-targeting siRNA transfected HECV cells showed upregulation, accounting for approximately a 10% increase to that of in non-targeting siRNA transfected ones when normalised to GAPDH and Actin (Figure 4-9 E, F). Interestingly, GAPDH normalised SOCS-4 protein expression levels in non-targeting siRNA HECV showed nearly 5% decrease to wild type HECV cells, whereas, once normalised to Actin, it demonstrated a greater than 30% increase (Figure 4-9 E, F).

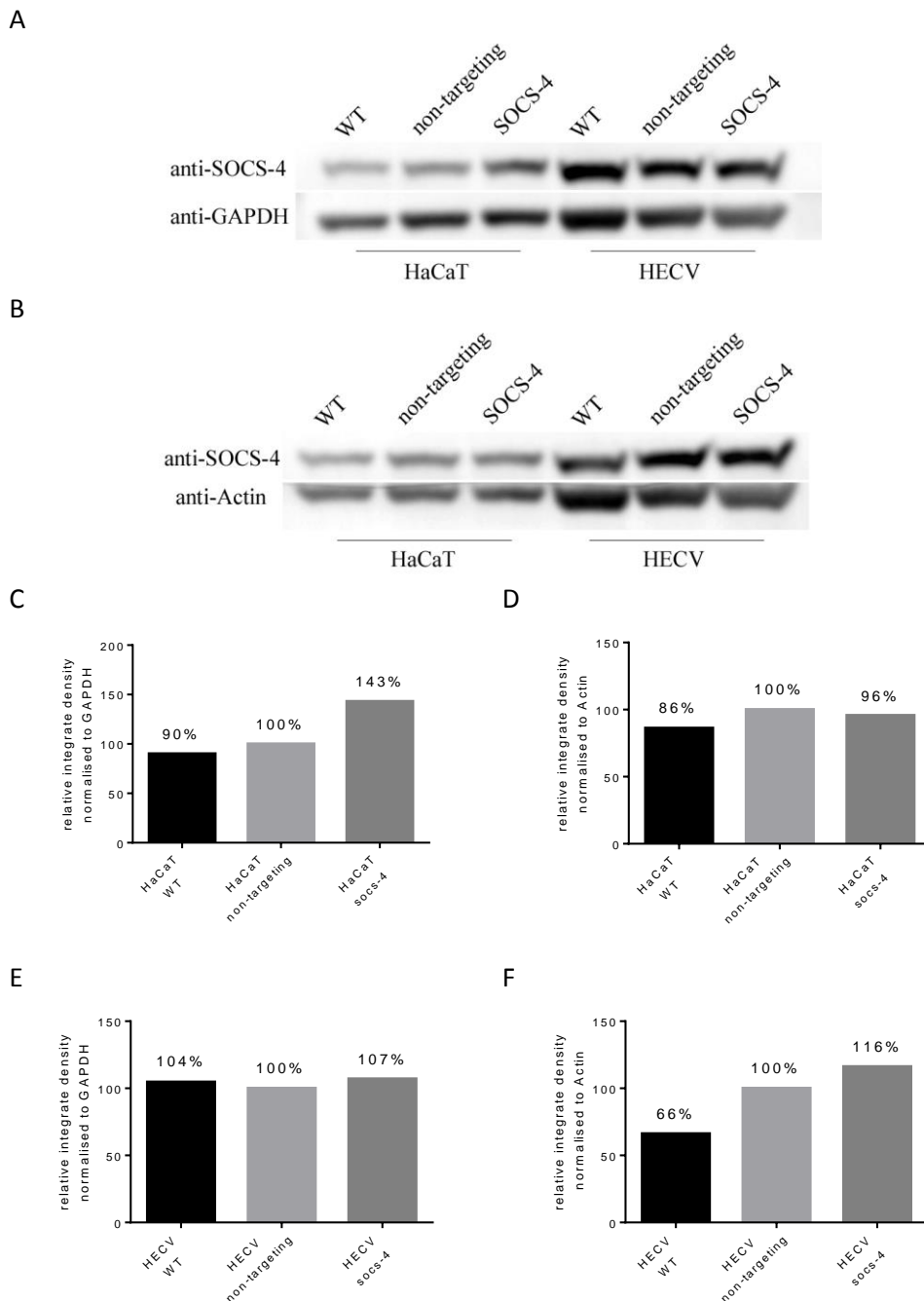


Figure 4-9: siRNA knockdown verification by western blotting

A, B. The normalised protein lysate from wild-type HaCaT, HECV, 25nM of non-targeting and SOCS-4-targeting siRNA transfected HaCaT, HECV were fractionated by SDS-PAGE and transferred to PVDF membrane. Anti-SOCS-4, anti-GAPDH and anti-Actin primary antibodies and anti-mouse as well as anti-goat IgG secondary antibodies were used for probing. Chemiluminescent reagent was used to detect the protein expression. Representative data was shown (n=3); **C, D, E, F.** The protein levels of SOCS-4 were quantified by semi-quantitative analysis using Image J, and normalised by the expression levels of GAPDH and Actin. Such normalised SOCS-4 expression levels in wild-type and SOCS-4-targeting siRNA transfected cells were compared with that of the non-targeting siRNA transfected cells and are represented graphically by percentage change.

4.3.2.4 Generation of SOCS-3 overexpression HaCaT and HECV models

4.3.2.4.1 Initial screening for SOCS-3 on various types of cell lines

Based on the literature review and the information from NCBI database, 8 cell lines available in our laboratory were selected screen for SOCS-3 expression together with HECV and HaCaT.

Positive SOCS-3 expression was found in the PLC-PRF-5, SKMES, A549, CAHPV-10, PC-3 and DU-145 cDNA samples, although SOCS-3 expression was much less in A549 compared to the other five cell lines tested. However, SOCS-3 expression was not detected in HaCaT, HECV, CaCo-2 and PZ-HPV-7 cell lines. Therefore, PLC-PRF-5 and SKMES were chosen for SOCS-3 coding sequence primer pair specificity test based on their high expression profile of SOCS-3 (Figure 4-10 A).

4.3.2.4.2 SOCS-3 coding sequence primer pair specificity check and annealing temperature confirmation

Five SOCS-3 coding sequence primer pairs were designed, and their amplification specificity were tested in the two cell lines displaying the greatest expression of SOCS-3, PLC-PRF-5 and SKMES. The primer combination of SOCS-3 exp F4 vs exp R was identified to be the most specific primer pairs since this primer pair amplified a single specific product at the correct size following 36 cycles of amplification both in PLC-PRF-5 and SKMES. Moreover, the amplification efficacy of SOCS-3 coding sequence was higher in PLC-PRF-5 than in SKMES when they were both amplified by such primer pairs under the same PCR conditions (Figure 4-10 B).

Furthermore, the appropriate annealing temperature was identified by the amplification of PLC-PRF-5 cDNA sample. It showed that 58°C was the most efficient annealing temperature in comparison to 52°C, 54°C and 56°C as this

temperature resulted in the strongest amplification of SOCS-3 coding sequence PCR product (Figure 4-10 C).

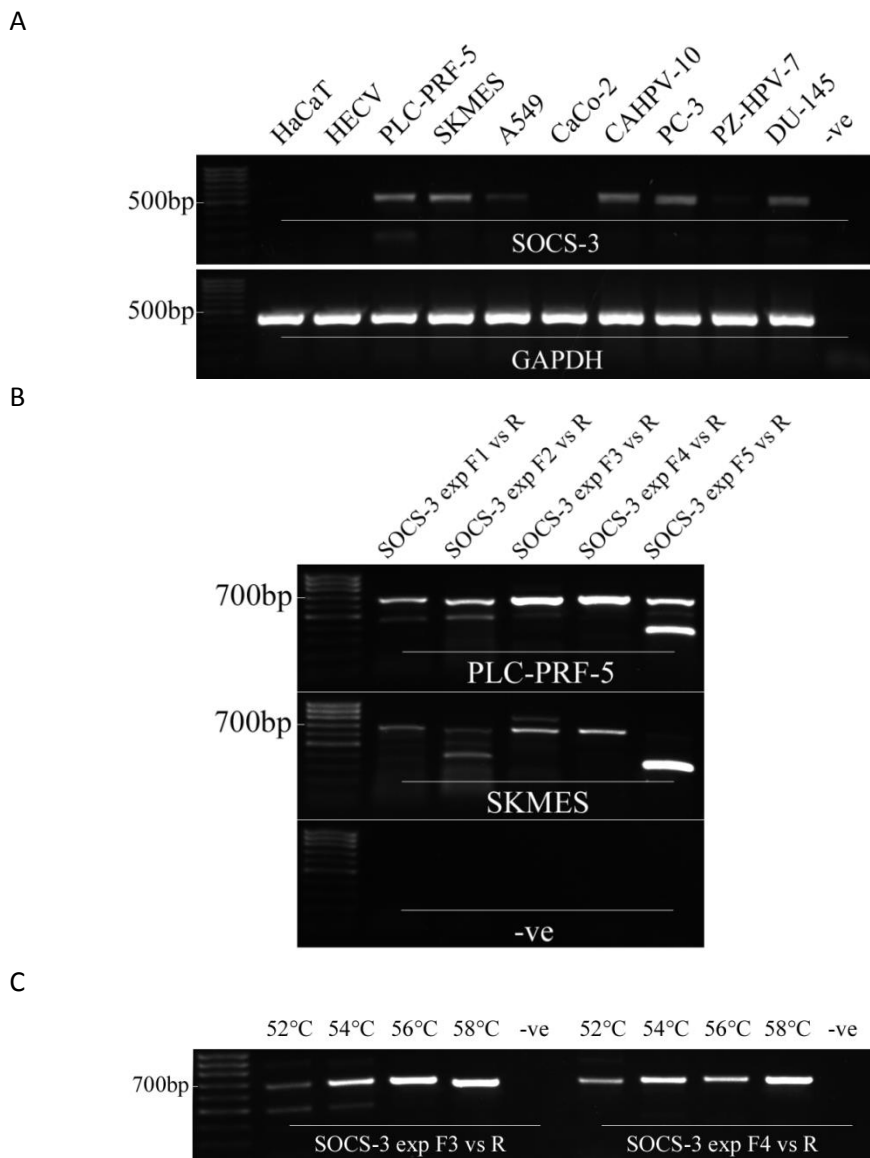


Figure 4-10: Initial screening for SOCS-3 expression on 10 potential cell lines

A. cDNA samples, reverse transcribed from the RNA from 10 cell lines, were amplified using the SOCS-3 F8 vs R8 primer pair and GAPDH F8 vs R8 respectively, and the PCR products were separated through gel electrophoresis. The predicted product size of SOCS-3 and GAPDH products are 521bp and 475bp respectively; **B.** cDNA samples reverse transcribed from RNA from PLC-RPF-5 and SKMES were amplified using four different primer pairs that all target SOCS-3 coding sequence, and the PCR products were separated by gel electrophoresis. The predicted size of all four PCR products is 678bp; **C.** cDNA sample reverse transcribed from RNA from PLC-RPF-5 was amplified using the of SOCS-3 exp F3 vs exp R and SOCS-3 exp F4 vs exp R primer pairs at four different annealing temperatures, and the PCR products were separated by gel electrophoresis. The predicted size of the two PCR products is 678bp.

4.3.2.4.3 Secondary screening of SOCS-3 on normal cell lines/tissues and SOCS-3 coding sequence amplification with high fidelity enzyme mix kit

The cDNA of six normal tissues and two normal cell lines preserved in our laboratory was selected according to the literature review and the information from NCBI database to test for potential SOCS-3 expression for further use in generating SOCS-3 coding sequence amplification. The cDNA from the MRC-5 and hFOB 1.19 was chosen because they are normal cell lines and exhibited the highest expression of SOCS-3 (Figure 4-11 A). A high fidelity enzyme mix kit was used to amplify SOCS-3 coding sequence and the PCR product was loaded on a 0.8% agarose gel and separated by gel electrophoresis followed by image capture. The amplified PCR product from MRC-5 cDNA was chosen for sample purification through excision and gel extraction due to it yielding the greater concentration of product (Figure 4-11 B).

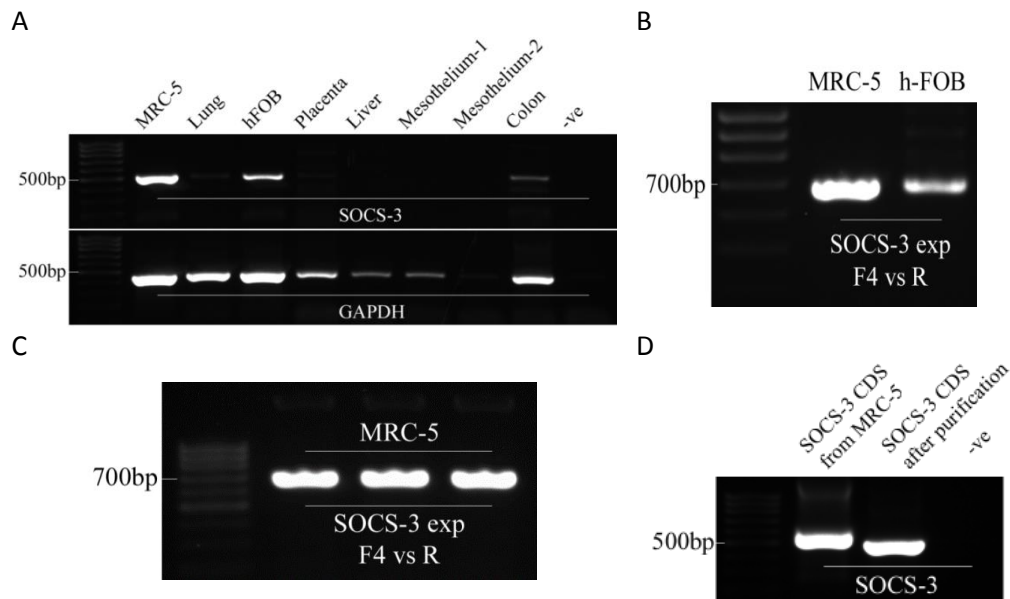


Figure 4- 11: SOCS-3 coding sequence synthesis, amplification and purification

A. cDNA samples, reverse transcribed from the RNA of 6 normal tissues and two normal cell lines were amplified by the primer pair of SOCS-3 F8 vs R8 and GAPDH F8 vs R8 respectively, and the PCR products were separated through gel electrophoresis. The predicted product size of SOCS-3 and GAPDH are 521bp and 475bp respectively; **B.** RNA samples from MRC-5 and h-FOB 1.19 were reverse transcribed to cDNA, and SOCS-3 coding sequence was amplified from these cDNA samples using the primer pair of SOCS-3 exp F4 vs exp R using high fidelity PCR enzyme mix followed by separation through gel electrophoresis. The predicted size of PCR products is 678bp; **C.** The high fidelity PCR enzyme mix and primer combination of SOCS-3 exp F4 vs exp R amplified SOCS-3 coding sequence product (predicted size: 678bp) from MRC-5 cell line were loaded on 0.8% agarose gel in triplicates followed by gel electrophoresis; **D.** The PCR product containing SOCS-3 coding sequence amplified from MRC-5 cell line and the purified SOCS-3 coding sequence product by gel extraction kit were both amplified using the primer pair of SOCS-3 F8 vs R8 and GoTaq Green master mix before being separated by gel electrophoresis to confirm presence of SOCS-3 sequence. The predicted product size is 521bp.

8µl of amplified PCR product from MRC-5 cDNA was loaded on three different lanes of a 0.8% agarose gel and separated by gel electrophoresis before being excised at the predicted size (Figure 4-11 C), then transferred into a 1.5ml microfuge tube. Such PCR product was extracted based upon the protocol provided by the manufacturer and detailed in Chapter II section 2.11.3. The concentration of such DNA product was measured and shown as follows (Table 4-2):

Table 4-2: Concentration measured for the purified SOCS-3 coding sequence product

Product name	A260/280	Concentration (ng/µl)	Sample volume (µl)
Purified SOCS-3 coding sequence	2.600	13	50

Each of the High Fidelity PCR Buffer amplified PCR product from MRC-5 cDNA sample and the SOCS-3 coding sequence from gel extraction were amplified by SOCS-3 F8 vs R8 primer pair using conditions identical to the initial screening excluding cycle numbers which was changed to 30 cycles. Subsequently, PCR products were loaded on a 0.8% agarose gel followed by gel electrophoresis and image capture (Figure 4-11 D). A more specific and clearer band was visualised on the purified SOCS-3 coding sequence sample lane. The presence of correctly sized products following SOCS-3 F8 vs R8 amplification gave initial confirmation that the amplified coding sequence was correct for SOCS-3, though more thorough confirmation was also undertaken following insertion and amplification of the SOCS-3 expression plasmid.

4.3.2.4.4 SOCS-3 coding sequence incorporation, transgene orientation check and plasmid extraction

The purified SOCS-3 coding sequence was incorporated into pEF6/V5-His-TOPO plasmid vector according to the cloning protocol outlined in the methodology section 2.11.2 to 2.11.3. These colonies were subject to orientation analysis using a combination of plasmid specific and sequence specific pairs to examine sequence insertion (T7F vs BGHR), incorrect orientation (T7F vs SOCS-3 exp F4) and correct orientation (T7F vs SOCS-3 exp R). As shown in Figure 4-12, the negative expression on both T7F vs SOCS-3 exp R and T7F vs SOCS-3 exp F4 combination lane and the positive expression but incorrect size on T7F vs BGHR primer pair lane, detecting from colony 1, 2, 4, 5, 6 and 8, indicated that there was no SOCS-3 coding sequence incorporated plasmids in those colonies. Colony 3, 7, 9 and 10 expressed the correct product size of SOCS-3 coding sequence insertion. Moreover, colony 7 and 10 showed positive expression in the incorrect primer pair lane, more so than in the correct orientation pair, indicating that the expression sequence was mostly inserted in the incorrect orientation. However, colony 3 and 9 exhibited positive expression in the correct orientation primer pair and negative expression in the incorrect orientation primer combination. This demonstrated that the majority of the plasmids in these two colonies were incorporated with the correct orientation of SOCS-3 coding sequence.

Colony 3 and 9 were then inoculated into two universal tubes containing 5ml of selective LB broth (containing 100µg/ml ampicillin) respectively, and both tubes were incubated overnight before plasmid extraction. The concentration of each extracted plasmid sample was measured and shown as follows (Table 4-3):

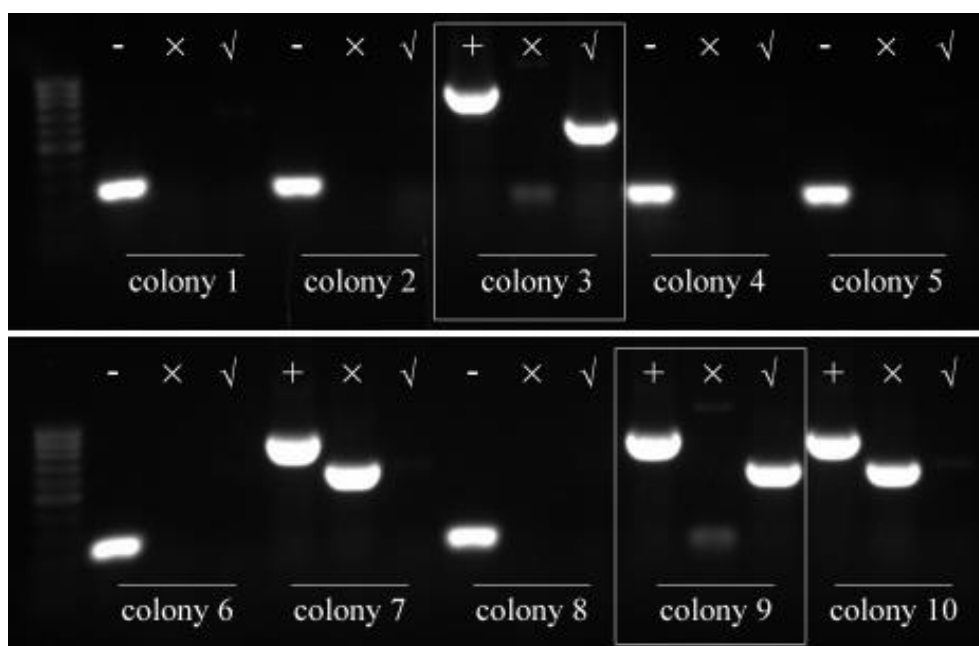


Figure 4-12: SOCS-3 coding sequence incorporation/orientation analysis

Colonies picked from the *E. coli*. Transformed with SOCS-3 coding sequence incorporated plasmid were inoculated into PCR reaction mixes for insertion and orientation checking. '+' represents SOCS-3 coding sequence insertion (T7F vs BGHR reaction with correctly sized product), '-' represents no SOCS-3 coding sequence incorporation (T7F vs BGHR reaction with incorrectly sized product). The 'v' mark represents correct orientation which was detected using primer combination of T7F vs SOCS-3 exp R (predicted size: 768bp), whereas, 'x' indicates incorrect orientation that was verified using the primer pair of T7F vs SOCS-3 exp F4 (predicted size: 768bp). The '□' mark was used to indicate colonies which were chosen for further plasmid amplification.

Table 4-3: Concentration measured for the SOCS-3 coding sequence incorporated plasmids

No.	Plasmid	A260/280	Concentration (ng/μl)
1	SOCS-3 coding sequence colony 3 (SOCS-3 exp1)	1.900	333
2	SOCS-3 coding sequence colony 9 (SOCS-3 exp2)	1.953	420

4.3.2.4.5 SOCS-3 coding sequence verification by sequencing

The appropriate concentration of the SOCS-3 coding sequence incorporated plasmids and purified SOCS-3 coding sequence PCR products were prepared with PCR water according to the protocol detailed in the methodology section and were sent for Sanger Sequencing (Source BioScience, Nottingham, UK). The sequencing results for the samples were queried by *Homo sapiens* (human) Nucleotide BLAST and indicated that all three tested sample were 100% identical to the targeted SOCS-3 coding sequence (Figure 4-13).

SOCS coding sequence - colony 3						
Alignments	Download	GenBank	Graphics	Distance tree of results		
	Max score	Total score	Query cover	E value	Ident	Accession
<input type="checkbox"/> Homo sapiens suppressor of cytokine signaling 3 (SOCS3), mRNA	1232	1232	98%	0.0	100%	NM_003955.4
SOCS coding sequence - colony 9						
Alignments	Download	GenBank	Graphics	Distance tree of results		
	Max score	Total score	Query cover	E value	Ident	Accession
<input type="checkbox"/> Homo sapiens suppressor of cytokine signaling 3 (SOCS3), mRNA	1247	1247	99%	0.0	100%	NM_003955.4
SOCS coding sequence - purified PCR product						
Alignments	Download	GenBank	Graphics	Distance tree of results		
	Max score	Total score	Query cover	E value	Ident	Accession
<input type="checkbox"/> Homo sapiens suppressor of cytokine signaling 3 (SOCS3), mRNA	1151	1151	100%	0.0	100%	NM_003955.4

Figure 4-13: SOCS-3 coding sequence verification

Sequencing results of the three samples sent for Sanger Sequencing were visualised and interpreted by Chromas Version 2.5.0 (Technelysium Pty Ltd), and were then checked by *Homo sapiens* (human) Nucleotide BLAST (NCBI). Two SOCS-3 coding sequence incorporated plasmids which were extracted from the orientation verified colonies were labelled as 'colony 3' and 'colony 9' respectively, and the purified SOCS-3 coding sequence sample was labelled as 'purified PCR product'. The 'black rectangular' and 'red rectangular' highlighted area indicate the coverage rate and identity rate of the tested samples to the targeted SOCS-3 coding sequence respectively.

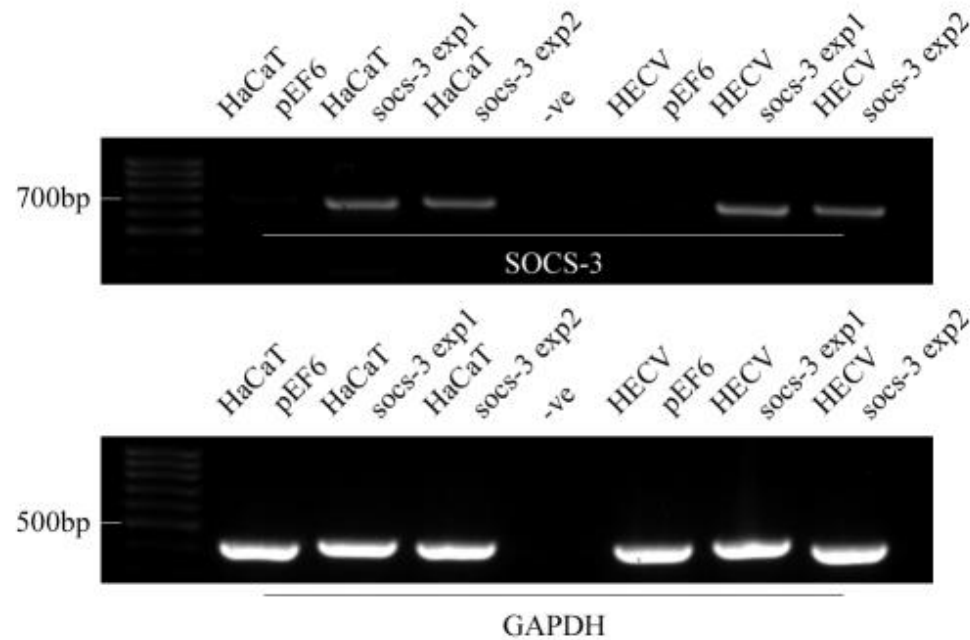
4.3.2.4.6 SOCS-3 overexpression verification in HaCaT and HECV models

SOCS-3 coding sequence incorporated plasmid and control plasmid (pEF6) were transfected using electroporation. Following the blasticidin selection period, RT-PCR, q-PCR and western blot were used to verify SOCS-3 overexpression in HaCaT and HECV. RNA was isolated from HaCaT and HECV cells transfected with control plasmid (pEF6) and SOCS-3 coding sequence incorporated plasmids (SOCS-3 exp1, SOCS-3 exp2) before reverse transcription was undertaken to obtain cDNA samples respectively. SOCS-3 and GAPDH transcript, targeted by primer pairs of SOCS-3 exp F4 vs R and GAPDH F8 vs R8, were amplified for 30 cycles by conventional PCR and the amplified products were loaded on 0.8% agarose gel for gel electrophoresis followed by visualising and image capture (Figure 4-14 A).

SOCS-3 expression was achieved through continuous synthesis of SOCS-3 coding sequence by T7F promoter in the pEF6/v5-His-TOPO plasmid in both transfected epithelial and endothelial cells (HaCaT and HECV). After 30 cycles of amplification, the transcript levels of SOCS-3 in both SOCS-3 coding sequence incorporated plasmid transfected HaCaT and HECV cell lines (SOCS-3 exp1 and SOCS-3 exp2) was obviously elevated (HaCaT SOCS-3exp1: 244%, HaCaT SOCS-3exp2: 223%; HECV SOCS-3exp1: 274%, HECV SOCS-3exp2: 232%) compared to the respective control cells (transfected with empty pEF6 plasmids alone), whereas, the expression level of GAPDH was approximately consistent throughout the samples (Figure 4-14 A). SOCS-3 exp2 plasmid transfected HaCaT and HECV cells were further verified using western blotting (Figure 4-14 B) and q-PCR (Figure 4-15 A, B, C, D), both methods demonstrating a good efficiency of SOCS-3 overexpression in comparison to the respective plasmid control cell lines, with q-PCR indicating an upregulation of greater than 4500% in HaCaT SOCS-3 expression cell lines and a greater than 8500% increase in HECV SOCS-3 expression cell lines

in comparison to respective plasmid controls. Fluctuation in percentage upregulation were obtained dependent on whether q-PCR was normalised to GAPDH or Actin housekeeping gene, though in all cases the enhanced expression of SOCS-3 in comparison to respective control cells was highly significant ($p < 0.001$ in all cases). Transfected HaCaT and HECV cells containing the SOCS-3 coding sequence plasmids were maintained in medium supplemented with blasticidin to promote stable expression of SOCS-3. Such cell lines were routinely tested to confirm SOCS-3 expression in comparison to empty vector controls. HaCaT and HECV cells transfected with control and SOCS-3 coding sequence plasmid were designated as HaCaT pEF6, HaCaT SOCS-3exp, HECV pEF6, HECV SOCS-3exp.

A



B

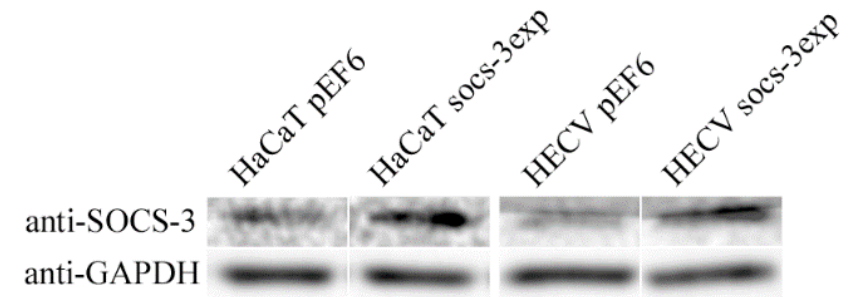
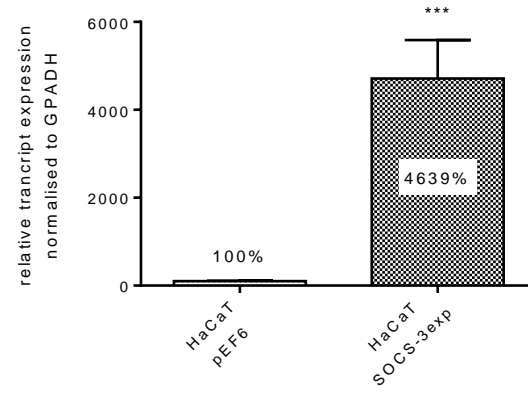


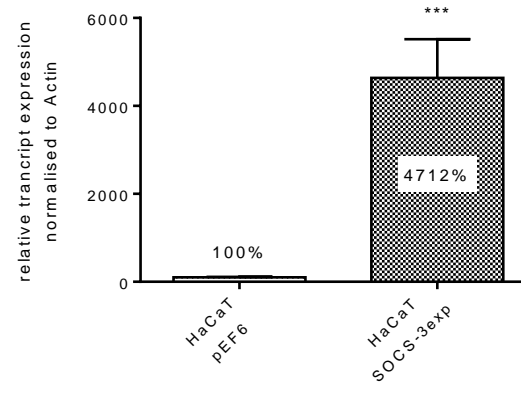
Figure 4-14: Verification of SOCS-3 expression in HaCaT and HECV by RT-PCR and western blotting

A. The transcript expression levels of SOCS-3 and GAPDH from different plasmid transfected cells was detected. Predicted product sizes for SOCS-3 and GAPDH primer pairs are 678bp and 475bp respectively; **B.** The protein expression level of SOCS-3 and GAPDH in HaCaT and HECV cells transfected with control plasmid and SOCS-3 coding sequence transgene incorporated plasmids were detected by western blotting (representative data is shown, n=3).

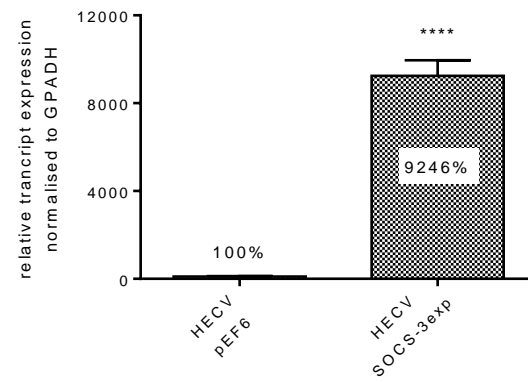
A



B



C



D

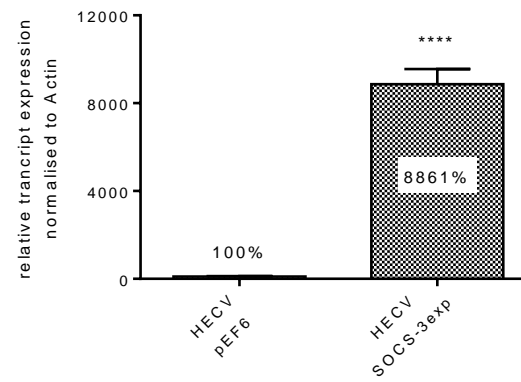


Figure 4-15: Verification of SOCS-3 expression in HaCaT and HECV by q-PCR

A, B, C, D. The transcript level of SOCS-3 in HaCaT and HECV cells transfected with control plasmid and SOCS-3 coding sequence transgene incorporated plasmids was detected using q-PCR and normalised by the expression levels of GAPDH and Actin respectively (***: $p < 0.001$, ****: $p < 0.0001$, error bars represent standard deviation; representative data is shown, $n=3$).

4.4 Discussion

The initial screening of the transcript levels of seven SOCS family members in chronic wound biopsies suggested that the gene levels of SOCS-3 and SOCS-4 exhibited higher expression in non-healing chronic wounds to that in the healing/healed chronic wound tissues. Moreover, the difference of SOCS-3 protein relocation between chronic non-healing and healing/healed wounds. The gene expression data, even though contrasted by protein expression analysis, when taken together with the literature highlights potential regulatory role of SOCS-3 and SOCS-4 during the chronic wound healing process. Hence, in order to further explore these highlighted proteins, the current chapter aimed to generate *in vitro* model systems for further functional characterisation in keratinocyte and endothelial cell lines. The establishment of SOCS-4 knockdown and SOCS-3 expression cell models in HaCaT and HECV cell lines respectively was determined based on the transcript expression profile of SOCS-3 and SOCS-4 which showed moderate expression of SOCS-4 and no expression of SOCS-3 in both HaCaT and HECV wild-type cell lines by RT-PCR. Two methodologies (ribozyme transgene and siRNA) were applied and optimised to generate SOCS-4 knockdown models in HaCaT and HECV cell lines. The SOCS-4 knockdown efficacy was verified by RT-PCR and q-PCR at transcript level and using western blotting at protein level. All three techniques successfully verified knockdown of SOCS-4 in both HaCaT and HECV cell lines by ribozyme transgene transfection. Routine verification of SOCS-4 knockdown was undertaken, and stable knockdown lines were used in future functional analysis.

Similar SOCS-4 targeting-ribozyme transgene incorporated plasmids that were extracted from different *E. coli* colonies (rib1 col4/rib1 col5 and rib2 col1/rib2 col2) were used to transfect HaCaT and HECV cells separately. After the

selection period, SOCS-4 knockdown ratio was verified by RT-PCR. Both HaCaT and HECV cells that received either ribozyme (ribozyme 1 or ribozyme 2) exhibited successfully decreased SOCS-4 transcript expression. This indicated that both ribozyme 1 and ribozyme 2 had an effect on the decrease of SOCS-4 transcript expression. However, HaCaT cells that acquired 'rib1 col4' plasmid showed obvious SOCS-4 downregulation at transcript level, whereas, those that were transfected with the 'rib1 col5' plasmid exhibited little decrease in SOCS-4 levels. This discrepancy could possibly be due to the different amount of plasmids that the cell acquired during the electroporation transfection stage and/or the selection stage, resulting in differential knockdown efficiencies.

The q-PCR results from the initial investigation on SOCS-4 knockdown by siRNA showed that, after 48 hours of siRNA transfection, SOCS-4 transcript levels were decreased in SOCS-4-targeting siRNA transfected HaCaT and HECV cells compared to that of the non-targeting transfected control cells. Interestingly, the transfect reagent seemed to have an effect on the expression level of GAPDH in HaCaT cells and Actin on HECV cells, since either decreased or increased SOCS-4 expression was seen in transfect reagent treated cells to that in wild-type cells once it was normalised to GAPDH or Actin expression respectively.

However, the q-PCR results from the different time point evaluation showed that, after 48 hours of siRNA treatment, there was no significant difference in SOCS-4 expression between HaCaT and HECV wild-type and transfect reagent treated cells following normalisation against either GAPDH or Actin. This was not in agreement with the results obtained from the initial investigation, suggesting the transfect reagent may affect the house-keeping gene expression by chance. Moreover, GAPDH normalised SOCS-4 transcript expression in SOCS-4-targeting siRNA transfected HaCaT exhibited significant knockdown, accounting

for less than 50% compared to non-targeting siRNA transfected cells. Comparing to the knockdown effect seen in the initial investigation, such low knockdown ratio indicated the poor reproducibility of the siRNA technique in the HaCaT cell line. Furthermore, after 72 hours of siRNA treatment, no differences in SOCS-4 expression could be found in any group following the normalisation of either GAPDH or Actin. This was in agreement with the traits of the siRNA technique, which only provides transient knockdown of the target gene. The western blotting results demonstrated siRNA transfection had a poor SOCS-4 protein knockdown efficiency in HaCaT cells after 48 hours treatment.

In summary, the poor SOCS-4 knockdown stability and the unpredicted house-keeping gene variation suggested that siRNA transfection technique may be not suitable for the generation of SOCS-4 knockdown HaCaT cell models. Another transfect reagent is required to be used to test the stability of house-keeping gene expression on HaCaT cells and to seeking optimised siRNA transfection conditions.

The results from different time point evaluation on siRNA transfected HECV groups showed that both GAPDH and Actin normalised SOCS-4 expression in SOCS-4-targeting siRNA transfected HECV cells decreased significantly in comparison to the non-targeting siRNA transfected ones following 48 hours transfection. This is consistent with the result from the initial investigation, although the knockdown ratio is approximately 15% less. This may be due to the lower concentration of transfect reagent applied for the time point evaluation experiment.

Furthermore, in agreement to the transient knockdown characteristics of siRNA, the SOCS-4 transcript knockdown ratio in HECV cell dropped 20% after 72 hours siRNA transfection. Interestingly, distinct from the initial investigation

results, the Actin normalised SOCS-4 expression in the transfect reagent treated HECV cells did not show any significant difference to that of wild-type cells after 48 hours treatment. However, the transfect reagents effect on house-keeping genes was observed after 72 hours of treatment, although such influence did not dramatically affect the SOCS-4 knockdown efficiency. Moreover, instead of achieving SOCS-4 knockdown at protein level, upregulation of SOCS-4 protein was observed following the normalisation against GAPDH and Actin expression after 48 hours of siRNA transfection. Therefore, different time points for protein screening, after 48 hours, is suggested to test the potentially delayed SOCS-4 protein decrease following SOCS-4 transcript level knockdown.

In brief, the HECV SOCS-4 knockdown model could potentially be achieved by siRNA technique after transfection condition optimisation and the verification of protein level downregulation for different time point. However, further cell functional assays and investigation of downstream mechanisms in long term experimentation may be affected due to the transient traits of such methodology, therefore, such characteristics needs to be taken into consideration while designing experiments based on HECV knockdown models utilising siRNA.

Additionally, the result presented here demonstrate an efficient model for SOCS-3 expression in the two cell lines chosen, HaCaT and HECV. SOCS-3 coding sequence was sucessfully generated and verified using a wide range of technique and sequencing and also confirmed substantial and signaificant expression of SOCS-3 in keratinocyte and endothelial cell models.

In conclusion, the HaCaT and HECV SOCS-4 knockdown model established by ribozyme transgene was considered to be the more robust of the tested techniques and, hence, was taken forward, in addition to the SOCS-3 expression

models, to conduct future experiments for cell functional assays and downstream mechanism investigations.

Chapter V

Functional significance of SOCS-4 knockdown in HaCaT and HECV models and potential downstream mechanisms

5.1 Introduction

According to the q-PCR and IHC screening on chronic wound biopsies reported and discussed in Chapter III, SOCS-4 is expressed primarily in all layers of keratinocytes of the epidermis and additionally distribution of SOCS-4 in microvessular-like structures in dermis also suggested its expression and implication in endothelial cells. Moreover, whilst in contrast to the protein data, higher gene expression of SOCS-4 was observed in non-healing chronic wound biopsies compared to that of in the healing/healed ones. Thus, this early data, whilst raising a number of questions, also raises the potential involvement of SOCS-4 in chronic wound biology or that its gene expression may be useful as a biomarker for chronic wound healing potential.

In order to further clarify the impact of SOCS-4 in wound biology the previous chapter established SOCS-4 knockdown models in keratinocyte (HaCaT) and endothelial (HECV) cells. Such knockdown was brought about by ribozyme transgenes as this method provided the more efficient/consistent knockdown efficiency and generated stable cell lines. HECV and HaCaT cell lines were chosen for the *in vitro* models since they have been successfully used in previous wound healing *in vitro* studies (Goren et al., 2006a, Liu et al., 2013, Tan et al., 2015) and represent two key cell types involved in healing.

The current chapter focuses on supplementing the previous clinical data with functional characterisation of the cellular impact of SOCS-4 knockdown, with regards to cell adhesion, proliferation, migration, spreading and angiogenic potential, within these keratinocyte and endothelial cell lines.

5.2 Methods and materials

5.2.1 *In vitro* MTT cell adhesion assay

This methodology is described in full in section 2.18.3 of Chapter II. In this chapter, the relative absorbance was normalised against the control group and transferred into percentage to the control in each repeat. The mean value was then calculated before being plotted in a bar chart as the final results.

5.2.2 *In vitro* MTT cell proliferation assay

This methodology is described in full in section 2.18.2 of Chapter II. In this chapter, the relative absorbance was normalised against the control group and transferred into a percentage relative to the control in each repeat. The mean value was then calculated before being plotted in a bar chart.

5.2.3 Kinexus protein array and data analysis

HaCaT pEF6 and HaCaT SOCS-4 KD protein samples were extracted as outlined in section 2.16 of chapter II. Such samples were subsequently sent to Kinexus Bioinformatics, Canada for protein microarray analysis.

The protein microarray used consists of 2 identical fields, allowing two samples to be analysed side by side at a time. Within each field, there are 16 subgrids of 11 x 10 spots. Diameters of spots average between 120 and 150µm. (Figure 5-1) 50µg of lysate protein from each sample are covalently labeled with a proprietary fluorescent dye combination. Free dye molecules are then removed at the completion of labeling reactions by gel filtration. After blocking non-specific binding sites on the array, an incubation chamber is mounted onto the microarray to permit the loading of control and SOCS-4 knockdown protein samples side by side on the same chip and prevent mixing of the samples. Following sample

incubation , unbound proteins are washed away. Each array produces a pair of 16-bit images, which are captured with a Perkin-Elmer ScanArray Reader laser array scanner (Waltham, MA). Signal quantification is performed with ImaGene 9.0 from BioDiscovery (El Segundo, CA) with predetermined settings for spot segmentation and background correction. The background-corrected raw intensity data are logarithmically transformed with base 2 for further Z scores calculation.

Globally Normalised Signal Intensity - Background corrected intensity values are globally normalised. The Globally Normalised Signal Intensity is calculated by summing the intensities of all the net signal median values for a sample. This is done for all samples within a comparison to find the average net signal median. Once the average net signal median is calculated, the sum of the net signal median for each sample is divided by the average net signal median to obtain a co-efficient for normalisation; using the co-efficient, the net signal mean for each sample is divided by the co-efficient to obtain the globally normalised signal intensity value.

%CFC (change from control in percentage) - The percent change of the treated sample in Normalised Intensity from the specified control. For example, a %CFC value of 100% corresponds to a 2-fold increase in signal intensity with the treatment. A negative %CFC value indicates the degree of reduction in signal intensity from the selected control.

Z Scores - Z scores represent where each signal falls in the overall distribution of values within a given sample, and they are calculated by subtracting the overall average intensity of all spots within a sample from the raw intensity of each spot, and dividing it by the SD of all of the measured intensities within each sample. Z score transformation corrects data internally within a single

sample. The background corrected spot intensity values for individual proteins are expressed as a unit of standard deviation (SD) from the normalised mean of zero. Since the transformation is done before sample-to-sample comparison, it is therefore comparison-independent.

Z Score Difference and Z ratio - The difference between the observed protein Z scores in samples in comparison. Z Ratios - Divide the Z Score Differences by the SD of all the differences for the comparison. Follow-up studies should be based largely on the values of the Z-Score Ratios as they reveal the most reliable changes between the control and treated samples.

This methodology has been described previously (Owen et al., 2016).

5.2.4 Statistical analysis

Statistical analysis was undertaken using the SigmaPlot 11 and Graphpad Prism 6 statistical software packages. Data was analysed using t-test or Mann Whitney test, depending on data parameters. Values of $p < 0.05$ (*), $p < 0.01$ (**), $p < 0.001$ (***) and $p < 0.0001$ (****) were regarded as statistically significant.

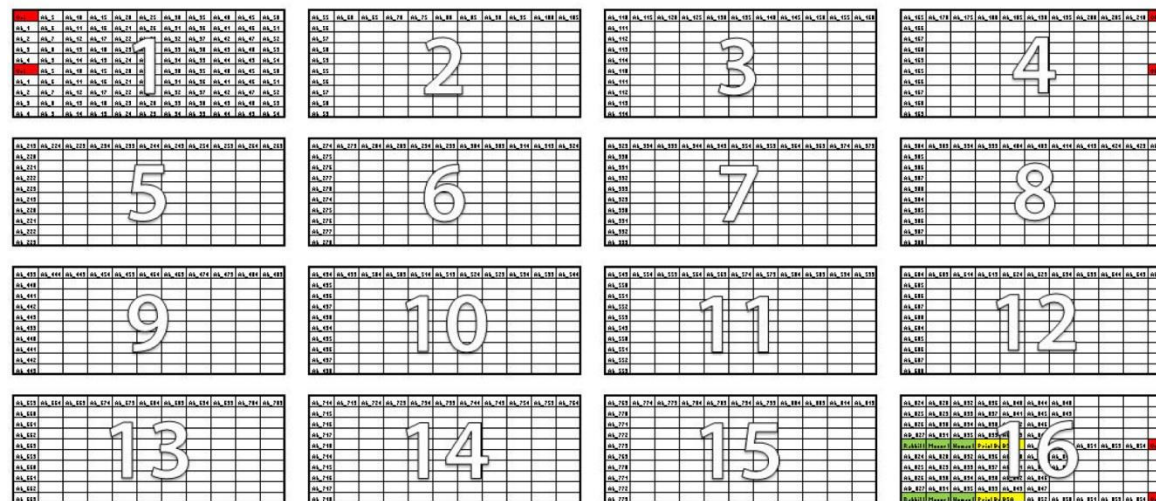
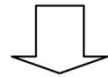
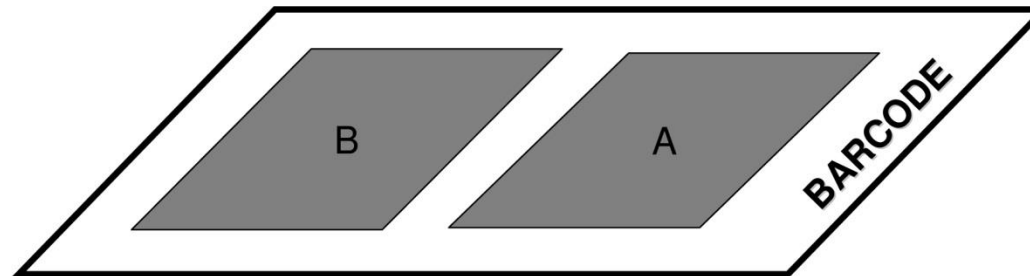


Figure 5-1: Diagram of protein microarray plate

5.3 Results

5.3.1 ECIS based initial attachment & spreading and migration assay

ECIS has been recognised as a synthetic cell function assay platform which relieves labour force and enables multiple functional assays in one experiment. Therefore, the adhesive and spreading as well as migratory ability of HaCaT and HECV SOCS-4 knockdown cells were tested using ECIS.

The initial attachment and spreading ability of HaCaT on gold electrode was attenuated by SOCS-4 knockdown, in comparison to respective control, and such trend was consistent over four hours following inoculation (1st to 3rd hour: $p < 0.01$, 4th hour: $p < 0.0001$; Figure 5-2 A). Moreover, at the 4th hour the HaCaT SOCS-4KD line showed 1897 ± 73 ohm average resistance change, representing 25% decrease compared to the HaCaT pEF6 line which had average resistance change of 2529 ± 194 ohm. Additionally, a similar trend was also found following the initial (1st hour: $p < 0.001$, 2nd to 4th hour: $p < 0.0001$) and the secondary (1st hour: $p < 0.001$, 2nd to 4th hour: $p < 0.0001$) electrical wounding, suggesting impaired migration of keratinocyte to the open gold electrode following SOCS-4 knockdown (Figure 5-2 B, C). Following the 1st electrical wounding, the average resistance change of HaCaT pEF6 and HaCaT SOCS-4KD were 2659 ± 65 ohm and 2173 ± 98 ohm respectively at the 4th hour, indicating 18% decrease following SOCS-4 knockdown. Furthermore, the 4th hour resistance change of HaCaT pEF6 and HaCaT SOCS-4KD were 2768 ± 110 ohm and 2021 ± 128 ohm respectively following the 2nd electrical wounding, displaying a 27% decrease in SOCS-4 deficient line.

However, contrasting results were observed in endothelial cells, indicating that SOCS-4 knockdown elevated the initial attachment and spreading of HECV on the gold electrode following cell seeding (1st to 4th hour: $p < 0.0001$; Figure 5-3 A). At the 4th hour following inoculation, the average resistance change of HECV

SOCS-4KD (4037 ± 1116 ohm) was 108% elevated compared to that of HECV pEF6 (1944 ± 482 ohm). In addition, the migration of HECV onto the open electrode was also enhanced by SOCS-4 deficiency following electrical wounding (1st to 4th hour: $p < 0.0001$; Figure 5-3 B), and such trend was also observed and validated following the second electrical wounding (1st to 4th hour: $p < 0.0001$; Figure 5-3 C). The average resistance change of HECV SOCS-4KD (4576 ± 837 ohm) was increased 116% compared to HECV pEF6 (2116 ± 622 ohm) at the 4th hour following the initial wounding, whereas such trend was enhanced as 172% at the 4th hour following the second wounding (HECV SOCS-4: 1948 ± 450 ohm vs HECV pEF6: 716 ± 195 ohm).

Taken together, SOCS-4 knockdown affected the initial attachment and spreading as well as migration of both keratinocytes and endothelial cells to gold electrode, albeit in an opposite manner.

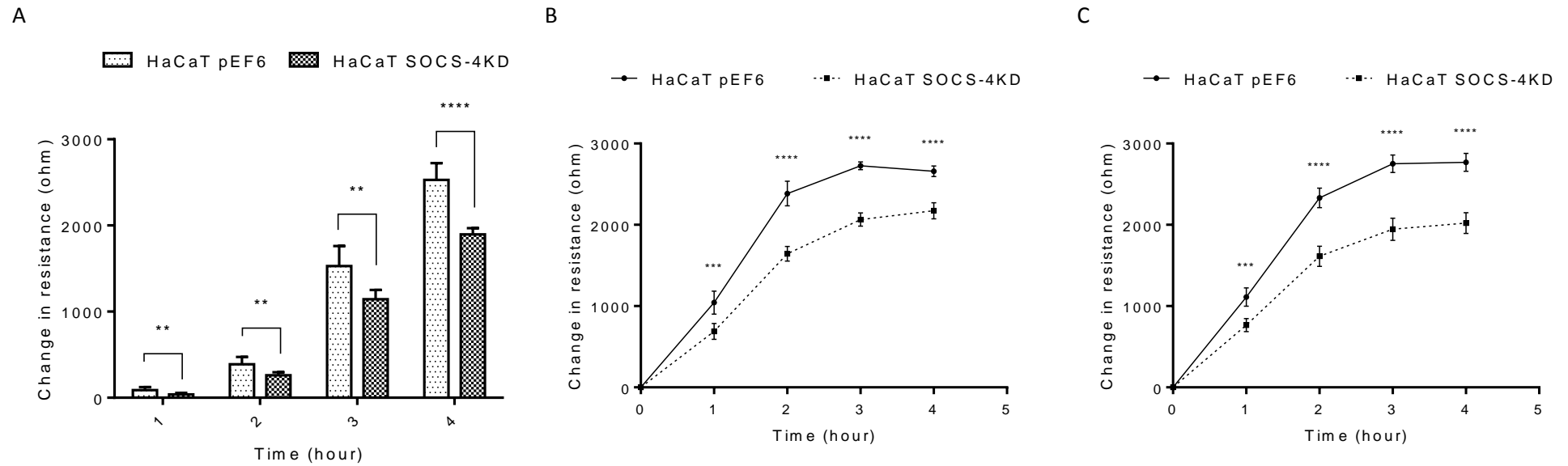


Figure 5-2: ECIS based initial adhesion and migration assay on SOCS-4 mutant HaCaT line

A. The resistance change at 4000Hz over the first four hours following inoculation; **B.** The resistance change at 4000Hz over the first four hours following the 1st electrical wounding; **C.** The resistance change at 4000Hz over the first four hours following the 2nd electrical wounding. (n=7; error bars represent standard deviation; representative data is shown; **: p < 0.01, ***: p < 0.001, ****: p < 0.0001).

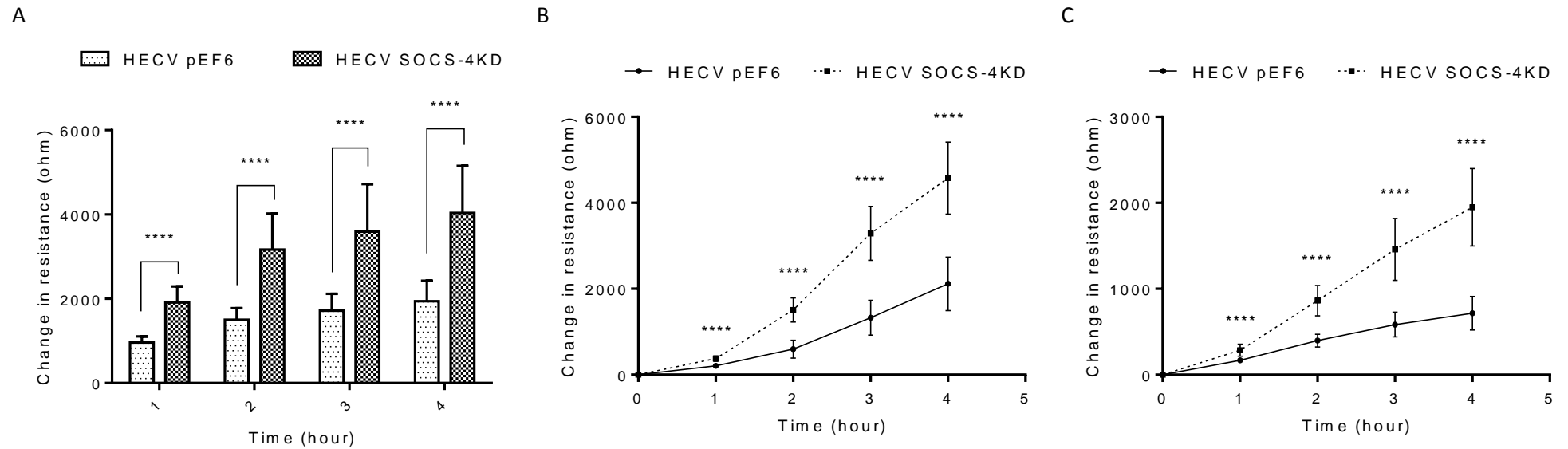


Figure 5-3: ECIS based initial adhesion and migration assay on SOCS-4 mutant HECV line

A. The resistance change at 4000Hz over the first four hours following inoculation; **B.** The resistance change at 4000Hz over the first four hours following the 1st electrical wounding; **C.** The resistance change at 4000Hz over the first four hours following the 2nd electrical wounding. (n=3; error bars represent standard deviation; representative data is shown; ****: p < 0.0001).

5.3.2 *In vitro* MTT cell adhesion assay

In vitro MTT cell adhesion assay was performed to determine if SOCS-4 affects the adhesive ability of HaCaT and HECV on matrigel matrix. Following 45 minutes incubation, the non-adherent cells were washed off, and the adherent viable cells were incubated in medium containing MTT for 4 hours to produce a purple coloured formazan product. Since the viable cell number corresponds to the amount of formazan product, following solubilisation with DMSO, the absorbance could be read and used to represent adherent cell numbers.

The *in vitro* MTT cell adhesion assay was repeated five times in HaCaT and HECV SOCS-4 knockdown cell models. The combined results from five repeats indicated that SOCS-4 knockdown did not significantly affect the adhesive ability of HaCaT, with only a 3% change in adherence noted ($p > 0.05$) whereas, the adhesion of HECV was decreased by 16% following the downregulation of SOCS-4 in comparison to control cells and this observation was found to be statistically significant ($p < 0.01$). (Figure 5-4)

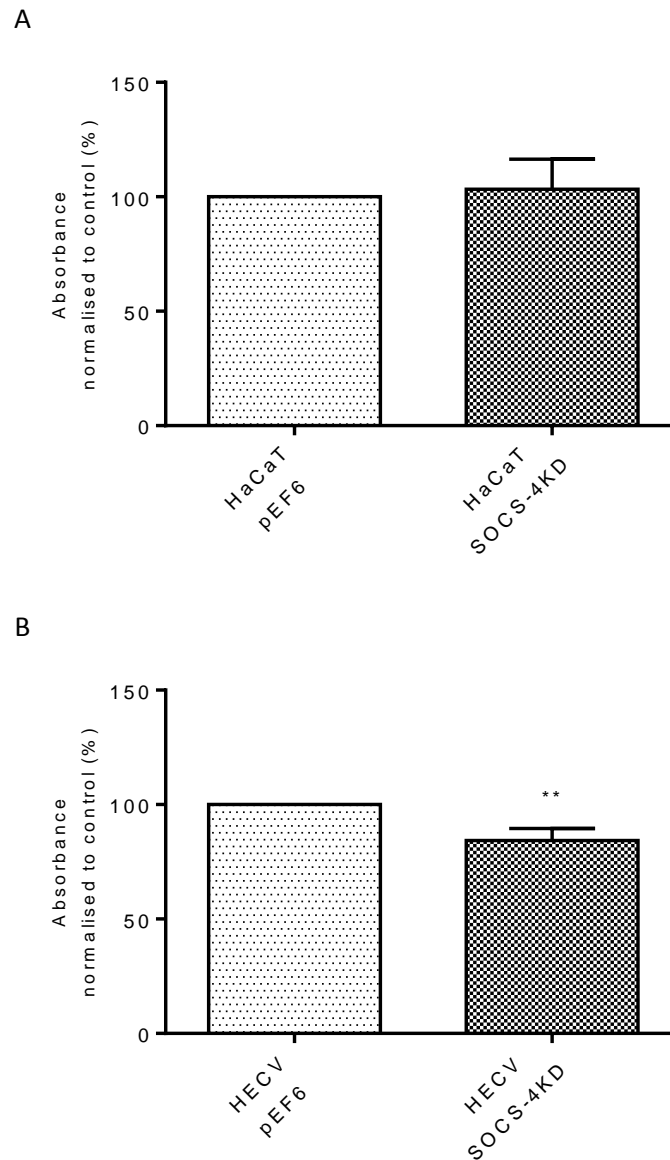


Figure 5-4: *In vitro* MTT cell adhesion assay on SOCS-4 mutant HaCaT and HECV lines

A. The absorbance, representing adherent HaCaT cell number, was analysed as a percentage against the control group in each repeat. Mean values are shown; **B.** The absorbance, representing adherent HECV cell number, was analysed as percentage against the control group in each repeat. Mean values are shown. (HaCaT, HECV: n=5; error bars represent standard error of the mean; **: $p < 0.01$)

5.3.3 *In vitro* MTT cell proliferation assay

In order to examine the impact of SOCS-4 knockdown on the proliferative ability of HaCaT and HECV cells, an *in vitro* MTT cell proliferation assay was conducted on the HaCaT and HECV SOCS-4 knockdown cell models.

SOCS-4 knockdown did not seem to influence the proliferative rates of the HaCaT cell line over a 3 or 5 day incubation. SOCS-4 knockdown resulted in a 8% increase at day 3 and a 6% decrease at day 5 in comparison to the HaCaT pEF6 control lines and neither change was seen to be statistically significant (Figure 5-5 A&B; $p > 0.05$). Similar SOCS-4 knockdown did not significantly influence the proliferative rates of HECV cells (day 3: 10% decrease; day 5: 2% decrease) in comparison to the HECV pEF6 control (Figure 5-5 C&D; $p > 0.05$)

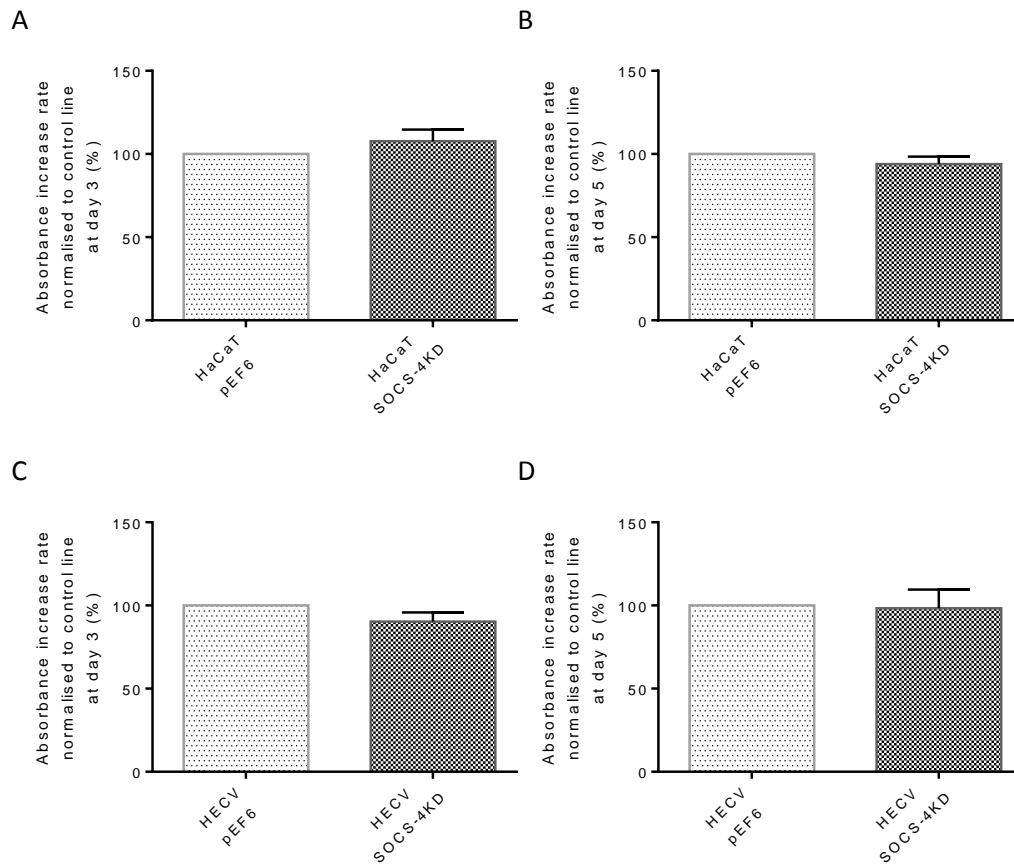


Figure 5-5: *In vitro* MTT cell proliferation assay on SOCS-4 mutant HaCaT and HECV lines

A. The proliferative rate of HaCaT cell on day 3 was analysed as percentage against the control group in each repeat. Mean values are shown; **B.** The proliferative rate of HaCaT cell on day 5 was analysed as percentage against the control group in each repeat. Mean values are shown; **C.** The proliferative rate of HECV cell on day 3 was analysed as percentage against the control group in each repeat. Mean values are shown; **D.** The proliferative rate of HECV cell on day 5 was analysed as percentage against the control group in each repeat. Mean values are shown. (n=5; error bars represent standard error of the mean)

5.3.4 *In vitro* cell migration assay (wound healing assay)

An *in vitro* wound healing assay was conducted to investigate the effect of SOCS-4 knockdown on HaCaT and HECV cells. The distance moved between two wound edges of wounded HaCaT pEF6 and HaCaT SOCS-4KD monolayers did not show any significant differences within the first eight hours ($p > 0.05$). However, starting from the 8th hour, the wound edges of HaCaT pEF6 began to migrate at a faster rate than that of HaCaT SOCS-4KD (8th hour to 10.5th hour: $p < 0.05$, 11th hour to 13th hour: $p < 0.01$), and such a trend was consistently significant until the 13th hour when at least one point of the two wound edges of HaCaT pEF6 met each other, with 91% of wound healed in general (Figure 5-6 A, B), whereas, the wound edges of HaCaT SOCS-4KD were still far from each other with only 57% wound healed (Figure 5-6 C). 15.5 hours following wounding, the wound front of HaCaT pEF6 was approximately closed, whereas, the wound of HaCaT SOCS-4KD remained open (Figure 5-6 B, C).

Similar trends were observed between HECV pEF6 and HECV SOCS-4KD though significant differences only appeared until the 12.5th hour following wounding ($p < 0.05$), and the wound of HECV pEF6 did not close within a 20 hour period when the experiment concluded (Figure 5-7 A, B). In addition, the wound of control line and SOCS-4 knockdown line were closed by 87% and 58% respectively at the 20th hour. Images captured at each critical time point (0, 12.5th and 20th hour) also demonstrated that the movement of the two wound edges of HECV pEF6 was faster than that of HECV SOCS-4KD at least between the 12.5th hour and the 20th hour following wounding (Figure 5-7 B, C).

In summary, downregulation of SOCS-4 decreased the migratory ability of epithelial cell by 34% at the 13th hour, and impaired the migration of endothelial

cell by 25% at 20th hour. Therefore, SOCS-4 knockdown attenuated the migration of both keratinocyte and endothelial cell.

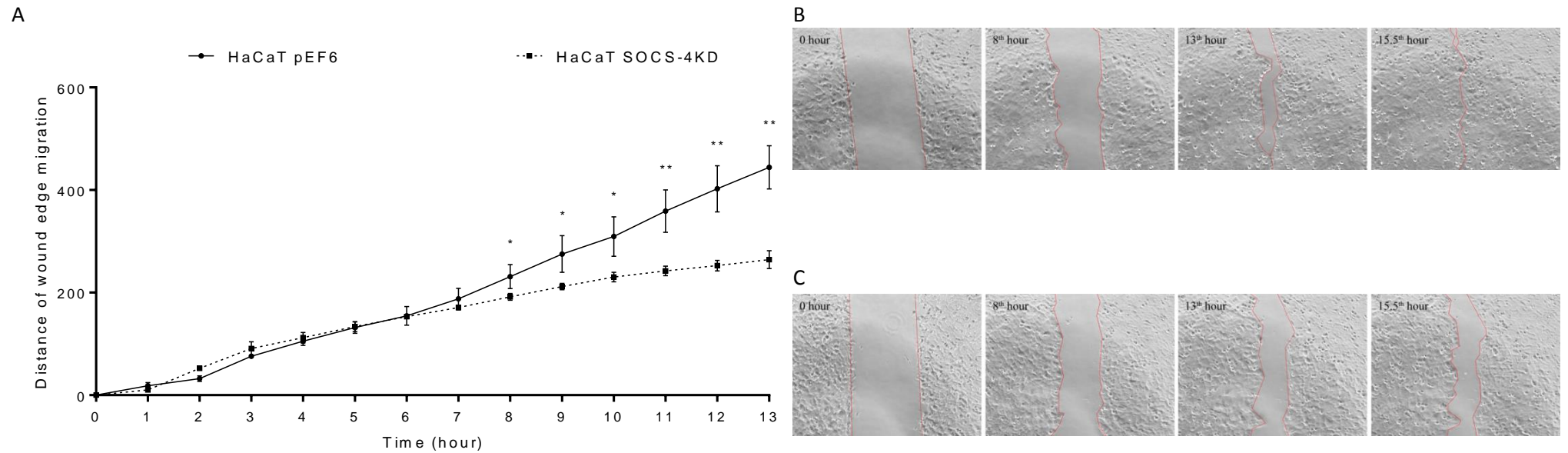


Figure 5-6: *In vitro* cell migration assay on SOCS-4 mutant HaCaT line

A. The distance migrated by wound edge at each hour are plotted on a line chart; **B.** Representative pictures of the wounded HaCaT pEF6 monolayer at the 0, 8th, 13th and 15.5th hour following wounding; **C.** Representative pictures of the wounded HaCaT SOCS4-KD monolayer at 0, 8th, 13th and 15.5th hour following wounding. (n=3, representative data is shown, error bars represent standard error of the mean; **: p < 0.01, *: p < 0.05; image was captured at X10 objective magnification; the red line indicates boundary of wound edge)

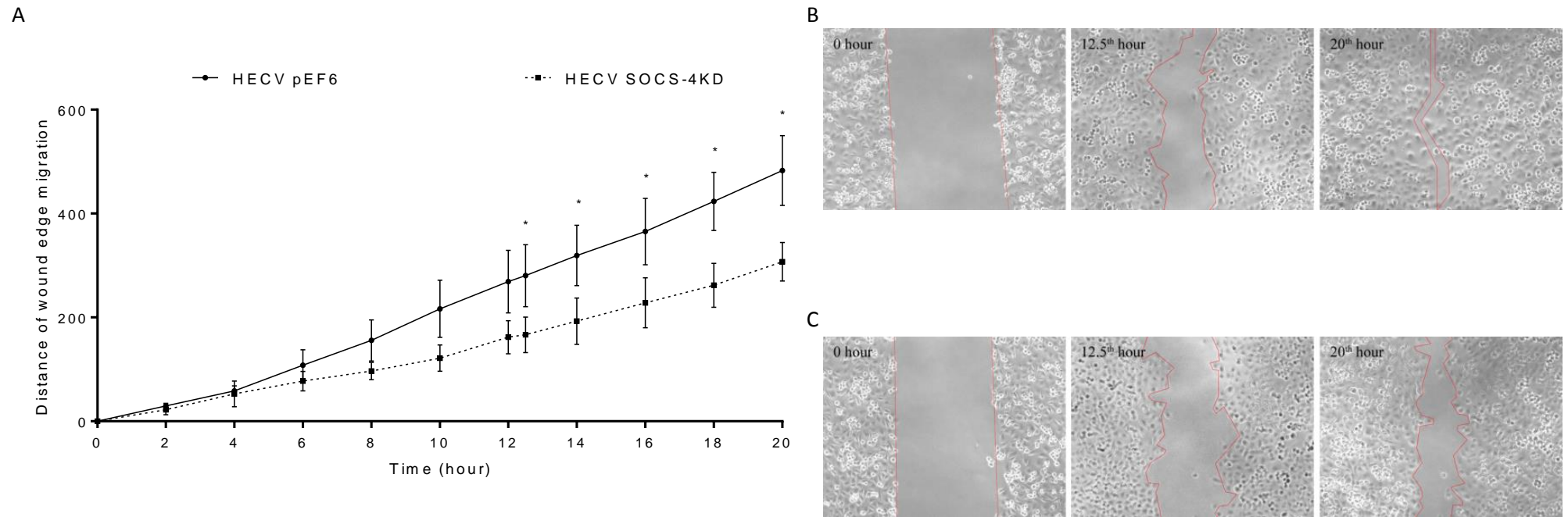


Figure 5-7: *In vitro* cell migration assay on SOCS-4 mutant HECV line

A. The distance migrated by wound edge at each two hours and at the 12.5th hour are plotted on a line chart; **B.** Representative pictures of the wounded HECV pEF6 monolayer at 0, 12.5th and 20th hour following wounding; **C.** Representative pictures of the wounded HECV SOCS4-KD monolayer at 0, 12.5th and 20th hour following wounding (n=3, representative data is shown, error bars represent standard error of the mean; *: p < 0.05; image was captured at X10 objective magnification; the red line indicates boundary of wound edge)

5.3.5 Tubule formation assay

An *in vitro* Matrigel tubule formation assay was conducted to explore the potential of SOCS-4 to impact on the microtubule formation capacity of HECV cells to investigate its potential to influence angiogenesis.

Two hours following inoculation, the control cells started to aggregate, showing the beginning of tube-like structures, whereas the SOCS-4 knockdown endothelial cells were more likely to cluster together. Furthermore, a general distribution of microtubule network with several complete tubes were obviously observed in the control line at the 4th hour, however, there was only a slight indication of tubule formation in the SOCS-4 knockdown cell at the same time point. This trend was more obvious over the next 6 hours until the conclusion of the experiment (Figure 5-8 A, B). After 10 hours of incubation, the number of tubules formed by the HECV SOCS-4KD line on matrigel matrix was much less compared to that of by HECV pEF6 according to the direct observation. In order to quantify this observed phenomenon, total perimeter, used as a quantification of total vessel coverage, was measured and compared between control and SOCS-4 knockdown lines. The total perimeter of the tubules formed by HECV SOCS-4KD was significantly less at the experimental end point (10 hours), representing a 31% decrease, than that of HECV pEF6 control line ($p < 0.01$; Figure 5-8 C). Therefore, SOCS-4 knockdown impaired the tubule formation ability of endothelial cells on matrigel matrix.

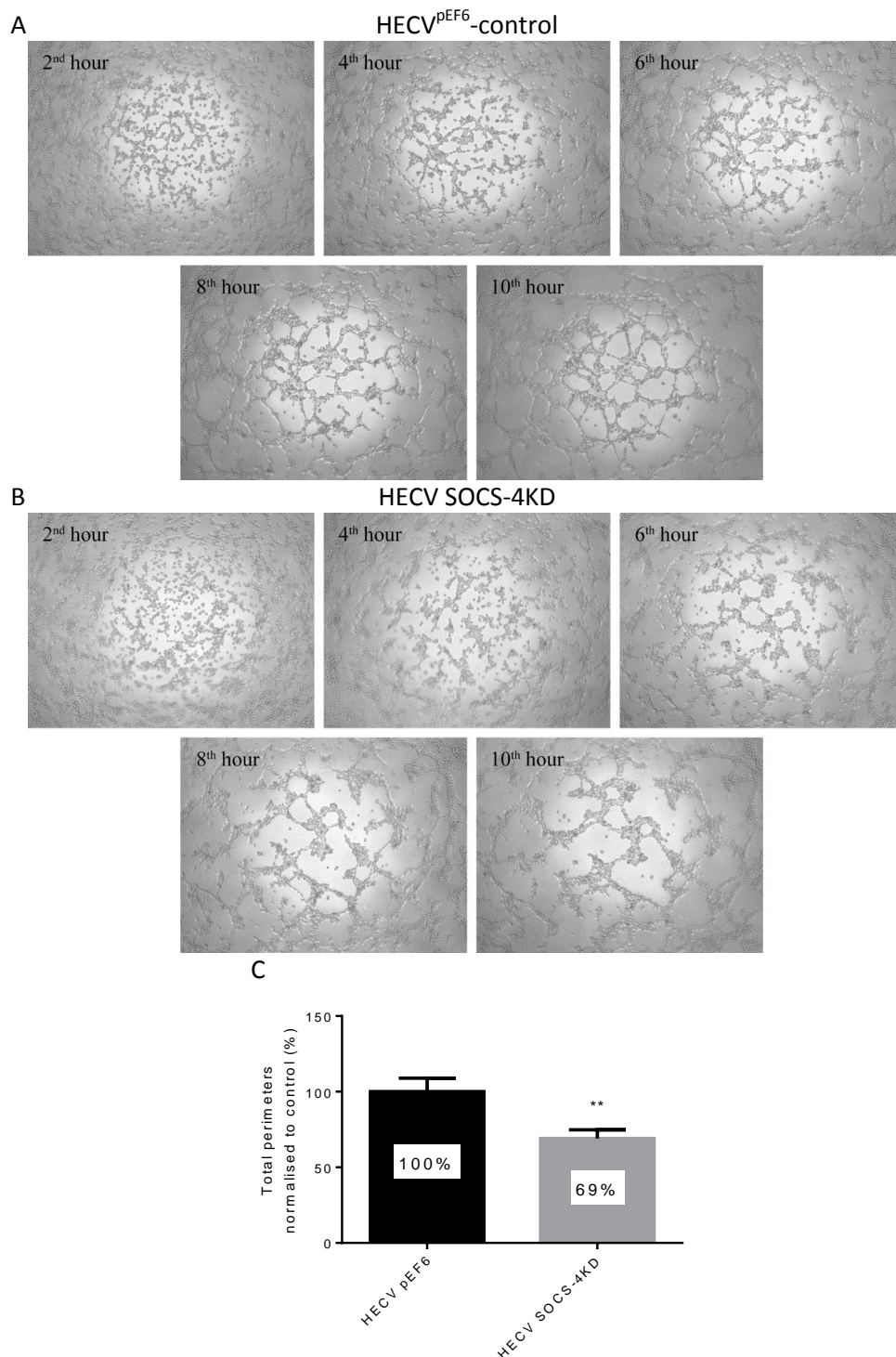


Figure 5-8: Tubule formation assay on SOCS-4 mutant HECV lines

A. Representative pictures of the formed tubules of HECV pEF6 at the 2nd, 4th, 6th, 8th and 10th hour; **B.** Representative pictures of the formed tubule of HECV SOCS-4KD at the 2nd, 4th, 6th, 8th and 10th hour; **C.** The perimeter of the formed tubules on each image at the experimental end point was manually traced and the total perimeter in pixels was quantified. The mean value was then calculated from the multiple replicates as the total average perimeter before being normalised to the value of the control line. Images were captured at X5 objective magnification. (n=3; representative data is shown; error bars represent standard deviation; **: p < 0.01)

5.3.6 Potential downstream signalling investigation

To explore global signalling event in HaCaT cells following SOCS-4 knockdown, a protein array analysis was carried out on the Kinexus850 platform (please refer to section 2.16 of Chapter II and section 5.2.3 of Chapter V). The array includes over 850 antibodies that recognise both total protein and phospho-proteins of a rather number of signalling proteins. Figure 5-9 shows a representative images from the array.

The results from the KinexusTM antibody microarray indicated that there were thirteen protein candidates which demonstrated a significantly decreased levels of phosphorylation following HaCaT SOCS-4 knockdown (Figure 5-10 A). One of the most significant changes was focal adhesion kinase (FAK) (Figure 5-10 B, C, D).

In the light of the significant role of FAK in cell signalling, matrix adhesion and cell migration, further investigation was focused on the verification of the protein expression level of total FAK and its phosphotyrosine site 397 (FAK Y397) between HaCaT pEF6 and HaCaT SOCS-4KD as this may be a key molecule governing the effects brought about by SOCS-4 suppression. It was found that downregulation of SOCS-4 correlated with the increase of total FAK and the decrease of FAK Y397 (Figure 5-11 A, B). Interestingly, the expression of SOCS-4 and FAK Y397 demonstrated similar expression pattern following the semi-quantitative analysis (Figure 5-11 C, D, E).

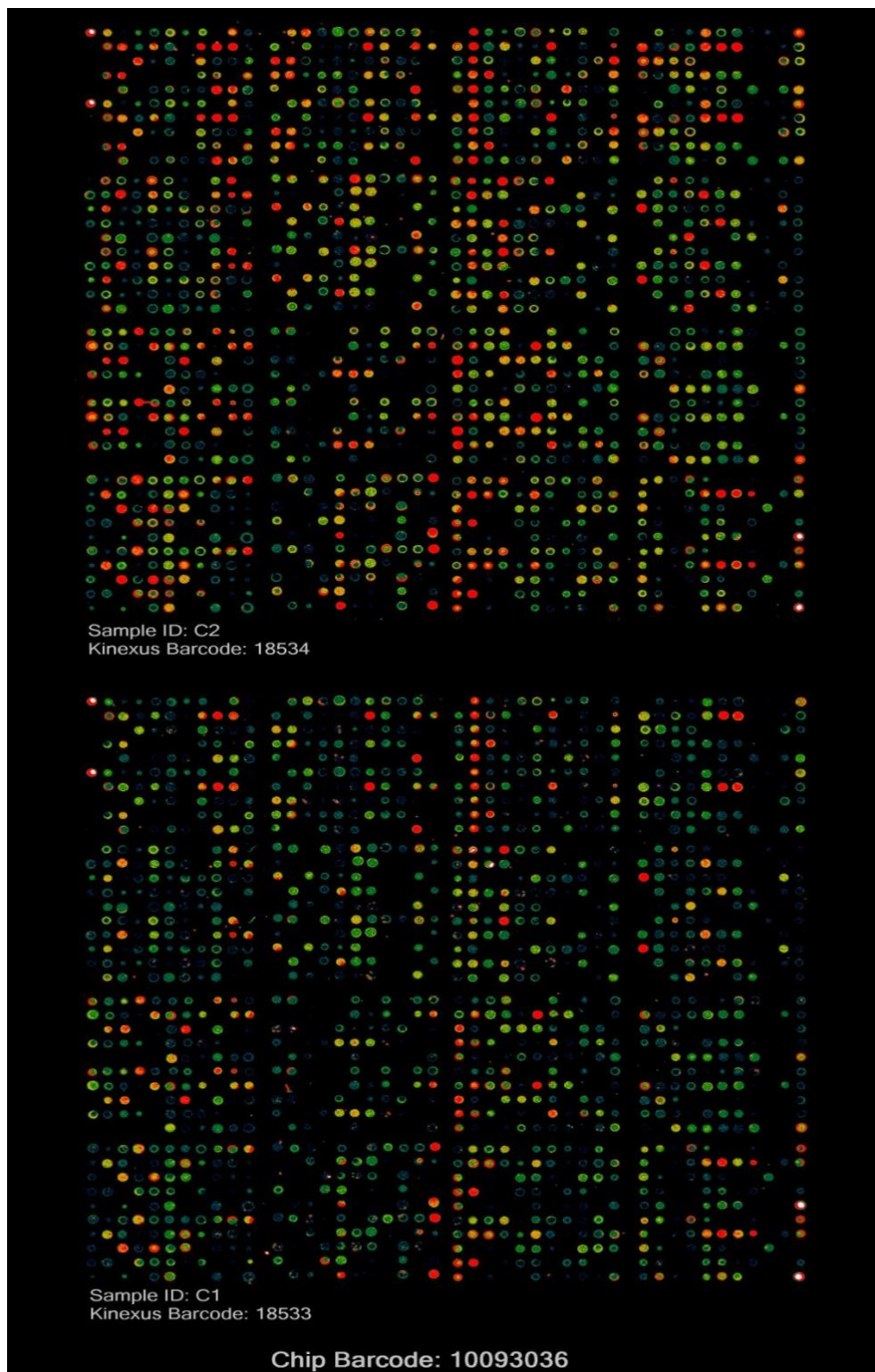


Figure 5-9: Kinexus 850 images in comparing proteins from HaCaT pEF6 (bottom, C1) and HaCaT SOCS-4KD (top, C2) cells.

The protein expression level correlates with the signal intensity. Different colours represent different signal intensity and decreasing signal intensity corresponds with a red to orange to yellow to green to blue transition.

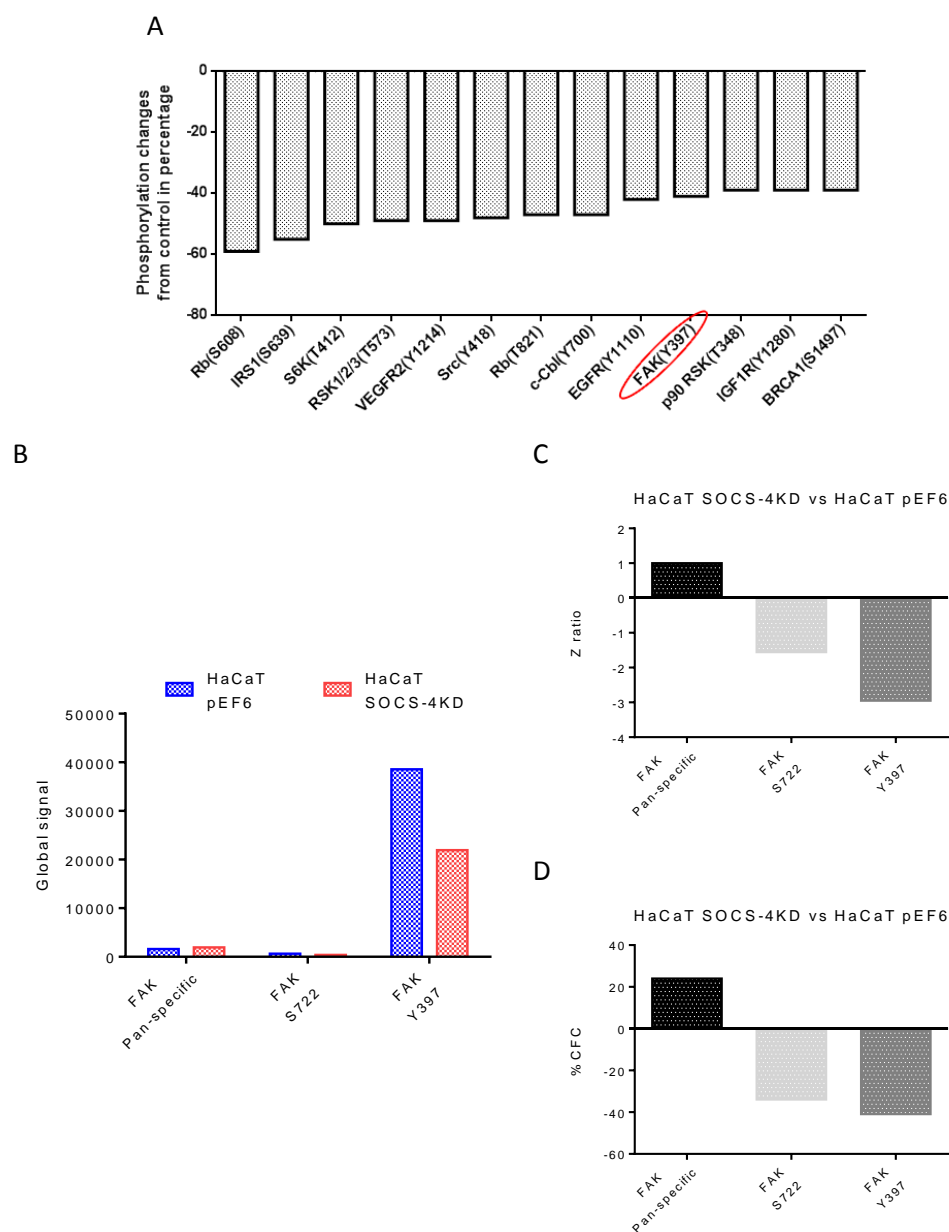


Figure 5-10: Investigation of potential molecular significance in HaCaT SOCS-4 mutant line

A. Significant protein phosphorylation decreases were seen in HaCaT SOCS-4KD compared to HaCaT pEF6 by the Kinexus™ antibody microarray. The red circle indicates the molecule chosen to be further investigated; **B, C, D.** The magnitude changes of FAK in the two cell models. Global signal of the respective protein (**B**), the Z ratio (**C**) and %CFC (**D**) of the respective protein.

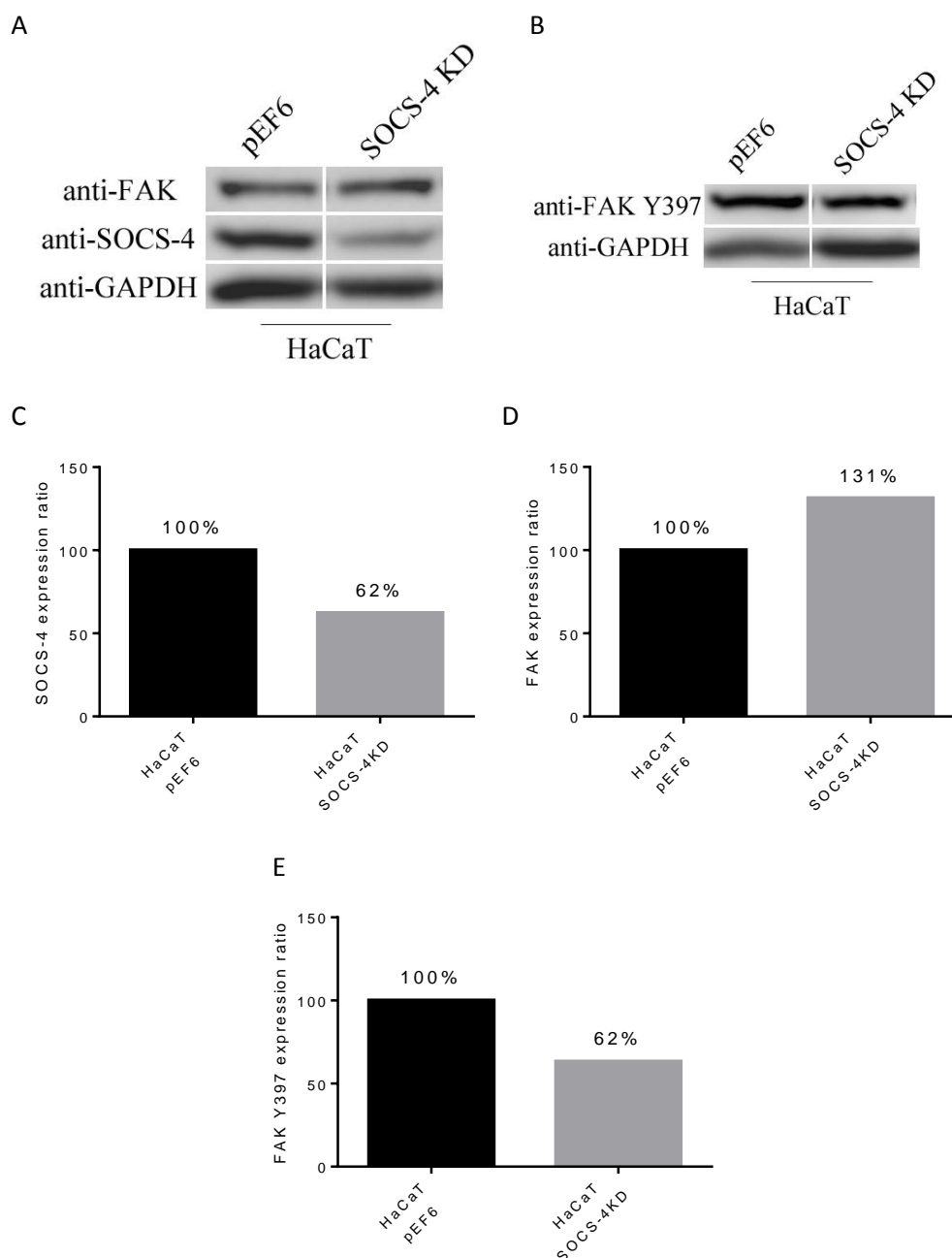


Figure 5-11: Investigation of potential downstream signalling events in HaCaT SOCS-4 mutant line

A, B. Western blotting verification on the protein expression level of SOCS-4, FAK and FAK Y397 in protein extracts from HaCaT pEF6 and HaCaT SOCS-4KD (n=1) **C, D, E.** Semi-quantitative analysis undertaken by Image J v1.50c on the western blotting results, the expression ratio is indicated as percentage control and plotted in bar charts.

5.4 Discussion

Keratinocytes are one of the pivotal cell types involved in the wound healing process, primarily exerting their function on re-epithelialisation. After activation, keratinocytes alter integrin expression to enable their migration over the wound bed and produce cytokines and chemokines to recruit and activate other cells to benefit the healing process (Pastar et al., 2008). Vascular endothelial cells are another important cell type involved in angiogenesis. The migration and proliferation of the activated vascular endothelial cell along with the interaction between ECM and such cell type contribute to neovascularisation and the formation of a vascular network in order to meet the significant increase in oxygen and nutrient requirement for local cell metabolism (Senger and Davis, 2011, Clark, 1996). Therefore, cell functional assays were conducted following the generation of HaCaT and HECV SOCS-4 knockdown mutant cell lines by ribozyme transgene to further investigate the potential effect of SOCS-4 to the behaviour of these critical cell types during the wound healing process.

The ECIS based initial attachment and spreading assay and migration assay demonstrated that the downregulation of SOCS-4 suppressed both HaCaT initial attachment and spreading as well as migratory ability to the gold electrode approximately 25%, whereas elevated initial attachment and spreading as well as migration were found in HECV SOCS-4 knockdown mutant lines, accounting for more than two times to the control line. This may imply that SOCS-4 potentially plays different roles in regulating adhesion, spreading and migration of HaCaT and HECV cells on gold electrode. Additionally, in contrast to the ECIS based initial adhesion assay, the MTT matrigel adhesion assay indicated that SOCS-4 knockdown had no effect on HaCaT cell matrigel adhesive ability, whereas the adhesive ability of HECV to the matrigel matrix was decreased by the

downregulation of SOCS-4. Such a discrepancy may account for the variant adhesive ability of HaCaT and HECV lines to the different matrix surface in the above two methodologies since different substratum matrix has been proved to modulate the expression profile of integrin differently, leading to altered cell morphology and adhesive ability (Delcommenne and Streuli, 1995). Again, the data suggests that SOCS-4 may differentially impact adhesion and spreading dependent on cell type and matrix conditions.

The results from the MTT proliferation assay indicated that SOCS-4 knockdown did not affect the cell proliferation within 5 days in both HaCaT and HECV lines. Whilst there is little data currently available as to SOCS-4's role in proliferation in wound healing models, a previous study, focusing on IL-23, miRNA-25 and SOCS-4 in thyroid cancer has suggested that SOCS-4 expression brought about minimal impact on cell growth in this model system (Mei et al., 2015). Hence, the observed effect in HaCaT and HECV cell lines appears to be in line with the limited data available within the literature.

The results from the scratch assay (cell migration assay) showed that the cell migration rates of HaCaT and HECV was not significantly affected by SOCS-4 knockdown at the initial migratory stage. Such results were again different from that seen in the ECIS based migration assay, which showed significant difference between the control and SOCS-4 mutant lines at the first hour following cell seeding. Such a discrepancy may be due to the different sensitivity of the measurement between the two methods or the variant migratory behaviour of the cells to different matrix surface. Together, both ECIS and EVOS scratch methodologies demonstrate a role for SOCS-4 in regulating keratinocyte and endothelial cell migration, though these do contrast between ECIS and EVOS in terms of the HECV cell line and time following wounding before this trait

demonstrates significance. The previously mentioned *in vitro* study on thyroid cancer cell lines demonstrated that SOCS-4 negatively regulated IL-23 induced cell migration, and such effect could be diminished by the presence of microRNA-25 through targeting the 3'-UTR of *SOCS-4* (Mei et al., 2015). The discrepancy of the cellular impact of SOCS-4 between this study and the findings presented here may be due to the variant downstream effect of SOCS-4 in different cell types, suggesting multiple regulatory roles of SOCS-4 in different cellular microenvironments.

The tubule formation assay on the HECV pEF6 and HECV SOCS-4KD lines indicated that SOCS-4 knockdown potentially decreased tubule formation by endothelial cell on matrigel matrix, and increased the cell-cell and cell-membrane attachment. Again, this observation seems more in line with the EVOS migration results, with such a negative impact on migration and tubule formation linking reduced SOCS-4 levels with a poor angiogenic response and again potentially implicating SOCS-4 in the wound healing process.

In order to further clarify the role of SOCS-4 and to identify potential mechanisms which bring about its observed functional effects a protein microarray was undertaken to compare control HaCaT and SOCS-4 knockdown HaCaT cell lines. This initial data has highlighted a number of molecules of interest which may aid in the explanation of the functional characterisation of SOCS-4 knockdown cell lines.

The screening of protein changes between HaCaT control line and HaCaT SOCS-4 deficient line showed a decrease of FAK Y397 was apparent following the downregulation of SOCS-4, indicating the potential effect of SOCS-4 on FAK activation. FAK Y397 is a key auto phosphorylation site which is able to be activated by many stimulus (such as integrin binding) and contributes to various

downstream signalling cascades including cell migration (Zhao and Guan, 2011). It has been documented that FAK activation promoted the migratory ability of keratinocyte during wound healing (Gates et al., 1994). In addition, decreased Src activation on Y418 was observed in the protein array results in this study. Previous studies indicated that Src activation requires FAK Y397 activation, and a well characterised pathway that FAK modulate cell migration is through the interaction of FAK/Src complex and p130cas (Cary et al., 1996, Cary et al., 1998). Taken together, a potential mechanism of the attenuated migration of SOCS-4 deficient HaCaT in wound healing assay in this chapter may due to the suppression of FAK/Src/p130cas pathway by the reduced FAK Y397 activation following SOCS-4 knockdown. Moreover, EGFR phosphorylation on Y1110 was also found reduced in the SOCS-4 knockdown keratinocytes. As previously described in the literature, the ligand binding, and subsequent activation of EGFR modulates a variety of keratinocyte functions (Schneider et al., 2008). Amongst the seven ligands of EGFR, heparin-binding EGF-like growth factor (HBEGF) has been demonstrated in promoting keratinocyte migration (Shirakata et al., 2005). Therefore, together with the result from wound healing assay in this chapter, decreased keratinocyte migration could potentially be explained as SOCS-4 deficiency reduced HBEGF production by keratinocyte, which in turn decreased EGFR activation. A previous study has also demonstrated that IGF-1 facilitated keratinocyte membrane protrusion and spreading, two prerequisite of cell migration, through stimulating PI3K (Haase et al., 2003). Given that the decreased IGF1R activation in SOCS-4 knockdown keratinocytes seen in the protein array and the reduced migration of SOCS-4 deficient HaCaT in wound healing assay, SOCS-4 may also potentiate IGF-1 signalling to improve keratinocyte migratory ability through the maintenance of PI3K activation. Furthermore, another growth factor

receptor, VEGFR-2, has been documented to be expressed in both HaCaT and a human primary keratinocytes and *in vitro* work on these two cell lines indicated that VEGFR-2 phosphorylation by VEGF stimulation could induce the migration of keratinocyte (Man et al., 2006, Yang et al., 2006). Therefore, based on the results of decreased phosphorylation of VEGFR-2 Y1214 from protein array and the decreased migration of keratinocyte following SOCS-4 knockdown from the wound healing assay, it is feasible that SOCS-4 could maintain the activation of VEGFR-2 to promote keratinocyte migration. Interestingly, a tumour suppressor protein BRCA1 was observed to have reduced phosphorylation of S1497. BRCA1 has been documented to negatively regulate cell proliferation (Holt et al., 1996, Randrianarison et al., 2001). However, *in vivo* study on epithelial tissue BRCA-1 conditional knockdown mice demonstrated that decreased activation of BRCA-1 rendered epidermal hyperproliferation and also enhanced cell apoptosis in epidermis, thus no obvious histological difference was observed (Berton et al., 2003). This again seems in line with the data obtained in this chapter suggesting SOCS-4 does not impact HaCaT cell proliferation.

In summary, the presence of SOCS-4 potentially has positive effects on the adhesion of HECV on matrigel matrix, whereas it has non-significant effects on this trait within the HaCaT cell line. Moreover, SOCS-4 may affect the adhesive ability of HaCaT and HECV to different matrix surface.

SOCS-4 also holds the potential to regulate HaCaT and HECV migration. Furthermore, SOCS-4 exhibited no significant effect on the growth of HaCaT and HECV cells. Therefore, the functional analysis of SOCS-4 mutant lines indicates a role for such molecule in a number of key traits associated with wound healing, this chapter also raises a number of interesting downstream signalling

mechanisms which may account for some of the functional observations following SOCS-4 knockdown.

Chapter VI

Functional significance of SOCS-3exp on HaCaT and HECV models

6.1 Introduction

SOCS proteins are a family of intracellular proteins containing eight members (Alexander, 2002) and were primarily found to exert their function as negative regulators of cytokine induced JAK-STAT signalling (Crocker et al., 2008a). Furthermore, several studies have suggested the involvement of SOCS-3 in components of wound healing. SOCS-3 deficient mice expressed a lethal inflammatory phenotype, suggesting its regulatory role in the inflammation response (Crocker et al., 2012) which is an essential stage in wound healing. This is in agreement with another study that indicated the exacerbated inflammation was related to the overexpression of SOCS-3 (Linke *et al.*, 2010a) further supporting a role for SOCS-3 in wound healing. However, the downstream mechanism of how SOCS-3 modulates wound healing still remain unclear.

Based on the q-PCR screening results obtained from the chronic wound biopsies in Chapter III, significantly higher gene expression levels of SOCS-3 was observed in non-healing chronic wound biopsies compared to that in the healing/healed ones, suggesting that the elevated SOCS-3 gene expression on wound site correlated with poor healing results. However, whilst this differential expression of SOCS-3 was not seen in the IHC staining of healing and non-healing chronic wounds, this data is in line with a study using SOCS-3 overexpression mouse model in a primary epithelial cell line, which demonstrated that the upregulation of SOCS-3 attenuated keratinocyte migration, contributing to impaired healing (Linke et al., 2010b). Moreover, according to the IHC screening on chronic wound biopsies in chapter III, SOCS-3 was found not only extensively expressed in all layers of keratinocytes of the epidermis, but in the surrounding blood vessels in dermis in all positive stained chronic wounds. Thus, SOCS-3 may also play some role in regulating endothelial cell function.

Therefore, it is of interest to further investigate the role of SOCS-3 in the human keratinocyte (HaCaT) and endothelial (HECV) cell model systems, as they represent two key cell types involved in wound healing and to explore the functional relevance of this molecule in conjunction with the clinical data. The PCR results presented in Chapter IV indicated no SOCS-3 expression in these two cell lines. Therefore, SOCS-3 coding sequence was incorporated into a vector and transfected into the two cell lines to generate SOCS-3 expression cell model, and the expression efficiency was verified by RT-PCR, q-PCR and western blotting (as described in Chapter IV). In this Chapter, functional assays were conducted on keratinocyte and endothelial SOCS-3 expression cell models.

6.2 Methods and materials

6.2.1 *In vitro* crystal violet matrigel adhesion assay

In order to enable the image capture to diversify the data presentation, another robust and reproducible methodology, crystal violet staining, was utilised instead of MTT for the cell adhesion assay on the SOCS-3exp cell models. The crystal violet staining method was originally conducted to evaluate the cytotoxic effects of chemicals due to the linear relationship between the absorbance of the stained cells and cell number (Saotome et al., 1989) and was later verified to be an alternative method to MTT assay (Chiba et al., 1998). The preparation of the matrigel matrix plate and the cell seeding density was as outlined in section 2.18.3 in chapter II.

Cells were seeded on the SFM rehydrated matrigel matrix that were prepared in six replicates and the plate was incubated at 37.0°C, 5% CO₂ and 95% humidity for 45 minutes. Subsequently, the plate wells were washed with 100µl of PBS three times to remove nonadherent cells. The adherent cells were then fixed in 100µl of 4% formalin for at least 15 minutes before being stained with 100µl of 1% crystal violet for at maximum of 15 minutes. The crystal violet was removed by gentle inversion of the plate, and was gently washed under a slow tap water flow. The plate was then placed in a fume cabinet until dried completely. Images were then captured for each well at X5 objective magnification using a Leica DMI1 microscope equipped with a MC120 HD camera and Leica Application Suite version 3.0.0 software (Leica Microsystems, Milton Keynes, UK) before the addition of the 10% acetic acid. The plate was tapped gently to enable the crystal violet to dissolve thoroughly.

The absorbance of each well was detected at 540nm using ELx800 plate reading spectrophotometer (Bio-Tek, Wolf laboratories, York, UK). Initial cell

adhesion in each well was determined by the absorbance. Experiments were repeated a minimum of three times.

6.2.2 Statistical analysis

Statistical analysis was undertaken using the SigmaPlot 11 and Graphpad Prism 6 statistical software packages. Data was analysed using t-test or Mann Whitney test, depending on data parameters. Values of $p < 0.05$ (*), $p < 0.01$ (**), $p < 0.001$ (***) and $p < 0.0001$ (****) were regarded as statistically significant.

6.3 Results

6.3.1 ECIS based initial attachment & spreading assay and migration assay

ECIS was performed to evaluate the impact of SOCS-3 expression on the initial attachment and spreading as well as migration of HaCaT and HECV.

As shown in Figure 6-1, the initial attachment and spreading of keratinocytes on gold electrode was elevated by SOCS-3 expression starting from the 1st hour ($p < 0.01$) and such effect was consistent until the 4th hour. At the 4th hour following inoculation, the average resistance change of HaCaT SOCS-3exp was 1854 ± 297 ohm, 103% elevated compared to that of HaCaT pEF6 which was 910 ± 203 ohm. (2nd hour: $p < 0.01$, 3rd hour: $p < 0.001$, 4th hour: $p < 0.0001$; Figure 6-1 A). In addition, increased migration over the open gold electrode was observed in the SOCS-3 expression HaCaT cell line in comparison to the control line over the 4 hours following the 1st electrical wounding, with highly significant differences noted. The average resistance change of HaCaT SOCS-3exp (2476 ± 252 ohm) was enhanced 86% compared to HaCaT pEF6 (1328 ± 430 ohm) at the 4th (1st and 2nd hour: $p < 0.0001$, 3rd and 4th hour: $p < 0.001$; Figure 6-1 B). Moreover, similar trends were seen following the 2nd electrical wounding, where SOCS-3 expression enhanced the migratory ability of HaCaT over the open gold electrode. At the 4th hour, the average resistance change of HaCaT SOCS-3exp (1701 ± 228 ohm) was 40% greater than that of HaCaT pEF6 (1218 ± 239 ohm) (1st to 4th hour: $p < 0.05$; Figure 6-1 C).

Interestingly, distinct from the results seen in keratinocyte, SOCS-3 expression in HECV cells did not affect the initial attachment and spreading on the gold electrode (1st to 4th hour: $p > 0.05$; Figure 6-2 A). However, similar to the HaCaT cell line, SOCS-3 expression resulted in an enhanced migration of HECV cells across the open gold electrode following both the initial (1st hour: $p < 0.001$,

2nd to 4th hour: $p < 0.01$) and secondary (1st and 2nd hour: $p < 0.0001$, 3rd and 4th hour: $p < 0.001$) electrical woundings (Figure 6-2 B, C). Following the 1st electrical wounding, the average resistance change of HECV pEF6 and HECV SOCS-3exp were 1683 ± 167 ohm and 2662 ± 646 ohm respectively at the 4th hour, 58% displaying enhancement following SOCS-3 expression. Furthermore, the 4th hour resistance change of HECV pEF6 and HECV SOCS-3exp were 741 ± 165 ohm and 2583 ± 650 ohm respectively following the 2nd electrical wounding, indicating a 248% elevation in the SOCS-3 expression line.

Therefore, SOCS-3 expression only increased the initial attachment and spreading of keratinocytes on the gold electrode, whereas the migratory ability of both keratinocytes and endothelial cells across the gold electrode were elevated by the expression of SOCS-3.

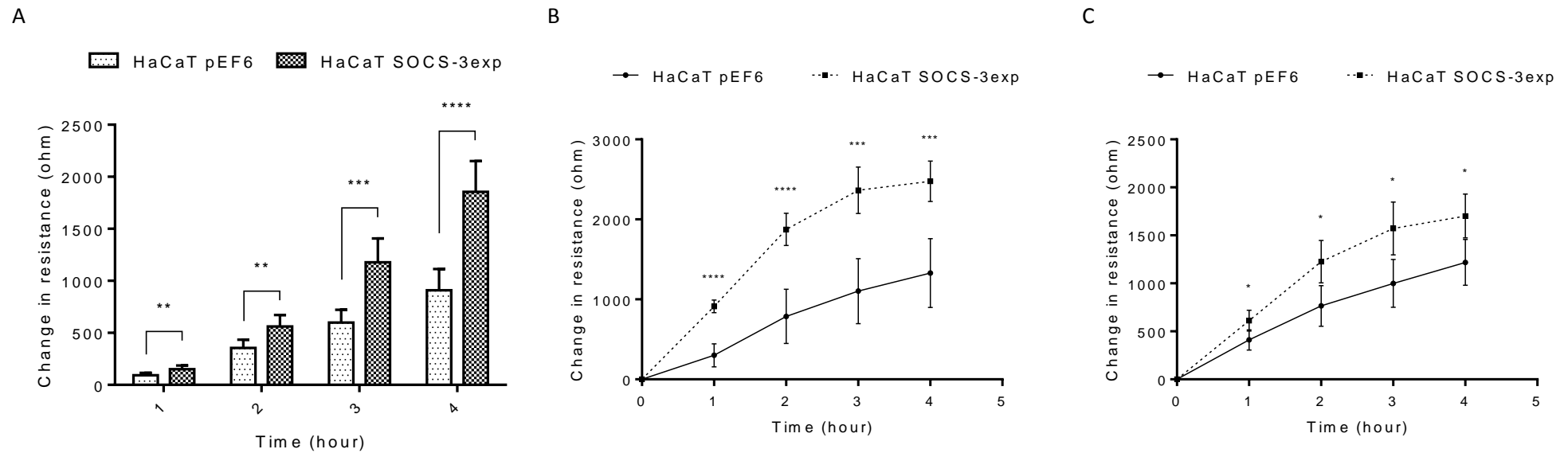


Figure 6-1: ECIS based initial adhesion and migration assay on SOCS-3 mutant HaCaT line

A. The resistance change at 4000Hz over the first four hours following inoculation; **B.** The resistance change at 4000Hz over the first four hours following the 1st electrical wounding; **C.** The resistance change at 4000Hz over the first four hours following the 2nd electrical wounding. (n=4, representative data is shown, error bars represent standard deviation; *: p < 0.05, **: p < 0.01, ***: p < 0.001, ****: p < 0.0001)

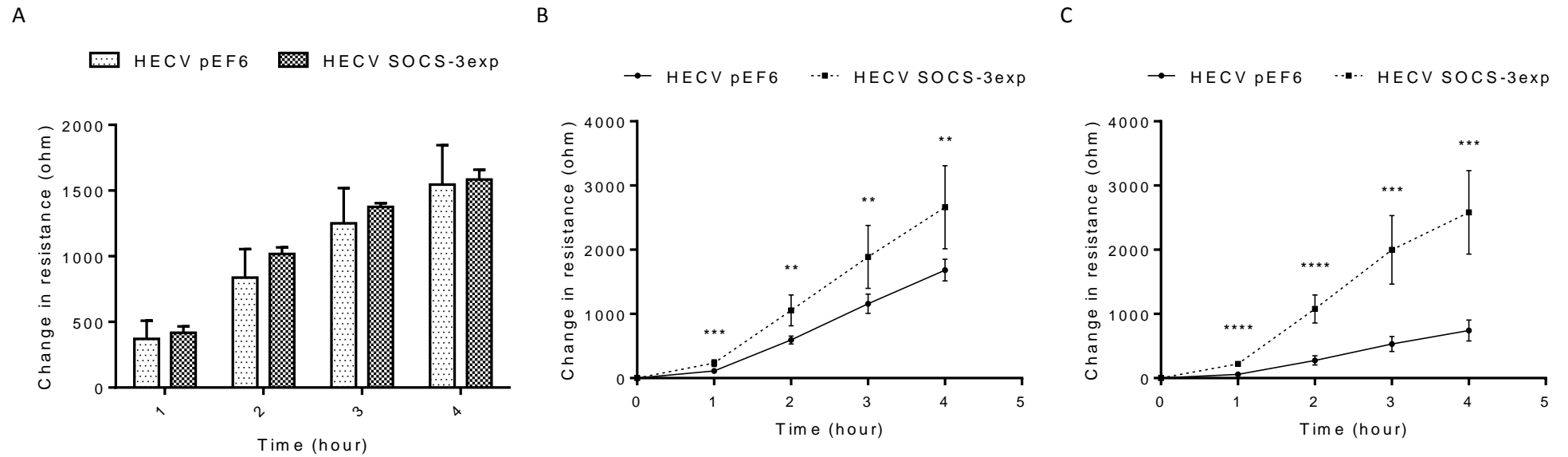


Figure 6-2: ECIS based initial adhesion and migration assay on SOCS-3 mutant HECV line

A. The resistance change at 4000Hz over the first four hours following inoculation; **B.** The resistance change at 4000Hz over the first four hours following the 1st electrical wounding; **C.** The resistance change at 4000Hz over the first four hours following the 2nd electrical wounding. (n=4, representative data is shown, error bars represent standard deviation; **: p < 0.01, ***: p < 0.001, ****: p < 0.0001)

6.3.2 *In vitro* crystal violet matrigel adhesion assay

Crystal violet staining assay was utilised to test if SOCS-3 expression affects the adhesive ability of keratinocyte and endothelial cells to matrigel matrix.

Analysis of the independent repeats indicated that SOCS-3 expression in HaCaT cell lines had little impact on cell matrigel matrix attachment with only a % difference noted between control and expression groups, which was not found to be statistically significant ($p > 0.05$; Figure 6-3 A). This is also apparent from the representative images, again suggestive that there was very little change in matrix attachment between control and SOCS-3 expression HaCaT cells (Figure 6-3 B, C). However, SOCS-3 expression in HECV endothelial cells was found to significantly enhance cell matrigel matrix adhesion and resulted in a 48% increase in adherent cell numbers ($p < 0.05$; Figure 6-3 D), a trend which was again apparent from the representative images (Figure 6-3 E, F). Hence, the data suggests that SOCS-3 expression elevated the adhesion of endothelial cell to matrigel matrix but had no effect on the adhesive ability of keratinocyte to the same matrix substratum.

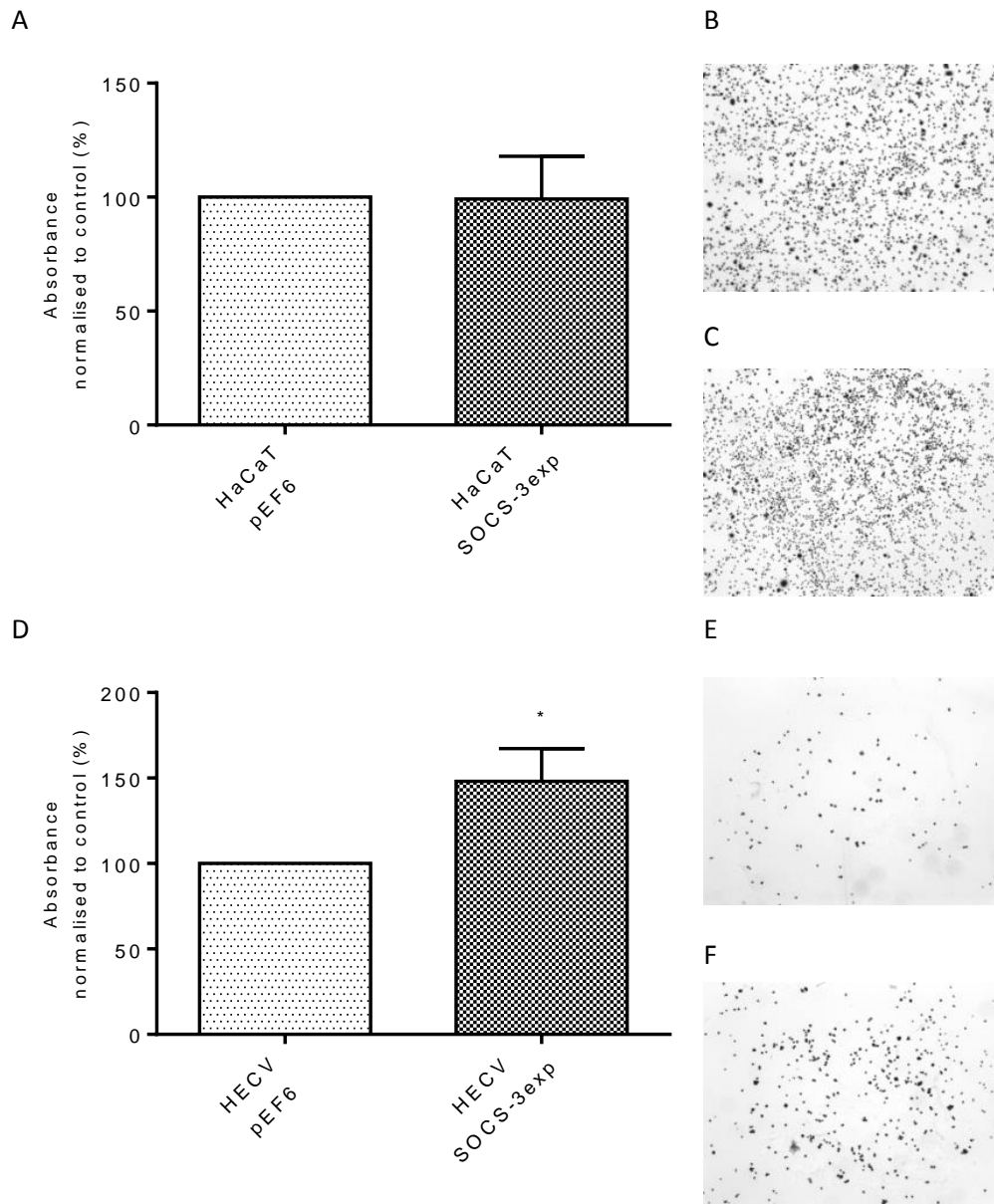


Figure 6-3: Crystal violet matrigel adhesion assay on SOCS-3 mutant HaCaT and HECV lines

A, The absorbance, representing adherent HaCaT cell number, was transformed into percentage against control group in each repeat. The mean value was calculated and plotted in a bar chart; **B**, **C**. Representative images captured for HaCaT pEF6 and HaCaT SOCS-3exp lines respectively following the crystal violet staining; **D**. The absorbance, representing adherent HECV cell number, was transformed into percentage against control group in each repeat. The mean value was calculated and plotted in a bar chart. **E**, **F**. Representative image captured on the HECV pEF6 and HECV SOCS-3exp lines respectively after the crystal violet staining. (HaCaT: n=6, HECV: n=5; error bars represent standard error of the mean; *: $p < 0.05$)

6.3.3 *In vitro* MTT cell proliferation assay

The MTT cell proliferation assay were conducted to investigate the impact of SOCS-3 expression on the proliferative ability of HaCaT and HECV cells, experiments were repeated for three times and the proliferation rate on day 3 and day 5 in each repeat was calculated based on the equation shown in chapter II section 2.18.2.

Statistical analysis of the keratinocyte SOCS-3 expression model indicated, no statistical difference between SOCS-3 expression and control keratinocytes on day 3 (1% decrease following SOCS-3 expression; $p > 0.05$; Figure 6-4 A). However, SOCS-3 expression attenuated the proliferation of keratinocytes on day 5, accounting for a 14% decrease compared to control keratinocytes ($p < 0.05$; Figure 6-4 B). Regarding the HECV endothelial cell model, no significant differences in proliferative rates between SOCS-3 expression and control HECV cells were observed either on day 3 (4% increase following SOCS-3 expression) and day 5 (27% increase following SOCS-3 expression) ($p > 0.05$; Figure 6-4 C, D). Taken together, SOCS-3 expression was found to decreased the proliferation of keratinocytes 5 days following inoculation but did not have influence the proliferative rates of endothelial cells.

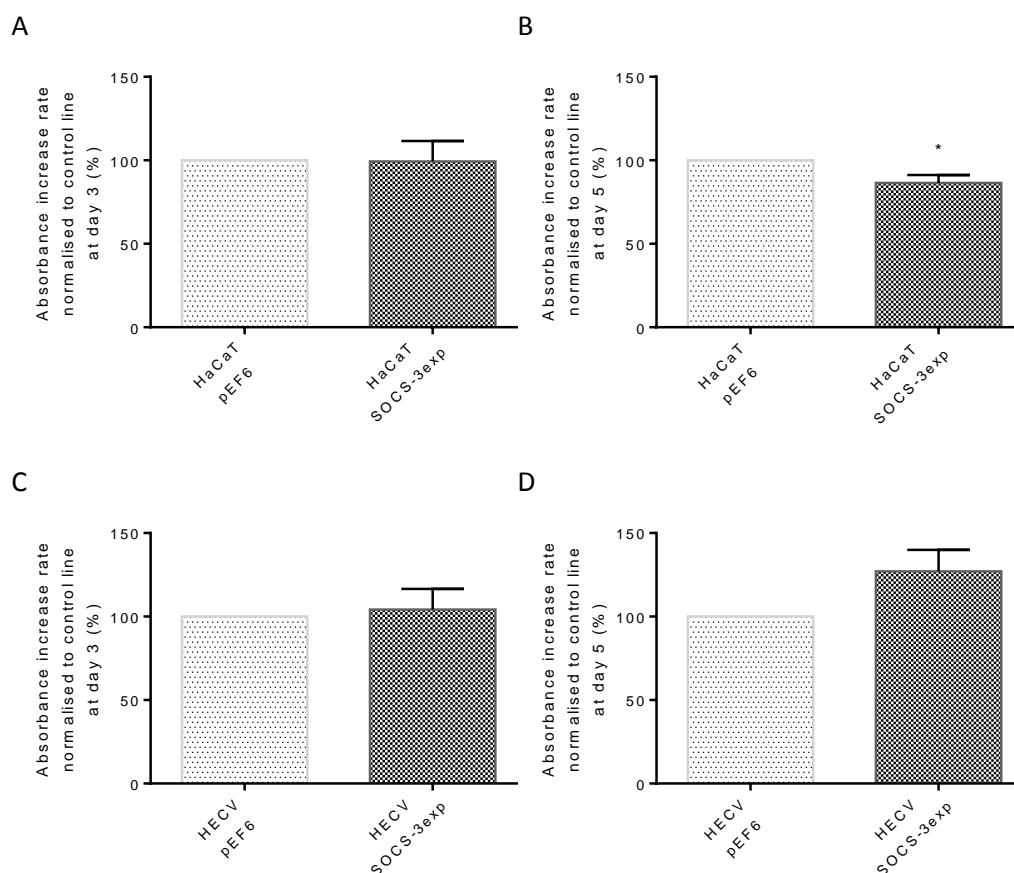


Figure 6-4: *In vitro* MTT cell proliferation assay on SOCS-3 mutant HaCaT and HECV lines by MTT

A. The proliferative rate of HaCaT cell on day 3 was transformed into percentage against control group in each repeat. The mean value was calculated and plotted in a bar chart; **B.** The proliferative rate of HaCaT cell on day 5 was transformed into percentage against control group in each repeat. The mean value was calculated and plotted in a bar chart; **C.** The proliferative rate of HECV cell on day 3 was transformed into percentage against control group in each repeat. The mean value was calculated and plotted in a bar chart; **D.** The proliferative rate of HECV cell on day 5 was transformed into percentage against control group in each repeat. The mean value was calculated and plotted in a bar chart. (n=3, error bars represent standard error of the mean; *: p < 0.05)

6.3.4 *In vitro* cell migration assay (wound healing assay)

An *in vitro* wound healing migration assay was undertaken to further explore the impact of SOCS-3 expression in human keratinocytes and endothelial cells. Surprisingly, there was no statistical difference observed in the rates of migration and wound closure between wounded HaCaT pEF6 and HaCaT SOCS-3exp monolayers at each 30-minute interval time point from the initial wounding point to the 15th hour when the experiment concluded ($p > 0.05$; Figure 6-5 A). This observation is further apparent in the representative images of the wound at 7.5th and 15th hour time points, demonstrating similar wound closure rates between HaCaT pEF6 and HaCaT SOCS-3exp (Figure 6-5 B, C).

Meanwhile, the *in vitro* wound healing assay was also conducted on SOCS-3 expression and control HECV cell lines. Similar results were also observed within the wounded monolayers of HECV pEF6 and HECV SOCS-3exp lines, showing no significant differences between the wound closure and migration rates of these two groups each 30-minute interval until the 20th hour ($p > 0.05$; Figure 6-6 A). Moreover, the wound width of the wounded HECV pEF6 and HECV SOCS-3exp, which both had a similar initial wound size, was found to display no obvious difference either at the 10th and the 20th hour (Figure 6-6 B, C).

Therefore, SOCS-3 expression seems have no effect on the migratory ability of human HaCaT keratinocytes or HECV endothelial cells on plasticware.

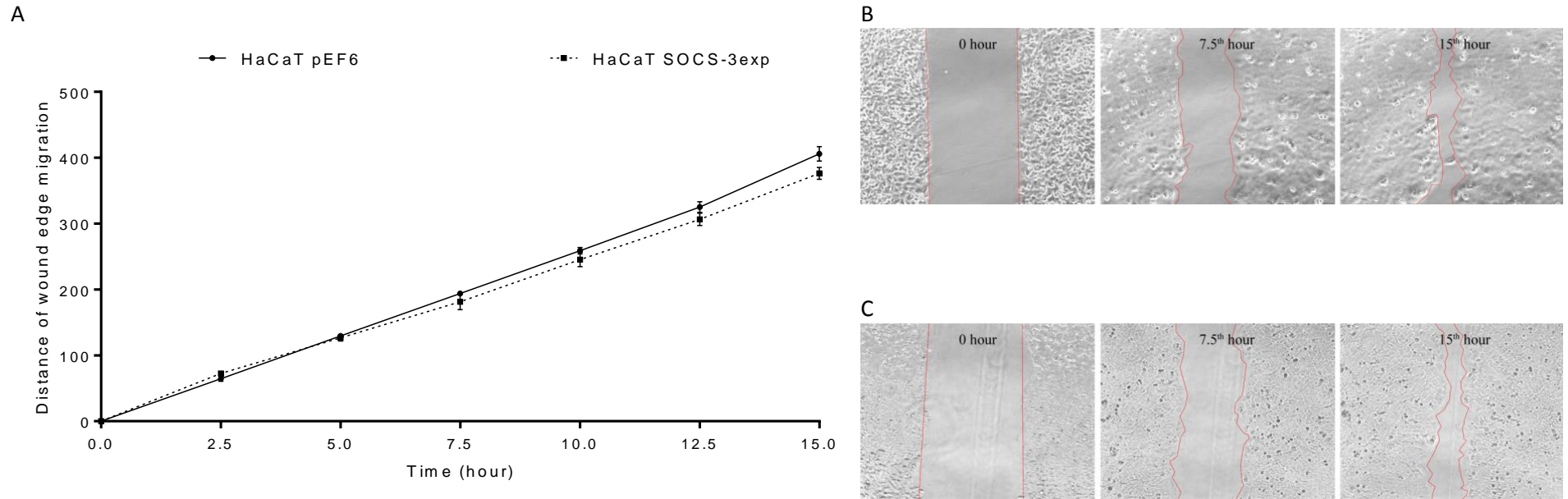


Figure 6-5: *In vitro* cell migration assay on SOCS-3 mutant HaCaT line

A. The distance migrated by the wound edge at each two and half hour interval were normalised to control line in percentage and plotted on a line chart; **B.** Representative pictures of the wounded HaCaT pEF6 monolayer at 0, 7.5th and 15th hour; **C.** Representative pictures of the wounded HaCaT SOCS3-exp monolayer at 0, 7.5th, and 15th hour following wounding. (n=3, representative data is shown; error bars represent standard error of the mean. Image was captured at X10 objective magnification; the red line indicates boundary of wound edge)

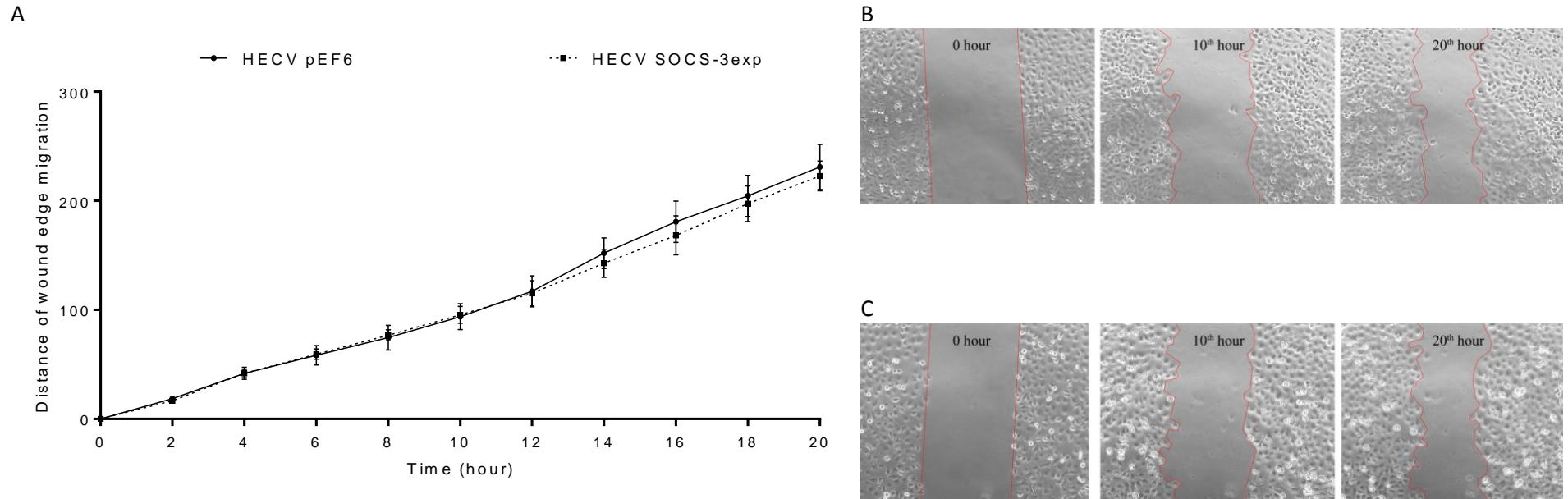


Figure 6-6: *In vitro* cell migration assay on SOCS-3 mutant HECV line

A. The distance migrated by the wound edge at each two hour interval were normalised to control line in percentage and plotted on a line chart; **B.** Representative pictures of the wounded HECV pEF6 monolayer at 0, 10th and 20th hour following wounding; **C.** Representative pictures of the wounded HECV SOCS3-exp monolayer at 0, 10th and 20th hour following wounding. (n=3, representative data is shown; error bars represent standard error of the mean. Image was captured at X10 objective magnification; the red line indicates boundary of wound edge)

6.3.5 Tubule formation assay

An *in vitro* Matrigel tubule formation assay was conducted to explore the potential of SOCS-3 expression to impact on the microtubule formation capacity of HECV cells and to investigate its potential to influence angiogenesis.

As displayed in Figure 6-7, at the 2nd hour following inoculation, both control and SOCS-3 expression cell lines began to form a tubule network, though the tube-like structure formed by the SOCS-3 expression line was more intensive than the control line. Furthermore, a microtubule network with more sprouts were clearly observed in the SOCS-3 expression line at the 4th hour in comparison to the control line. This trend was consistent over the next 6 hours until the conclusion of the experiment (Figure 6-7 A, B). The tubule formation ability was quantified at the 10th hour following cell seeding. Total perimeter of the formed tubules, giving an indication of total tubule coverage, was measured and compared between control and SOCS-3 expression lines. The total perimeter of the tubules formed by the SOCS-3 expression HECV cell line on matrigel matrix was 51% higher than that of by control cells and this trend was found to be statistically significant ($p < 0.01$; Figure 6-7 C). Therefore, SOCS-3 expression enhanced the tubule formation ability of endothelial cell on matrigel matrix.

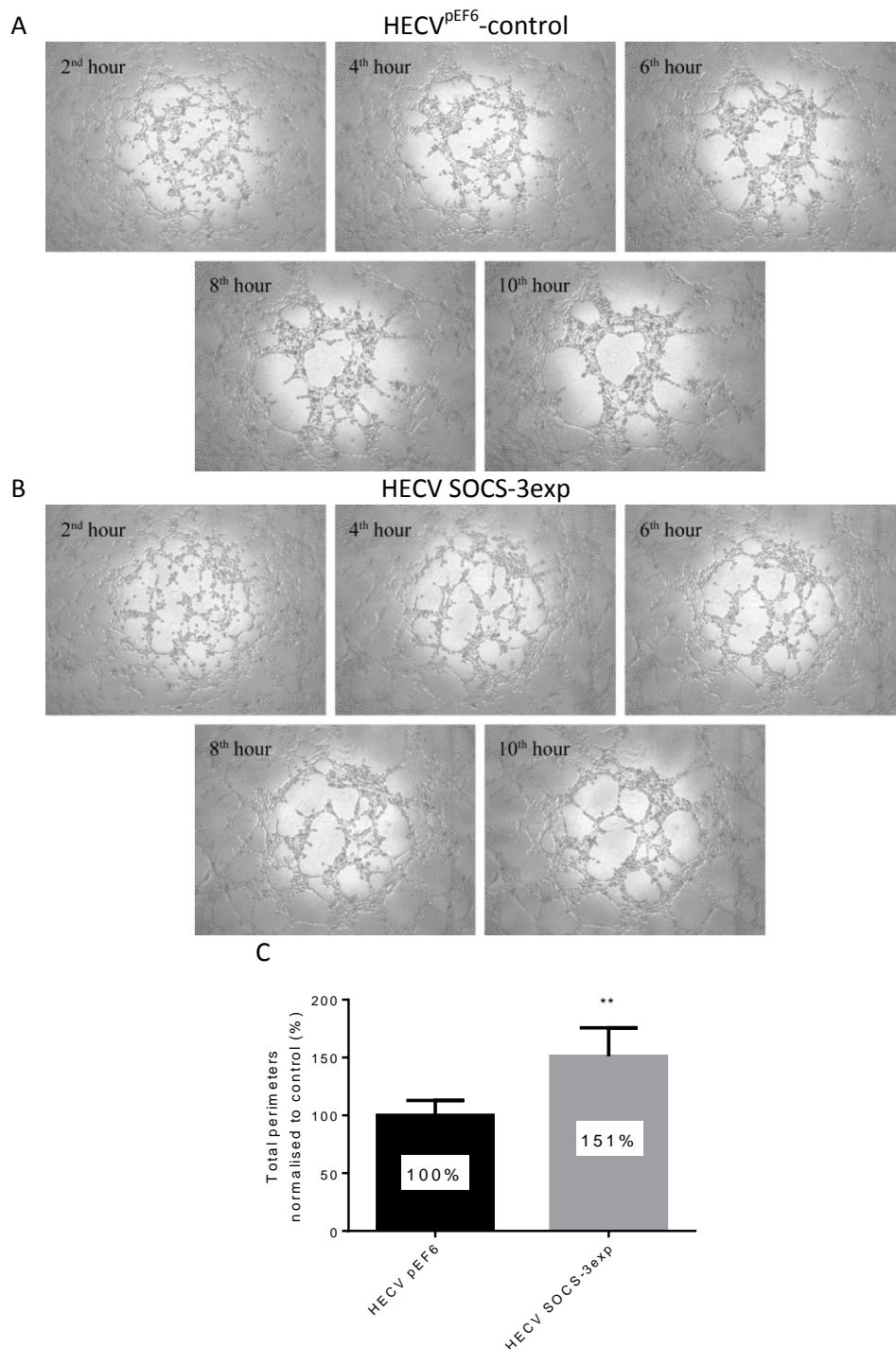


Figure 6-7: Tubule formation assay on SOCS-3 mutant HECV line

A. Representative pictures of the formed tubule of HECV pEF6 at the 2nd, 4th, 6th, 8th and 10th hour; **B.** Representative pictures of the formed tubule of HECV SOCS-3exp at the 2nd, 4th, 6th, 8th and 10th hour; **C.** The perimeter of the formed tubules on each image at the experimental endpoint was manually traced and the total perimeter in pixels was quantified. The mean value was then calculated from the multiple replicates as the total average perimeter before being normalised to the value of the control line. (images were captured at X5 objective magnification; n=3; representative data is shown; error bars represent standard deviation; **: p < 0.01)

6.4 Discussion

In addition to SOCS-4, explored in the previous chapter, the results obtained from Chapter III suggested that gene expression of SOCS-3 was differentially expressed between healing and non-healing chronic wounds and though the IHC data did not indicate differential expression it did highlight a potential relocation of SOCS-3 between the two clinical subgroups within the cohort. These observations combined with the literature, also suggest interesting links between SOCS-3 and wound healing, leading to the endeavor to further characterise the significance of SOCS-3 expression in two wound healing *in vitro* models, HaCaT and HECV. In Chapter IV it was suggested that neither HECV nor HaCaT cell lines expressed SOCS-3. This observation was surprising given that IHC analysis showed positive expression of SOCS-3 in both keratinocyte and endothelial components of the tissue, the precise reason for this is unknown but may represent inherent differences between immortalised cell lines and human tissue. A similar absence of SOCS-3 was also observed in mouse keratinocytes in studies by Linke *et al*, reporting the significance of SOCS-3 expression in transgenic mouse models (Linke *et al.*, 2010b), and, in agreement with our observations, in the HaCaT cell line (Goren *et al.*, 2006a).

In order to characterise the functional impact of SOCS-3 expression in human keratinocytes and endothelial cells the same functional assays conducted on the SOCS-4 mutant lines were also applied to the SOCS-3 expression HaCaT and HECV lines. The results from ECIS based initial attachment and spreading assay and migration assay showed that SOCS-3 expression elevated the initial attachment and spreading as well as migratory ability of HaCaT to the gold electrode. Interestingly, instead of observing contradictory results on SOCS-3 mutant HECV lines, as seen in Chapter V between HaCaT and HECV cells following

SOCS-4 knockdown, elevated rates of migration were similarly observed in HECV SOCS-3exp compared to HECV pEF6, whereas no statistical significance was observed on their initial attachment and spreading to the gold electrode. This suggested that SOCS-3 may potentially play a similar role in the migration, but not initial attachment and spreading in HaCaT and HECV cells.

However, the crystal violet matrigel adhesion assay indicated no statistical differences in matrigel adhesive ability between SOCS-3 expression HaCaT and control HaCaT cell lines, whereas HECV adhesion to the matrigel matrix was promoted by the SOCS-3 expression. The discrepancy between ECIS based initial adhesion assay and the crystal violet matrigel adhesion assay may suggest the alternative adhesive ability of HaCaT and HECV lines to the different matrix surface (from gold electrode to matrigel matrix). A previous study has showed enhanced expression of $\beta 1$ integrin in SOCS-3 expression cells, indicating a regulatory role for SOCS-3 in integrin expression (Stevenson et al., 2010). In addition, the matrigel utilised in this study consists of laminin and collagen IV which are both ligands of $\beta 1$ integrin (Diamond and Springer, 1994). Therefore, it is feasible that SOCS-3 increased cell adhesion to matrigel matrix through the enhancement of $\beta 1$ integrin, potentially accounting for the differential attachment to alternate substratum. It is also possible that such a role of SOCS-3 may be cell specific, depending on the expression profiles and active pathways within the cell lines.

The results from the *In vitro* cell migration assay (wound healing assay) indicated that the cell migration of HaCaT and HECV was not significantly affected by SOCS-3 expression, which was again different from that observed in the ECIS based migration assay, which showed significantly enhanced migration resulting from SOCS-3 expression following cell seeding. SOCS-3 has also been proposed

to influence keratinocyte migration within the literature, and a wound healing assay performed on a murine primary epithelial cell line demonstrated that SOCS-3 attenuated the migration of keratinocyte on fibronectin (Linke et al., 2010b). These contrasting results are likely to attribute to the different integrin expression profiles and receptors present in distinct substratum utilised in different experiment, since it has been documented that extracellular matrix controlled the expression of $\beta 1$ integrin, resulting different cell behaviour (Delcommenne and Streuli, 1995).

The results from the *in vitro* MTT cell proliferation assay indicated that the presence of SOCS-3 impaired the proliferation of HaCaT cells. Additionally, a previous study generated a successfully stable SOCS-3 expression HaCaT cell model utilising the pcDNATM3.1 Expression Vector and demonstrated that keratinocyte proliferation was impaired by the upregulation of SOCS-3 (Goren et al., 2006a). This is in line with the finding in the *in vitro* MTT cell proliferation assay in this chapter, suggesting the effectiveness of the SOCS-3 expression model established in this study. However, the impaired proliferation of HaCaT cells were seen in the 24th hour in the previous publication instead of 5 days observed in this chapter. This may due to the differing SOCS-3 expression levels, potentially resulting from differing SOCS-3 expression plasmid efficiencies between the two studies. Nevertheless, these, taken together, support the role of SOCS-3 in suppressing HaCaT proliferation. Moreover, an *in vivo* study observed decreased mitogenic marker in the epidermis of SOCS-3 overexpression mouse model with impaired healing phenotype, which further strengthening the role of SOCS-3 in suppressing keratinocyte proliferation (Linke et al., 2010b). However, the data presented here, whilst supporting the role of SOCS-3 in HaCaT cells, also suggests

a cell specific role of SOCS-3 in regards to proliferation as SOCS-3 expression brought about no significant changes in HECV proliferative rates.

According to the images taken from the tubule formation assay, reduced cell aggregation was observed in the SOCS-3 expression endothelial cells compared to the control lines starting from the 4th hour following cell seeding. This may be explained by a previous study on murine myeloid cell, which demonstrated that SOCS-3 attenuated homotypic cell aggregation through the suppression of STAT-3 activation (Wooten et al., 2000). Moreover, the elevated tubule formation on matrigel matrix by SOCS-3 expression in endothelial cells observed in the tubule formation assay may due to both the enhancement of adhesion and the promotion of spreading on such substratum, based on the fact that SOCS-3 was found to increase $\beta 1$ integrin expression (Stevenson et al., 2010) and that $\alpha 1\beta 1$ and $\alpha 1\beta 2$ was required for VEGF promoted endothelial cell spreading (Senger et al., 1997, Senger et al., 2002). Therefore, SOCS-3 expression may enhance endothelial cell adhesion to the matrigel matrix by upregulating the expression of $\beta 1$ integrin, and subsequently promotes the migration and sprouting through modulation of $\alpha 1\beta 1$ and $\alpha 2\beta 1$ integrins, resulting in enhanced tubule formation. Interestingly, silencing SOCS-3 in human and mouse retinal endothelial cell promoted the IGF-1- and TNF- α -stimulated cell proliferation (Stahl et al., 2012). In addition, SOCS-3 conditional knockdown mice exhibited increased pathologic retinal neovascularization but not physiologic vascular development, indicating an endogenous negative regulatory role of SOCS-3 in pathologic angiogenesis (Stahl et al., 2012). This is in contrast to the results in this current study suggesting pro-angiogenic effect of SOCS-3. This may be because the *in vitro* tubule formation assay used in this study is an *in vitro* approach in comparison to the complex microenvironment existing in the *in vivo* model. Alternatively, the

anti-angiogenic role of SOCS-3 observed in the *in vivo* study may be due to pathological stress since such effect was not seen in physiological murine models.

In summary, SOCS-3 does not influence the migration of HaCaT and HECV to the plastic cultureware matrix surface, whereas it appears to increase the migratory ability of such cell lines to the gold electrode. Furthermore, the presence of SOCS-3 improves the adhesion of HECV on matrigel matrix potentially by regulating $\beta 1$ integrin expression, whereas promote endothelial cell spreading the same substratum via modulating $\alpha 1\beta 1$ and $\alpha 2\beta 1$, however, this hypothesis requires further validation. Moreover, SOCS-3 may affect the migratory and adhesive ability of HaCaT and HECV to different matrix surfaces due to the regulatory effect of different substratum on integrin expression. In addition, SOCS-3 also holds the potential to impair HaCaT proliferation. Therefore, the functional analysis of SOCS-3 mutant cell lines indicates a role for this molecule in the key cell types involved in wound healing process.

Chapter VII

General discussion

The aim of the studies in this thesis was to investigate the importance of the SOCS family in the wound healing process, exploring their potential to act as prognostic factors in clinical cohorts and exploring the potential of SOCS-3 and -4 to influence key cellular traits linked to the healing process.

7.1 The clinical significance of SOCS family members in chronic wounds

Detection of SOCS family members within a clinical venous leg healing/healed and non-healing cohort (Cohort 1) using q-PCR highlighted significant elevations in SOCS-3 and -4 gene expression in non-healing chronic wounds compared to healing/healed chronic wounds. In addition, SOCS-1, SOCS-2, SOCS-5 and SOCS-6 exhibited a similar trend, though this did not reach statistical significance. However, the expression profile of SOCS-7 showed a contrasting trend to the other six family members examined, demonstrating enhanced gene expression in healing/healed chronic wounds compared to non-healing chronic wounds, though again, this did not display any significant differences. Hence, this data suggests some association between gene level expression of SOCS-3 and -4 and the healing potential of chronic wounds or may represent a predictive marker to identify healing potential of such wounds though such applications requires more intense investigation in larger gene expression cohorts to fully realise this potential.

In addition to the gene expression profile, IHC analysis was also undertaken to explore protein expression localisation in chronic wound tissues. The IHC screening was conducted using a different venous leg cohort (Cohort 2) which was defined using the same selection and grouping criteria as the cohort (Cohort 1) used for q-PCR analysis. Unfortunately, staining of a subset of this cohort showed no clear differences in the expression of SOCS-1 to SOCS-6

between non-healing and healing/healed chronic wounds. The majority of the chronic wounds exhibited positive staining for all six proteins predominantly in epidermis and partially in dermis and SOCS-7 staining appeared to be very weak or negative throughout the cohort following staining with two independent antibodies. However, IHC staining potentially indicated the relocalisation of SOCS-3 protein, from wound edge to epidermis distal to the wound edge, in the non-healing chronic wounds (4 out of 10 positive stained biopsies) in comparison to the healing/healed tissues (1 out of 8 positive stained biopsies). This phenomenon, whilst only observed in a small number of sections, again indicates that SOCS-3 may play differing roles within the tissues of healing/healed and non-healing chronic wounds and again warrants further establishment in larger cohorts to clarify.

The expression profile of SOCS-3 in normal skin tissues demonstrated that SOCS-3 expression was seldomly detected in epithelium (White et al., 2011, Goren et al., 2006a, Linke et al., 2010b). This is in line with the PCR screening data exploring the expression profile of SOCS-3 in the HaCaT cell line presented in chapter VI, which demonstrated no SOCS-3 expression in human HaCaT keratinocytes. Additionally, positive expression of SOCS-3 was found in inflammatory tissues (White et al., 2011), which is in agreement with the results in the IHC screening in the chronic wound biopsies (Cohort 2) in Chapter III, since a number of pro-inflammatory SOCS-3-inducible cytokines including IL-6, TNF- α , IFN- γ are produced and secreted by the recruited cells in the wound site during the healing process (Table 1-8). Together, this may suggest that SOCS-3 is induced by cytokine receptor activation through cytokine stimulation following wounding, and may have an effect on the regulation of keratinocyte behaviour. Due to the fact that a non-healing chronic wound is constitutively trapped in the

inflammation stage (Powers et al., 2016), the elevated expression of SOCS-3 protein may be due to the constant stimulation by the continuously produced pro-inflammatory cytokines.

SOCS-4 is a poorly characterised member of the SOCS family and its role in wound healing remains uncharacterised. Whilst not directly explored in the context of wound healing, SOCS-4 has been shown to be induced upon EGF stimulation and to inhibit EGFR via competing with STAT-3 and enhancing EGFR degradation (Kario et al., 2005, Bullock et al., 2007). A potential role of SOCS-4 has also been implicated in the regulation of other STAT family members (Hu et al., 2010). Given the significance of EGF in wound healing (Barrientos et al., 2008, Yu et al., 2010) and the ability of SOCS-4 to impact EGF/STAT signalling it is likely that represent a level of control for SOCS-4 in healing. Indeed conditional knockout of STAT-3 in the epidermis of mice impaired EGF dependant migration and wound healing (Sano et al., 1999). Hence, SOCS-4, acting at this level, may also be able to regulate healing. These observations are somewhat supported by the results of Chapter III, showing an increase in gene expression of chronic wounds, potentially interferes with EGF-STAT signalling to impair healing, though further work to clarify this is needed. However, whilst an interesting theory, this is limited by contrasts seen between gene level and protein level expression. In the IHC analysis of the clinical cohort, no difference in SOCS-4 expression was observed within the subset of tissues stained. This requires further study in larger cohorts to clarify the differences seen. Moreover, given the evidence that EGFR distributes in keratinocyte in human skin tissue (Nanney et al., 1990), the expression of SOCS-4 in all layers of the epidermis in the chronic wound biopsies observed in Chapter III may attribute to EGF-induced EGFR activation, further suggesting the negative regulatory role of SOCS-4 in EGF signalling in chronic wound tissues.

Overall, the clinical data has highlighted some interesting potential links, but also raised some interesting points requiring future work. The differential patterns seen between the gene expression and the IHC analysis needs further analysis utilising larger cohorts of chronic wounds but also acute wounds and normal skin. Certainly, the results give an early indication that gene analysis of SOCS-3 and -4 levels may have some prognostic function and may prove useful in patient management. The clinical data presented here also suggests that SOCS-1, SOCS-2, SOCS-5, SOCS-6 and SOCS-7 do not have great clinical significance in terms of chronic wounds and their healing potential.

7.2 The cellular traits of SOCS-4 in essential cell types involved in the wound healing and its potential mechanism

One of the aims of this thesis was to characterise the effect of SOCS-4 on the functional characteristics of key keratinocyte and endothelial cell lines and the potential of this to impact healing. To achieve this, stable SOCS-4 knockdown lines were established as described in Chapter IV. To date there are no clear studies focusing directly on the role of SOCS-4 in chronic wound healing or in general wound healing.

The functional characterisation on the established HaCaT and HECV knockdown mutant cell lines demonstrated that SOCS-4 did not have any effect on the proliferative rate of these cell types at least within 5 days incubation. Whilst not in the context of wound healing, SOCS-4 inhibition has also been shown not to influence the growth of K1 thyroid cancer cell lines (Mei et al., 2015). This evidence partially support the results seen in the *in vitro* MTT proliferation assay conducted in Chapter V, and suggest that SOCS-4 does not have significant impact on the proliferation of keratinocyte and endothelial cell.

Regarding the ECIS based assays, according to previous literature, the initial 10 hours of resistance increase following inoculation in ECIS assay reflects the initial attachment and spreading ability of the seeded cells (Wegener et al., 2000). Interestingly, the ECIS assay in Chapter V demonstrated that SOCS-4 downregulation reduced the initial attachment and spreading of keratinocyte, whereas this ability in endothelial cells was elevated following SOCS-4 knockdown. This discrepancy may attributed to the different integrins expression profile of keratinocyte and endothelial cell (Longmate and Dipersio, 2014, Hynes, 2007), which render them different adherent and migratory abilities influenced by the interaction of integrins and substratum matrix. This requires further clarification from additional scientific study.

Cell attachment was further studied using a Matrigel matrix assay. Matrigel matrix is a protein substrate that resembles the ECM found in many tissues and it has been utilised in numerous studies to generate more *in vivo*-like cell culture environments to measure cellular behaviours. Therefore, the results observed in the *in vitro* MTT cell adhesion assay are more likely to represent physiological conditions. MTT matrigel matrix adhesion assays conducted in Chapter V demonstrated that SOCS-4 did not influence HaCaT keratinocyte Matrigel attachment but suppression of SOCS-4 significantly reduced HECV endothelial cell matrigel attachment rates. This phenomenon may also be explain through a potentially different integrin expression profile present within the two cell types, rendering different adhesive ability to matrigel matrix, as the matrigel matrix used in this study primarily consists of laminin and collagen IV (<https://www.corning.com/media/worldwide/cls/documents/CLS-DL-CC-026%20DL.pdf>). SOCS-4 may potentially modulate the expression profile of laminin receptors $\alpha 3\beta 1$, $\alpha 6\beta 1$, $\alpha 6\beta 4$ and collagen receptors $\alpha 1\beta 1$ $\alpha 2\beta 1$ (Hynes,

2007) in endothelial cells and maintain its adhesive ability to laminin and collagen IV. Though this again requires further scientific clarification.

Regarding the *in vitro* migration assays, keratinocyte migratory ability was significantly impaired by SOCS-4 downregulation and such a trend was consistent between both scratch and ECIS based methodologies, albeit that impairment of migration was seen following different time periods. Such a discrepancy may due to the variant sensitivity between electrode sensor measurements and manually measuring wound edge distances in distinct methodologies. Interestingly, the investigation on the migration of SOCS-4 mutant endothelial cells demonstrated contradictory results, namely, elevated migration of SOCS-4 knockdown endothelial cell on gold electrode and decreased migration following SOCS-4 downregulation on plastic cultureware in the above mentioned two methodologies. This may suggest the diverse effect of SOCS-4 on the migratory ability on different matrix surface, since the substratum matrix is capable of regulating the integrin expression profile, leading to different cell behaviour (Delcommenne and Streuli, 1995). Therefore, the transwell migration assay, another method to investigate cell migration, may be required to further clarify the hypothesis raised above. Nonetheless, the ECIS based migration assay and the wound healing assay, despite presenting some contradicting data, suggested a role for SOCS-4 in the regulation of migration within HaCaT keratinocyte and HECV endothelial cells. Previous work in a thyroid cancer model has suggested that SOCS-4 could inhibit IL-23 mediated migration, suggesting a potentially constraining role of SOCS in the regulation of thyroid cancer cells (Mei et al., 2015). Taken together with this study, the migrational results presented in Chapter V are novel in the context of keratinocyte, endothelial cell and wound based background and

furthermore highlight a potential cell type-specific regulatory role of SOCS-4 in migration.

A tubule formation assay was utilised to investigate the angiogenic ability of HECV endothelial cells, following SOCS-4 knockdown and demonstrated a decreased formation of tubules, in terms of the number and the total perimeter, suggesting loss of SOCS-4 decreases angiogenic potential of this cell line. This is in line with observation of the matrigel matrix adhesion assay, and further supports the theory that SOCS-4 may play a role in altering the integrin expression profile in endothelial cells, not only contributing to its adhesion, but the migration, cell membrane assembly and sprouting on laminin and type IV collagen (Senger and Davis, 2011). Moreover, the SOCS-4 deficient cells tended to migrate less, an observation potentially linked to the results observed in the *in vitro* wound assay, considering migration is one of the prerequisite of sprouting (Ausprunk and Folkman, 1977). Therefore, the presence of SOCS-4 may contribute to a positive angiogenic response, in another words, SOCS-4 may act as a pro-angiogenic regulator in wound healing.

To explore potential mechanisms account for these function effects, a kinexus protein microarray was undertaken to assess changes in protein phosphorylation brought about by SOCS-4 knockdown. The screening on the potential variation of the protein expression following SOCS-4 knockdown in keratinocytes, conducted in Chapter V, highlighted the significant decrease of FAK Y397. FAK has been implicated as a critical factor of cell adhesion and migration, and Y397 of FAK, an auto phosphorylation site, is able to be activated in response to a number of stimuli, including recognition of matrix and initiate a variety of downstream signalling cascades contributing to migration (Wozniak et al., 2004, Zhao and Guan, 2011). A study showed that FAK mutations on the Y397 site

impaired the FAK-mediated cell migration, indicating the indispensable role of Y397 in the promotion of cell migration (Cary et al., 1996). This may explain the correlation between the decreased FAK Y397 and the downregulation of keratinocyte migration following SOCS-4 knockdown in HaCaT observed in Chapter V. Therefore, SOCS-4 may potentially affect keratinocyte migration through modulating the activation of FAK Y397. Moreover, another study on a FAK deficient mouse model and a FAK knockdown endothelial cell model discovered endothelial FAK is required for pathological angiogenesis (Tavora et al., 2010). This is also in line with the results observed in Chapter V, demonstrating that decreased FAK phosphorylation correlated with reduced HECV endothelial cell tubule formation following SOCS-4 knockdown. Furthermore, Src Y418 phosphorylation was also decreased following the downregulation of SOCS-4 in keratinocyte. It has been demonstrated that FAK phosphorylation is the prerequisite of Src activation as well as the formation of FAK/Src complex, and cell migration is mediated by the interaction of FAK/Src complex and p130cas (Cary et al., 1996, Cary et al., 1998). Taken together, the potential mechanism of SOCS-4 modulating the migration of keratinocyte is through the FAK/Src/p130cas pathway. Further intense study required to clarify and establish the importance of FAK/Src in relation to SOCS-4 and wound healing.

SOCS-4 has been poorly characterised in terms of wound healing. EGFR signalling is relatively well documented within the wound healing pathway and evidence has also suggested that SOCS-4 can regulate EGFR signalling, as outlined previously (Kario et al., 2005). In the protein array results in Chapter V, EGFR phosphorylation on Y1110 was also found reduced in the SOCS-4 knockdown keratinocytes. Moreover, SOCS-4 deficiency attenuated the migration of HaCaT keratinocytes. EGFR activation by heparin-binding EGF-like growth factor (HBEGF)

binding has been proved to facilitate keratinocyte migration (Shirakata et al., 2005). Therefore, it could be theorised that SOCS-4 downregulation may lead to reduced HBEGF production by keratinocytes, which in turn decreased the EGFR activation, resulting in decreased migration.

VEGFR-2 is another growth factor involved in wound healing whose phosphorylation was found decreased in SOCS-4 deficient keratinocyte in Chapter V. The activation of VEGFR-2 has been proved to promote keratinocyte migration (Yang et al., 2006). Thus, the impaired migration of keratinocyte following SOCS-4 knockdown may attribute to the decreased VEGFR-2 activation, raising another potential mechanism of SOCS-4 regulating keratinocyte migration through sustaining the activation of VEGFR-2.

In addition, protein array and wound healing assays conducted in Chapter V exhibited reduced phosphorylation of IGF-1R on Y1280 and decreased migration of keratinocyte following SOCS-4 knockdown. Since IGF-1-induced IGF-1R activation promotes keratinocyte migration via the activation of PI3K (Haase et al., 2003), SOCS-4 may potentially affect the keratinocyte migration through the maintenance of either IGF-1R or PI3K activation. In summary, the study on SOCS-4 deficient endothelial cells suggested a potential regulatory role for SOCS-4 in regulating the interaction of endothelial cells and ECM as well as angiogenesis and it could be theorised that this may be through modulation of the integrin profile within endothelial cells. Furthermore, the investigation on keratinocyte SOCS-4 knockdown model demonstrated the importance of SOCS-4 on the human keratinocyte migration, and highlighted a number of mechanisms potentially responsible for this effect. Therefore, the data suggests that SOCS-4 is an important protein that is potentially required for epithelialisation and angiogenesis in the wound healing process.

7.3 The cellular traits of SOCS-3 in essential cell types involved in the wound healing

Another aim of this thesis was to explore and clarify the impact of SOCS-3 on keratinocyte and endothelial cells in an attempt to highlight its importance in key healing traits. *In vitro* cell functional assays were conducted on the SOCS-3 expression HaCaT and HECV mutant lines. The expression of SOCS-3 did not significantly affect the proliferative rate of the endothelial cell during 5-day period, whereas, a significantly decreased proliferation was seen in SOCS-3 expression HaCaT cells on the 5th day after cell seeding. This is consistent with an *in vivo* study demonstrated overexpression of SOCS-3 attenuated the healing process with reduced mitogenic marker (Linke et al., 2010b), strengthening the negative regulatory role of SOCS-3 in keratinocyte proliferation.

The ECIS based initial attachment and spreading assay on SOCS-3 mutant HaCaT and HECV models demonstrated elevated initial attachment and spreading of keratinocytes following SOCS-3 expression, whereas no difference was shown between SOCS-3 expression endothelial cell and its control line. Similar to the discrepancy found in the same assay on SOCS-4 mutant keratinocyte and endothelial cells, this may due to different integrin expression profile in the two cell types which play different roles (keratinocyte for epithelialisation, endothelial cell for angiogenesis) in wound healing (Longmate and Dipersio, 2014, Hynes, 2007). Moreover, ECIS based migration assays, conducted in Chapter VI, indicated that SOCS-3 enhanced the migratory ability of both keratinocyte and endothelial cells over the gold electrode, which did not agree with the *in vitro* wound healing migration assay, indicating no difference in migration of either keratinocyte or endothelial cell following SOCS-3 expression. Interestingly, an *in vitro* wound

healing assay conducted in a previous study on murine primary keratinocytes demonstrated reduced migration of such cells on fibronectin following SOCS-3 overexpression (Linke et al., 2010b), which is contrast to the results observed from the ECIS based migration assay in Chapter VI. Again, this may be explained by the different integrin expression caused by different substratum matrix (gold electrode on ECIS assay; plastic cultureware in wound healing assay in Chapter VI; fibronectin in previous study) (Delcommenne and Streuli, 1995).

The crystal violet adhesion assay demonstrated that SOCS-3 expression enhanced the adhesion of endothelial cell to matrigel matrix, whereas SOCS-3 upregulation had no effect on such ability of keratinocyte. Previous studies have shown that SOCS-3 can enhance the $\beta 1$ integrins expression, and that $\beta 1$ interins are ligands that bind to laminin and type IV collagen of basement membrane (Stevenson et al., 2010, Diamond and Springer, 1994). Given that the primary components of matrigel matrix are laminin and type IV collagen, the enhanced adhesion of endothelial cells on matrigel matrix could be explained by the endothelial cell-dependent elevation of $\beta 1$ integrin expression following SOCS-3 upregulation.

The tubule formation assay conducted on the HECV SOCS-3 expressing line demonstrated that the expression of SOCS-3 significantly enhanced tubule formation ability of endothelial cells on matrigel matrix. This result is consistent with the *in vitro* crystal violet adhesion assay indicated previously. Previous evidence suggestes that $\alpha 1\beta 1$ and $\alpha 1\beta 2$ facilitate VEGF-dependent endothelial cell sprouting (Senger et al., 1997, Senger et al., 2002). Therefore, the potential rationale of increased tubule formation by SOCS-3 expression could be explained by the elevation of $\beta 1$ integrins following SOCS-3 expression, which benefit both adhesion and spreading of endothelial cell on the pre-coated laminin and type IV

collagen substratum. The tube formation assay further emphasises that SOCS-3 may hold the potential to regulate the integrin expression in endothelial cell, and subsequently contribute to angiogenesis..

7.4 Main findings and significance

The q-PCR screening on chronic wound cohort 1 demonstrated 81% and 93% elevated SOCS-3 and SOCS-4 expression in non-healing chronic wounds in comparison to healing/healed group respectively suggesting gene expression of SOCS-3 and SOCS-4 may be implicated in the healing profile and may present useful tools as genetic biomarkers for healing progression. IHC screening on chronic wound cohort 2 demonstrated that SOCS-1 to SOCS-6 were expressed primarily in all layers of epidermis with higher expression levels in the nucleus of the basal layer keratinocytes, whereas much less intensive expression of SOCS-1 to SOCS-6 were observed in dermis. However, no different distribution or intensity of SOCS-1 to SOCS-6 was observed between the non-healing chronic wounds and healing/healed chronic wounds, although there was an intimation of SOCS-3 relocalisation in non-healing chronic wounds since 75% (3 out of 4) of increased SOCS-3 expression in epidermis distal to the wound edge were seen in non-healing chronic wound tissues. These results suggest that elevated SOCS-3 and SOCS-4 gene expression may potentially predict poor healing result of chronic wound, although this hypothesis requires further verification on protein level based on larger non-healing and healing/healed chronic wound cohort or the cohort consisting of normal, acute and chronic wound tissues.

Characterisation of SOCS-4 knockdown mutants has led to the implication that the presence of SOCS-4 in keratinocytes acts in a pro-migratory fashion, as well as promoting cell-matrix adhesion. This further suggests that this is

potentially achieved through its regulation of FAK/Src/p130cas pathway, HBEGF/EGFR pathway, VEGF/VEGFR-2 pathway and IGF-1/IGF-1R/PI3K pathway. Furthermore, the role of SOCS-4 in endothelial cells appears more relative to the particular substratum and environment the cells are located on, though it does appear to have a pro-angiogenic function. Such effects may be due to integrin profiling of such cells though more work is needed to characterise this in the context of SOCS-4. Given the importance of traits such as migration and angiogenesis within the wound healing process (Pastar et al., 2014, Tonnesen et al., 2000, Senger and Davis, 2011), the functional data suggests that the presence of SOCS-4 would promote healing. This again appears to be in contrast to the gene expression profile, indicating higher SOCS-4 gene expression in non-healing chronic wounds, a trait not confirmed at the protein level. This study has suggested a role for SOCS-4 as a potential biomarker and has similarly implicated it in regulating key characteristics and pathways relative to wound healing. Hence SOCS-4 appears to play some complex role in the wound healing process and this requires more intense scientific research to be fully elucidated.

SOCS-3 expression in HaCaT keratinocytes reduced the proliferation and appeared to have substrate specific effects on attachment and migration, enhancing these traits in regards to the gold electrode but not plastic cultureware or matrigel. The conflict between the different assays and also the negative impact on proliferation and in some aspects, pro-migratory impact make it difficult to conclude a definitive role in promoting or inhibiting wound healing. In terms of the endothelial model, even though there is conflict between the experimental assays, overall the characterisation suggests a pro-angiogenic impact of SOCS-3 expression and this in turn may be significant in the re-epithelialisation and proliferation stage of wound healing where angiogenesis in a

key component. When analysed in conjunction with the clinical data, a pro-angiogenic phenotype would seem to oppose the observation that SOCS-3 gene expression is enhanced in non-healing chronic wounds and displays some relocalisation in such wounds compared to healing/healed ones. This may be explained by the housekeeping gene (CK-19), an epithelial cell biomarker, used in the clinical q-PCR screening. Hence, the results may only represent SOCS-3 expression profile in keratinocytes but not in endothelial cells. Therefore, SOCS-3 may potentially exert anti-proliferative role in keratinocytes, whereas play pro-angiogenic role in endothelial cells in the re-epithelialisation and the proliferation stage.

Taken together, this thesis has furthered the understanding of the role played by SOCS-3 and SOCS-4, in chronic wound healing. This study has identified differential gene expression between chronic healing and non-healing wounds, and also demonstrated a potential shift in localisation of SOCS-3 between these chronic wound types. Furthermore the study has established a role for SOCS-3 and -4 in several cellular processes of wound healing, such as migration and angiogenesis. Whilst highlighting these interesting aspects of SOCS role in wound healing, this thesis also raises some questions. Most importantly, there appears to be some contrast between clinical observations, where higher gene level expression of SOCS-3 and SOCS-4 associated with the non-healing wounds, and cellular functions, where SOCS-3 and 4 appear to confer pro-migratory and pro-angiogenic traits. This may in part be due to the differing nature of basic *in vitro* models and the more complex nature within a multi-cellular tissue environment, in this case, a chronic wound environment. This thesis has also implied a potential clinical role for SOCS-3 and SOCS-4 gene expression to be used as a potential biomarker. Further research to clarify the potential of SOCS family members in

chronic wound healing, their implications in much larger clinical cohorts as well as in normal wound healing processes would be of benefit and is warranted.

7.5 Future work

Since the clinical chronic wound biopsies chosen for the IHC screening on SOCS members was less than the amount used for transcript expression screening, a larger cohort of chronic wounds would be required to further investigate the clinical significance of SOCS protein expression pattern in chronic wounds. In addition, based on the fact that a possible relocalisation of SOCS-3 was seen in chronic wounds distal to the wound edge, the gene expression levels and the protein expression pattern between cohorts of acute and chronic wounds is also of great interest and this should be investigated fully in future investigations.

In terms of cellular and molecular study, future work is needed to focus on the verification of the potential link between SOCS-4 and FAK and FAK Y397. This study looked at the functional impact of SOCS-4, either in a dual SOCS-4/FAK knockdown and in combination with small molecule inhibitors targeting FAK and Y397 phosphorylation is warranted to expand the knowledge in this area. Given the significance of FAK and its downstream signalling and its implications in a wide variety of processes, future work is also needed to profile changes in expression of FAK and FAK Y397 in the endothelial cells and to apply similar dual knockdown/small molecule inhibitor techniques to explore the significance of this pathway in the angiogenic response. Furthermore, in addition to the FAK link, the Kinexus microarray has provided a number of other very interesting leads to follow up, particularly wound relevant pathways such as EGFR, VEGFR and IGF. Full verification and follow up of this precious resource will be instrumental in fully elucidating the role of SOCS-4 and its significance in wound biology. In

addition to these mechanistic studies in relation to SOCS-4, future work should be undertaken to explore some of these pathways in SOCS-3 models, particularly the FAK link, as previous literature has suggested that SOCS-3 can associate with FAK through SH2 and KIR domains in a FAK Y397-dependent manner, subsequently enhancing FAK turnover via SOCS box-dependent-proteasomal degradation (Liu et al., 2003).

Moreover, given the significance of the experimental matrix present within a number of the assays, the detection of integrin expression profiles following SOCS-4 knockdown and SOCS-3 expression in these cell models is also of interest to further clarify the mechanisms through which SOCS-3 and -4 may mediating the adhesion, migration and spreading of keratinocytes/endothelial cells on matrigel matrix.

Further understanding of these downstream signalling pathways may aid in the full realisation of the clinical significance of these molecules, potentially allowing multi-target therapeutic design.

Chapter VIII

References

- ADAMS, T. E., HANSEN, J. A., STARR, R., NICOLA, N. A., HILTON, D. J. & BILLESTRUP, N. 1998. Growth hormone preferentially induces the rapid, transient expression of SOCS-3, a novel inhibitor of cytokine receptor signaling. *J Biol Chem*, 273, 1285-7.
- ALEXANDER, W. S. 2002. Suppressors of cytokine signalling (SOCS) in the immune system. *Nat Rev Immunol*, 2, 410-6.
- ALEXANDER, W. S., STARR, R., FENNER, J. E., SCOTT, C. L., HANDMAN, E., SPRIGG, N. S., CORBIN, J. E., CORNISH, A. L., DARWICHE, R., OWCZAREK, C. M., KAY, T. W., NICOLA, N. A., HERTZOG, P. J., METCALF, D. & HILTON, D. J. 1999. SOCS1 is a critical inhibitor of interferon gamma signaling and prevents the potentially fatal neonatal actions of this cytokine. *Cell*, 98, 597-608.
- AMAN, M. J., MIGONE, T. S., SASAKI, A., ASCHERMAN, D. P., ZHU, M., SOLDAINI, E., IMADA, K., MIYAJIMA, A., YOSHIMURA, A. & LEONARD, W. J. 1999. CIS associates with the interleukin-2 receptor beta chain and inhibits interleukin-2-dependent signaling. *J Biol Chem*, 274, 30266-72.
- ANSEL, J. C., TIESMAN, J. P., OLERUD, J. E., KRUEGER, J. G., KRANE, J. F., TARA, D. C., SHIPLEY, G. D., GILBERTSON, D., USUI, M. L. & HART, C. E. 1993. Human keratinocytes are a major source of cutaneous platelet-derived growth factor. *J Clin Invest*, 92, 671-8.
- ARAKAWA, S., HATANO, Y. & KATAGIRI, K. 2004. Differential expression of mRNA for Th1 and Th2 cytokine-associated transcription factors and suppressors of cytokine signalling in peripheral blood mononuclear cells of patients with atopic dermatitis. *Clin Exp Immunol*, 135, 505-10.
- ARTS, P., PLANTINGA, T. S., VAN DEN BERG, J. M., GILISSEN, C., VELTMAN, J. A., VAN TROTSBURG, A. S., VAN DE VEERDONK, F. L., KUIJPERS, T. W., HOISCHEN, A. & NETEA, M. G. 2015. A missense mutation underlies defective SOCS4 function in a family with autoimmunity. *J Intern Med*, 278, 203-10.
- AUERNHAMMER, C. J. & MELMED, S. 1999. Interleukin-11 stimulates proopiomelanocortin gene expression and adrenocorticotropin secretion in corticotroph cells: evidence for a redundant cytokine network in the hypothalamo-pituitary-adrenal axis. *Endocrinology*, 140, 1559-66.
- AUSPRUNK, D. H. & FOLKMAN, J. 1977. Migration and proliferation of endothelial cells in preformed and newly formed blood vessels during tumor angiogenesis. *Microvasc Res*, 14, 53-65.
- BABON, J. J., MCMANUS, E. J., YAO, S., DESOUZA, D. P., MIELKE, L. A., SPRIGG, N. S., WILLSON, T. A., HILTON, D. J., NICOLA, N. A., BACA, M., NICHOLSON, S. E. & NORTON, R. S. 2006. The structure of SOCS3 reveals the basis of the extended SH2 domain function and identifies an unstructured insertion that regulates stability. *Mol Cell*, 22, 205-16.
- BABON, J. J., SABO, J. K., SOETOPO, A., YAO, S., BAILEY, M. F., ZHANG, J. G., NICOLA, N. A. & NORTON, R. S. 2008. The SOCS box domain of SOCS3: structure and interaction with the elonginBC-cullin5 ubiquitin ligase. *J Mol Biol*, 381, 928-40.
- BABON, J. J., SABO, J. K., ZHANG, J. G., NICOLA, N. A. & NORTON, R. S. 2009. The SOCS box encodes a hierarchy of affinities for Cullin5: implications for ubiquitin ligase formation and cytokine signalling suppression. *J Mol Biol*, 387, 162-74.
- BAIRD, A., MORMEDE, P. & BOHLEN, P. 1985. Immunoreactive fibroblast growth factor in cells of peritoneal exudate suggests its identity with

- macrophage-derived growth factor. *Biochem Biophys Res Commun*, 126, 358-64.
- BANERJEE, A., BANKS, A. S., NAWIJN, M. C., CHEN, X. P. & ROTHMAN, P. B. 2002. Cutting edge: Suppressor of cytokine signaling 3 inhibits activation of NFATp. *J Immunol*, 168, 4277-81.
- BANKS, A. S., LI, J., MCKEAG, L., HRIBAL, M. L., KASHIWADA, M., ACCILI, D. & ROTHMAN, P. B. 2005. Deletion of SOCS7 leads to enhanced insulin action and enlarged islets of Langerhans. *J Clin Invest*, 115, 2462-71.
- BARRIENTOS, S., STOJADINOVIC, O., GOLINKO, M. S., BREM, H. & TOMIC-CANIC, M. 2008. Growth factors and cytokines in wound healing. *Wound Repair Regen*, 16, 585-601.
- BARSHEES, N. R., SIGIREDDI, M., WROBEL, J. S., MAHANKALI, A., ROBBINS, J. M., KOUGIAS, P. & ARMSTRONG, D. G. 2013. The system of care for the diabetic foot: objectives, outcomes, and opportunities. *Diabet Foot Ankle*, 4.
- BAYLE, J., LETARD, S., FRANK, R., DUBREUIL, P. & DE SEPULVEDA, P. 2004. Suppressor of cytokine signaling 6 associates with KIT and regulates KIT receptor signaling. *J Biol Chem*, 279, 12249-59.
- BAYLE, J., LOPEZ, S., IWAI, K., DUBREUIL, P. & DE SEPULVEDA, P. 2006. The E3 ubiquitin ligase HOIL-1 induces the polyubiquitination and degradation of SOCS6 associated proteins. *FEBS Lett*, 580, 2609-14.
- BEHM, B., BABILAS, P., LANDTHALER, M. & SCHREML, S. 2012. Cytokines, chemokines and growth factors in wound healing. *J Eur Acad Dermatol Venereol*, 26, 812-20.
- BELLEZZA, I., NEUWIRT, H., NEMES, C., CAVARRETTA, I. T., PUHR, M., STEINER, H., MINELLI, A., BARTSCH, G., OFFNER, F., HOBISCH, A., DOPPLER, W. & CULIG, Z. 2006. Suppressor of cytokine signaling-3 antagonizes cAMP effects on proliferation and apoptosis and is expressed in human prostate cancer. *Am J Pathol*, 169, 2199-208.
- BELLO, Y. M. & PHILLIPS, T. J. 2000. Recent advances in wound healing. *JAMA*, 283, 716-8.
- BERGAMIN, E., WU, J. & HUBBARD, S. R. 2006. Structural basis for phosphotyrosine recognition by suppressor of cytokine signaling-3. *Structure*, 14, 1285-92.
- BERLATO, C., CASSATELLA, M. A., KINJYO, I., GATTO, L., YOSHIMURA, A. & BAZZONI, F. 2002. Involvement of suppressor of cytokine signaling-3 as a mediator of the inhibitory effects of IL-10 on lipopolysaccharide-induced macrophage activation. *J Immunol*, 168, 6404-11.
- BERTON, T. R., MATSUMOTO, T., PAGE, A., CONTI, C. J., DENG, C. X., JORCANO, J. L. & JOHNSON, D. G. 2003. Tumor formation in mice with conditional inactivation of Brca1 in epithelial tissues. *Oncogene*, 22, 5415-26.
- BICKERS, D. R., LIM, H. W., MARGOLIS, D., WEINSTOCK, M. A., GOODMAN, C., FAULKNER, E., GOULD, C., GEMMEN, E., DALL, T., AMERICAN ACADEMY OF DERMATOLOGY, A. & SOCIETY FOR INVESTIGATIVE, D. 2006. The burden of skin diseases: 2004 a joint project of the American Academy of Dermatology Association and the Society for Investigative Dermatology. *J Am Acad Dermatol*, 55, 490-500.
- BJORBAEK, C., ELMQUIST, J. K., EL-HASCHIMI, K., KELLY, J., AHIMA, R. S., HILEMAN, S. & FLIER, J. S. 1999. Activation of SOCS-3 messenger ribonucleic acid in the hypothalamus by ciliary neurotrophic factor. *Endocrinology*, 140, 2035-43.

- BJORBAEK, C., ELMQUIST, J. K., FRANTZ, J. D., SHOELSON, S. E. & FLIER, J. S. 1998. Identification of SOCS-3 as a potential mediator of central leptin resistance. *Mol Cell*, 1, 619-25.
- BLATTI, S. P., FOSTER, D. N., RANGANATHAN, G., MOSES, H. L. & GETZ, M. J. 1988. Induction of fibronectin gene transcription and mRNA is a primary response to growth-factor stimulation of AKR-2B cells. *Proc Natl Acad Sci U S A*, 85, 1119-23.
- BLOTNICK, S., PEOPLES, G. E., FREEMAN, M. R., EBERLEIN, T. J. & KLAGSBRUN, M. 1994. T lymphocytes synthesize and export heparin-binding epidermal growth factor-like growth factor and basic fibroblast growth factor, mitogens for vascular cells and fibroblasts: differential production and release by CD4+ and CD8+ T cells. *Proc Natl Acad Sci U S A*, 91, 2890-94.
- BOISCLAIR, Y. R., WANG, J., SHI, J., HURST, K. R. & OOI, G. T. 2000. Role of the suppressor of cytokine signaling-3 in mediating the inhibitory effects of interleukin-1beta on the growth hormone-dependent transcription of the acid-labile subunit gene in liver cells. *J Biol Chem*, 275, 3841-7.
- BORDER, W. A. & RUOSLAHTI, E. 1992. Transforming growth factor-beta in disease: the dark side of tissue repair. *J Clin Invest*, 90, 1-7.
- BORISH, L. C. & STEINKE, J. W. 2003. 2. Cytokines and chemokines. *J Allergy Clin Immunol*, 111, S460-75.
- BOSANQUET, D. C., HARDING, K. G., RUGE, F., SANDERS, A. J. & JIANG, W. G. 2012. Expression of IL-24 and IL-24 receptors in human wound tissues and the biological implications of IL-24 on keratinocytes. *Wound Repair Regen*, 20, 896-903.
- BOUKAMP, P., PETRUSSEVSKA, R. T., BREITKREUTZ, D., HORNING, J., MARKHAM, A. & FUSENIG, N. E. 1988. Normal keratinization in a spontaneously immortalized aneuploid human keratinocyte cell line. *J Cell Biol*, 106, 761-71.
- BOYLE, K., EGAN, P., RAKAR, S., WILLSON, T. A., WICKS, I. P., METCALF, D., HILTON, D. J., NICOLA, N. A., ALEXANDER, W. S., ROBERTS, A. W. & ROBB, L. 2007. The SOCS box of suppressor of cytokine signaling-3 contributes to the control of G-CSF responsiveness in vivo. *Blood*, 110, 1466-74.
- BREM, H., STOJADINOVIC, O., DIEGELMANN, R. F., ENTERO, H., LEE, B., PASTAR, I., GOLINKO, M., ROSENBERG, H. & TOMIC-CANIC, M. 2007. Molecular markers in patients with chronic wounds to guide surgical debridement. *Mol Med*, 13, 30-9.
- BREM, H. & TOMIC-CANIC, M. 2007. Cellular and molecular basis of wound healing in diabetes. *J Clin Invest*, 117, 1219-22.
- BRENDER, C., COLUMBUS, R., METCALF, D., HANDMAN, E., STARR, R., HUNTINGTON, N., TARLINTON, D., ODUM, N., NICHOLSON, S. E., NICOLA, N. A., HILTON, D. J. & ALEXANDER, W. S. 2004. SOCS5 is expressed in primary B and T lymphoid cells but is dispensable for lymphocyte production and function. *Mol Cell Biol*, 24, 6094-103.
- BRENDER, C., LOVATO, P., SOMMER, V. H., WOETMANN, A., MATHIESEN, A. M., GEISLER, C., WASIK, M. & ODUM, N. 2005. Constitutive SOCS-3 expression protects T-cell lymphoma against growth inhibition by IFNalpha. *Leukemia*, 19, 209-13.
- BRENDER, C., NIELSEN, M., KALTOFT, K., MIKKELSEN, G., ZHANG, Q., WASIK, M., BILLESTRUP, N. & ODUM, N. 2001a. STAT3-mediated constitutive expression of SOCS-3 in cutaneous T-cell lymphoma. *Blood*, 97, 1056-62.

- BRENDER, C., NIELSEN, M., ROPKE, C., NISSEN, M. H., SVEJGAARD, A., BILLESTRUP, N., GEISLER, C. & ODUM, N. 2001b. Interferon-alpha induces transient suppressors of cytokine signalling expression in human T cells. *Exp Clin Immunogenet*, 18, 80-5.
- BRENDER, C., TANNAHILL, G. M., JENKINS, B. J., FLETCHER, J., COLUMBUS, R., SARIS, C. J., ERNST, M., NICOLA, N. A., HILTON, D. J., ALEXANDER, W. S. & STARR, R. 2007. Suppressor of cytokine signaling 3 regulates CD8 T-cell proliferation by inhibition of interleukins 6 and 27. *Blood*, 110, 2528-36.
- BROGI, E., SCHATTEMAN, G., WU, T., KIM, E. A., VARTICOVSKI, L., KEYT, B. & ISNER, J. M. 1996. Hypoxia-induced paracrine regulation of vascular endothelial growth factor receptor expression. *J Clin Invest*, 97, 469-76.
- BROUGHTON, G., 2ND, JANIS, J. E. & ATTINGER, C. E. 2006a. A brief history of wound care. *Plast Reconstr Surg*, 117, 6S-11S.
- BROUGHTON, G., 2ND, JANIS, J. E. & ATTINGER, C. E. 2006b. Wound healing: an overview. *Plast Reconstr Surg*, 117, 1e-S-32e-S.
- BROWN, G. L., NANNEY, L. B., GRIFFEN, J., CRAMER, A. B., YANCEY, J. M., CURTSINGER, L. J., 3RD, HOLTZIN, L., SCHULTZ, G. S., JURKIEWICZ, M. J. & LYNCH, J. B. 1989. Enhancement of wound healing by topical treatment with epidermal growth factor. *N Engl J Med*, 321, 76-9.
- BROWN, L. F., YEO, K. T., BERSE, B., YEO, T. K., SENGHER, D. R., DVORAK, H. F. & VAN DE WATER, L. 1992. Expression of vascular permeability factor (vascular endothelial growth factor) by epidermal keratinocytes during wound healing. *J Exp Med*, 176, 1375-9.
- BRUMANN, M., MATZ, M., KUSMENKOV, T., STEGMAIER, J., BIBERTHALER, P., KANZ, K. G., MUTSCHLER, W. & BOGNER, V. 2014. Impact of STAT/SOCS mRNA expression levels after major injury. *Mediators Inflamm*, 2014, 749175.
- BRYANT, R. & NIX, D. 2015. *Acute and chronic wounds*, Elsevier Health Sciences.
- BUCALO, B., EAGLSTEIN, W. H. & FALANGA, V. 1993. Inhibition of cell proliferation by chronic wound fluid. *Wound Repair Regen*, 1, 181-6.
- BUCKLEY-STURROCK, A., WOODWARD, S. C., SENIOR, R. M., GRIFFIN, G. L., KLAGSBRUN, M. & DAVIDSON, J. M. 1989. Differential stimulation of collagenase and chemotactic activity in fibroblasts derived from rat wound repair tissue and human skin by growth factors. *J Cell Physiol*, 138, 70-8.
- BULLOCK, A. N., DEBRECZENI, J. E., EDWARDS, A. M., SUNDSTROM, M. & KNAPP, S. 2006. Crystal structure of the SOCS2-elongin C-elongin B complex defines a prototypical SOCS box ubiquitin ligase. *Proc Natl Acad Sci U S A*, 103, 7637-42.
- BULLOCK, A. N., RODRIGUEZ, M. C., DEBRECZENI, J. E., SONGYANG, Z. & KNAPP, S. 2007. Structure of the SOCS4-ElonginB/C complex reveals a distinct SOCS box interface and the molecular basis for SOCS-dependent EGFR degradation. *Structure*, 15, 1493-504.
- BURGESS, W. H. & MACIAG, T. 1989. The heparin-binding (fibroblast) growth factor family of proteins. *Annu Rev Biochem*, 58, 575-606.
- CACALANO, N. A., SANDEN, D. & JOHNSTON, J. A. 2001. Tyrosine-phosphorylated SOCS-3 inhibits STAT activation but binds to p120 RasGAP and activates Ras. *Nat Cell Biol*, 3, 460-5.
- CALEGARI, V. C., BEZERRA, R. M., TORSONI, M. A., TORSONI, A. S., FRANCHINI, K. G., SAAD, M. J. & VELLOSO, L. A. 2003. Suppressor of cytokine signaling 3

- is induced by angiotensin II in heart and isolated cardiomyocytes, and participates in desensitization. *Endocrinology*, 144, 4586-96.
- CALLUS, B. A. & MATHEY-PREVOT, B. 2002. SOCS36E, a novel Drosophila SOCS protein, suppresses JAK/STAT and EGF-R signalling in the imaginal wing disc. *Oncogene*, 21, 4812-21.
- CARMELIET, P., FERREIRA, V., BREIER, G., POLLEFEYT, S., KIECKENS, L., GERTSENSTEIN, M., FAHRIG, M., VANDENHOECK, A., HARPAL, K., EBERHARDT, C., DECLERCQ, C., PAWLING, J., MOONS, L., COLLEN, D., RISAU, W. & NAGY, A. 1996. Abnormal blood vessel development and lethality in embryos lacking a single VEGF allele. *Nature*, 380, 435-9.
- CARY, L. A., CHANG, J. F. & GUAN, J. L. 1996. Stimulation of cell migration by overexpression of focal adhesion kinase and its association with Src and Fyn. *J Cell Sci*, 109 (Pt 7), 1787-94.
- CARY, L. A., HAN, D. C., POLTE, T. R., HANKS, S. K. & GUAN, J. L. 1998. Identification of p130Cas as a mediator of focal adhesion kinase-promoted cell migration. *J Cell Biol*, 140, 211-21.
- CHEDID, M., RUBIN, J. S., CSAKY, K. G. & AARONSON, S. A. 1994. Regulation of keratinocyte growth factor gene expression by interleukin 1. *J Biol Chem*, 269, 10753-7.
- CHEN, J. D., KIM, J. P., ZHANG, K., SARRET, Y., WYNN, K. C., KRAMER, R. H. & WOODLEY, D. T. 1993. Epidermal growth factor (EGF) promotes human keratinocyte locomotion on collagen by increasing the alpha 2 integrin subunit. *Exp Cell Res*, 209, 216-23.
- CHEN, J. D., LAPIERE, J. C., SAUDER, D. N., PEAHEY, C. & WOODLEY, D. T. 1995. Interleukin-1 alpha stimulates keratinocyte migration through an epidermal growth factor/transforming growth factor-alpha-independent pathway. *J Invest Dermatol*, 104, 729-33.
- CHEN, T. L., BATES, R. L., XU, Y., AMMANN, A. J. & BECK, L. S. 1992. Human recombinant transforming growth factor-beta 1 modulation of biochemical and cellular events in healing of ulcer wounds. *J Invest Dermatol*, 98, 428-35.
- CHEN, Z., LAURENCE, A., KANNO, Y., PACHER-ZAVISIN, M., ZHU, B. M., TATO, C., YOSHIMURA, A., HENNIGHAUSEN, L. & O'SHEA, J. J. 2006. Selective regulatory function of Socs3 in the formation of IL-17-secreting T cells. *Proc Natl Acad Sci U S A*, 103, 8137-42.
- CHIBA, K., KAWAKAMI, K. & TOHYAMA, K. 1998. Simultaneous evaluation of cell viability by neutral red, MTT and crystal violet staining assays of the same cells. *Toxicol In Vitro*, 12, 251-8.
- CHOI, Y. B., SON, M., PARK, M., SHIN, J. & YUN, Y. 2010. SOCS-6 negatively regulates T cell activation through targeting p56lck to proteasomal degradation. *J Biol Chem*, 285, 7271-80.
- CHONG, M. M., CORNISH, A. L., DARWICHE, R., STANLEY, E. G., PURTON, J. F., GODFREY, D. I., HILTON, D. J., STARR, R., ALEXANDER, W. S. & KAY, T. W. 2003. Suppressor of cytokine signaling-1 is a critical regulator of interleukin-7-dependent CD8+ T cell differentiation. *Immunity*, 18, 475-87.
- CLARK, R. 1996. *The Molecular and Cellular Biology of Wound Repair*, Springer Science & Business Media.
- CLARK, R. A., FOLKVORD, J. M., HART, C. E., MURRAY, M. J. & MCPHERSON, J. M. 1989. Platelet isoforms of platelet-derived growth factor stimulate fibroblasts to contract collagen matrices. *J Clin Invest*, 84, 1036-40.

- CLARK, R. A., NIELSEN, L. D., WELCH, M. P. & MCPHERSON, J. M. 1995. Collagen matrices attenuate the collagen-synthetic response of cultured fibroblasts to TGF-beta. *J Cell Sci*, 108 (Pt 3), 1251-61.
- CLARKE, P., GRAY, A. & HOLMAN, R. 2002. Estimating utility values for health states of type 2 diabetic patients using the EQ-5D (UKPDS 62). *Med Decis Making*, 22, 340-9.
- COFFEY, R. J., JR., DERYNCK, R., WILCOX, J. N., BRINGMAN, T. S., GOUSTIN, A. S., MOSES, H. L. & PITTELKOW, M. R. 1987. Production and auto-induction of transforming growth factor-alpha in human keratinocytes. *Nature*, 328, 817-20.
- COHNEY, S. J., SANDEN, D., CACALANO, N. A., YOSHIMURA, A., MUI, A., MIGONE, T. S. & JOHNSTON, J. A. 1999. SOCS-3 is tyrosine phosphorylated in response to interleukin-2 and suppresses STAT5 phosphorylation and lymphocyte proliferation. *Mol Cell Biol*, 19, 4980-8.
- COONDOO, A. 2011. Cytokines in dermatology - a basic overview. *Indian J Dermatol*, 56, 368-74.
- CORDEIRO, M. F., REICHEL, M. B., GAY, J. A., D'ESPOSITA, F., ALEXANDER, R. A. & KHAW, P. T. 1999. Transforming growth factor-beta1, -beta2, and -beta3 in vivo: effects on normal and mitomycin C-modulated conjunctival scarring. *Invest Ophthalmol Vis Sci*, 40, 1975-82.
- CORNISH, A. L., DAVEY, G. M., METCALF, D., PURTON, J. F., CORBIN, J. E., GREENHALGH, C. J., DARWICHE, R., WU, L., NICOLA, N. A., GODFREY, D. I., HEATH, W. R., HILTON, D. J., ALEXANDER, W. S. & STARR, R. 2003. Suppressor of cytokine signaling-1 has IFN-gamma-independent actions in T cell homeostasis. *J Immunol*, 170, 878-86.
- COX, D. A., KUNZ, S., CERLETTI, N., MCMASTER, G. K. & BURK, R. R. 1992. Wound healing in aged animals--effects of locally applied transforming growth factor beta 2 in different model systems. *EXS*, 61, 287-95.
- CRESPO, A., FILLA, M. B., RUSSELL, S. W. & MURPHY, W. J. 2000. Indirect induction of suppressor of cytokine signalling-1 in macrophages stimulated with bacterial lipopolysaccharide: partial role of autocrine/paracrine interferon-alpha/beta. *Biochem J*, 349, 99-104.
- CROKER, B. A., KIU, H. & NICHOLSON, S. E. 2008a. SOCS regulation of the JAK/STAT signalling pathway. *Semin Cell Dev Biol*, 19, 414-22.
- CROKER, B. A., KIU, H., PELLEGRINI, M., TOE, J., PRESTON, S., METCALF, D., O'DONNELL, J. A., CENGIA, L. H., MCARTHUR, K., NICOLA, N. A., ALEXANDER, W. S. & ROBERTS, A. W. 2012. IL-6 promotes acute and chronic inflammatory disease in the absence of SOCS3. *Immunol Cell Biol*, 90, 124-9.
- CROKER, B. A., KREBS, D. L., ZHANG, J. G., WORMALD, S., WILLSON, T. A., STANLEY, E. G., ROBB, L., GREENHALGH, C. J., FORSTER, I., CLAUSEN, B. E., NICOLA, N. A., METCALF, D., HILTON, D. J., ROBERTS, A. W. & ALEXANDER, W. S. 2003. SOCS3 negatively regulates IL-6 signaling in vivo. *Nat Immunol*, 4, 540-5.
- CROKER, B. A., METCALF, D., ROBB, L., WEI, W., MIFSUD, S., DIRAGO, L., CLUSE, L. A., SUTHERLAND, K. D., HARTLEY, L., WILLIAMS, E., ZHANG, J. G., HILTON, D. J., NICOLA, N. A., ALEXANDER, W. S. & ROBERTS, A. W. 2004. SOCS3 is a critical physiological negative regulator of G-CSF signaling and emergency granulopoiesis. *Immunity*, 20, 153-65.
- CROKER, B. A., MIELKE, L. A., WORMALD, S., METCALF, D., KIU, H., ALEXANDER, W. S., HILTON, D. J. & ROBERTS, A. W. 2008b. Socs3 maintains the specificity

- of biological responses to cytokine signals during granulocyte and macrophage differentiation. *Exp Hematol*, 36, 786-98.
- DARBY, I. A., LAVERDET, B., BONTE, F. & DESMOULIERE, A. 2014. Fibroblasts and myofibroblasts in wound healing. *Clin Cosmet Investig Dermatol*, 7, 301-11.
- DE SEPULVEDA, P., OKKENHAUG, K., ROSE, J. L., HAWLEY, R. G., DUBREUIL, P. & ROTTAPPEL, R. 1999. Socs1 binds to multiple signalling proteins and suppresses steel factor-dependent proliferation. *EMBO J*, 18, 904-15.
- DELCOMMENNE, M. & STREULI, C. H. 1995. Control of integrin expression by extracellular matrix. *J Biol Chem*, 270, 26794-801.
- DELGADO-ORTEGA, M., MELO, S. & MEURENS, F. 2011. Expression of SOCS1-7 and CIS mRNA in porcine tissues. *Vet Immunol Immunopathol*, 144, 493-8.
- DELLI BOVI, P., CURATOLA, A. M., KERN, F. G., GRECO, A., ITTMANN, M. & BASILICO, C. 1987. An oncogene isolated by transfection of Kaposi's sarcoma DNA encodes a growth factor that is a member of the FGF family. *Cell*, 50, 729-37.
- DEUEL, T. F., SENIOR, R. M., HUANG, J. S. & GRIFFIN, G. L. 1982. Chemotaxis of monocytes and neutrophils to platelet-derived growth factor. *J Clin Invest*, 69, 1046-9.
- DEY, B. R., FURLANETTO, R. W. & NISSLEY, P. 2000. Suppressor of cytokine signaling (SOCS)-3 protein interacts with the insulin-like growth factor-I receptor. *Biochem Biophys Res Commun*, 278, 38-43.
- DEY, B. R., SPENCE, S. L., NISSLEY, P. & FURLANETTO, R. W. 1998. Interaction of human suppressor of cytokine signaling (SOCS)-2 with the insulin-like growth factor-I receptor. *J Biol Chem*, 273, 24095-101.
- DIAMOND, M. S. & SPRINGER, T. A. 1994. The dynamic regulation of integrin adhesiveness. *Curr Biol*, 4, 506-17.
- DIF, F., SAUNIER, E., DEMENEIX, B., KELLY, P. A. & EDERY, M. 2001. Cytokine-inducible SH2-containing protein suppresses PRL signaling by binding the PRL receptor. *Endocrinology*, 142, 5286-93.
- DOGUSAN, Z., HOOGHE-PETERS, E. L., BERUS, D., VELKENIERS, B. & HOOGHE, R. 2000. Expression of SOCS genes in normal and leukemic human leukocytes stimulated by prolactin, growth hormone and cytokines. *J Neuroimmunol*, 109, 34-9.
- DOMINEY, A. M., WANG, X. J., KING, L. E., JR., NANNY, L. B., GAGNE, T. A., SELLHEYER, K., BUNDMAN, D. S., LONGLEY, M. A., ROTHNAGEL, J. A., GREENHALGH, D. A. & ET AL. 1993. Targeted overexpression of transforming growth factor alpha in the epidermis of transgenic mice elicits hyperplasia, hyperkeratosis, and spontaneous, squamous papillomas. *Cell Growth Differ*, 4, 1071-82.
- DREW, P., POSNETT, J., RUSLING, L. & WOUND CARE AUDIT, T. 2007. The cost of wound care for a local population in England. *Int Wound J*, 4, 149-55.
- DUNCAN, M. R. & BERMAN, B. 1985. Gamma interferon is the lymphokine and beta interferon the monokine responsible for inhibition of fibroblast collagen production and late but not early fibroblast proliferation. *J Exp Med*, 162, 516-27.
- EFRON, P. A. & MOLDAWER, L. L. 2004. Cytokines and wound healing: the role of cytokine and anticytokine therapy in the repair response. *J Burn Care Rehabil*, 25, 149-60.
- EGWUAGU, C. E., YU, C. R., ZHANG, M., MAHDI, R. M., KIM, S. J. & GERY, I. 2002. Suppressors of cytokine signaling proteins are differentially expressed in

- Th1 and Th2 cells: implications for Th cell lineage commitment and maintenance. *J Immunol*, 168, 3181-7.
- EMANUELLI, B., PERALDI, P., FILLoux, C., SAWKA-VERHELLE, D., HILTON, D. & VAN OBBERGHEN, E. 2000. SOCS-3 is an insulin-induced negative regulator of insulin signaling. *J Biol Chem*, 275, 15985-91.
- ENDO, T. A., MASUHARA, M., YOKOUCHI, M., SUZUKI, R., SAKAMOTO, H., MITSUI, K., MATSUMOTO, A., TANIMURA, S., OHTSUBO, M., MISAWA, H., MIYAZAKI, T., LEONOR, N., TANIGUCHI, T., FUJITA, T., KANAKURA, Y., KOMIYA, S. & YOSHIMURA, A. 1997. A new protein containing an SH2 domain that inhibits JAK kinases. *Nature*, 387, 921-4.
- EYLES, J. L., METCALF, D., GRUSBY, M. J., HILTON, D. J. & STARR, R. 2002. Negative regulation of interleukin-12 signaling by suppressor of cytokine signaling-1. *J Biol Chem*, 277, 43735-40.
- FADERL, S., HARRIS, D., VAN, Q., KANTARJIAN, H. M., TALPAZ, M. & ESTROV, Z. 2003. Granulocyte-macrophage colony-stimulating factor (GM-CSF) induces antiapoptotic and proapoptotic signals in acute myeloid leukemia. *Blood*, 102, 630-7.
- FALANGA, V. 2000. Classifications for wound bed preparation and stimulation of chronic wounds. *Wound Repair Regen*, 8, 347-52.
- FALANGA, V. 2005. Wound healing and its impairment in the diabetic foot. *Lancet*, 366, 1736-43.
- FAVRE, H., BENHAMOU, A., FINIDORI, J., KELLY, P. A. & EDERY, M. 1999. Dual effects of suppressor of cytokine signaling (SOCS-2) on growth hormone signal transduction. *FEBS Lett*, 453, 63-6.
- FENG, Y., SANDERS, A. J., MORGAN, L. D., HARDING, K. G. & JIANG, W. G. 2016. Potential roles of suppressor of cytokine signaling in wound healing. *Regen Med*, 11, 193-209.
- FENG, Z. P., CHANDRASHEKARAN, I. R., LOW, A., SPEED, T. P., NICHOLSON, S. E. & NORTON, R. S. 2012. The N-terminal domains of SOCS proteins: a conserved region in the disordered N-termini of SOCS4 and 5. *Proteins*, 80, 946-57.
- FLAUMENHAFT, R., KOJIMA, S., ABE, M. & RIFKIN, D. B. 1993. Activation of latent transforming growth factor beta. *Adv Pharmacol*, 24, 51-76.
- FLAUMENHAFT, R. & RIFKIN, D. B. 1991. Extracellular matrix regulation of growth factor and protease activity. *Curr Opin Cell Biol*, 3, 817-23.
- FOLKMAN, J. & KLAGSBRUN, M. 1987. Angiogenic factors. *Science*, 235, 442-7.
- FOLKMAN, J. & SHING, Y. 1992. Angiogenesis. *J Biol Chem*, 267, 10931-4.
- FORSTER, A. C. & SYMONS, R. H. 1987. Self-cleavage of plus and minus RNAs of a virusoid and a structural model for the active sites. *Cell*, 49, 211-20.
- FREEDBERG, I. M., TOMIC-CANIC, M., KOMINE, M. & BLUMENBERG, M. 2001. Keratins and the keratinocyte activation cycle. *J Invest Dermatol*, 116, 633-40.
- FUJIMOTO, M., NAKA, T., NAKAGAWA, R., KAWAZOE, Y., MORITA, Y., TATEISHI, A., OKUMURA, K., NARAZAKI, M. & KISHIMOTO, T. 2000. Defective thymocyte development and perturbed homeostasis of T cells in STAT-induced STAT inhibitor-1/suppressors of cytokine signaling-1 transgenic mice. *J Immunol*, 165, 1799-806.
- GALIANO, R. D., TEPPER, O. M., PELO, C. R., BHATT, K. A., CALLAGHAN, M., BASTIDAS, N., BUNTING, S., STEINMETZ, H. G. & GURTNER, G. C. 2004. Topical vascular endothelial growth factor accelerates diabetic wound

- healing through increased angiogenesis and by mobilizing and recruiting bone marrow-derived cells. *Am J Pathol*, 164, 1935-47.
- GALKOWSKA, H., WOJEWODZKA, U. & OLSZEWSKI, W. L. 2006. Chemokines, cytokines, and growth factors in keratinocytes and dermal endothelial cells in the margin of chronic diabetic foot ulcers. *Wound Repair Regen*, 14, 558-65.
- GATES, R. E., KING, L. E., JR., HANKS, S. K. & NANNEY, L. B. 1994. Potential role for focal adhesion kinase in migrating and proliferating keratinocytes near epidermal wounds and in culture. *Cell Growth Differ*, 5, 891-9.
- GERBER, H. P., MCMURTREY, A., KOWALSKI, J., YAN, M., KEYT, B. A., DIXIT, V. & FERRARA, N. 1998. Vascular endothelial growth factor regulates endothelial cell survival through the phosphatidylinositol 3'-kinase/Akt signal transduction pathway. Requirement for Flk-1/KDR activation. *J Biol Chem*, 273, 30336-43.
- GIBRAN, N. S., JANG, Y. C., ISIK, F. F., GREENHALGH, D. G., MUFFLEY, L. A., UNDERWOOD, R. A., USUI, M. L., LARSEN, J., SMITH, D. G., BUNNETT, N., ANSEL, J. C. & OLERUD, J. E. 2002. Diminished neuropeptide levels contribute to the impaired cutaneous healing response associated with diabetes mellitus. *J Surg Res*, 108, 122-8.
- GOHEL, M. S. & POSKITT, K. R. 2009. Venous ulceration. *ABC of Arterial and Venous Disease*, 78, 84.
- GOLDSHMIT, Y., WALTERS, C. E., SCOTT, H. J., GREENHALGH, C. J. & TURNLEY, A. M. 2004. SOCS2 induces neurite outgrowth by regulation of epidermal growth factor receptor activation. *J Biol Chem*, 279, 16349-55.
- GOODRIDGE, D., TREPMAN, E., SLOAN, J., GUSE, L., STRAIN, L. A., MCINTYRE, J. & EMBIL, J. M. 2006. Quality of life of adults with unhealed and healed diabetic foot ulcers. *Foot Ankle Int*, 27, 274-80.
- GOREN, I., LINKE, A., MULLER, E., PFEILSCHIFTER, J. & FRANK, S. 2006a. The suppressor of cytokine signaling-3 is upregulated in impaired skin repair: implications for keratinocyte proliferation. *J Invest Dermatol*, 126, 477-85.
- GOREN, I., MULLER, E., PFEILSCHIFTER, J. & FRANK, S. 2006b. Severely impaired insulin signaling in chronic wounds of diabetic ob/ob mice: a potential role of tumor necrosis factor-alpha. *Am J Pathol*, 168, 765-77.
- GRANSTEIN, R. D., MURPHY, G. F., MARGOLIS, R. J., BYRNE, M. H. & AMENTO, E. P. 1987. Gamma-interferon inhibits collagen synthesis in vivo in the mouse. *J Clin Invest*, 79, 1254-8.
- GREENHALGH, C. J., BERTOLINO, P., ASA, S. L., METCALF, D., CORBIN, J. E., ADAMS, T. E., DAVEY, H. W., NICOLA, N. A., HILTON, D. J. & ALEXANDER, W. S. 2002a. Growth enhancement in suppressor of cytokine signaling 2 (SOCS-2)-deficient mice is dependent on signal transducer and activator of transcription 5b (STAT5b). *Mol Endocrinol*, 16, 1394-406.
- GREENHALGH, C. J., METCALF, D., THAUS, A. L., CORBIN, J. E., UREN, R., MORGAN, P. O., FABRI, L. J., ZHANG, J. G., MARTIN, H. M., WILLSON, T. A., BILLESTRUP, N., NICOLA, N. A., BACA, M., ALEXANDER, W. S. & HILTON, D. J. 2002b. Biological evidence that SOCS-2 can act either as an enhancer or suppressor of growth hormone signaling. *J Biol Chem*, 277, 40181-4.
- GREENHALGH, C. J., RICO-BAUTISTA, E., LORENTZON, M., THAUS, A. L., MORGAN, P. O., WILLSON, T. A., ZERVOUDAKIS, P., METCALF, D., STREET, I., NICOLA, N. A., NASH, A. D., FABRI, L. J., NORSTEDT, G., OHLSSON, C., FLORES-MORALES, A., ALEXANDER, W. S. & HILTON, D. J. 2005. SOCS2 negatively

- regulates growth hormone action in vitro and in vivo. *J Clin Invest*, 115, 397-406.
- GREY, J. E., HARDING, K. G. & ENOCH, S. 2006. Venous and arterial leg ulcers. *BMJ*, 332, 347-50.
- GRINNELL, F. 1994. Fibroblasts, myofibroblasts, and wound contraction. *J Cell Biol*, 124, 401-4.
- GROSS, J. L., MOSCATELLI, D. & RIFKIN, D. B. 1983. Increased capillary endothelial cell protease activity in response to angiogenic stimuli in vitro. *Proc Natl Acad Sci U S A*, 80, 2623-7.
- GROTENDORST, G. R., SEPPA, H. E., KLEINMAN, H. K. & MARTIN, G. R. 1981. Attachment of smooth muscle cells to collagen and their migration toward platelet-derived growth factor. *Proc Natl Acad Sci U S A*, 78, 3669-72.
- GULLBERG, D., TINGSTROM, A., THURESSON, A. C., OLSSON, L., TERRACIO, L., BORG, T. K. & RUBIN, K. 1990. Beta 1 integrin-mediated collagen gel contraction is stimulated by PDGF. *Exp Cell Res*, 186, 264-72.
- GUPTA, S., MISHRA, K., SUROLIA, A. & BANERJEE, K. 2011. Suppressor of cytokine signalling-6 promotes neurite outgrowth via JAK2/STAT5-mediated signalling pathway, involving negative feedback inhibition. *PLoS One*, 6, e26674.
- GURTNER, G. C., WERNER, S., BARRANDON, Y. & LONGAKER, M. T. 2008. Wound repair and regeneration. *Nature*, 453, 314-21.
- HAAN, S., FERGUSON, P., SOMMER, U., HIREMATH, M., MCVICAR, D. W., HEINRICH, P. C., JOHNSTON, J. A. & CACALANO, N. A. 2003. Tyrosine phosphorylation disrupts elongin interaction and accelerates SOCS3 degradation. *J Biol Chem*, 278, 31972-9.
- HAASE, I., EVANS, R., POFAHL, R. & WATT, F. M. 2003. Regulation of keratinocyte shape, migration and wound epithelialization by IGF-1- and EGF-dependent signalling pathways. *J Cell Sci*, 116, 3227-38.
- HANADA, T., YOSHIDA, H., KATO, S., TANAKA, K., MASUTANI, K., TSUKADA, J., NOMURA, Y., MIMATA, H., KUBO, M. & YOSHIMURA, A. 2003. Suppressor of cytokine signaling-1 is essential for suppressing dendritic cell activation and systemic autoimmunity. *Immunity*, 19, 437-50.
- HANSEN, J. A., LINDBERG, K., HILTON, D. J., NIELSEN, J. H. & BILLESTRUP, N. 1999. Mechanism of inhibition of growth hormone receptor signaling by suppressor of cytokine signaling proteins. *Mol Endocrinol*, 13, 1832-43.
- HARDING, K. G., MORRIS, H. L. & PATEL, G. K. 2002. Science, medicine and the future: healing chronic wounds. *BMJ*, 324, 160-3.
- HARLAN, J. M., THOMPSON, P. J., ROSS, R. R. & BOWEN-POPE, D. F. 1986. Alpha-thrombin induces release of platelet-derived growth factor-like molecule(s) by cultured human endothelial cells. *J Cell Biol*, 103, 1129-33.
- HARRIS, J., STANFORD, P. M., SUTHERLAND, K., OAKES, S. R., NAYLOR, M. J., ROBERTSON, F. G., BLAZEK, K. D., KAZLAUSKAS, M., HILTON, H. N., WITTLIN, S., ALEXANDER, W. S., LINDEMAN, G. J., VISVADER, J. E. & ORMANDY, C. J. 2006. Socs2 and elf5 mediate prolactin-induced mammary gland development. *Mol Endocrinol*, 20, 1177-87.
- HASELOFF, J. & GERLACH, W. L. 1988. Simple RNA enzymes with new and highly specific endoribonuclease activities. *Nature*, 334, 585-91.
- HE, B., YOU, L., UEMATSU, K., ZANG, K., XU, Z., LEE, A. Y., COSTELLO, J. F., MCCORMICK, F. & JABLONS, D. M. 2003. SOCS-3 is frequently silenced by

- hypermethylation and suppresses cell growth in human lung cancer. *Proc Natl Acad Sci U S A*, 100, 14133-8.
- HEBENSTREIT, D., LUFT, P., SCHMIEDLECHNER, A., REGL, G., FRISCHAUF, A. M., ABERGER, F., DUSCHL, A. & HOREJS-HOECK, J. 2003. IL-4 and IL-13 induce SOCS-1 gene expression in A549 cells by three functional STAT6-binding motifs located upstream of the transcription initiation site. *J Immunol*, 171, 5901-7.
- HELDIN, P., LAURENT, T. C. & HELDIN, C. H. 1989. Effect of growth factors on hyaluronan synthesis in cultured human fibroblasts. *Biochem J*, 258, 919-22.
- HELMAN, D., SANDOWSKI, Y., COHEN, Y., MATSUMOTO, A., YOSHIMURA, A., MERCHAV, S. & GERTLER, A. 1998. Cytokine-inducible SH2 protein (CIS3) and JAK2 binding protein (JAB) abolish prolactin receptor-mediated STAT5 signaling. *FEBS Lett*, 441, 287-91.
- HIGLEY, H. R., KSANDER, G. A., GERHARDT, C. O. & FALANGA, V. 1995. Extravasation of macromolecules and possible trapping of transforming growth factor-beta in venous ulceration. *Br J Dermatol*, 132, 79-85.
- HILTON, D. J., RICHARDSON, R. T., ALEXANDER, W. S., VINEY, E. M., WILLSON, T. A., SPRIGG, N. S., STARR, R., NICHOLSON, S. E., METCALF, D. & NICOLA, N. A. 1998. Twenty proteins containing a C-terminal SOCS box form five structural classes. *Proc Natl Acad Sci U S A*, 95, 114-9.
- HINO, K., SATOU, Y., YAGI, K. & SATOH, N. 2003. A genomewide survey of developmentally relevant genes in *Ciona intestinalis*. VI. Genes for Wnt, TGFbeta, Hedgehog and JAK/STAT signaling pathways. *Dev Genes Evol*, 213, 264-72.
- HIRANO, S., REES, R. S. & GILMONT, R. R. 2002. MAP kinase pathways involving hsp27 regulate fibroblast-mediated wound contraction. *J Surg Res*, 102, 77-84.
- HIWATASHI, K., TAMIYA, T., HASEGAWA, E., FUKAYA, T., HASHIMOTO, M., KAKOI, K., KASHIWAGI, I., KIMURA, A., INOUE, N., MORITA, R., YASUKAWA, H. & YOSHIMURA, A. 2011. Suppression of SOCS3 in macrophages prevents cancer metastasis by modifying macrophage phase and MCP2/CCL8 induction. *Cancer Lett*, 308, 172-80.
- HOLMES, D. I. & ZACHARY, I. 2005. The vascular endothelial growth factor (VEGF) family: angiogenic factors in health and disease. *Genome Biol*, 6, 209.
- HOLT, J. T., THOMPSON, M. E., SZABO, C., ROBINSON-BENION, C., ARTEAGA, C. L., KING, M. C. & JENSEN, R. A. 1996. Growth retardation and tumour inhibition by BRCA1. *Nat Genet*, 12, 298-302.
- HONG, F., NGUYEN, V. A. & GAO, B. 2001. Tumor necrosis factor alpha attenuates interferon alpha signaling in the liver: involvement of SOCS3 and SHP2 and implication in resistance to interferon therapy. *FASEB J*, 15, 1595-7.
- HORVAT, S. & MEDRANO, J. F. 2001. Lack of Socs2 expression causes the high-growth phenotype in mice. *Genomics*, 72, 209-12.
- HOWARD, J. K., CAVE, B. J., OKSANEN, L. J., TZAMELI, I., BJORBAEK, C. & FLIER, J. S. 2004. Enhanced leptin sensitivity and attenuation of diet-induced obesity in mice with haploinsufficiency of Socs3. *Nat Med*, 10, 734-8.
- HU, G., ZHOU, R., LIU, J., GONG, A. Y. & CHEN, X. M. 2010. MicroRNA-98 and let-7 regulate expression of suppressor of cytokine signaling 4 in biliary epithelial cells in response to *Cryptosporidium parvum* infection. *J Infect Dis*, 202, 125-35.

- HUNTER, M. G., JACOB, A., O'DONNELL L. C., AGLER, A., DRUHAN, L. J., COGGESHALL, K. M. & AVALOS, B. R. 2004. Loss of SHIP and CIS recruit to the granulocyte colony-stimulating factor receptor contribute to hyperproliferative responses in severe congenital neutropenia/acute myelogenous leukemia. *J Immunol*, 173, 5036-45.
- HWANG, M. N., MIN, C. H., KIM, H. S., LEE, H., YOON, K. A., PARK, S. Y., LEE, E. S. & YOON, S. 2007. The nuclear localization of SOCS6 requires the N-terminal region and negatively regulates Stat3 protein levels. *Biochem Biophys Res Commun*, 360, 333-8.
- HYNES, R. O. 2007. Cell-matrix adhesion in vascular development. *J Thromb Haemost*, 5 Suppl 1, 32-40.
- IGAZ, P., TOTH, S. & FALUS, A. 2001. Biological and clinical significance of the JAK-STAT pathway; lessons from knockout mice. *Inflamm Res*, 50, 435-41.
- ILANGUMARAN, S., RAMANATHAN, S., NING, T., LA ROSE, J., REINHART, B., POUSSIER, P. & ROTTAPPEL, R. 2003. Suppressor of cytokine signaling 1 attenuates IL-15 receptor signaling in CD8+ thymocytes. *Blood*, 102, 4115-22.
- INAGAKI-OHARA, K., MAYUZUMI, H., KATO, S., MINOKOSHI, Y., OTSUBO, T., KAWAMURA, Y. I., DOHI, T., MATSUZAKI, G. & YOSHIMURA, A. 2014. Enhancement of leptin receptor signaling by SOCS3 deficiency induces development of gastric tumors in mice. *Oncogene*, 33, 74-84.
- IRANDOUST, M. I., AARTS, L. H., ROOVERS, O., GITS, J., ERKELAND, S. J. & TOUW, I. P. 2007. Suppressor of cytokine signaling 3 controls lysosomal routing of G-CSF receptor. *EMBO J*, 26, 1782-93.
- ISAKSEN, D. E., BAUMANN, H., TROBRIDGE, P. A., FARR, A. G., LEVIN, S. D. & ZIEGLER, S. F. 1999. Requirement for stat5 in thymic stromal lymphopoietin-mediated signal transduction. *J Immunol*, 163, 5971-7.
- ITO, A., SATO, T., IGA, T. & MORI, Y. 1990. Tumor necrosis factor bifunctionally regulates matrix metalloproteinases and tissue inhibitor of metalloproteinases (TIMP) production by human fibroblasts. *FEBS Lett*, 269, 93-5.
- JAKSA, P. J. & MAHONEY, J. L. 2010. Quality of life in patients with diabetic foot ulcers: validation of the Cardiff Wound Impact Schedule in a Canadian population. *Int Wound J*, 7, 502-7.
- JEONG, H. W. & KIM, I. S. 2004. TGF-beta1 enhances betaig-h3-mediated keratinocyte cell migration through the alpha3beta1 integrin and PI3K. *J Cell Biochem*, 92, 770-80.
- JIANG, C. K., FLANAGAN, S., OHTSUKI, M., SHUAI, K., FREEDBERG, I. M. & BLUMENBERG, M. 1994. Disease-activated transcription factor: allergic reactions in human skin cause nuclear translocation of STAT-91 and induce synthesis of keratin K17. *Mol Cell Biol*, 14, 4759-69.
- JOHNSON, K. E. & WILGUS, T. A. 2014. Vascular Endothelial Growth Factor and Angiogenesis in the Regulation of Cutaneous Wound Repair. *Adv Wound Care (New Rochelle)*, 3, 647-661.
- JONES, A. M., GRIFFITHS, J. L., SANDERS, A. J., OWEN, S., RUGE, F., HARDING, K. G. & JIANG, W. G. 2016. The clinical significance and impact of interleukin 15 on keratinocyte cell growth and migration. *Int J Mol Med*, 38, 679-86.
- JONES, S. C., CURTSINGER, L. J., WHALEN, J. D., PIETSCH, J. D., ACKERMAN, D., BROWN, G. L. & SCHULTZ, G. S. 1991. Effect of topical recombinant TGF-beta on healing of partial thickness injuries. *J Surg Res*, 51, 344-52.

- JORGENSEN, S. B., O'NEILL, H. M., SYLOW, L., HONEYMAN, J., HEWITT, K. A., PALANIVEL, R., FULLERTON, M. D., OBERG, L., BALENDRAN, A., GALIC, S., VAN DER POEL, C., TROUNCE, I. A., LYNCH, G. S., SCHERTZER, J. D. & STEINBERG, G. R. 2013. Deletion of skeletal muscle SOCS3 prevents insulin resistance in obesity. *Diabetes*, 62, 56-64.
- KAMURA, T., MAENAKA, K., KOTOSHIBA, S., MATSUMOTO, M., KOHDA, D., CONAWAY, R. C., CONAWAY, J. W. & NAKAYAMA, K. I. 2004. VHL-box and SOCS-box domains determine binding specificity for Cul2-Rbx1 and Cul5-Rbx2 modules of ubiquitin ligases. *Genes Dev*, 18, 3055-65.
- KANDA, S., LANDGREN, E., LJUNGSTROM, M. & CLAESSION-WELSH, L. 1996. Fibroblast growth factor receptor 1-induced differentiation of endothelial cell line established from tsA58 large T transgenic mice. *Cell Growth Differ*, 7, 383-95.
- KANDEL, J., BOSSY-WETZEL, E., RADVANYI, F., KLAGSBRUN, M., FOLKMAN, J. & HANAHAN, D. 1991. Neovascularization is associated with a switch to the export of bFGF in the multistep development of fibrosarcoma. *Cell*, 66, 1095-104.
- KARIO, E., MARMOR, M. D., ADAMSKY, K., CITRI, A., AMIT, I., AMARIGLIO, N., RECHAVI, G. & YARDEN, Y. 2005. Suppressors of cytokine signaling 4 and 5 regulate epidermal growth factor receptor signaling. *J Biol Chem*, 280, 7038-48.
- KARLSEN, A. E., RONN, S. G., LINDBERG, K., JOHANNESSEN, J., GALSGAARD, E. D., POCIOT, F., NIELSEN, J. H., MANDRUP-POULSEN, T., NERUP, J. & BILLESTRUP, N. 2001. Suppressor of cytokine signaling 3 (SOCS-3) protects beta -cells against interleukin-1beta - and interferon-gamma -mediated toxicity. *Proc Natl Acad Sci U S A*, 98, 12191-6.
- KARSTEN, P., HADER, S. & ZEIDLER, M. P. 2002. Cloning and expression of Drosophila SOCS36E and its potential regulation by the JAK/STAT pathway. *Mech Dev*, 117, 343-6.
- KATO, H., NOMURA, K., OSABE, D., SHINOHARA, S., MIZUMORI, O., KATASHIMA, R., IWASAKI, S., NISHIMURA, K., YOSHINO, M., KOBORI, M., ICHIISHI, E., NAKAMURA, N., YOSHIKAWA, T., TANAHASHI, T., KESHAVARZ, P., KUNIKA, K., MORITANI, M., KUDO, E., TSUGAWA, K., TAKATA, Y., HAMADA, D., YASUI, N., MIYAMOTO, T., SHIOTA, H., INOUE, H. & ITAKURA, M. 2006. Association of single-nucleotide polymorphisms in the suppressor of cytokine signaling 2 (SOCS2) gene with type 2 diabetes in the Japanese. *Genomics*, 87, 446-58.
- KAWAZOE, Y., NAKA, T., FUJIMOTO, M., KOHZAKI, H., MORITA, Y., NARAZAKI, M., OKUMURA, K., SAITOH, H., NAKAGAWA, R., UCHIYAMA, Y., AKIRA, S. & KISHIMOTO, T. 2001. Signal transducer and activator of transcription (STAT)-induced STAT inhibitor 1 (SSI-1)/suppressor of cytokine signaling 1 (SOCS1) inhibits insulin signal transduction pathway through modulating insulin receptor substrate 1 (IRS-1) phosphorylation. *J Exp Med*, 193, 263-9.
- KAZI, J. U. & RONNSTRAND, L. 2013. Suppressor of cytokine signaling 2 (SOCS2) associates with FLT3 and negatively regulates downstream signaling. *Mol Oncol*, 7, 693-703.
- KAZI, J. U., SUN, J., PHUNG, B., ZADJALI, F., FLORES-MORALES, A. & RONNSTRAND, L. 2012. Suppressor of cytokine signaling 6 (SOCS6) negatively regulates Flt3 signal transduction through direct binding to phosphorylated tyrosines 591 and 919 of Flt3. *J Biol Chem*, 287, 36509-17.

- KEDZIERSKI, L., LINOSSI, E. M., KOLESNIK, T. B., DAY, E. B., BIRD, N. L., KILE, B. T., BELZ, G. T., METCALF, D., NICOLA, N. A., KEDZIERSKA, K. & NICHOLSON, S. E. 2014. Suppressor of cytokine signaling 4 (SOCS4) protects against severe cytokine storm and enhances viral clearance during influenza infection. *PLoS Pathog*, 10, e1004134.
- KERSHAW, N. J., LAKTYUSHIN, A., NICOLA, N. A. & BABON, J. J. 2014. Reconstruction of an active SOCS3-based E3 ubiquitin ligase complex in vitro: identification of the active components and JAK2 and gp130 as substrates. *Growth Factors*, 32, 1-10.
- KERSHAW, N. J., MURPHY, J. M., LIAU, N. P., VARGHESE, L. N., LAKTYUSHIN, A., WHITLOCK, E. L., LUCET, I. S., NICOLA, N. A. & BABON, J. J. 2013. SOCS3 binds specific receptor-JAK complexes to control cytokine signaling by direct kinase inhibition. *Nat Struct Mol Biol*, 20, 469-76.
- KIEVIT, P., HOWARD, J. K., BADMAN, M. K., BALTHASAR, N., COPPARI, R., MORI, H., LEE, C. E., ELMQUIST, J. K., YOSHIMURA, A. & FLIER, J. S. 2006. Enhanced leptin sensitivity and improved glucose homeostasis in mice lacking suppressor of cytokine signaling-3 in POMC-expressing cells. *Cell Metab*, 4, 123-32.
- KINJYO, I., HANADA, T., INAGAKI-OHARA, K., MORI, H., AKI, D., OHISHI, M., YOSHIDA, H., KUBO, M. & YOSHIMURA, A. 2002. SOCS1/JAB is a negative regulator of LPS-induced macrophage activation. *Immunity*, 17, 583-91.
- KISSELEVA, T., BHATTACHARYA, S., BRAUNSTEIN, J. & SCHINDLER, C. W. 2002. Signaling through the JAK/STAT pathway, recent advances and future challenges. *Gene*, 285, 1-24.
- KLAGSBRUN, M. 1989. The fibroblast growth factor family: structural and biological properties. *Prog Growth Factor Res*, 1, 207-35.
- KNISZ, J., BANKS, A., MCKEAG, L., METCALFE, D. D., ROTHMAN, P. B. & BROWN, J. M. 2009. Loss of SOCS7 in mice results in severe cutaneous disease and increased mast cell activation. *Clin Immunol*, 132, 277-84.
- KOBAYASHI, D., NOMOTO, S., KODERA, Y., FUJIWARA, M., KOIKE, M., NAKAYAMA, G., OHASHI, N. & NAKAO, A. 2012. Suppressor of cytokine signaling 4 detected as a novel gastric cancer suppressor gene using double combination array analysis. *World J Surg*, 36, 362-72.
- KOO, Y. & YUN, Y. 2016. Effects of polydeoxyribonucleotides (PDRN) on wound healing: Electric cell-substrate impedance sensing (ECIS). *Mater Sci Eng C Mater Biol Appl*, 69, 554-60.
- KOTENKO, S. V., IZOTOVA, L. S., MIROCHNITCHENKO, O. V., ESTEROVA, E., DICKENSHEETS, H., DONNELLY, R. P. & PESTKA, S. 2001. Identification, cloning, and characterization of a novel soluble receptor that binds IL-22 and neutralizes its activity. *J Immunol*, 166, 7096-103.
- KREBS, D. L. & HILTON, D. J. 2001. SOCS proteins: negative regulators of cytokine signaling. *Stem Cells*, 19, 378-87.
- KREBS, D. L., METCALF, D., MERSON, T. D., VOSS, A. K., THOMAS, T., ZHANG, J. G., RAKAR, S., O'BRYAN M, K., WILLSON, T. A., VINEY, E. M., MIELKE, L. A., NICOLA, N. A., HILTON, D. J. & ALEXANDER, W. S. 2004. Development of hydrocephalus in mice lacking SOCS7. *Proc Natl Acad Sci U S A*, 101, 15446-51.
- KREBS, D. L., UREN, R. T., METCALF, D., RAKAR, S., ZHANG, J. G., STARR, R., DE SOUZA, D. P., HANZINIKOLAS, K., EYLES, J., CONNOLLY, L. M., SIMPSON, R. J., NICOLA, N. A., NICHOLSON, S. E., BACA, M., HILTON, D. J. & ALEXANDER, W. S. 2002. SOCS-6 binds to insulin receptor substrate 4, and mice lacking

- the SOCS-6 gene exhibit mild growth retardation. *Mol Cell Biol*, 22, 4567-78.
- KREMER, B. E., ADANG, L. A. & MACARA, I. G. 2007. Septins regulate actin organization and cell-cycle arrest through nuclear accumulation of NCK mediated by SOCS7. *Cell*, 130, 837-50.
- KSANDER, G. A., CHU, G. H., MCMULLIN, H., OGAWA, Y., PRATT, B. M., ROSENBLATT, J. S. & MCPHERSON, J. M. 1990. Transforming growth factors-beta 1 and beta 2 enhance connective tissue formation in animal models of dermal wound healing by secondary intent. *Ann N Y Acad Sci*, 593, 135-47.
- KSANDER, G. A., GERHARDT, C. O. & OLSEN, D. R. 1993. Exogenous transforming growth factor-beta(2) enhances connective tissue formation in transforming growth factor-beta(1)-deficient, healing-impaired dermal wounds in mice. *Wound Repair Regen*, 1, 137-48.
- KURKINEN, M., VAHERI, A., ROBERTS, P. J. & STENMAN, S. 1980. Sequential appearance of fibronectin and collagen in experimental granulation tissue. *Lab Invest*, 43, 47-51.
- LADWIG, G. P., ROBSON, M. C., LIU, R., KUHN, M. A., MUIR, D. F. & SCHULTZ, G. S. 2002. Ratios of activated matrix metalloproteinase-9 to tissue inhibitor of matrix metalloproteinase-1 in wound fluids are inversely correlated with healing of pressure ulcers. *Wound Repair Regen*, 10, 26-37.
- LAITEERAPONG, N., KARTER, A. J., LIU, J. Y., MOFFET, H. H., SUDORE, R., SCHILLINGER, D., JOHN, P. M. & HUANG, E. S. 2011. Correlates of quality of life in older adults with diabetes: the diabetes & aging study. *Diabetes Care*, 34, 1749-53.
- LANG, R., PAULEAU, A. L., PARGANAS, E., TAKAHASHI, Y., MAGES, J., IHLE, J. N., RUTSCHMAN, R. & MURRAY, P. J. 2003. SOCS3 regulates the plasticity of gp130 signaling. *Nat Immunol*, 4, 546-50.
- LAVENS, D., MONTOYE, T., PIESSEVAUX, J., ZABEAU, L., VANDEKERCKHOVE, J., GEVAERT, K., BECKER, W., EYCKERMAN, S. & TAVERNIER, J. 2006. A complex interaction pattern of CIS and SOCS2 with the leptin receptor. *J Cell Sci*, 119, 2214-24.
- LAZARUS, G. S., COOPER, D. M., KNIGHTON, D. R., PERCORARO, R. E., RODEHEAVER, G. & ROBSON, M. C. 1994. Definitions and guidelines for assessment of wounds and evaluation of healing. *Wound Repair Regen*, 2, 165-70.
- LE, Y., ZHU, B. M., HARLEY, B., PARK, S. Y., KOBAYASHI, T., MANIS, J. P., LUO, H. R., YOSHIMURA, A., HENNIGHAUSEN, L. & SILBERSTEIN, L. E. 2007. SOCS3 protein developmentally regulates the chemokine receptor CXCR4-FAK signaling pathway during B lymphopoiesis. *Immunity*, 27, 811-23.
- LEE, C., KOLESNIK, T. B., CAMINSCHI, I., CHAKRAVORTY, A., CARTER, W., ALEXANDER, W. S., JONES, J., ANDERSON, G. P. & NICHOLSON, S. E. 2009. Suppressor of cytokine signalling 1 (SOCS1) is a physiological regulator of the asthma response. *Clin Exp Allergy*, 39, 897-907.
- LEE, S. H., YUN, S., PIAO, Z. H., JEONG, M., KIM, D. O., JUNG, H., LEE, J., KIM, M. J., KIM, M. S., CHUNG, J. W., KIM, T. D., YOON, S. R., GREENBERG, P. D. & CHOI, I. 2010. Suppressor of cytokine signaling 2 regulates IL-15-primed human NK cell function via control of phosphorylated Pyk2. *J Immunol*, 185, 917-28.
- LEJEUNE, D., DEMOULIN, J. B. & RENAULD, J. C. 2001. Interleukin 9 induces expression of three cytokine signal inhibitors: cytokine-inducible SH2-

- containing protein, suppressor of cytokine signalling (SOCS)-2 and SOCS-3, but only SOCS-3 overexpression suppresses interleukin 9 signalling. *Biochem J*, 353, 109-116.
- LESINA, M., KURKOWSKI, M. U., LUDES, K., ROSE-JOHN, S., TREIBER, M., KLOPPPEL, G., YOSHIMURA, A., REINDL, W., SIPOS, B., AKIRA, S., SCHMID, R. M. & ALGUL, H. 2011. Stat3/Socs3 activation by IL-6 transsignaling promotes progression of pancreatic intraepithelial neoplasia and development of pancreatic cancer. *Cancer Cell*, 19, 456-69.
- LEUNG, D. W., CACHIANES, G., KUANG, W. J., GOEDEL, D. V. & FERRARA, N. 1989. Vascular endothelial growth factor is a secreted angiogenic mitogen. *Science*, 246, 1306-9.
- LEUNG, D. Y. 1995. Atopic dermatitis: the skin as a window into the pathogenesis of chronic allergic diseases. *J Allergy Clin Immunol*, 96, 302-18; quiz 319.
- LEUNG, K. C., DOYLE, N., BALLESTEROS, M., SJOGREN, K., WATTS, C. K., LOW, T. H., LEONG, G. M., ROSS, R. J. & HO, K. K. 2003. Estrogen inhibits GH signaling by suppressing GH-induced JAK2 phosphorylation, an effect mediated by SOCS-2. *Proc Natl Acad Sci U S A*, 100, 1016-21.
- LI, J., ZHANG, Y. P. & KIRSNER, R. S. 2003. Angiogenesis in wound repair: angiogenic growth factors and the extracellular matrix. *Microsc Res Tech*, 60, 107-14.
- LI, L., GRONNING, L. M., ANDERSON, P. O., LI, S., EDVARSEN, K., JOHNSTON, J., KIOUSSIS, D., SHEPHERD, P. R. & WANG, P. 2004. Insulin induces SOCS-6 expression and its binding to the p85 monomer of phosphoinositide 3-kinase, resulting in improvement in glucose metabolism. *J Biol Chem*, 279, 34107-14.
- LI, Y., CHU, N., ROSTAMI, A. & ZHANG, G. X. 2006. Dendritic cells transduced with SOCS-3 exhibit a tolerogenic/DC2 phenotype that directs type 2 Th cell differentiation in vitro and in vivo. *J Immunol*, 177, 1679-88.
- LINKE, A., GOREN, I., BOSL, M. R., PFEILSCHIFTER, J. & FRANK, S. 2010a. Epithelial overexpression of SOCS-3 in transgenic mice exacerbates wound inflammation in the presence of elevated TGF-beta1. *J Invest Dermatol*, 130, 866-75.
- LINKE, A., GOREN, I., BOSL, M. R., PFEILSCHIFTER, J. & FRANK, S. 2010b. The suppressor of cytokine signaling (SOCS)-3 determines keratinocyte proliferative and migratory potential during skin repair. *J Invest Dermatol*, 130, 876-85.
- LIONGUE, C., O'SULLIVAN, L. A., TRENGOVE, M. C. & WARD, A. C. 2012. Evolution of JAK-STAT pathway components: mechanisms and role in immune system development. *PLoS One*, 7, e32777.
- LIU, C. L., TAM, J. C., SANDERS, A. J., KO, C. H., FUNG, K. P., LEUNG, P. C., HARDING, K. G., JIANG, W. G. & LAU, C. B. 2013. Molecular angiogenic events of a two-herb wound healing formula involving MAPK and Akt signaling pathways in human vascular endothelial cells. *Wound Repair Regen*, 21, 579-87.
- LIU, E., COTE, J. F. & VUORI, K. 2003. Negative regulation of FAK signaling by SOCS proteins. *EMBO J*, 22, 5036-46.
- LIU, X., MAMEZA, M. G., LEE, Y. S., ESEONU, C. I., YU, C. R., KANG DERWENT, J. J. & EGWUAGU, C. E. 2008a. Suppressors of cytokine-signaling proteins induce insulin resistance in the retina and promote survival of retinal cells. *Diabetes*, 57, 1651-8.

- LIU, X., ZHANG, Y., YU, Y., YANG, X. & CAO, X. 2008b. SOCS3 promotes TLR4 response in macrophages by feedback inhibiting TGF-beta1/Smad3 signaling. *Mol Immunol*, 45, 1405-13.
- LOBB, R. R., ALDERMAN, E. M. & FETT, J. W. 1985. Induction of angiogenesis by bovine brain derived class 1 heparin-binding growth factor. *Biochemistry*, 24, 4969-73.
- LOBMANN, R., AMBROSCH, A., SCHULTZ, G., WALDMANN, K., SCHIWECK, S. & LEHNERT, H. 2002. Expression of matrix-metalloproteinases and their inhibitors in the wounds of diabetic and non-diabetic patients. *Diabetologia*, 45, 1011-6.
- LONGMATE, W. M. & DIPERSIO, C. M. 2014. Integrin Regulation of Epidermal Functions in Wounds. *Adv Wound Care (New Rochelle)*, 3, 229-246.
- LOSMAN, J. A., CHEN, X. P., HILTON, D. & ROTHMAN, P. 1999. Cutting edge: SOCS-1 is a potent inhibitor of IL-4 signal transduction. *J Immunol*, 162, 3770-4.
- LOVATO, P., BRENDER, C., AGNHOLT, J., KELSEN, J., KALTOFT, K., SVEJGAARD, A., ERIKSEN, K. W., WOETMANN, A. & ODUM, N. 2003. Constitutive STAT3 activation in intestinal T cells from patients with Crohn's disease. *J Biol Chem*, 278, 16777-81.
- MACHADO, F. S., JOHNDROW, J. E., ESPER, L., DIAS, A., BAFICA, A., SERHAN, C. N. & ALIBERTI, J. 2006. Anti-inflammatory actions of lipoxin A4 and aspirin-triggered lipoxin are SOCS-2 dependent. *Nat Med*, 12, 330-4.
- MADONNA, S., SCARPONI, C., DE PITA, O. & ALBANESI, C. 2008. Suppressor of cytokine signaling 1 inhibits IFN-gamma inflammatory signaling in human keratinocytes by sustaining ERK1/2 activation. *FASEB J*, 22, 3287-97.
- MADONNA, S., SCARPONI, C., PALLOTTA, S., CAVANI, A. & ALBANESI, C. 2012. Anti-apoptotic effects of suppressor of cytokine signaling 3 and 1 in psoriasis. *Cell Death Dis*, 3, e334.
- MAGRANGEAS, F., APIOU, F., DENIS, S., WEIDLE, U., JACQUES, Y. & MINVIELLE, S. 2000. Cloning and expression of CIS6, chromosome assignment to 3p22 and 2p21 by in situ hybridization. *Cytogenet Cell Genet*, 88, 78-81.
- MAGRANGEAS, F., BOISTEAU, O., DENIS, S., JACQUES, Y. & MINVIELLE, S. 2001a. Negative cross-talk between interleukin-3 and interleukin-11 is mediated by suppressor of cytokine signalling-3 (SOCS-3). *Biochem J*, 353, 223-30.
- MAGRANGEAS, F., BOISTEAU, O., DENIS, S., JACQUES, Y. & MINVIELLE, S. 2001b. Negative regulation of oncostatin M signaling by suppressor of cytokine signaling (SOCS-3). *Eur Cytokine Netw*, 12, 309-15.
- MAN, X. Y., YANG, X. H., CAI, S. Q., YAO, Y. G. & ZHENG, M. 2006. Immunolocalization and expression of vascular endothelial growth factor receptors (VEGFRs) and neuropilins (NRPs) on keratinocytes in human epidermis. *Mol Med*, 12, 127-36.
- MARINE, J. C., MCKAY, C., WANG, D., TOPHAM, D. J., PARGANAS, E., NAKAJIMA, H., PENDEVILLE, H., YASUKAWA, H., SASAKI, A., YOSHIMURA, A. & IHLE, J. N. 1999a. SOCS3 is essential in the regulation of fetal liver erythropoiesis. *Cell*, 98, 617-27.
- MARINE, J. C., TOPHAM, D. J., MCKAY, C., WANG, D., PARGANAS, E., STRAVOPODIS, D., YOSHIMURA, A. & IHLE, J. N. 1999b. SOCS1 deficiency causes a lymphocyte-dependent perinatal lethality. *Cell*, 98, 609-16.
- MARTENS, N., UZAN, G., WERY, M., HOOGHE, R., HOOGHE-PETERS, E. L. & GERTLER, A. 2005. Suppressor of cytokine signaling 7 inhibits prolactin, growth hormone, and leptin signaling by interacting with STAT5 or STAT3 and attenuating their nuclear translocation. *J Biol Chem*, 280, 13817-23.

- MARTENS, N., WERY, M., WANG, P., BRAET, F., GERTLER, A., HOOGHE, R., VANDENHAUTE, J. & HOOGHE-PETERS, E. L. 2004. The suppressor of cytokine signaling (SOCS)-7 interacts with the actin cytoskeleton through vinexin. *Exp Cell Res*, 298, 239-48.
- MARTIN, P. & LEBOVICH, S. J. 2005. Inflammatory cells during wound repair: the good, the bad and the ugly. *Trends Cell Biol*, 15, 599-607.
- MARUYAMA, K., ASAI, J., II, M., THORNE, T., LOSORDO, D. W. & D'AMORE, P. A. 2007. Decreased macrophage number and activation lead to reduced lymphatic vessel formation and contribute to impaired diabetic wound healing. *Am J Pathol*, 170, 1178-91.
- MARX, M., PERLMUTTER, R. A. & MADRI, J. A. 1994. Modulation of platelet-derived growth factor receptor expression in microvascular endothelial cells during in vitro angiogenesis. *J Clin Invest*, 93, 131-9.
- MASUHIRO, Y., KAYAMA, K., FUKUSHIMA, A., BABA, K., SOUTSU, M., KAMIYA, Y., GOTOH, M., YAMAGUCHI, N. & HANAZAWA, S. 2008. SOCS-3 inhibits E2F/DP-1 transcriptional activity and cell cycle progression via interaction with DP-1. *J Biol Chem*, 283, 31575-83.
- MATSUMOTO, A., MASUHARA, M., MITSUI, K., YOKOUCHI, M., OHTSUBO, M., MISAWA, H., MIYAJIMA, A. & YOSHIMURA, A. 1997. CIS, a cytokine inducible SH2 protein, is a target of the JAK-STAT5 pathway and modulates STAT5 activation. *Blood*, 89, 3148-54.
- MATSUMOTO, A., SEKI, Y., KUBO, M., OHTSUKA, S., SUZUKI, A., HAYASHI, I., TSUJI, K., NAKAHATA, T., OKABE, M., YAMADA, S. & YOSHIMURA, A. 1999. Suppression of STAT5 functions in liver, mammary glands, and T cells in cytokine-inducible SH2-containing protein 1 transgenic mice. *Mol Cell Biol*, 19, 6396-407.
- MATSUMOTO, A., SEKI, Y., WATANABE, R., HAYASHI, K., JOHNSTON, J. A., HARADA, Y., ABE, R., YOSHIMURA, A. & KUBO, M. 2003. A role of suppressor of cytokine signaling 3 (SOCS3/CIS3/SSI3) in CD28-mediated interleukin 2 production. *J Exp Med*, 197, 425-36.
- MATUOKA, K., MIKI, H., TAKAHASHI, K. & TAKENAWA, T. 1997. A novel ligand for an SH3 domain of the adaptor protein Nck bears an SH2 domain and nuclear signaling motifs. *Biochem Biophys Res Commun*, 239, 488-92.
- MCFARLAND-MANCINI, M. M., FUNK, H. M., PALUCH, A. M., ZHOU, M., GIRIDHAR, P. V., MERCER, C. A., KOZMA, S. C. & DREW, A. F. 2010. Differences in wound healing in mice with deficiency of IL-6 versus IL-6 receptor. *J Immunol*, 184, 7219-28.
- MEI, Z., CHEN, S., CHEN, C., XIAO, B., LI, F., WANG, Y. & TAO, Z. 2015. Interleukin-23 Facilitates Thyroid Cancer Cell Migration and Invasion by Inhibiting SOCS4 Expression via MicroRNA-25. *PLoS One*, 10, e0139456.
- MENDEZ, M. V., RAFFETTO, J. D., PHILLIPS, T., MENZOIAN, J. O. & PARK, H. Y. 1999. The proliferative capacity of neonatal skin fibroblasts is reduced after exposure to venous ulcer wound fluid: A potential mechanism for senescence in venous ulcers. *J Vasc Surg*, 30, 734-43.
- MENKE, N. B., WARD, K. R., WITTEN, T. M., BONCHEV, D. G. & DIEGELMANN, R. F. 2007. Impaired wound healing. *Clin Dermatol*, 25, 19-25.
- METCALF, D., ALEXANDER, W. S., ELEFANTY, A. G., NICOLA, N. A., HILTON, D. J., STARR, R., MIFSUD, S. & DI RAGO, L. 1999. Aberrant hematopoiesis in mice with inactivation of the gene encoding SOCS-1. *Leukemia*, 13, 926-34.

- METCALF, D., GREENHALGH, C. J., VINEY, E., WILLSON, T. A., STARR, R., NICOLA, N. A., HILTON, D. J. & ALEXANDER, W. S. 2000. Gigantism in mice lacking suppressor of cytokine signalling-2. *Nature*, 405, 1069-73.
- METCALF, D., MIFSUD, S., DI RAGO, L., NICOLA, N. A., HILTON, D. J. & ALEXANDER, W. S. 2002. Polycystic kidneys and chronic inflammatory lesions are the delayed consequences of loss of the suppressor of cytokine signaling-1 (SOCS-1). *Proc Natl Acad Sci U S A*, 99, 943-8.
- MIGNATTI, P., TSUBOI, R., ROBBINS, E. & RIFKIN, D. B. 1989. In vitro angiogenesis on the human amniotic membrane: requirement for basic fibroblast growth factor-induced proteinases. *J Cell Biol*, 108, 671-82.
- MILLER, M. E., MICHAYLIRA, C. Z., SIMMONS, J. G., NEY, D. M., DAHLY, E. M., HEATH, J. K. & LUND, P. K. 2004. Suppressor of cytokine signaling-2: a growth hormone-inducible inhibitor of intestinal epithelial cell proliferation. *Gastroenterology*, 127, 570-81.
- MINAMOTO, S., Ikegame, K., UENO, K., NARAZAKI, M., NAKA, T., YAMAMOTO, H., MATSUMOTO, T., SAITO, H., HOSOE, S. & KISHIMOTO, T. 1997. Cloning and functional analysis of new members of STAT induced STAT inhibitor (SSI) family: SSI-2 and SSI-3. *Biochem Biophys Res Commun*, 237, 79-83.
- MIYANAKA, Y., UENO, Y., TANAKA, S., YOSHIOKA, K., HATAKEYAMA, T., SHIMAMOTO, M., SUMII, M. & CHAYAMA, K. 2007. Clinical significance of mucosal suppressors of cytokine signaling 3 expression in ulcerative colitis. *World J Gastroenterol*, 13, 2939-44.
- MONTESANO, R., VASSALLI, J. D., BAIRD, A., GUILLEMIN, R. & ORCI, L. 1986. Basic fibroblast growth factor induces angiogenesis in vitro. *Proc Natl Acad Sci U S A*, 83, 7297-301.
- MOONEY, R. A., SENN, J., CAMERON, S., INAMDAR, N., BOIVIN, L. M., SHANG, Y. & FURLANETTO, R. W. 2001. Suppressors of cytokine signaling-1 and -6 associate with and inhibit the insulin receptor. A potential mechanism for cytokine-mediated insulin resistance. *J Biol Chem*, 276, 25889-93.
- MOREO, K. 2005. Understanding and overcoming the challenges of effective case management for patients with chronic wounds. *Case Manager*, 16, 62-3, 67.
- MORI, H., HANADA, R., HANADA, T., AKI, D., MASHIMA, R., NISHINAKAMURA, H., TORISU, T., CHIEN, K. R., YASUKAWA, H. & YOSHIMURA, A. 2004. Socs3 deficiency in the brain elevates leptin sensitivity and confers resistance to diet-induced obesity. *Nat Med*, 10, 739-43.
- MORITA, Y., NAKA, T., KAWAZOE, Y., FUJIMOTO, M., NARAZAKI, M., NAKAGAWA, R., FUKUYAMA, H., NAGATA, S. & KISHIMOTO, T. 2000. Signals transducers and activators of transcription (STAT)-induced STAT inhibitor-1 (SSI-1)/suppressor of cytokine signaling-1 (SOCS-1) suppresses tumor necrosis factor alpha-induced cell death in fibroblasts. *Proc Natl Acad Sci U S A*, 97, 5405-10.
- MORIWAKI, A., INOUE, H., NAKANO, T., MATSUNAGA, Y., MATSUNO, Y., MATSUMOTO, T., FUKUYAMA, S., KAN, O. K., MATSUMOTO, K., TSUDA-EGUCHI, M., NAGAKUBO, D., YOSHIE, O., YOSHIMURA, A., KUBO, M. & NAKANISHI, Y. 2011. T cell treatment with small interfering RNA for suppressor of cytokine signaling 3 modulates allergic airway responses in a murine model of asthma. *Am J Respir Cell Mol Biol*, 44, 448-55.
- MOTTA, M., ACCORNERO, P. & BARATTA, M. 2004. Leptin and prolactin modulate the expression of SOCS-1 in association with interleukin-6 and tumor

- necrosis factor-alpha in mammary cells: a role in differentiated secretory epithelium. *Regul Pept*, 121, 163-70.
- MUSTOE, T. A., O'SHAUGHNESSY, K. & KLOETERS, O. 2006. Chronic wound pathogenesis and current treatment strategies: a unifying hypothesis. *Plast Reconstr Surg*, 117, 35S-41S.
- MUSTOE, T. A., PIERCE, G. F., MORISHIMA, C. & DEUEL, T. F. 1991. Growth factor-induced acceleration of tissue repair through direct and inductive activities in a rabbit dermal ulcer model. *J Clin Invest*, 87, 694-703.
- MUSTOE, T. A., PIERCE, G. F., THOMASON, A., GRAMATES, P., SPORN, M. B. & DEUEL, T. F. 1987. Accelerated healing of incisional wounds in rats induced by transforming growth factor-beta. *Science*, 237, 1333-6.
- NAKA, T., MATSUMOTO, T., NARAZAKI, M., FUJIMOTO, M., MORITA, Y., OHSAWA, Y., SAITO, H., NAGASAWA, T., UCHIYAMA, Y. & KISHIMOTO, T. 1998. Accelerated apoptosis of lymphocytes by augmented induction of Bax in SSI-1 (STAT-induced STAT inhibitor-1) deficient mice. *Proc Natl Acad Sci U S A*, 95, 15577-82.
- NAKA, T., NARAZAKI, M., HIRATA, M., MATSUMOTO, T., MINAMOTO, S., AONO, A., NISHIMOTO, N., KAJITA, T., TAGA, T., YOSHIZAKI, K., AKIRA, S. & KISHIMOTO, T. 1997. Structure and function of a new STAT-induced STAT inhibitor. *Nature*, 387, 924-9.
- NAKAGAWA, R., NAKA, T., TSUTSUI, H., FUJIMOTO, M., KIMURA, A., ABE, T., SEKI, E., SATO, S., TAKEUCHI, O., TAKEDA, K., AKIRA, S., YAMANISHI, K., KAWASE, I., NAKANISHI, K. & KISHIMOTO, T. 2002. SOCS-1 participates in negative regulation of LPS responses. *Immunity*, 17, 677-87.
- NANNEY, L. B., STOSCHECK, C. M., KING, L. E., JR., UNDERWOOD, R. A. & HOLBROOK, K. A. 1990. Immunolocalization of epidermal growth factor receptors in normal developing human skin. *J Invest Dermatol*, 94, 742-8.
- NEWMAN, S. L., HENSON, J. E. & HENSON, P. M. 1982. Phagocytosis of senescent neutrophils by human monocyte-derived macrophages and rabbit inflammatory macrophages. *J Exp Med*, 156, 430-42.
- NICHOLSON, S. E., METCALF, D., SPRIGG, N. S., COLUMBUS, R., WALKER, F., SILVA, A., CARY, D., WILLSON, T. A., ZHANG, J. G., HILTON, D. J., ALEXANDER, W. S. & NICOLA, N. A. 2005. Suppressor of cytokine signaling (SOCS)-5 is a potential negative regulator of epidermal growth factor signaling. *Proc Natl Acad Sci U S A*, 102, 2328-33.
- NICHOLSON, S. E., WILLSON, T. A., FARLEY, A., STARR, R., ZHANG, J. G., BACA, M., ALEXANDER, W. S., METCALF, D., HILTON, D. J. & NICOLA, N. A. 1999. Mutational analyses of the SOCS proteins suggest a dual domain requirement but distinct mechanisms for inhibition of LIF and IL-6 signal transduction. *EMBO J*, 18, 375-85.
- NIEMAND, C., NIMMESGER, A., HAAN, S., FISCHER, P., SCHAPER, F., ROSSAINT, R., HEINRICH, P. C. & MULLER-NEWEN, G. 2003. Activation of STAT3 by IL-6 and IL-10 in primary human macrophages is differentially modulated by suppressor of cytokine signaling 3. *J Immunol*, 170, 3263-72.
- O'KEEFE, E. J., CHIU, M. L. & PAYNE, R. E., JR. 1988. Stimulation of growth of keratinocytes by basic fibroblast growth factor. *J Invest Dermatol*, 90, 767-9.
- O'TOOLE, E. A. 2001. Extracellular matrix and keratinocyte migration. *Clin Exp Dermatol*, 26, 525-30.
- ODLAND, G. & ROSS, R. 1968. Human wound repair. I. Epidermal regeneration. *J Cell Biol*, 39, 135-51.

- OKABE, S., TAUCHI, T., MORITA, H., OHASHI, H., YOSHIMURA, A. & OHYASHIKI, K. 1999. Thrombopoietin induces an SH2-containing protein, CIS1, which binds to Mpl: involvement of the ubiquitin proteasome pathway. *Exp Hematol*, 27, 1542-7.
- ORTIZ-MUNOZ, G., MARTIN-VENTURA, J. L., HERNANDEZ-VARGAS, P., MALLAVIA, B., LOPEZ-PARRA, V., LOPEZ-FRANCO, O., MUNOZ-GARCIA, B., FERNANDEZ-VIZARRA, P., ORTEGA, L., EGIDO, J. & GOMEZ-GUERRERO, C. 2009. Suppressors of cytokine signaling modulate JAK/STAT-mediated cell responses during atherosclerosis. *Arterioscler Thromb Vasc Biol*, 29, 525-31.
- OWEN, S., ZHAO, H., DART, A., WANG, Y., RUGE, F., GAO, Y., WEI, C., WU, Y. & JIANG, W. G. 2016. Heat shock protein 27 is a potential indicator for response to YangZheng XiaoJi and chemotherapy agents in cancer cells. *Int J Oncol*.
- OZAKI, A., SEKI, Y., FUKUSHIMA, A. & KUBO, M. 2005. The control of allergic conjunctivitis by suppressor of cytokine signaling (SOCS)3 and SOCS5 in a murine model. *J Immunol*, 175, 5489-97.
- PARK, E. S., KIM, H., SUH, J. M., PARK, S. J., KWON, O. Y., KIM, Y. K., RO, H. K., CHO, B. Y., CHUNG, J. & SHONG, M. 2000. Thyrotropin induces SOCS-1 (suppressor of cytokine signaling-1) and SOCS-3 in FRTL-5 thyroid cells. *Mol Endocrinol*, 14, 440-8.
- PARK, J. E. & BARBUL, A. 2004. Understanding the role of immune regulation in wound healing. *Am J Surg*, 187, 11S-16S.
- PASTAR, I., STOJADINOVIC, O., KRZYZANOWSKA, A., BARRIENTOS, S., STUELLEN, C., ZIMMERMAN, K., BLUMENBERG, M., BREM, H. & TOMIC-CANIC, M. 2010. Attenuation of the transforming growth factor beta-signaling pathway in chronic venous ulcers. *Mol Med*, 16, 92-101.
- PASTAR, I., STOJADINOVIC, O. & TOMIC-CANIC, M. 2008. Role of keratinocytes in healing of chronic wounds. *Surg Technol Int*, 17, 105-12.
- PASTAR, I., STOJADINOVIC, O., YIN, N. C., RAMIREZ, H., NUSBAUM, A. G., SAWAYA, A., PATEL, S. B., KHALID, L., ISSEROFF, R. R. & TOMIC-CANIC, M. 2014. Epithelialization in Wound Healing: A Comprehensive Review. *Adv Wound Care (New Rochelle)*, 3, 445-464.
- PAULSSON, Y., HAMMACHER, A., HELDIN, C. H. & WESTERMARK, B. 1987. Possible positive autocrine feedback in the prereplicative phase of human fibroblasts. *Nature*, 328, 715-7.
- PEZET, A., FAVRE, H., KELLY, P. A. & EDERY, M. 1999. Inhibition and restoration of prolactin signal transduction by suppressors of cytokine signaling. *J Biol Chem*, 274, 24497-502.
- PHILLIPS, G. D., WHITEHEAD, R. A. & KNIGHTON, D. R. 1992. Inhibition by methylprednisolone acetate suggests an indirect mechanism for TGF-B induced angiogenesis. *Growth Factors*, 6, 77-84.
- PIESSEVAUX, J., LAVENS, D., MONTOYE, T., WAUMAN, J., CATTEEUW, D., VANDEKERCKHOVE, J., BELSHAM, D., PEELMAN, F. & TAVERNIER, J. 2006. Functional cross-modulation between SOCS proteins can stimulate cytokine signaling. *J Biol Chem*, 281, 32953-66.
- PITTELKOW, M. R., COOK, P. W., SHIPLEY, G. D., DERYNCK, R. & COFFEY, R. J., JR. 1993. Autonomous growth of human keratinocytes requires epidermal growth factor receptor occupancy. *Cell Growth Differ*, 4, 513-21.
- POSNETT, J. & FRANKS, P. J. 2008. The burden of chronic wounds in the UK. *Nurs Times*, 104, 44-5.

- POWERS, J. G., HIGHAM, C., BROUSSARD, K. & PHILLIPS, T. J. 2016. Wound healing and treating wounds: Chronic wound care and management. *J Am Acad Dermatol*, 74, 607-25; quiz 625-6.
- PRICE, P. E., FAGERVIK-MORTON, H., MUDGE, E. J., BEELE, H., RUIZ, J. C., NYSTROM, T. H., LINDHOLM, C., MAUME, S., MELBY-OSTERGAARD, B., PETER, Y., ROMANELLI, M., SEPPANEN, S., SERENA, T. E., SIBBALD, G., SORIANO, J. V., WHITE, W., WOLLINA, U., WOO, K. Y., WYNDHAM-WHITE, C. & HARDING, K. G. 2008. Dressing-related pain in patients with chronic wounds: an international patient perspective. *Int Wound J*, 5, 159-71.
- PUHR, M., SANTER, F. R., NEUWIRT, H., SUSANI, M., NEMETH, J. A., HOBISCH, A., KENNER, L. & CULIG, Z. 2009. Down-regulation of suppressor of cytokine signaling-3 causes prostate cancer cell death through activation of the extrinsic and intrinsic apoptosis pathways. *Cancer Res*, 69, 7375-84.
- QIN, H., NIYONGERE, S. A., LEE, S. J., BAKER, B. J. & BENVENISTE, E. N. 2008. Expression and functional significance of SOCS-1 and SOCS-3 in astrocytes. *J Immunol*, 181, 3167-76.
- QIN, H., WILSON, C. A., ROBERTS, K. L., BAKER, B. J., ZHAO, X. & BENVENISTE, E. N. 2006. IL-10 inhibits lipopolysaccharide-induced CD40 gene expression through induction of suppressor of cytokine signaling-3. *J Immunol*, 177, 7761-71.
- QUENTMEIER, H., GEFFERS, R., JOST, E., MACLEOD, R. A., NAGEL, S., ROHRS, S., ROMANI, J., SCHERR, M., ZABORSKI, M. & DREXLER, H. G. 2008. SOCS2: inhibitor of JAK2V617F-mediated signal transduction. *Leukemia*, 22, 2169-75.
- RAFFETTO, J. D., MENDEZ, M. V., MARIEN, B. J., BYERS, H. R., PHILLIPS, T. J., PARK, H. Y. & MENZOIAN, J. O. 2001. Changes in cellular motility and cytoskeletal actin in fibroblasts from patients with chronic venous insufficiency and in neonatal fibroblasts in the presence of chronic wound fluid. *J Vasc Surg*, 33, 1233-41.
- RAM, P. A. & WAXMAN, D. J. 1999. SOCS/CIS protein inhibition of growth hormone-stimulated STAT5 signaling by multiple mechanisms. *J Biol Chem*, 274, 35553-61.
- RAM, P. A. & WAXMAN, D. J. 2000. Role of the cytokine-inducible SH2 protein CIS in desensitization of STAT5b signaling by continuous growth hormone. *J Biol Chem*, 275, 39487-96.
- RANDRIANARISON, V., MAROT, D., FORAY, N., CABANNES, J., MERET, V., CONNAULT, E., VITRAT, N., OPOLON, P., PERRICAUDET, M. & FEUNTEUN, J. 2001. BRCA1 carries tumor suppressor activity distinct from that of p53 and p21. *Cancer Gene Ther*, 8, 759-70.
- RAWLINGS, J. S., RENNEBECK, G., HARRISON, S. M., XI, R. & HARRISON, D. A. 2004a. Two Drosophila suppressors of cytokine signaling (SOCS) differentially regulate JAK and EGFR pathway activities. *BMC Cell Biol*, 5, 38.
- RAWLINGS, J. S., ROSLER, K. M. & HARRISON, D. A. 2004b. The JAK/STAT signaling pathway. *J Cell Sci*, 117, 1281-3.
- REED, A. S., UNGER, E. K., OLOFSSON, L. E., PIPER, M. L., MYERS, M. G., JR. & XU, A. W. 2010. Functional role of suppressor of cytokine signaling 3 upregulation in hypothalamic leptin resistance and long-term energy homeostasis. *Diabetes*, 59, 894-906.
- REUTERDAHL, C., SUNDBERG, C., RUBIN, K., FUNA, K. & GERDIN, B. 1993. Tissue localization of beta receptors for platelet-derived growth factor and

- platelet-derived growth factor B chain during wound repair in humans. *J Clin Invest*, 91, 2065-75.
- RICO-BAUTISTA, E., FLORES-MORALES, A. & FERNANDEZ-PEREZ, L. 2006. Suppressor of cytokine signaling (SOCS) 2, a protein with multiple functions. *Cytokine Growth Factor Rev*, 17, 431-9.
- RIGBY, R. J., SIMMONS, J. G., GREENHALGH, C. J., ALEXANDER, W. S. & LUND, P. K. 2007. Suppressor of cytokine signaling 3 (SOCS3) limits damage-induced crypt hyper-proliferation and inflammation-associated tumorigenesis in the colon. *Oncogene*, 26, 4833-41.
- RISAU, W., DREXLER, H., MIRONOV, V., SMITS, A., SIEGBAHN, A., FUNA, K. & HELDIN, C. H. 1992. Platelet-derived growth factor is angiogenic in vivo. *Growth Factors*, 7, 261-6.
- RISS, T. L., MORAVEC, R. A., NILES, A. L., DUELLMAN, S., BENINK, H. A., WORZELLA, T. J. & MINOR, L. 2004. Cell Viability Assays. In: SITTAMPALAM, G. S., COUSSENS, N. P., BRIMACOMBE, K., GROSSMAN, A., ARKIN, M., AULD, D., AUSTIN, C., BEJCEK, B., GLICKSMAN, M., INGLESE, J., IVERSEN, P. W., LI, Z., MCGEE, J., MCMANUS, O., MINOR, L., NAPPER, A., PELTIER, J. M., RISS, T., TRASK, O. J., JR. & WEIDNER, J. (eds.) *Assay Guidance Manual*. Bethesda (MD).
- ROBB, L., BOYLE, K., RAKAR, S., HARTLEY, L., LOCHLAND, J., ROBERTS, A. W., ALEXANDER, W. S. & METCALF, D. 2005. Genetic reduction of embryonic leukemia-inhibitory factor production rescues placentation in SOCS3-null embryos but does not prevent inflammatory disease. *Proc Natl Acad Sci U S A*, 102, 16333-8.
- ROBERTS, A. B. & SPORN, M. B. 1988. Transforming growth factor- β . *The molecular and cellular biology of wound repair*. Springer.
- ROBERTS, A. B., SPORN, M. B., ASSOIAN, R. K., SMITH, J. M., ROCHE, N. S., WAKEFIELD, L. M., HEINE, U. I., LIOTTA, L. A., FALANGA, V., KEHRL, J. H. & ET AL. 1986. Transforming growth factor type beta: rapid induction of fibrosis and angiogenesis in vivo and stimulation of collagen formation in vitro. *Proc Natl Acad Sci U S A*, 83, 4167-71.
- ROBERTS, A. W., ROBB, L., RAKAR, S., HARTLEY, L., CLUSE, L., NICOLA, N. A., METCALF, D., HILTON, D. J. & ALEXANDER, W. S. 2001. Placental defects and embryonic lethality in mice lacking suppressor of cytokine signaling 3. *Proc Natl Acad Sci U S A*, 98, 9324-9.
- ROBSON, M. C., PHILLIP, L. G., COOPER, D. M., LYLE, W. G., ROBSON, L. E., ODOM, L., HILL, D. P., HANHAM, A. F. & KSANDER, G. A. 1995. Safety and effect of transforming growth factor-beta(2) for treatment of venous stasis ulcers. *Wound Repair Regen*, 3, 157-67.
- ROSS, R. 1993. The pathogenesis of atherosclerosis: a perspective for the 1990s. *Nature*, 362, 801-9.
- RUBIN, K., TERRACIO, L., RONNSTRAND, L., HELDIN, C. H. & KLARESKOG, L. 1988. Expression of platelet-derived growth factor receptors is induced on connective tissue cells during chronic synovial inflammation. *Scand J Immunol*, 27, 285-94.
- RUI, L., YUAN, M., FRANTZ, D., SHOELSON, S. & WHITE, M. F. 2002. SOCS-1 and SOCS-3 block insulin signaling by ubiquitin-mediated degradation of IRS1 and IRS2. *J Biol Chem*, 277, 42394-8.
- SACHITHANANDAN, N., FAM, B. C., FYNCH, S., DZAMKO, N., WATT, M. J., WORMALD, S., HONEYMAN, J., GALIC, S., PROIETTO, J., ANDRIKOPOULOS, S., HEVENER, A. L., KAY, T. W. & STEINBERG, G. R. 2010. Liver-specific

- suppressor of cytokine signaling-3 deletion in mice enhances hepatic insulin sensitivity and lipogenesis resulting in fatty liver and obesity. *Hepatology*, 52, 1632-42.
- SADOWSKI, C. L., CHOI, T. S., LE, M., WHEELER, T. T., WANG, L. H. & SADOWSKI, H. B. 2001. Insulin Induction of SOCS-2 and SOCS-3 mRNA expression in C2C12 Skeletal Muscle Cells Is Mediated by Stat5*. *J Biol Chem*, 276, 20703-10.
- SAKAI, I., TAKEUCHI, K., YAMAUCHI, H., NARUMI, H. & FUJITA, S. 2002. Constitutive expression of SOCS3 confers resistance to IFN-alpha in chronic myelogenous leukemia cells. *Blood*, 100, 2926-31.
- SANKAR, S., MAHOOTI-BROOKS, N., BENSEN, L., MCCARTHY, T. L., CENTRELLA, M. & MADRI, J. A. 1996. Modulation of transforming growth factor beta receptor levels on microvascular endothelial cells during in vitro angiogenesis. *J Clin Invest*, 97, 1436-46.
- SANO, S., ITAMI, S., TAKEDA, K., TARUTANI, M., YAMAGUCHI, Y., MIURA, H., YOSHIKAWA, K., AKIRA, S. & TAKEDA, J. 1999. Keratinocyte-specific ablation of Stat3 exhibits impaired skin remodeling, but does not affect skin morphogenesis. *EMBO J*, 18, 4657-68.
- SAOTOME, K., MORITA, H. & UMEDA, M. 1989. Cytotoxicity test with simplified crystal violet staining method using microtitre plates and its application to injection drugs. *Toxicol In Vitro*, 3, 317-21.
- SASAKI, A., YASUKAWA, H., SHOUDA, T., KITAMURA, T., DIKIC, I. & YOSHIMURA, A. 2000. CIS3/SOCS-3 suppresses erythropoietin (EPO) signaling by binding the EPO receptor and JAK2. *J Biol Chem*, 275, 29338-47.
- SASAKI, A., YASUKAWA, H., SUZUKI, A., KAMIZONO, S., SYODA, T., KINJO, I., SASAKI, M., JOHNSTON, J. A. & YOSHIMURA, A. 1999. Cytokine-inducible SH2 protein-3 (CIS3/SOCS3) inhibits Janus tyrosine kinase by binding through the N-terminal kinase inhibitory region as well as SH2 domain. *Genes Cells*, 4, 339-51.
- SASI, W., JIANG, W. G., SHARMA, A. & MOKBEL, K. 2010. Higher expression levels of SOCS 1,3,4,7 are associated with earlier tumour stage and better clinical outcome in human breast cancer. *BMC Cancer*, 10, 178.
- SATO, N., BEITZ, J. G., KATO, J., YAMAMOTO, M., CLARK, J. W., CALABRESI, P., RAYMOND, A. & FRACKELTON, A. R., JR. 1993. Platelet-derived growth factor indirectly stimulates angiogenesis in vitro. *Am J Pathol*, 142, 1119-30.
- SATO, Y. & RIFKIN, D. B. 1988. Autocrine activities of basic fibroblast growth factor: regulation of endothelial cell movement, plasminogen activator synthesis, and DNA synthesis. *J Cell Biol*, 107, 1199-205.
- SCHAPER, N. C., ANDROS, G., APELQVIST, J., BAKKER, K., LAMMER, J., LEPANTALO, M., MILLS, J. L., REEKERS, J., SHEARMAN, C. P., ZIERLER, R. E., HINCHLIFFE, R. J. & INTERNATIONAL WORKING GROUP ON DIABETIC, F. 2012. Specific guidelines for the diagnosis and treatment of peripheral arterial disease in a patient with diabetes and ulceration of the foot 2011. *Diabetes Metab Res Rev*, 28 Suppl 1, 236-7.
- SCHEITZ, C. J., LEE, T. S., MCDERMITT, D. J. & TUMBAR, T. 2012. Defining a tissue stem cell-driven Runx1/Stat3 signalling axis in epithelial cancer. *EMBO J*, 31, 4124-39.
- SCHNEIDER, M. R., WERNER, S., PAUS, R. & WOLF, E. 2008. Beyond wavy hairs: the epidermal growth factor receptor and its ligands in skin biology and pathology. *Am J Pathol*, 173, 14-24.

- SCHREML, S., SZEIMIES, R. M., PRANTL, L., KARRER, S., LANDTHALER, M. & BABILAS, P. 2010. Oxygen in acute and chronic wound healing. *Br J Dermatol*, 163, 257-68.
- SCHULTZ, G. S., BARILLO, D. J., MOZINGO, D. W., CHIN, G. A. & WOUND BED ADVISORY BOARD, M. 2004. Wound bed preparation and a brief history of TIME. *Int Wound J*, 1, 19-32.
- SCHULTZ, G. S., SIBBALD, R. G., FALANGA, V., AYELLO, E. A., DOWSETT, C., HARDING, K., ROMANELLI, M., STACEY, M. C., TEOT, L. & VANSCHIEDT, W. 2003. Wound bed preparation: a systematic approach to wound management. *Wound Repair Regen*, 11 Suppl 1, S1-28.
- SCHWEIGERER, L., NEUFELD, G., FRIEDMAN, J., ABRAHAM, J. A., FIDDES, J. C. & GOSPODAROWICZ, D. 1987. Capillary endothelial cells express basic fibroblast growth factor, a mitogen that promotes their own growth. *Nature*, 325, 257-9.
- SEKI, E., KONDO, Y., IIMURO, Y., NAKA, T., SON, G., KISHIMOTO, T., FUJIMOTO, J., TSUTSUI, H. & NAKANISHI, K. 2008. Demonstration of cooperative contribution of MET- and EGFR-mediated STAT3 phosphorylation to liver regeneration by exogenous suppressor of cytokine signalings. *J Hepatol*, 48, 237-45.
- SEKI, Y., HAYASHI, K., MATSUMOTO, A., SEKI, N., TSUKADA, J., RANSOM, J., NAKA, T., KISHIMOTO, T., YOSHIMURA, A. & KUBO, M. 2002. Expression of the suppressor of cytokine signaling-5 (SOCS5) negatively regulates IL-4-dependent STAT6 activation and Th2 differentiation. *Proc Natl Acad Sci U S A*, 99, 13003-8.
- SEKI, Y., INOUE, H., NAGATA, N., HAYASHI, K., FUKUYAMA, S., MATSUMOTO, K., KOMINE, O., HAMANO, S., HIMENO, K., INAGAKI-OHARA, K., CACALANO, N., O'GARRA, A., OSHIDA, T., SAITO, H., JOHNSTON, J. A., YOSHIMURA, A. & KUBO, M. 2003. SOCS-3 regulates onset and maintenance of T(H)2-mediated allergic responses. *Nat Med*, 9, 1047-54.
- SELLHEYER, K., BICKENBACH, J. R., ROTHNAGEL, J. A., BUNDMAN, D., LONGLEY, M. A., KRIEG, T., ROCHE, N. S., ROBERTS, A. B. & ROOP, D. R. 1993. Inhibition of skin development by overexpression of transforming growth factor beta 1 in the epidermis of transgenic mice. *Proc Natl Acad Sci U S A*, 90, 5237-41.
- SENGER, D. R., CLAFFEY, K. P., BENES, J. E., PERRUZZI, C. A., SERGIOU, A. P. & DETMAR, M. 1997. Angiogenesis promoted by vascular endothelial growth factor: regulation through alpha1beta1 and alpha2beta1 integrins. *Proc Natl Acad Sci U S A*, 94, 13612-7.
- SENGER, D. R. & DAVIS, G. E. 2011. Angiogenesis. *Cold Spring Harb Perspect Biol*, 3, a005090.
- SENGER, D. R., GALLI, S. J., DVORAK, A. M., PERRUZZI, C. A., HARVEY, V. S. & DVORAK, H. F. 1983. Tumor cells secrete a vascular permeability factor that promotes accumulation of ascites fluid. *Science*, 219, 983-5.
- SENGER, D. R., PERRUZZI, C. A., STREIT, M., KOTELIANSKY, V. E., DE FOUGEROLLES, A. R. & DETMAR, M. 2002. The alpha(1)beta(1) and alpha(2)beta(1) integrins provide critical support for vascular endothelial growth factor signaling, endothelial cell migration, and tumor angiogenesis. *Am J Pathol*, 160, 195-204.
- SEPPA, H., GROTENDORST, G., SEPPA, S., SCHIFFMANN, E. & MARTIN, G. R. 1982. Platelet-derived growth factor in chemotactic for fibroblasts. *J Cell Biol*, 92, 584-8.

- SHAH, M., FOREMAN, D. M. & FERGUSON, M. W. 1995. Neutralisation of TGF-beta 1 and TGF-beta 2 or exogenous addition of TGF-beta 3 to cutaneous rat wounds reduces scarring. *J Cell Sci*, 108 (Pt 3), 985-1002.
- SHANMUGAM, V. K., PRICE, P., ATTINGER, C. E. & STEEN, V. D. 2010. Lower extremity ulcers in systemic sclerosis: features and response to therapy. *Int J Rheumatol*, 2010.
- SHEN, X., HONG, F., NGUYEN, V. A. & GAO, B. 2000. IL-10 attenuates IFN-alpha-activated STAT1 in the liver: involvement of SOCS2 and SOCS3. *FEBS Lett*, 480, 132-6.
- SHI, H., CAVE, B., INOUE, K., BJORBAEK, C. & FLIER, J. S. 2006. Overexpression of suppressor of cytokine signaling 3 in adipose tissue causes local but not systemic insulin resistance. *Diabetes*, 55, 699-707.
- SHI, H., TZAMELI, I., BJORBAEK, C. & FLIER, J. S. 2004. Suppressor of cytokine signaling 3 is a physiological regulator of adipocyte insulin signaling. *J Biol Chem*, 279, 34733-40.
- SHIMOKADO, K., RAINES, E. W., MADTES, D. K., BARRETT, T. B., BENDITT, E. P. & ROSS, R. 1985. A significant part of macrophage-derived growth factor consists of at least two forms of PDGF. *Cell*, 43, 277-86.
- SHIPLEY, G. D., KEEBLE, W. W., HENDRICKSON, J. E., COFFEY, R. J., JR. & PITTELKOW, M. R. 1989. Growth of normal human keratinocytes and fibroblasts in serum-free medium is stimulated by acidic and basic fibroblast growth factor. *J Cell Physiol*, 138, 511-8.
- SHIRAKATA, Y., KIMURA, R., NANBA, D., IWAMOTO, R., TOKUMARU, S., MORIMOTO, C., YOKOTA, K., NAKAMURA, M., SAYAMA, K., MEKADA, E., HIGASHIYAMA, S. & HASHIMOTO, K. 2005. Heparin-binding EGF-like growth factor accelerates keratinocyte migration and skin wound healing. *J Cell Sci*, 118, 2363-70.
- SHOUDA, T., YOSHIDA, T., HANADA, T., WAKIOKA, T., OISHI, M., MIYOSHI, K., KOMIYA, S., KOSAI, K., HANAKAWA, Y., HASHIMOTO, K., NAGATA, K. & YOSHIMURA, A. 2001. Induction of the cytokine signal regulator SOCS3/CIS3 as a therapeutic strategy for treating inflammatory arthritis. *J Clin Invest*, 108, 1781-8.
- SHWEIKI, D., ITIN, A., SOFFER, D. & KESHET, E. 1992. Vascular endothelial growth factor induced by hypoxia may mediate hypoxia-initiated angiogenesis. *Nature*, 359, 843-5.
- SIEGBAHN, A., HAMMACHER, A., WESTERMARK, B. & HELDIN, C. H. 1990. Differential effects of the various isoforms of platelet-derived growth factor on chemotaxis of fibroblasts, monocytes, and granulocytes. *J Clin Invest*, 85, 916-20.
- SIEWERT, E., MULLER-ESTERL, W., STARR, R., HEINRICH, P. C. & SCHAPER, F. 1999. Different protein turnover of interleukin-6-type cytokine signalling components. *Eur J Biochem*, 265, 251-7.
- SINGER, A. J. & CLARK, R. A. 1999. Cutaneous wound healing. *N Engl J Med*, 341, 738-46.
- SNYDER, R. J. 2005. Treatment of nonhealing ulcers with allografts. *Clin Dermatol*, 23, 388-95.
- SONG, M. M. & SHUAI, K. 1998. The suppressor of cytokine signaling (SOCS) 1 and SOCS3 but not SOCS2 proteins inhibit interferon-mediated antiviral and antiproliferative activities. *J Biol Chem*, 273, 35056-62.
- SORIANO, S. F., HERNANZ-FALCON, P., RODRIGUEZ-FRADE, J. M., DE ANA, A. M., GARZON, R., CARVALHO-PINTO, C., VILA-CORO, A. J., ZABALLOS, A.,

- BALOMENOS, D., MARTINEZ, A. C. & MELLADO, M. 2002. Functional inactivation of CXC chemokine receptor 4-mediated responses through SOCS3 up-regulation. *J Exp Med*, 196, 311-21.
- SPORN, M. B., ROBERTS, A. B., SHULL, J. H., SMITH, J. M., WARD, J. M. & SODEK, J. 1983. Polypeptide transforming growth factors isolated from bovine sources and used for wound healing in vivo. *Science*, 219, 1329-31.
- SPORRI, B., KOVANEN, P. E., SASAKI, A., YOSHIMURA, A. & LEONARD, W. J. 2001. JAB/SOCS1/SSI-1 is an interleukin-2-induced inhibitor of IL-2 signaling. *Blood*, 97, 221-6.
- STAHL, A., JOYAL, J. S., CHEN, J., SAPIEHA, P., JUAN, A. M., HATTON, C. J., PEI, D. T., HURST, C. G., SEAWARD, M. R., KRAH, N. M., DENNISON, R. J., GREENE, E. R., BOSCOLO, E., PANIGRAHY, D. & SMITH, L. E. 2012. SOCS3 is an endogenous inhibitor of pathologic angiogenesis. *Blood*, 120, 2925-9.
- STARR, R., METCALF, D., ELEFANTY, A. G., BRYSHA, M., WILLSON, T. A., NICOLA, N. A., HILTON, D. J. & ALEXANDER, W. S. 1998. Liver degeneration and lymphoid deficiencies in mice lacking suppressor of cytokine signaling-1. *Proc Natl Acad Sci U S A*, 95, 14395-9.
- STARR, R., WILLSON, T. A., VINEY, E. M., MURRAY, L. J., RAYNER, J. R., JENKINS, B. J., GONDA, T. J., ALEXANDER, W. S., METCALF, D., NICOLA, N. A. & HILTON, D. J. 1997. A family of cytokine-inducible inhibitors of signalling. *Nature*, 387, 917-21.
- STEED, D. L. 2004. Debridement. *Am J Surg*, 187, 71S-74S.
- STENN, K. S. & DEPALMA, L. 1988. Re-epithelialization. *The molecular and cellular biology of wound repair*. Springer.
- STEPHAN, C. M., WANG, J., WHITEMAN, E. L., BIRNBAUM, M. J. & LAZAR, M. A. 2005. Activation of SOCS-3 by resistin. *Mol Cell Biol*, 25, 1569-75.
- STEVENSON, N. J., MCFARLANE, C., ONG, S. T., NAHLIK, K., KELVIN, A., ADDLEY, M. R., LONG, A., GREAVES, D. R., O'FARRELLY, C. & JOHNSTON, J. A. 2010. Suppressor of cytokine signalling (SOCS) 1 and 3 enhance cell adhesion and inhibit migration towards the chemokine eotaxin/CCL11. *FEBS Lett*, 584, 4469-74.
- SUTHERLAND, J. M., KEIGHTLEY, R. A., NIXON, B., ROMAN, S. D., ROBKER, R. L., RUSSELL, D. L. & MCLAUGHLIN, E. A. 2012. Suppressor of cytokine signaling 4 (SOCS4): moderator of ovarian primordial follicle activation. *J Cell Physiol*, 227, 1188-98.
- SUTHERLAND, K. D., LINDEMAN, G. J., CHOONG, D. Y., WITTLIN, S., BRENTZELL, L., PHILLIPS, W., CAMPBELL, I. G. & VISVADER, J. E. 2004. Differential hypermethylation of SOCS genes in ovarian and breast carcinomas. *Oncogene*, 23, 7726-33.
- SZULCEK, R., BOGAARD, H. J. & VAN NIEUW AMERONGEN, G. P. 2014. Electric cell-substrate impedance sensing for the quantification of endothelial proliferation, barrier function, and motility. *J Vis Exp*.
- TAKAHASHI, Y., CARPINO, N., CROSS, J. C., TORRES, M., PARGANAS, E. & IHLE, J. N. 2003. SOCS3: an essential regulator of LIF receptor signaling in trophoblast giant cell differentiation. *EMBO J*, 22, 372-84.
- TAKASE, H., YU, C. R., LIU, X., FUJIMOTO, C., GERY, I. & EGWUAGU, C. E. 2005. Induction of suppressors of cytokine signaling (SOCS) in the retina during experimental autoimmune uveitis (EAU): potential neuroprotective role of SOCS proteins. *J Neuroimmunol*, 168, 118-27.
- TALEB, S., ROMAIN, M., RAMKHELAWON, B., UYTENHOVE, C., PASTERKAMP, G., HERBIN, O., ESPOSITO, B., PEREZ, N., YASUKAWA, H., VAN SNICK, J.,

- YOSHIMURA, A., TEDGUI, A. & MALLAT, Z. 2009. Loss of SOCS3 expression in T cells reveals a regulatory role for interleukin-17 in atherosclerosis. *J Exp Med*, 206, 2067-77.
- TAN, Y., SANDERS, A. J., ZHANG, Y., MARTIN, T. A., OWEN, S., RUGE, F. & JIANG, W. G. 2015. Interleukin-24 (IL-24) Expression and Biological Impact on HECV Endothelial Cells. *Cancer Genomics Proteomics*, 12, 243-50.
- TANAKA, K., ICHIYAMA, K., HASHIMOTO, M., YOSHIDA, H., TAKIMOTO, T., TAKAESU, G., TORISU, T., HANADA, T., YASUKAWA, H., FUKUYAMA, S., INOUE, H., NAKANISHI, Y., KOBAYASHI, T. & YOSHIMURA, A. 2008. Loss of suppressor of cytokine signaling 1 in helper T cells leads to defective Th17 differentiation by enhancing antagonistic effects of IFN-gamma on STAT3 and Smads. *J Immunol*, 180, 3746-56.
- TANNAHILL, G. M., ELLIOTT, J., BARRY, A. C., HIBBERT, L., CACALANO, N. A. & JOHNSTON, J. A. 2005. SOCS2 can enhance interleukin-2 (IL-2) and IL-3 signaling by accelerating SOCS3 degradation. *Mol Cell Biol*, 25, 9115-26.
- TAVORA, B., BATISTA, S., REYNOLDS, L. E., JADEJA, S., ROBINSON, S., KOSTOUROU, V., HART, I., FRUTTIGER, M., PARSONS, M. & HODIVALA-DILKE, K. M. 2010. Endothelial FAK is required for tumour angiogenesis. *EMBO Mol Med*, 2, 516-28.
- TELGENHOFF, D. & SHROOT, B. 2005. Cellular senescence mechanisms in chronic wound healing. *Cell Death Differ*, 12, 695-8.
- TEPASS, U. 2009. FERM proteins in animal morphogenesis. *Curr Opin Genet Dev*, 19, 357-67.
- TERSTEGEN, L., GATSIOS, P., BODE, J. G., SCHAPER, F., HEINRICH, P. C. & GRAEVE, L. 2000. The inhibition of interleukin-6-dependent STAT activation by mitogen-activated protein kinases depends on tyrosine 759 in the cytoplasmic tail of glycoprotein 130. *J Biol Chem*, 275, 18810-7.
- TONKO-GEYMAYER, S., GOUPILLE, O., TONKO, M., SORATROI, C., YOSHIMURA, A., STREULI, C., ZIEMIECKI, A., KOFLER, R. & DOPPLER, W. 2002. Regulation and function of the cytokine-inducible SH-2 domain proteins, CIS and SOCS3, in mammary epithelial cells. *Mol Endocrinol*, 16, 1680-95.
- TONNESEN, M. G., FENG, X. & CLARK, R. A. 2000. Angiogenesis in wound healing. *J Invest Dermatol Symp Proc*, 5, 40-6.
- TORISU, T., NAKAYA, M., WATANABE, S., HASHIMOTO, M., YOSHIDA, H., CHINEN, T., YOSHIDA, R., OKAMOTO, F., HANADA, T., TORISU, K., TAKAESU, G., KOBAYASHI, T., YASUKAWA, H. & YOSHIMURA, A. 2008. Suppressor of cytokine signaling 1 protects mice against concanavalin A-induced hepatitis by inhibiting apoptosis. *Hepatology*, 47, 1644-54.
- TORISU, T., SATO, N., YOSHIGA, D., KOBAYASHI, T., YOSHIOKA, T., MORI, H., IIDA, M. & YOSHIMURA, A. 2007. The dual function of hepatic SOCS3 in insulin resistance in vivo. *Genes Cells*, 12, 143-54.
- TRENGOVE, M. C. & WARD, A. C. 2013. SOCS proteins in development and disease. *Am J Clin Exp Immunol*, 2, 1-29.
- TRENGOVE, N. J., BIELEFELDT-OHMANN, H. & STACEY, M. C. 2000. Mitogenic activity and cytokine levels in non-healing and healing chronic leg ulcers. *Wound Repair Regen*, 8, 13-25.
- TRENGOVE, N. J., STACEY, M. C., MACAULEY, S., BENNETT, N., GIBSON, J., BURSLEM, F., MURPHY, G. & SCHULTZ, G. 1999. Analysis of the acute and chronic wound environments: the role of proteases and their inhibitors. *Wound Repair Regen*, 7, 442-52.

- TROP, S., DE SEPULVEDA, P., ZUNIGA-PFLUCKER, J. C. & ROTTAPPEL, R. 2001. Overexpression of suppressor of cytokine signaling-1 impairs pre-T-cell receptor-induced proliferation but not differentiation of immature thymocytes. *Blood*, 97, 2269-77.
- TSUBOI, R., SATO, C., KURITA, Y., RON, D., RUBIN, J. S. & OGAWA, H. 1993. Keratinocyte growth factor (FGF-7) stimulates migration and plasminogen activator activity of normal human keratinocytes. *J Invest Dermatol*, 101, 49-53.
- TURNLEY, A. M., FAUX, C. H., RIETZE, R. L., COONAN, J. R. & BARTLETT, P. F. 2002. Suppressor of cytokine signaling 2 regulates neuronal differentiation by inhibiting growth hormone signaling. *Nat Neurosci*, 5, 1155-62.
- UEKI, K., KONDO, T., TSENG, Y. H. & KAHN, C. R. 2004. Central role of suppressors of cytokine signaling proteins in hepatic steatosis, insulin resistance, and the metabolic syndrome in the mouse. *Proc Natl Acad Sci U S A*, 101, 10422-7.
- UHLENBECK, O. C. 1987. A small catalytic oligoribonucleotide. *Nature*, 328, 596-600.
- UREN, R. T., TURBIC, A., WONG, A. W., KLEIN, R., MURRAY, S. S. & TURNLEY, A. M. 2014. A novel role of suppressor of cytokine signaling-2 in the regulation of TrkA neurotrophin receptor biology. *J Neurochem*, 129, 614-27.
- UTO-KONOMI, A., MIYAUCHI, K., OZAKI, N., MOTOMURA, Y., SUZUKI, Y., YOSHIMURA, A., SUZUKI, S., CUA, D. & KUBO, M. 2012. Dysregulation of suppressor of cytokine signaling 3 in keratinocytes causes skin inflammation mediated by interleukin-20 receptor-related cytokines. *PLoS One*, 7, e40343.
- UYTTENDAELE, I., LEMMENS, I., VERHEE, A., DE SMET, A. S., VANDEKERCKHOVE, J., LAVENS, D., PEELMAN, F. & TAVERNIER, J. 2007. Mammalian protein-protein interaction trap (MAPPIT) analysis of STAT5, CIS, and SOCS2 interactions with the growth hormone receptor. *Mol Endocrinol*, 21, 2821-31.
- VALENCIA, I. C., FALABELLA, A., KIRSNER, R. S. & EAGLSTEIN, W. H. 2001. Chronic venous insufficiency and venous leg ulceration. *J Am Acad Dermatol*, 44, 401-21; quiz 422-4.
- VAN DE GEIJN, G. J., GITS, J. & TOUW, I. P. 2004. Distinct activities of suppressor of cytokine signaling (SOCS) proteins and involvement of the SOCS box in controlling G-CSF signaling. *J Leukoc Biol*, 76, 237-44.
- VERDIER, F., RABIONET, R., GOUILLEUX, F., BEISENHERZ-HUSS, C., VARLET, P., MULLER, O., MAYEUX, P., LACOMBE, C., GISSELBRECHT, S. & CHRETIEN, S. 1998. A sequence of the CIS gene promoter interacts preferentially with two associated STAT5A dimers: a distinct biochemical difference between STAT5A and STAT5B. *Mol Cell Biol*, 18, 5852-60.
- VESTERLUND, M., ZADJALI, F., PERSSON, T., NIELSEN, M. L., KESSLER, B. M., NORSTEDT, G. & FLORES-MORALES, A. 2011. The SOCS2 ubiquitin ligase complex regulates growth hormone receptor levels. *PLoS One*, 6, e25358.
- VLACICH, G., NAWIJN, M. C., WEBB, G. C. & STEINER, D. F. 2010. Pim3 negatively regulates glucose-stimulated insulin secretion. *Islets*, 2, 308-17.
- VLODAVSKY, I., FRIDMAN, R., SULLIVAN, R., SASSE, J. & KLAGSBRUN, M. 1987. Aortic endothelial cells synthesize basic fibroblast growth factor which remains cell associated and platelet-derived growth factor-like protein which is secreted. *J Cell Physiol*, 131, 402-8.

- WANG, L., ZHANG, Z., ZHANG, R., HAFNER, M. S., WONG, H. K., JIAO, Z. & CHOPP, M. 2004. Erythropoietin up-regulates SOCS2 in neuronal progenitor cells derived from SVZ of adult rat. *Neuroreport*, 15, 1225-9.
- WANG, Q., MIYAKAWA, Y., FOX, N. & KAUSHANSKY, K. 2000. Interferon-alpha directly represses megakaryopoiesis by inhibiting thrombopoietin-induced signaling through induction of SOCS-1. *Blood*, 96, 2093-9.
- WANG, Z., MA, T., MA, J., HAN, J., DING, L. & QIU, Q. 2015. Convergent evolution of SOCS4 between yak and Tibetan antelope in response to high-altitude stress. *Gene*, 572, 298-302.
- WATANABE, H., KUBO, M., NUMATA, K., TAKAGI, K., MIZUTA, H., OKADA, S., ITO, T. & MATSUKAWA, A. 2006. Overexpression of suppressor of cytokine signaling-5 in T cells augments innate immunity during septic peritonitis. *J Immunol*, 177, 8650-7.
- WEGENER, J., KEESE, C. R. & GIAEVER, I. 2000. Electric cell-substrate impedance sensing (ECIS) as a noninvasive means to monitor the kinetics of cell spreading to artificial surfaces. *Exp Cell Res*, 259, 158-66.
- WELCH, M. P., ODLAND, G. F. & CLARK, R. A. 1990. Temporal relationships of F-actin bundle formation, collagen and fibronectin matrix assembly, and fibronectin receptor expression to wound contraction. *J Cell Biol*, 110, 133-45.
- WERDIN, F., TENNENHAUS, M., SCHALLER, H. E. & RENNEKAMPFF, H. O. 2009. Evidence-based management strategies for treatment of chronic wounds. *Eplasty*, 9, e19.
- WERNER, S. & GROSE, R. 2003. Regulation of wound healing by growth factors and cytokines. *Physiol Rev*, 83, 835-70.
- WHITE, G. E., COTTERILL, A., ADDLEY, M. R., SOILLEUX, E. J. & GREAVES, D. R. 2011. Suppressor of cytokine signalling protein SOCS3 expression is increased at sites of acute and chronic inflammation. *J Mol Histol*, 42, 137-51.
- WILLIAMS, G. T. 1991. Programmed cell death: apoptosis and oncogenesis. *Cell*, 65, 1097-8.
- WONG, P. K., EGAN, P. J., CROKER, B. A., O'DONNELL, K., SIMS, N. A., DRAKE, S., KIU, H., MCMANUS, E. J., ALEXANDER, W. S., ROBERTS, A. W. & WICKS, I. P. 2006. SOCS-3 negatively regulates innate and adaptive immune mechanisms in acute IL-1-dependent inflammatory arthritis. *J Clin Invest*, 116, 1571-81.
- WOODLEY, D. T., BACHMANN, P. M. & O'KEEFE, E. J. 1988. Laminin inhibits human keratinocyte migration. *J Cell Physiol*, 136, 140-6.
- WOODLEY, D. T., KALEBEC, T., BANES, A. J., LINK, W., PRUNIERAS, M. & LIOTTA, L. 1986. Adult human keratinocytes migrating over nonviable dermal collagen produce collagenolytic enzymes that degrade type I and type IV collagen. *J Invest Dermatol*, 86, 418-23.
- WOOTEN, D. K., XIE, X., BARTOS, D., BUSCHE, R. A., LONGMORE, G. D. & WATOWICH, S. S. 2000. Cytokine signaling through Stat3 activates integrins, promotes adhesion, and induces growth arrest in the myeloid cell line 32D. *J Biol Chem*, 275, 26566-75.
- WORMALD, S. & HILTON, D. J. 2004. Inhibitors of cytokine signal transduction. *J Biol Chem*, 279, 821-4.
- WOZNIAK, M. A., MODZELEWSKA, K., KWONG, L. & KEELY, P. J. 2004. Focal adhesion regulation of cell behavior. *Biochim Biophys Acta*, 1692, 103-19.
- WYSOCKI, A. B. & GRINNELL, F. 1990. Fibronectin profiles in normal and chronic wound fluid. *Lab Invest*, 63, 825-31.

- WYSOCKI, A. B., STAIANO-COICO, L. & GRINNELL, F. 1993. Wound fluid from chronic leg ulcers contains elevated levels of metalloproteinases MMP-2 and MMP-9. *J Invest Dermatol*, 101, 64-8.
- XIANG, S., DONG, N. G., LIU, J. P., WANG, Y., SHI, J. W., WEI, Z. J., HU, X. J. & GONG, L. 2013. Inhibitory effects of suppressor of cytokine signaling 3 on inflammatory cytokine expression and migration and proliferation of IL-6/IFN-gamma-induced vascular smooth muscle cells. *J Huazhong Univ Sci Technolog Med Sci*, 33, 615-22.
- YAGER, D. R. & NWOMEH, B. C. 1999. The proteolytic environment of chronic wounds. *Wound Repair Regen*, 7, 433-41.
- YAGER, D. R., ZHANG, L. Y., LIANG, H. X., DIEGELMANN, R. F. & COHEN, I. K. 1996. Wound fluids from human pressure ulcers contain elevated matrix metalloproteinase levels and activity compared to surgical wound fluids. *J Invest Dermatol*, 107, 743-8.
- YAMAMOTO, K., YAMAGUCHI, M., MIYASAKA, N. & MIURA, O. 2003. SOCS-3 inhibits IL-12-induced STAT4 activation by binding through its SH2 domain to the STAT4 docking site in the IL-12 receptor beta2 subunit. *Biochem Biophys Res Commun*, 310, 1188-93.
- YAN, C., CAO, J., WU, M., ZHANG, W., JIANG, T., YOSHIMURA, A. & GAO, H. 2010. Suppressor of cytokine signaling 3 inhibits LPS-induced IL-6 expression in osteoblasts by suppressing CCAAT/enhancer-binding protein {beta} activity. *J Biol Chem*, 285, 37227-39.
- YANG, X. H., MAN, X. Y., CAI, S. Q., YAO, Y. G., BU, Z. Y. & ZHENG, M. 2006. Expression of VEGFR-2 on HaCaT cells is regulated by VEGF and plays an active role in mediating VEGF induced effects. *Biochem Biophys Res Commun*, 349, 31-8.
- YANG, Z., HULVER, M., MCMILLAN, R. P., CAI, L., KERSHAW, E. E., YU, L., XUE, B. & SHI, H. 2012. Regulation of insulin and leptin signaling by muscle suppressor of cytokine signaling 3 (SOCS3). *PLoS One*, 7, e47493.
- YARKONY, G. M. 1994. Pressure ulcers: a review. *Arch Phys Med Rehabil*, 75, 908-17.
- YASUKAWA, H., HOSHIJIMA, M., GU, Y., NAKAMURA, T., PRADERVAND, S., HANADA, T., HANAKAWA, Y., YOSHIMURA, A., ROSS, J., JR. & CHIEN, K. R. 2001. Suppressor of cytokine signaling-3 is a biomechanical stress-inducible gene that suppresses gp130-mediated cardiac myocyte hypertrophy and survival pathways. *J Clin Invest*, 108, 1459-67.
- YASUKAWA, H., MISAWA, H., SAKAMOTO, H., MASUHARA, M., SASAKI, A., WAKIOKA, T., OHTSUKA, S., IMAIZUMI, T., MATSUDA, T., IHLE, J. N. & YOSHIMURA, A. 1999. The JAK-binding protein JAB inhibits Janus tyrosine kinase activity through binding in the activation loop. *EMBO J*, 18, 1309-20.
- YASUKAWA, H., OHISHI, M., MORI, H., MURAKAMI, M., CHINEN, T., AKI, D., HANADA, T., TAKEDA, K., AKIRA, S., HOSHIJIMA, M., HIRANO, T., CHIEN, K. R. & YOSHIMURA, A. 2003. IL-6 induces an anti-inflammatory response in the absence of SOCS3 in macrophages. *Nat Immunol*, 4, 551-6.
- YIN, Y., LIU, W., JI, G. & DAI, Y. 2013. The essential role of p38 MAPK in mediating the interplay of oxLDL and IL-10 in regulating endothelial cell apoptosis. *Eur J Cell Biol*, 92, 150-9.
- YOSHIMURA, A., OHKUBO, T., KIGUCHI, T., JENKINS, N. A., GILBERT, D. J., COPELAND, N. G., HARA, T. & MIYAJIMA, A. 1995. A novel cytokine-inducible gene CIS encodes an SH2-containing protein that binds to

- tyrosine-phosphorylated interleukin 3 and erythropoietin receptors. *EMBO J*, 14, 2816-26.
- YU, F. S., YIN, J., XU, K. & HUANG, J. 2010. Growth factors and corneal epithelial wound healing. *Brain Res Bull*, 81, 229-35.
- ZADJALI, F., PIKE, A. C., VESTERLUND, M., SUN, J., WU, C., LI, S. S., RONNSTRAND, L., KNAPP, S., BULLOCK, A. N. & FLORES-MORALES, A. 2011. Structural basis for c-KIT inhibition by the suppressor of cytokine signaling 6 (SOCS6) ubiquitin ligase. *J Biol Chem*, 286, 480-90.
- ZAFRA, M. P., MAZZEO, C., GAMEZ, C., RODRIGUEZ MARCO, A., DE ZULUETA, A., SANZ, V., BILBAO, I., RUIZ-CABELLO, J., ZUBELDIA, J. M. & DEL POZO, V. 2014. Gene silencing of SOCS3 by siRNA intranasal delivery inhibits asthma phenotype in mice. *PLoS One*, 9, e91996.
- ZHAN, X., BATES, B., HU, X. G. & GOLDFARB, M. 1988. The human FGF-5 oncogene encodes a novel protein related to fibroblast growth factors. *Mol Cell Biol*, 8, 3487-95.
- ZHANG, J. G., FARLEY, A., NICHOLSON, S. E., WILLSON, T. A., ZUGARO, L. M., SIMPSON, R. J., MORITZ, R. L., CARY, D., RICHARDSON, R., HAUSMANN, G., KILE, B. J., KENT, S. B., ALEXANDER, W. S., METCALF, D., HILTON, D. J., NICOLA, N. A. & BACA, M. 1999. The conserved SOCS box motif in suppressors of cytokine signaling binds to elongins B and C and may couple bound proteins to proteasomal degradation. *Proc Natl Acad Sci U S A*, 96, 2071-6.
- ZHANG, J. G., METCALF, D., RAKAR, S., ASIMAKIS, M., GREENHALGH, C. J., WILLSON, T. A., STARR, R., NICHOLSON, S. E., CARTER, W., ALEXANDER, W. S., HILTON, D. J. & NICOLA, N. A. 2001. The SOCS box of suppressor of cytokine signaling-1 is important for inhibition of cytokine action in vivo. *Proc Natl Acad Sci U S A*, 98, 13261-5.
- ZHAO, X. & GUAN, J. L. 2011. Focal adhesion kinase and its signaling pathways in cell migration and angiogenesis. *Adv Drug Deliv Rev*, 63, 610-5.
- ZOLK, O., NG, L. L., O'BRIEN, R. J., WEYAND, M. & ESCHENHAGEN, T. 2002. Augmented expression of cardiotrophin-1 in failing human hearts is accompanied by diminished glycoprotein 130 receptor protein abundance. *Circulation*, 106, 1442-6.
- ZONG, C. S., CHAN, J., LEVY, D. E., HORVATH, C., SADOWSKI, H. B. & WANG, L. H. 2000. Mechanism of STAT3 activation by insulin-like growth factor I receptor. *J Biol Chem*, 275, 15099-105.
- ZUKER, M. 2003. Mfold web server for nucleic acid folding and hybridization prediction. *Nucleic Acids Res*, 31, 3406-15.
- ARAVINDAN, R, YE, L., SANDERS, AJ., PATRICIA, E. Price., KEITH, G. Harding, & **WEN, G. Jiang**. 2017. The molecular and cellular impact of Psoriasin (S100A7) on the healing of human wounds. *Molecular and Therapeutic Medicine*, in press.